LINK LAYER PROTOCOL PERFORMANCE OF INDOOR INFRARED WIRELESS COMMUNICATIONS

VASILEIOS VITSAS

A thesis submitted in partial fulfillment of the requirements of Bournemouth University for the degree of Doctor of Philosophy

June 2002

Bournemouth University

LINK LAYER PROTOCOL PERFORMANCE OF INDOOR INFRARED WIRELESS COMMUNICATIONS

Vasileios Vitsas

ABSTRACT

The increasing deployment of portable computers and mobile devices leads to an increasing demand for wireless connections. Infrared presents several advantages over radio for indoor wireless connectivity but infrared link quality is affected by ambient infrared noise and by low power transmission levels due to eye safety limitations. The Infrared Data Association (IrDA) has developed the widely used IrDA 1.x protocol standard for short range, narrow beam, point to point connections. IrDA addressed the requirement for indoor multipoint connectivity with the development of the Advanced Infrared (AIr) protocol stack.

This work analyses infrared link layer design based on IrDA proposals for addressing link layer topics and suggests implementation issues and protocol modifications that improve the operation of short range infrared connections. The performance of optical wireless links is measured by the utilization, which can be drawn at the data link layer. A new mathematical model is developed that reaches a simple equation that calculates IrDA 1.x utilization. The model is validated by comparing its outcome with simulation results obtained using the OPNET modeler. The mathematical model is employed to study the effectiveness on utilization of physical and link layer parameters. The simple equation gives insights for the optimum control of the infrared link for maximum utilization. By differentiating the utilization equation, simple formulas are derived for optimum values of the window and frame size parameters. Analytical results indicate that significant utilization increase is observed if the optimum values are implemented, especially for high error rate links. A protocol improvement that utilizes special Supervisory frames (S-frames) to pass transmission control is proposed to deal with delays introduced by F-timer expiration. Results indicate that employing the special S-frame highly improves utilization when optimum window and frame size values are implemented. The achieved practical utilization increase for optimum parameter implementation is confirmed by means of simulation.

AIr protocol trades speed for range by employing Repetition Rate (RR) coding to achieve the increased transmission range required for wireless LAN connectivity. AIr employs the RTS/CTS medium reservation scheme to cope with hidden stations and CSMA/CA techniques with linear contention window (CW) adjustment for medium access. A mathematical model is developed for the AIr collision avoidance (CA) procedures and validated by comparing analysis with simulation results. The model is employed to examine the effectiveness of the CA parameters on utilization. By differentiating the utilization equation, the optimum CW size that maximises utilization as a function of the number of the transmitting stations is derived. The proposed linear CW adjustment is very effective in implementing CW values close to optimum and thus minimizing CA delays. AIr implements a Go-Back-N retransmission scheme at high or low level to cope with transmission errors. AIr optionally implements a Stop-and-Wait retransmission scheme to efficiently implement RR coding. Analytical models for the AIr retransmission schemes are developed and employed to compare protocol utilization for different link parameter values. Finally, the effectiveness of the proposed RR coding on utilization for different retransmission schemes is explored.

DEDICATION

Αφιερώνεται στην μητέρα μου Αννα

και στον πατέρα μου Κωνσταντίνο

PUBLICATIONS RESULTING FROM THESIS

I. Awards

[1] V. Vitsas and A. C. Boucouvalas, 'IrDA IrLAP Protocol Throughput Performance Analysis for Optical Wireless Links', Proc. of 2nd International Workshop on Networked Appliances (IWNA 2000), Nov. 30- Dec. 1, 2000, Rutgers Univ., New Jersey, USA **(Best paper award).**

II. Journal publications

[2] V. Vitsas and A. C. Boucouvalas, 'Optimisation of IrDA IrLAP Link Access Protocol', IEEE Journal on Selected Areas in Communications, accepted for publication.

[3] V. Vitsas and A. C. Boucouvalas, 'Performance Analysis of the Advanced Infrared (AIr) CSMA/CA MAC Protocol for Wireless LANs', Wireless Networks, accepted for publication.

[4] V. Vitsas and A.C. Boucouvalas, 'Automatic repeat request schemes for infrared wireless communications', IEE Electronics Letters, vol. 38, no. 5, pp. 244-246, 28th February 2002.

[5] V. Vitsas and A.C. Boucouvalas, 'Simultaneous optimisation of window and frame size for maximum throughput IrDA links', IEE Electronics Letters, vol. 37, no. 16, pp. 1042-1043, 2nd August 2001.

[6] A. C. Boucouvalas and V. Vitsas, 'Optimum window and frame size for IrDA links', IEE Electronics Letters, vol. 37, no. 3, pp. 194-196, 1st February 2001.

[7] P. Barker, A.C. Boucouvalas and V. Vitsas, 'Performance modelling of the IrDA infrared wireless communications protocol', International Journal of Communication Systems, vol. 13, pp. 589-604, 2000.

[8] P. Barker, V. Vitsas and Boucouvalas A.C., 'Simulation analysis of the Advanced Infrared (AIr) MAC wireless communications protocol', accepted for publication in IEE Proceedings Circuits and Systems.

III. International conference refereed publications

[9] V. Vitsas and A. C. Boucouvalas, 'Effectiveness of packet level acknowledgement in infrared wireless LANs', IEEE 55th Vehicular

Technology Conference 2002, VTC Spring 2002, vol. 4, pp. 1814-1818, Birmingham, AL, May 6-9, 2002.

[10] V. Vitsas and A. C. Boucouvalas, 'Performance analysis of the collision avoidance procedure of the Advanced Infrared (AIr) CSMA/CA protocol for wireless LANs', IEEE 55th Vehicular Technology Conference 2002, VTC Spring 2002, vol. 3, pp. 1502-1506, Birmingham, AL, May 6-9, 2002.

[11] V. Vitsas and A. C. Boucouvalas, 'Effectiveness of Selective Reject (SREJ) Automatic Repeat Request (ARQ) scheme with RR-coding in infrared wireless LANs', accepted for publication in CSNDSP 2002, July 15-17, 2002, Staffordshire, UK.

[12] V. Vitsas and A.C. Boucouvalas, 'Window and frame size adaptivity for maximum throughput in IrDA links', Proc. of the 3rd Electronic Circuits and Systems Conference, pp. 147-152, Slovak University of Technology in Bratislava, Bratislava, Slovakia, September 5-7, 2001.

[13] V. Vitsas and A. C. Boucouvalas, 'Performance evaluation of IrDA Advanced Infrared AIr-MAC Protocol', Proc. of the 5th Multi-Conference on Systemics, Cybernetics, and Informatics, vol. IV, pp. 347-352, Orlando, USA, 2001.

[14] V. Vitsas and A.C. Boucouvalas, 'Performance Analysis of the AIr-MAC optical wireless protocol', International Conference on System Engineering, Communications and Information Technologies, (ICSECIT 2001), Department of Electrical Engineering, University of Magallanes, Punta Arenas, Chile, April 16-19, 2001.

[15] V. Vitsas and A.C. Boucouvalas, 'Throughput analysis of the IrDA IrLAP optical wireless link access protocol', Proc. of the 3rd Conference on Telecommunications (ConfTele 2001), pp. 225-229, April 23-24, 2001, Figueira da Foz, Portugal.

[16] A. C. Boucouvalas and V. Vitsas, '100 Mb/s IrDA protocol performance evaluation', IASTED International Conference on Wireless and Optical Communications, (WOC 2001), June 27-29, 2001 Banff, Canada, pp. 49-57.

NOTE: Most of these publications are available at:

http://dec.bournemouth.ac.uk/staff/tboucouvalas/acbpub.htm

ACKNOWLEDGMENTS

I would like to acknowledge the advice, encouragement and support I received from my supervisor, Prof. Anthony Boucouvalas, throughout the duration of my project. Although he was usually very busy, he was always able to find a few (long) minutes to discuss issues of my project. I also thank him for giving me the freedom to follow aspects of my own research interests in this project.

I would also like to thank Achilleas Arslanoglou, Andonis Vafiadis and Dimitris Kleftouris for their constant encouragement, and my friends in Bournemouth, Dimitris Vikeloudas , Periklis Chatzimisios and Angeliki Chrevatidis for their friendship and for the relaxing moments when playing biriba.

Last but not least, I would like to thank Martha and my mother for their patience and support over these years.

CONTENTS

LIST OF FIGURES

LIST OF TABLES

ABBREVIATIONS

4PPM/VR	4-slot Pulse Position Modulation with Variable Repetition Rate encoding
ACK	Acknowledgement
AIr	Advanced Infrared
AIr MAC	AIr Medium Access Control
AIr LC	AIr Link Control
AIr LM	AIr Link Manager
AP	Access Point
ARQ	Automatic Repeat reQuest
BER	Bit Error Rate
CA	Collision Avoidance
CAS	Collision Avoidance Slot
CDMA	Code Division Multiple Access
CRC	Cyclic Redundancy Check
CSMA/CA	Carrier Sense Multiple Access with Collision Avoidance
CT	CAS Timer
CTS	Clear To Send
CW	Contention Window
DA	Destination Address
DCF	Distributed Coordination Function
DD	Direct Detection
DSSS	Direct Sequence Spread Spectrum
EOB	End Of Burst
EOBC	End Of Burst Confirm
ETSI	European Telecommunication Standards Institute
F-bit	Final bit
FCS	Frame Check Sequence
FER	Frame Error Rate
FH	Frequency Hopping
FHSS	Frequency Hopping Spread Spectrum
FIR	Fast Infrared
FLACK	Frame Level Acknowledgment
FLACK-M	Frame Level Acknowledgment MAC
FOV	Field Of View
GBN	Go-Back-N
HiperLAN	High Performance Radio LAN
I-frame	Information frame
IrDA	Infrared Data Association
IrLAP	IrDA Link Access Protocol
IM	Intensity Modulation
IR	Infrared
ISM	Industrial / Scientific / Medical
L-PPM	*L*-slot Pulse Position Modulation
LAN	Local Area Network
LOS	Line Of Sight
MAC	Medium Access Control

MACA	Multiple Access with Collision Avoidance
MBR	Main Body
MT	Mobile Terminal
NoFLACK	No Frame Level Acknowledgment
NoFLACK-ACK	No Frame Level Acknowledgment utilizing LC ACK frames
NDM	Normal Disconnect Mode
NRM	Normal Response Mode
OFDM	Orthogonal Frequency Division Multiplexing
P-bit	Poll bit
P/F bit	Poll/Final bit
PA	Preamble
PAN	Personal Area Network
PCF	Point Coordination Function
PDA	Personal Digital Assistant
PSAP	Physical layer Service Access Point
QoS	Quality of Service
RH	Robust Header
RR	Repetition Rate
RR S-frame	Receive Ready Supervisory frame
RT	Reservation Time
RTS	Request To Send
S-frame	Supervisory frame
SA	Source Address
SEQ-NoFLACK	Sequential No Frame Level Acknowledgment
SIR	Serial Infrared
SNR	Signal-to-Noise Ratio
SREJ	Selective Reject
SYNC	Synchronisation
SW	Stop-and-Wait
TAT	Turn Around Time
TDMA	Time Division Multiple Access
U-frame	Unnumbered frame
VFIR	Very Fast Infrared
VTT	Virtual Transmission Time
WFCTS	Wait For CTS
WLAN	Wireless LAN
WPAN	Wireless Personal Area Network
WTT	Window Transmission Time

CHAPTER 1

Introduction

1.1 Motivation

The exponential increase in deployment and use of "information appliances" such as digital still and video cameras, PDAs, music players, watches, mobile phones, laptops and handheld computers, leads to a demand for connectivity between them in a wireless manner. New devices have powerful "computer like" capabilities for storing, retrieving and processing of information such as portable information gathering appliances and palmtop computers. Laptop computers demand high-speed data wireless connections for accessing all services that are available on high-speed wired networks. Laptop users also wish to establish short-period wireless data connections for printing and for information exchange with a portable device.

Infrared and radio are considered as candidates for wireless connectivity. Infrared radiation offers several advantages over radio [8][57]. Infrared links utilize low cost components with small physical size and low power consumption. In addition, infrared spectrum is unregulated worldwide and can achieve high data rates. However, the infrared medium is not without drawbacks. Infrared emissions must obey eye safety limitations and are confined to the room of operation because infrared radiation cannot penetrate walls. Link quality can be detrimental due to ambient infrared noise and third user interference.

There are difficult challenges in designing wireless connectivity. Transmission range, transmitted power and modulation format issues must be addressed differently when a wireless medium is utilized. Carrier sensing and collision detection is more difficult in wireless than in wired connections. The desired station mobility and security issues must also be considered. In addition, there are different requirements for wireless connections. Depending on the application and on the devices involved, a wireless point to point or multipoint connection may be needed. For example, a digital camera requires a point to point connection with a laptop to transfer the pictures it holds in memory; a laptop requires LAN connectivity in order to share information with other laptops in range.

In order to avoid the development of non-interoperable single-vendor proprietary infrared link designs, the Infrared Data Association (IrDA) was established in 1993 by major IT companies aiming to develop standards for infrared connectivity. IrDA developed the IrDA 1.x protocol stack for short range, narrow beam, point to point connections. IrPHY, the IrDA 1.x physical layer, supports data rates up to 16Mbit/s. IrDA 1.x is widely adopted [16], fully supported by popular operating systems [106] and millions of devices are shipped every year embedding an infrared port for their wireless transfer needs [101].

IrDA addressed the requirement for multipoint connections with the development of the Advanced Infrared (AIr) protocol stack. The AIr proposal preserves the investment in IrDA 1.x upper layer applications by replacing the physical and the link layer of the IrDA 1.x protocol stack. A new physical layer, AIr PHY, is proposed that supports wide-angle infrared ports in order to achieve multipoint connectivity. AIr PHY base rate is 4 Mbit/s. AIr PHY employs Repetition Rate (RR) coding to achieve the increased transmission range required for wireless LAN connectivity. The transmitter trades speed for range by repeating the transmitted information RR times in order to increase the capture probability at the receiver. IrLAP, the IrDA 1.x link layer is divided into three sub-layers, the AIr Medium Access Control (AIr MAC), the AIr Link Manager (AIr LM) and the AIr Link Control (AIr LC) sub layers. AIr MAC is responsible for coordinating access to the shared infrared medium and for efficiently implementing RR coding. AIr LC provides guaranteed information delivery to the remote device.

The performance of wireless links may be measured by the link utilization, which can be drawn at the data link layer. Utilization is defined as the percentage of time the medium successfully transfers information between stations. Utilization takes into account all significant factors that affect performance such as (a) the physical layer delays (e.g. hardware latency), (b) the medium access mechanism, (c) the transmission control passing scheme, (d) the transmission errors introduced by the wireless medium and (e) the acknowledgement delays. Link layer design is very important as it must minimize physical and link layer delays and increase performance for the information transfer scenarios that will utilize the considered infrared link.

1.2 Statement of the problem

Link layer design must minimize physical and link layer delays such as hardware

latency, medium access and retransmission delays. An efficient link layer must minimize utilization loss due to hardware latency delays and transmit large amounts of information before reversing link direction in order to decrease link turn around frequency. A single transmission error may result in the retransmission of a large amount of information data and utilization degradation. The determination of the optimum information amount that simultaneously minimizes retransmission overhead and hardware latency delays is addressed in this work. The implementation of an efficient transmission control passing mechanism for the specific link quality is also a link layer design challenge. In multipoint infrared connectivity, the development of an efficient medium access mechanism that minimizes collisions and channel idle time when many stations wish to utilize the shared medium at the same time is a challenge. The efficient implementation of coding schemes used to reach stations far away from the transmitter combined with retransmission schemes that cope with transmission errors is studied in this work.

1.3 Outline of research work

This work focuses on the efficient link layer design of infrared links based on IrDA proposals. The following issues are addressed:

a) **point to point infrared connections**

- The effect on utilization of wireless specific physical layer parameters is examined in order to determine the physical layer requirements for high performance. As the IrPHY supports half-duplex connections only, transmission control is passed at the IrLAP layer. The performance of different transmission control passing mechanisms is studied.
- Transmission errors are more likely to occur in wireless media. For example, the strict IrPHY range restriction (1m) can not be always met. A greater link distance may cause an increased error rate and utilization degradation. We derive optimum link layer parameter values that maximize utilization at high error rates. The utilization improvement of implementing optimum values for window size and the frame length is examined.

b) **Infrared wireless LANs**

- Access to shared infrared medium is coordinated by Carrier Sense Multiple

Access with Collision Avoidance (CSMA/CA) techniques. A station that is not able to hear transmissions originating from another station is called a hidden station. As hidden stations are likely to appear in infrared wireless LANs, the Request To Send / Clear To Send (RTS/CTS) medium reservation scheme is utilized to cope with the hidden station problem. AIr MAC always terminates medium reservation by an End Of Burst / End Of Burst Confirm (EOB/EOBC) frame exchange to inform all stations that current reservation is over and that the next contention period starts. The RTS and CTS control frames are transmitted using the maximum RR value (RR=16) in order to increase their transmission range. Thus, the employed CSMA/CA scheme may cause significant utilization degradation if it results in a significant number of collisions or empty collision avoidance slots. The performance of the proposed AIr MAC collision avoidance (CA) procedures is studied analytically. A mathematical model is developed assuming a finite number of stations and error free transmissions. The significance of the collision avoidance parameters and their effectiveness on utilization is examined.

- AIr LC employs a Go-Back-N (GBN) Automatic Repeat Request (ARQ) retransmission scheme to cope with transmission errors. However, AIr MAC optionally implements a Stop-and-Wait (SW) ARQ scheme as it may utilize frame level acknowledgments to efficiently implement RR coding. AIr MAC may also implement a GBN ARQ scheme acknowledging correctly received frames using the EOBC frame that terminates a reservation. We define five link layer protocols, which are referred to as a) frame level acknowledgement, b) frame level acknowledgement MAC, c) no frame level acknowledgement, d) no frame level acknowledgement utilizing LC ACK frames and e) sequential no frame level acknowledgment. These protocols provide a one or two layer ARQ scheme that copes with transmission errors. The effectiveness of the proposed ARQ protocols is compared under different channel conditions and for various application requirements.
- AIr MAC is responsible for implementing the suitable RR value for a specific link quality. The receiver monitors link quality and recommends RR values to the transmitter. The transmitter selects the RR it utilizes based (a) on the receiver

recommendations, (b) on the ARQ protocol it utilizes and (c) on the window size and frame length it implements. An analytical model that evaluates frame error rate as a function of SNR and RR is presented. The selection of ARQ protocol, RR value, window size and frame length that maximizes utilization is finally examined.

1.4 Thesis outline

The main scope of this thesis is to develop algorithms to support high speed and robust indoor infrared wireless connections. It focuses on the data link layer procedures that determine the performance of these links. Infrared point to point as well as LAN connectivity is considered. This thesis has four parts; chapter 2 discusses indoor connectivity, chapters 3 and 4 consider infrared point-to-point link layer issues, chapters 5, 6 and 7 study infrared multipoint connectivity and chapter 8 presents the conclusions.

Chapter 2 introduces wireless personal and local area networks, compares radio and infrared transmission media for indoor connectivity and discusses current standards for indoor links focusing on link layer issues. It presents the special characteristics of the infrared medium and discusses the link layer design challenges when the infrared medium is utilized at the physical layer. Chapter 2 also presents the two methods used in this work to address link layer design challenges; computer simulation and mathematical modeling. It finally presents the performance measures that evaluate performance and critically reviews current research in this area.

Chapter 3 presents the IrDA 1.x protocol stack and the IrLAP layer. It examines the IrLAP performance by developing a new analytical model for IrLAP utilization. The new model is compared with existing models in the literature and validated by comparing simulation with analysis results. The performance of IrDA 1.x links for various error rate conditions is presented and the effectiveness of physical and link layer parameters to link performance is studied. The IrLAP performance in the predicted future increases of IrPHY data rate is also examined.

Chapter 4 examines link utilization improvement for specific error rate conditions. It derives optimum window size values for fixed frame length and optimum frame length values for fixed window size by differentiating the utilization equation. Simple equations are derived that calculate optimum window and frame size values as a function of the link error rate and of physical layer parameters. The performance

improvement when optimum values are implemented is discussed. If window and frame size can be simultaneously adjusted, new equations for optimum window and frame size are derived. Simultaneous window and frame size adjustment always achieves higher utilization. The practical IrLAP performance improvement that can be achieved if the transmitter utilizes optimum window and frame size values is examined using simulation techniques.

Chapter 5 presents the AIr protocol stack proposal for wireless LANs and focuses on the AIr MAC sublayer. It presents the interface between AIr MAC and PHY layers and analyses the AIr MAC collision avoidance procedures and transfer schemes, including the Reserved and Unreserved transfer modes of the protocol. It examines AIr performance using simulation techniques and analyses the performance of the Unreserved transfer mode for the particular PHY/MAC interface and collision avoidance scheme.

Chapter 6 develops an analytical model that calculates the performance of the collision avoidance (CA) procedures of the AIr protocol assuming no hidden stations and a finite number of contending stations. The model is validated by comparing analysis with simulation results and is employed to evaluate the effectiveness of the physical and link layer parameters to utilization assuming error free transmissions.

Chapter 7 considers link layer performance when transmission errors occur. It develops analytical models for five ARQ schemes that cope with transmission errors. It employs these models to examine the retransmission delays and the model developed in chapter 6 for the collision avoidance delays. It also presents an analytical model that calculates frame error rate as a function of signal to noise ratio when RR coding is implemented. By combining these analytical models, we calculate utilization as a function of the station's SNR, the implemented RR, the employed ARQ scheme, the turn around time delay and the utilized window and frame size values.

Chapter 8 presents the conclusions of this thesis and proposes direction for future research in the field of indoor infrared connectivity.

CHAPTER 2

Background

In this chapter we introduce the technologies that support short-range wireless communications. We classify the proposed technologies using two criteria. First, we distinguish point-to-point connections utilized to form Wireless Personal Area Networks from multipoint connections used to form Wireless LANs. Second, we classify technologies according to the medium they utilize, radio or infrared optical.

Wireless Personal Area Networks (PANs) allow mobile devices to function together in ad hoc networks within a personal space [62]. Wireless PANs aim to replace wired connectivity between devices such as still and video cameras, laptops and MP3 players. Wireless LANs (WLANs) provide computer connectivity in a small area such as an office complex, a building or a hallway by extending or replacing a wired LAN. The main attraction in wireless LANs is the flexibility and mobility; bandwidth considerations are of secondary importance [88]. Portable terminals forming the WLAN should have access to all services provided for wired terminals. Unlike wired stations, portable terminals suffer from severe limitations in size, weight and power consumption. In addition, WLAN design addresses the special properties of the wireless medium.

Bluetooth [32] and IrDA 1.x [101] protocol stacks support indoor point to point links utilizing the radio and infrared spectrum respectively. HomeRF [70] and HiperLAN [55] support multipoint WLAN connectivity using radio. IEEE 802.11 standard supports multipoint connectivity and offers several choices of physical medium such as spread spectrum radio and infrared [26]. IrDA AIr protocol proposal utilizes the infrared spectrum to implement wireless LANs [73].

The outline of this chapter is as follows. Section 2.1 describes wireless indoor connectivity and section 2.2 presents current standards for wireless PANs and LANs focusing on transmission techniques and medium access procedures. Section 2.3 compares radio and infrared transmission media for indoor wireless connectivity and section 2.4 categorizes indoor infrared communication systems. Infrared radiation exhibits special characteristics when utilized for indoor connectivity. The link layer design challenges arising from these characteristics are discussed in section 2.5. Section

2.6 presents the advantages and disadvantages of computer simulation and mathematical modeling techniques that evaluate the performance of communication systems and section 2.7 presents the performance measures used to evaluate the system performance. Finally, section 2.8 reviews current research related to infrared link layer design challenges.

2.1 Wireless indoor communications

Indoor connectivity is required in the home and office environment to carry telephone conversations, music, television, video (MPEG1, MPEG2 and MPEG4), pictures (JPEG), signals from surveillance cameras and alarm sensors, commands for controlling appliances and multimedia information from the Internet [27]. Portable computers, such as laptops, palmtops and PDAs, also require connections for Internet access, printing and information exchange. Although wired connections can be employed to provide the required information transfer, their use in many cases is impractical or undesirable. For example, it is impractical to install a new wiring system to connect two computers in different rooms at home. Wireless connections provide an attractive alternative, especially when a mobile device is involved and when a low bandwidth is required. At present, the applications utilizing short-range indoor wireless connections fall into two main areas [27]:

- Controlling items, such as climate control systems, electric appliances (television, video, etc.), lights and surveillance cameras
- Connecting PCs and peripherals for information exchange and entertainment.

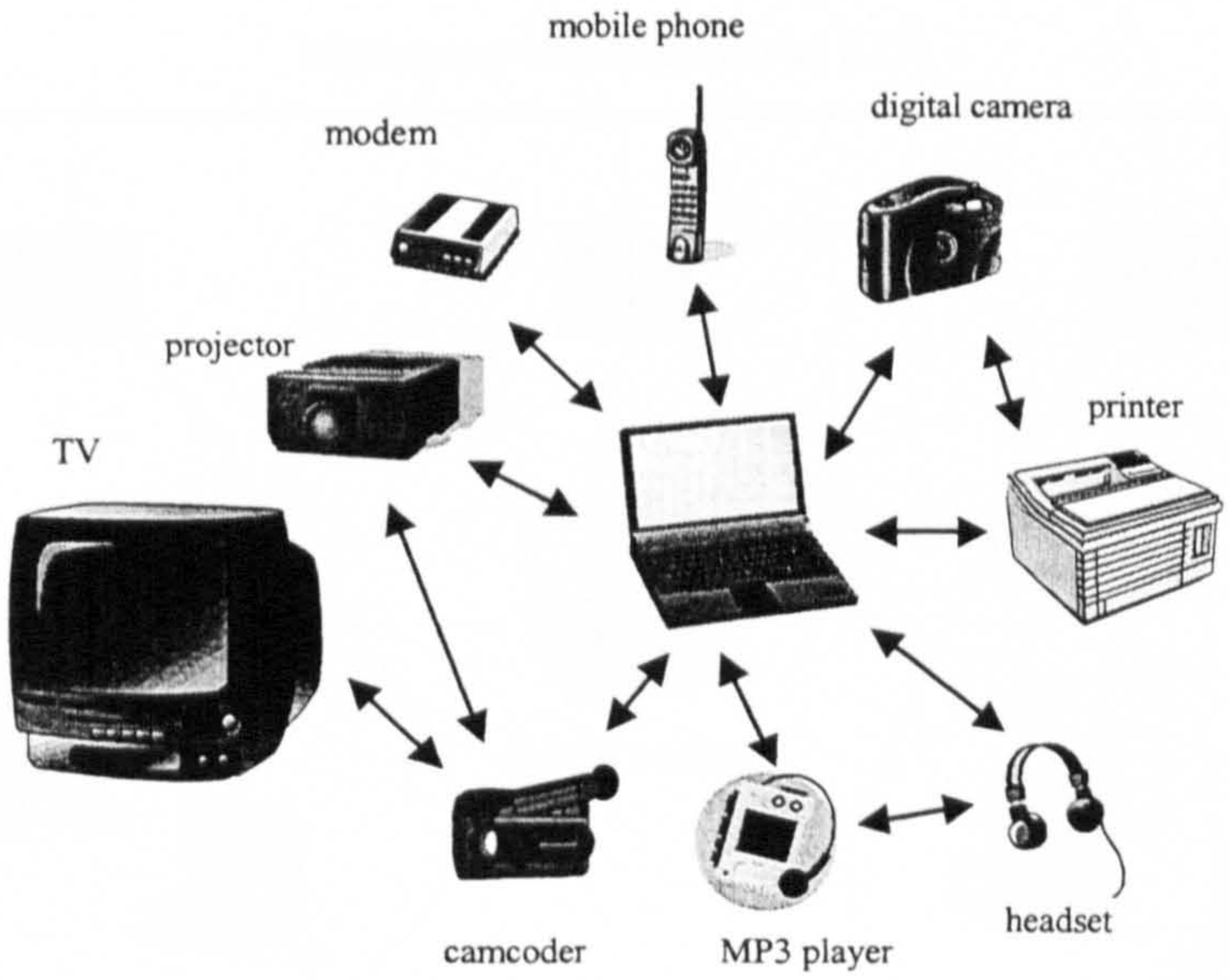

Figure 2.1 WPAN applications

This work considers the information exchange between two or more PCs and/or peripherals. Depending on user applications, two categories are defined for wireless information exchange:

a) **Wireless PANs.** A wireless PAN (WPAN) (Fig. 2.1) enables short-range ad hoc connectivity among portable consumer electronics and communications devices, such as laptops, PDAs, MP3 players, still and video cameras, modems, printers, mobile phones and TVs [59]. Wireless PAN technology aims to replace cables between these devices and to provide fast and reliable information transfer abilities to the single user. WPAN technology is often utilized for point-to-point information transfer and implements master/slave communication techniques.

b) **Wireless LANs.** A wireless LAN (WLAN) aims to offer wireless stations the same capabilities that wired LANs provide to stationary stations. WLANs are not widely used due to high prices, low data rates, security issues and license requirements. These drawbacks have been recently addressed and a rapid wireless LAN deployment is expected [86]. Wireless LAN connectivity can be categorized as follows:

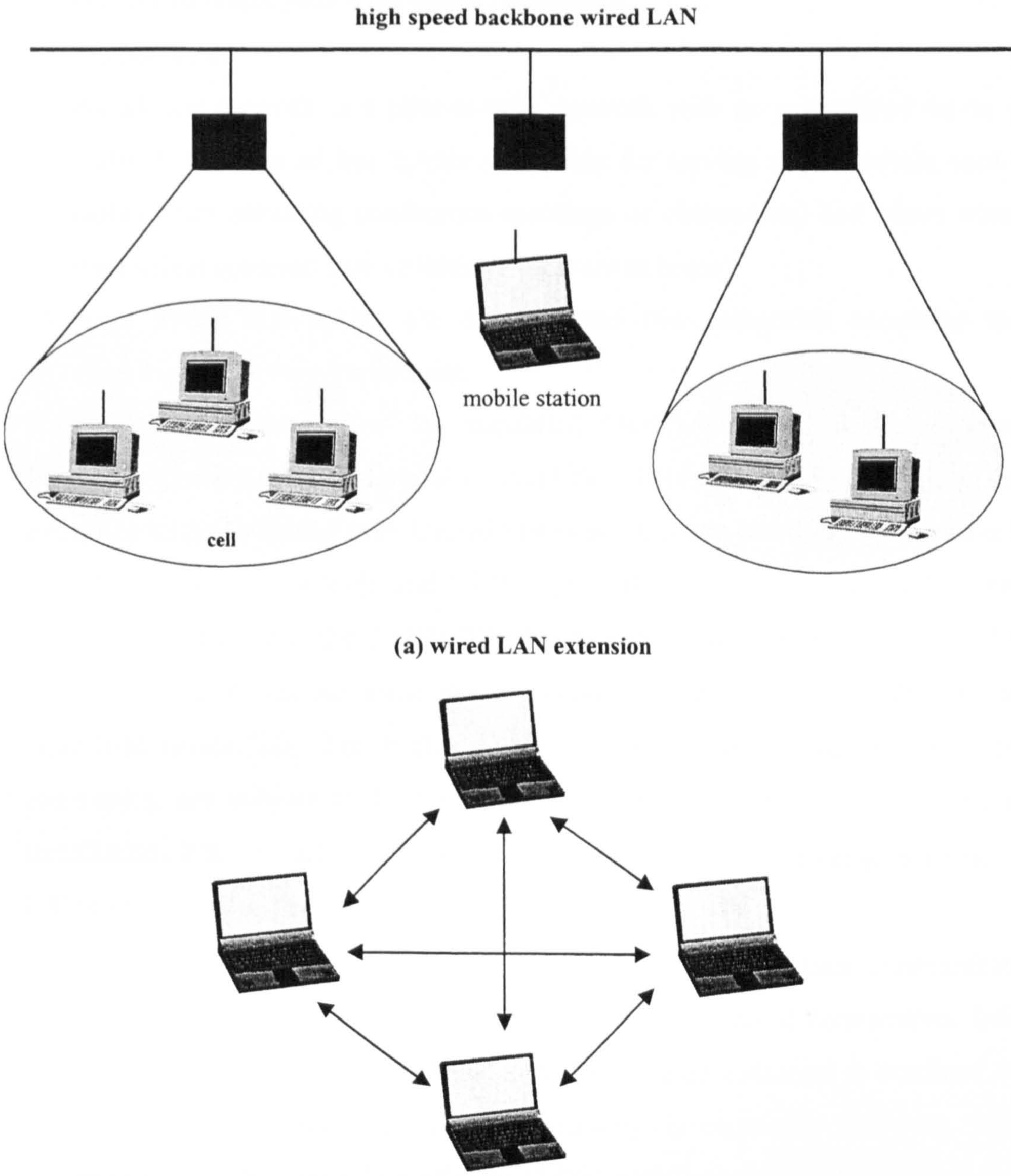

Figure 2.2 Wireless LAN configurations

- LAN extension and nomadic access

A wireless LAN extension of an existing high-speed backbone wired LAN, (Fig. 2.2a), saves the cost of installing wires and eases the relocation of stationary computers [85]. It also provides easy network access to mobile computers. This scheme is suitable for buildings where wiring is difficult or prohibited (e.g. manufacturing plants, stock exchanges, trading floors and historical buildings). It is also suitable for businesses operating in many buildings and having a large

number of employees with laptop computers.

- Ad hoc LAN

  An ad hoc network is a peer-to-peer network with no centralized server (Fig. 2.2b). A wireless ad hoc LANs is suitable for serving an immediate need (e.g. laptop users attending conference meetings or classrooms) and where wiring is impractical (connect two or three computers at home).

Wireless PANs and LANs are divided into two categories according to the transmission technique they implement:

a) **Radio.** Radio transmissions are regulated worldwide and require government licensing. However, the Industrial / Scientific / Medical (ISM) radio bands are an exception to the licensing rule. United States and Canada allocate ISM bands at 902-928 MHz, 2,400–2,484 MHz and 5,725-5,850 MHz [87][2]. They are called the 900 MHz, the 2.4 GHz and the 5 GHz ISM bands respectively. The 2.4 GHz ISM band is allocated worldwide but some countries allocate slightly different 900 MHz and 5 GHz ISM bands [80]. The higher frequency ISM bands require more expensive electronics, are subject to higher interference from microwave ovens and radar installations but can achieve higher data rates. To avoid licensing, wireless radio PANs and LANs utilize the ISM bands.

b) **Infrared (IR).** Infrared waves are suitable for short-range indoor communications. Remote controls for TVs, videos and stereos utilize infrared connections. Infrared components are cheap, easy to build and the infrared radiation is confined to the room of operation. As a result, no licensing is required. However, infrared connections may require a line of sight (LOS) path between the transmitter and the receiver. In fact, as we go from radio to light frequencies, transmissions behave more like rays and less like waves. The infrared spectrum offers virtually unlimited bandwidth capable of accommodating high data rates [57].

2.2 Wireless PAN and LAN standards

The great range of applications requiring wireless information transfers has led to the development of many standards. Devices for wireless PANs and LANs follow specifications developed by independent standard bodies or industry consortia. This section briefly describes current standards for wireless PANs and LANs focusing on physical layer and medium access issues. Table 2.1 gives an overview of the attributes

	applica-tion	Peak data rate (Mbit/s)	cost	range	frequency	modulation	data network support	organization
IrDA 1.x	WPAN	16	Low	<2m LOS	infrared	RZI/ 4PPM/ HHH(1,13)	via PPP	IrDA
Bluetooth	WPAN	1	Medium	10-100m	2.4 GHz	FHSS	via PPP	Bluetooth Special Interest Group
HiperLAN	WLAN	24	High	>30m	5 GHz	OFDM	TCP/IP	ETSI
802.11	WLAN	2	Medium/high	>50m	2.4 GHz/ infrared	FHSS/ DSSS/ 4PPM	TCP/IP	IEEE
802.11a	WLAN	54	High	100m	5 GHz	OFDM	TCP/IP	IEEE
802.11b	WLAN	11	Medium/high	100m	2.4 GHz	DSSS	TCP/IP	IEEE
HomeRF	WLAN	1.6	Medium	50m	2.4 GHz	FHSS	TCP/IP	Home Radio Frequency WG
IrDA AIr	WLAN	4	Medium	<10 LOS	infrared	4PPM	via PPP	IrDA

Table 2.1 WPAN and WLAN technologies

of the proposed technologies. Comparisons should be made bearing in mind that these technologies are more complementary than competitive [2][70].

2.2.1 Wireless PANs

2.2.1.1 IrDA 1.x

IrDA 1.x protocol specification was developed by IBM, Hewlett-Packard and Sharp for short-range, low-cost, half duplex, point-to-point links utilizing the IR spectrum. IrDA 1.x links aim to replace cables between devices such as laptop computers, personal digital assistants (PDAs), digital still and video cameras, mobile phones and printers. Computer manufacturers have widely adopted the IrDA 1.x standard [16] and popular operating systems fully support the IrDA 1.x specification [106]. Almost every portable computer and all Windows CE devices on market today contain an IrDA 1.x infrared port. More than 40 million devices are shipped every year equipped with IrDA 1.x ports and IrDA 1.x technology achieved a widespread deployment in a wide range of devices in a short time [101].

IrDA 1.x supports data rates up to 115,200 bit/s using the standard UART serial hardware and data rates up to 4Mbit/s and 16 Mbit/s using the high speed extension [52]. It utilizes narrow angle IR ports with a viewing of axis angle of between 15 and 30 degrees [67]. The IrDA 1.x link distance is at least 1m. The specified narrow angle and

short range allow the operation of multiple independent links in the same room at the same time. IrDA 1.x implements master/slave communication techniques. Any station can claim the master role at the negotiation phase but only one is assigned the master role when the link is established. The remaining (one or more) stations are slaves. The master station coordinates all transmissions and all data flows through the master station; only transmissions between the master and a slave station are permitted.

2.2.1.2 Bluetooth

Bluetooth was originally developed by Ericsson as a cable replacement for laptop to mobile phone connections for Internet access. The Bluetooth Special Interest Group (BSIG) [104] is an industry consortium formed by leading computer and mobile phone manufacturers to develop a standard for wireless connectivity for devices such as cordless and mobile phones, modems, headsets, PDAs, computers, printers, keyboards, MP3 players and projectors. BSIG published Bluetooth ver. 1.0 specification in 1999. Bluetooth is royalty-free and offers a low-cost, low-power, radio based cable replacement [32][33]. It also provides error correction, power management, security, and implements a Code Division Multiple Access (CDMA) transmission scheme.

Bluetooth utilizes the 2.4 GHz ISM radio band to achieve a data rate of 1 Mb/s at a range of 10 or 100 meters, depending on the power of the radio transceiver being used [81]. Devices in range form small networks called piconets. A station in the piconet is assigned the master role. The master implements centralized control; only transmissions between the master and one or more slaves is allowed [32]. A slave can only communicate with the master and only with the granted permission of the master. A piconet can contain up to eight devices (one master and up to seven slaves). Any station can be assigned the master role and master and slave roles are assigned for the piconet time duration. Bluetooth device discovery is a slow procedure but can be accelerated by techniques used in the IrDA specifications [103].

Bluetooth utilizes Frequency Hopping (FH) with carrier spacing of 1MHz. Typically, up to 80 different carrier frequencies can be used in the 2.4 GHz ISM bandwidth of 80 MHz. Devices in a piconet change frequency after every transmission following a well known hopping sequence to minimize radio interference. The master of a piconet provides the piconet identity, the hop sequence and the system clock that coordinates all piconet transmissions.

Many piconets can co-exist in the same area. If it wishes, a device participating in a piconet can also join another piconet that covers its geographical position. This form of overlapping is called scatternet [86]. Piconets in the same space implement different hop sequences. The signal in a piconet is spread over the 80 MHz frequency range but instantaneously only a bandwidth of 1 MHz is occupied. As a result, the 80 MHz bandwidth can support up to 80 simultaneous 1 MHz transmissions, each with a data rate of 1 Mb/s. However, collisions occur when devices in different piconets use the same hop frequency at the same time resulting in performance degradation.

2.2.2 Wireless LANs

2.2.2.1 HomeRF

The Home Radio Frequency Working Group (HRFWG) was launched in 1998 by leading computer companies (most in North America) to develop and promote wireless standards for voice and data communication around the home using radio. The key goal of the group is to enable interoperable wireless voice and data networking around the home at an affordable price. HRFWG proposed the HomeRF standard [105] for connecting PCs, peripherals, cordless phones and other consumer electronic devices using Frequency Hopping Spread Spectrum (FHSS) techniques in the 2.4 GHz ISM band [70][27]. The HomeRF data rate is 1.6 Mb/s and the distance range is 45 meters. HomeRF supports up to 127 data connections (PCs and peripherals) and four high quality voice connections (cordless telephones) [81].

HomeRF MAC layer utilizes contention-free periods and a Time Division Multiple Access (TDMA) scheme for the delay sensitive voice data from cordless phones. It also utilizes contention periods and a CSMA/CA scheme for the delay insensitive data connections [70]. The CSMA/CA scheme is derived from the IEEE 802.11 protocol. HomeRF also provides simultaneous voice and data calls, data security, and power management for both voice and data connections.

2.2.2.2 HiperLAN

The European Telecommunication Standards Institute (ETSI) proposed the High Performance Radio LAN (HiperLAN) protocol. HiperLAN considers a wireless extension of a wired network where Mobile Terminals (MTs), such as laptops and

PDAs, establish wireless connections to Access Points (APs) of a wired network. HiperLAN utilizes the 5 GHz ISM band [81], which provides larger frequency bandwidth than the 2.4 GHz band. By employing an efficient power amplifier and the larger frequency range, a data rate of 24 Mb/s is offered. HiperLAN provides connection-oriented information exchange, power save, quality of service (QoS) support, automatic frequency allocation, security, mobility support and easy integration with a variety of wired networks.

HiperLAN physical layer utilizes Orthogonal Frequency Division Multiplexing (OFDM), which is a special form of multicarrier modulation. OFDM divides data into several interleaved parallel bit steams and every stream modulates a separate sub-carrier. HiperLAN physical layer supports seven data rates ranging from 3 Mb/s to 25 Mb/s and several modulation and coding alternatives. HiperLAN also adapts data rate to current radio link quality. HiperLAN MAC layer utilizes a centralized controller at the AP [63]. It controls medium access using time division duplex (TDD) and dynamic time division multiple access (TDMA) techniques [55].

2.2.2.3 IEEE 802.11

IEEE has proposed the 802.11 standard for wireless LANs. IEEE 802.11 standard proposes three different physical layers utilizing:

a) Frequency Hopping Spread-Spectrum (FHSS) modulation in the 2.4 GHz ISM band
b) Direct Sequence Spread-Spectrum (DSSS) modulation in the 2.4 GHz ISM band
c) Infrared (IR) light using non-directed transmissions and both line-of-sight and reflected reception

All three physical layers support a data rate of 2 Mb/s. Both radio physical layers provide a range of up to 100 m indoors and the IR physical layer provides a range of up to 20 m but it is confined to the room of operation [86]. IEEE 802.11 standard considers interference and reliability, security, power saving, human safety and station mobility [26]. It supports access-point oriented and ad hoc networking topologies [65]. IEEE 802.11 MAC layer supports two medium access methods, the Distributed Coordination Function (DCF) and the Point Coordination Function (PCF). In DCF, all stations utilize CSMA/CA schemes for medium access. DCF is used for relatively insensitive to time delay information exchange, such as electronic mail and file transfers and it is suitable

for ad hoc networking topologies. PCF is based on polling that is controlled by a point coordinator, which is called the PCF station. The PCF station coordinates medium access and allows only one station to transmit at any time. PCF is suitable for time-bounded services such as voice and video transmissions [26]. As the PCF station is always an access point, the support of time-bounded services is limited to networks with infrastructure [65].

IEEE recently released the 802.11a and 802.11b standards. IEEE 802.11a utilizes the 5 GHz ISM band and achieves a data rate of 54 Mbps using OFDM. IEEE 802.11b is an extension of the 802.11 DSSS scheme and achieves a data rate of 11Mb/s by utilizing the complex Complementary Code Keying (CCK) modulation scheme [69].

2.2.2.4 IrDA AIr

IrDA proposed the Advanced Infrared (AIr) standard for wireless LANs by extending the IrDA 1.x protocol stack and relaxing the range and viewing angle restrictions posed by the IrDA 1.x physical layer [73][54]. AIr ports have a viewing of axis angle of between 60 and 75 degrees to achieve multipoint connectivity with other devices in range. AIr devices take advantage of line of sight (LOS) propagation paths but they can also communicate relying on infrared signal reflections from the ceiling and walls if the LOS path is obstructed. AIr data rate is 4Mbit/s but lower data rates (up to 256Kbit/s) can be utilized if the link quality is low due to high link distance, intense background light and/or non-LOS path. Adaptive data rate aims to reach all AIr stations operating in the same office or room. AIr transmission range is approximately 5m at 4Mbit/s and 10m at 256 Kbit/s for LOS links [40][41].

AIr standard provides dynamic device discovery procedures, priority delivery service for time sensitive data, power management and co-existence with IrDA 1.x devices [44]. AIr utilizes CSMA/CA techniques for medium access and does not assign master and slave roles to communicating stations.

2.3 Infrared versus radio

Infrared radiation has several advantages over radio for short-range wireless communication [8][57][58]. The infrared spectrum is unregulated worldwide and has a virtually unlimited bandwidth. Infrared detectors and emitters are available at low cost. Infrared is close in wavelength to visible light and exhibits similar behavior. Both are

directionally reflected from flat surfaces, diffusely reflected by rough surfaces, absorbed by dark objects and do not penetrate opaque barriers and walls. As a result, infrared transmissions are restricted to the room in which they originate and do not interfere with infrared transmissions in neighboring rooms. The signal room confinement simplifies security issues and offers a high aggregate capacity because the same spectrum can be safely reused in different rooms.

It is very difficult to design a low cost and sensitive infrared detector that collects significant signal power. Receiver sensitivity gets more difficult as we go from radio to infrared spectrum. Thus, the widely ASK and FSK modulation techniques used in radio are less attractive for low cost infrared links. A suitable solution is to implement Intensity Modulation (IM), in which the desired waveform is modulated onto the instantaneous power of the optical carrier [57]. The receiver utilizes a Direct Detection (DD) technique, in which the receiver's output current is proportional to the received instantaneous infrared power. The IM/DD modulation technique simplifies infrared port design and prevents multipath fading [57].

However, indoor infrared communication has several drawbacks. The room confinement is the main infrared disadvantage because it restricts communication range. Communication between different rooms requires the installation of infrared access points interconnected via a wired backbone or radio links. Infrared link quality is affected by infrared noise arising from incandescent and fluorescent lighting, sunlight and other infrared devices such as TV remote controls. Infrared links operate at short distances and although higher transmitter power is needed if the link distance is increased, the transmitter power levels must obey the eye safety regulations. In addition, some form of alignment between infrared ports may be required to achieve a high communication quality. This required alignment between the infrared transmitter and receiver may restrict the desired station mobility.

Infrared links can achieve high data rates; high-speed laboratory systems are presented in [56][57][102]. However, to increase infrared data rate above 10 Mbit/s requires more expensive components [35]. Radio communication can achieve high rates but suffers from interference from other radio transmitters. As radio passes through walls, radio links operating in different rooms of the same building must utilize different frequencies from the limited radio spectrum in order to minimize interference.

	Radio	Infrared	Implication for IR
Bandwidth regulated?	Yes	No	License not required Worldwide compatibility
Passes through walls?	Yes	No	Restricted coverage Simplifies security issues Reuse spectrum in different rooms
Multipath fading?	Yes	No	Simple and cheap link design
Dominant noise	Other users	Background light	Limited range
Range	High	Low	
Security	Low	High	
Pocket receiver	Yes	No	
Electrical interference	Yes	No	

Table 2.2 Infrared versus radio

In addition, the same radio spectrum may be utilized from other applications. For example, Bluetooth WPANs and IEEE 802.11 WLANs operate at the same 2.4 GHz ISM band. When a Bluetooth PAN co-exists in the same room with an IEEE 802.11 WLAN, a serious interference problem arises, which is examined in [22][64][82].

Radio and infrared can be considered as complementary transmission media [2][57]. Radio is preferred when long range transmission or transmission through walls is required [85]. Radio is also preferable when user mobility is of prime importance. Infrared is preferred when the aggregate system capacity must be maximized, when simple and low-cost components must be used and when international compatibility is required [8][57].

2.4 IR wireless communication systems

Depending on the application needs, infrared links can be utilized in different configurations and employ narrow-angle or wide-angle transmitters and receivers. Narrow-angle IR ports have a narrow beam transmission pattern and a narrow reception field of view (FOV). Wide-angle IR ports have a broad beam radiation pattern and a wide FOV.

Infrared links are also classified as line-of-sight (LOS) and non-LOS links. In LOS links, there is always an unobstructed line-of-sight path between the communicating devices. Fig. 2.3 shows the basic configuration of a point-to-point narrow angle LOS link. The transmitter consists of a modulation and encoding circuitry, an amplifier and an infrared LED with a beam-shaping lens. The receiver consists of a photo-detector with a collimating lens, an amplifier and a demodulation and decoding circuitry. Fig. 2.4 presents a narrow-angle LOS infrared communication. Non-LOS links rely on

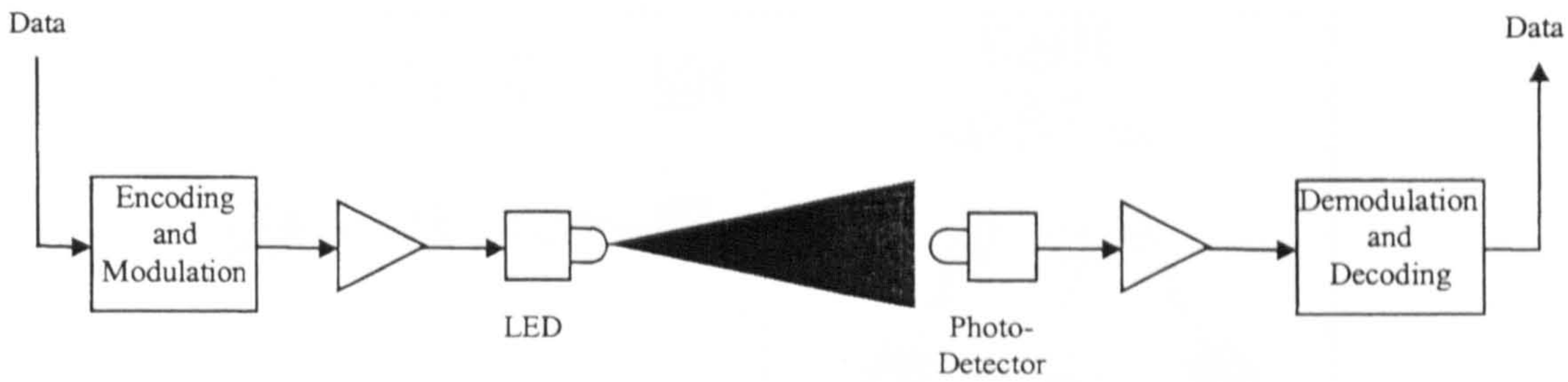

Figure 2.3 Basic line of sight infrared link

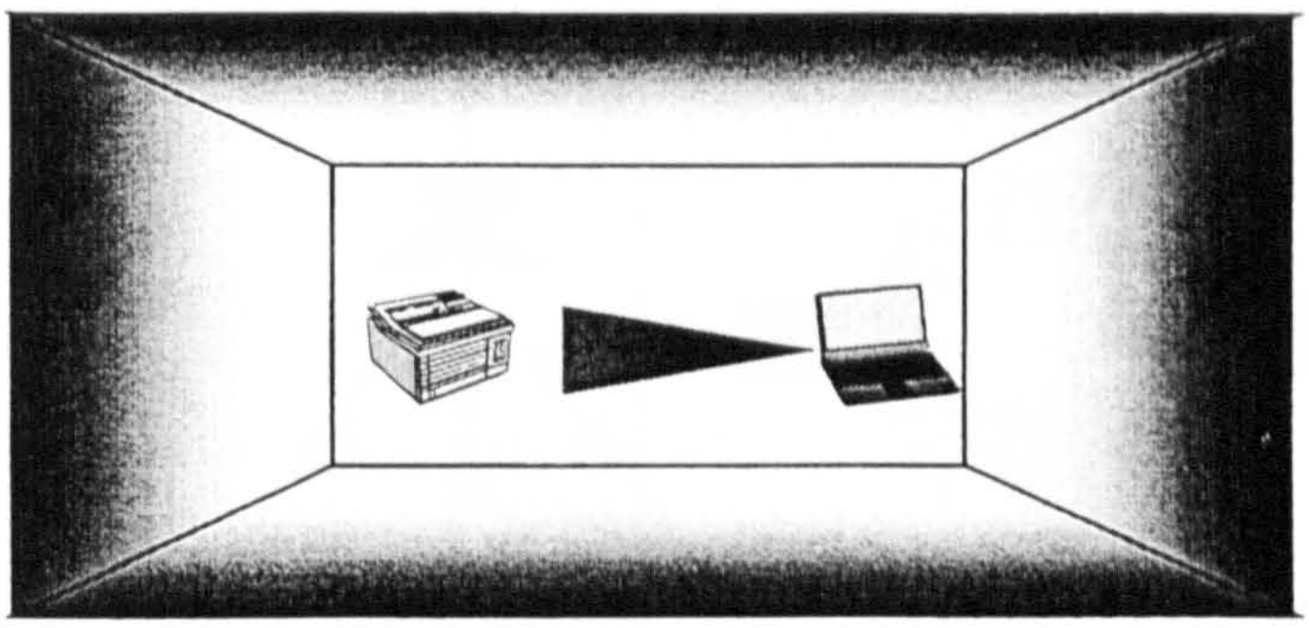

Figure 2.4 Line of sight infrared communication

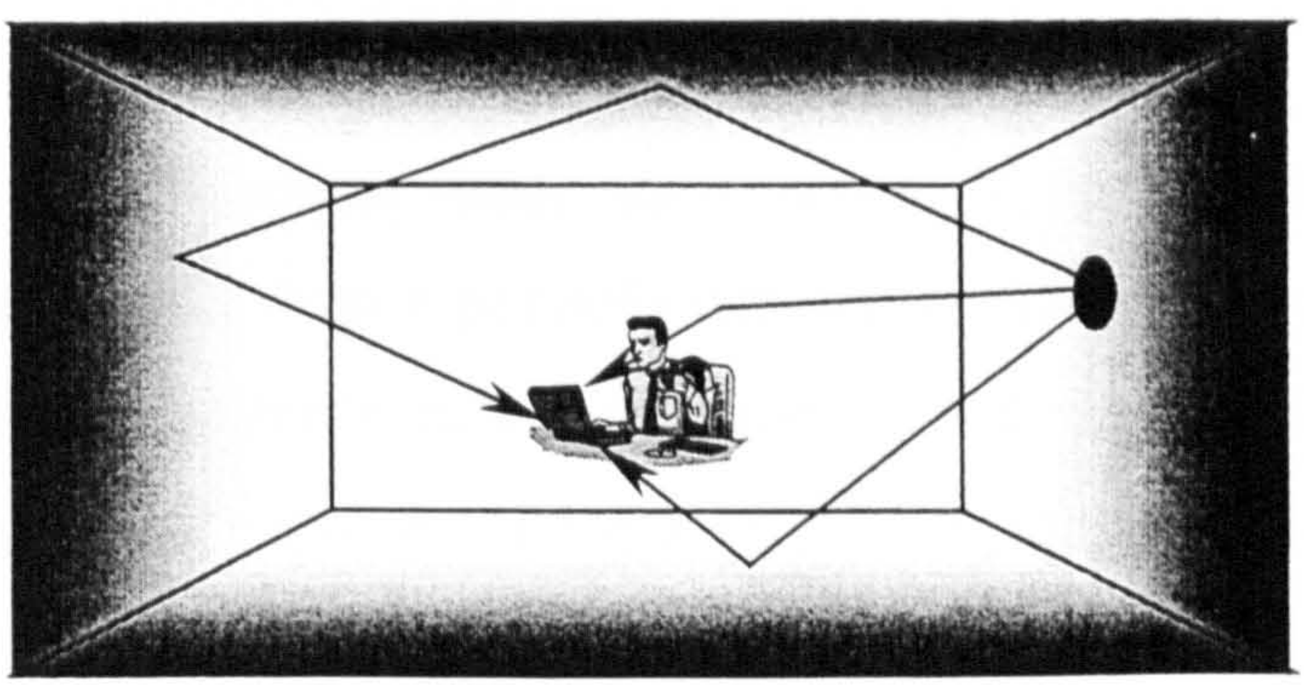

Figure 2.5 Non-line of sight infrared communication

reflections of the infrared radiation from the ceiling or other reflecting surfaces (Fig. 2.5). Non-LOS links are most convenient from the user's perspective, because the user does not have to maintain alignment and a LOS path. As a result, user mobility is increased if a non-LOS link is utilized. LOS links make more efficient use of the optical power and minimize interference because most of the ambient light is rejected by the narrow FOV of the receiver.

The IrDA 1.x standard defines LOS point-to-point infrared links utilizing narrow angle IR ports. The IrDA AIr standard considers LOS and non-LOS multipoint infrared communication employing wide-angle IR ports. Depending on the topology, infrared communications are divided into the following categories:

- **point to point communication** (Fig. 2.6(a)): Two narrow angle infrared devices

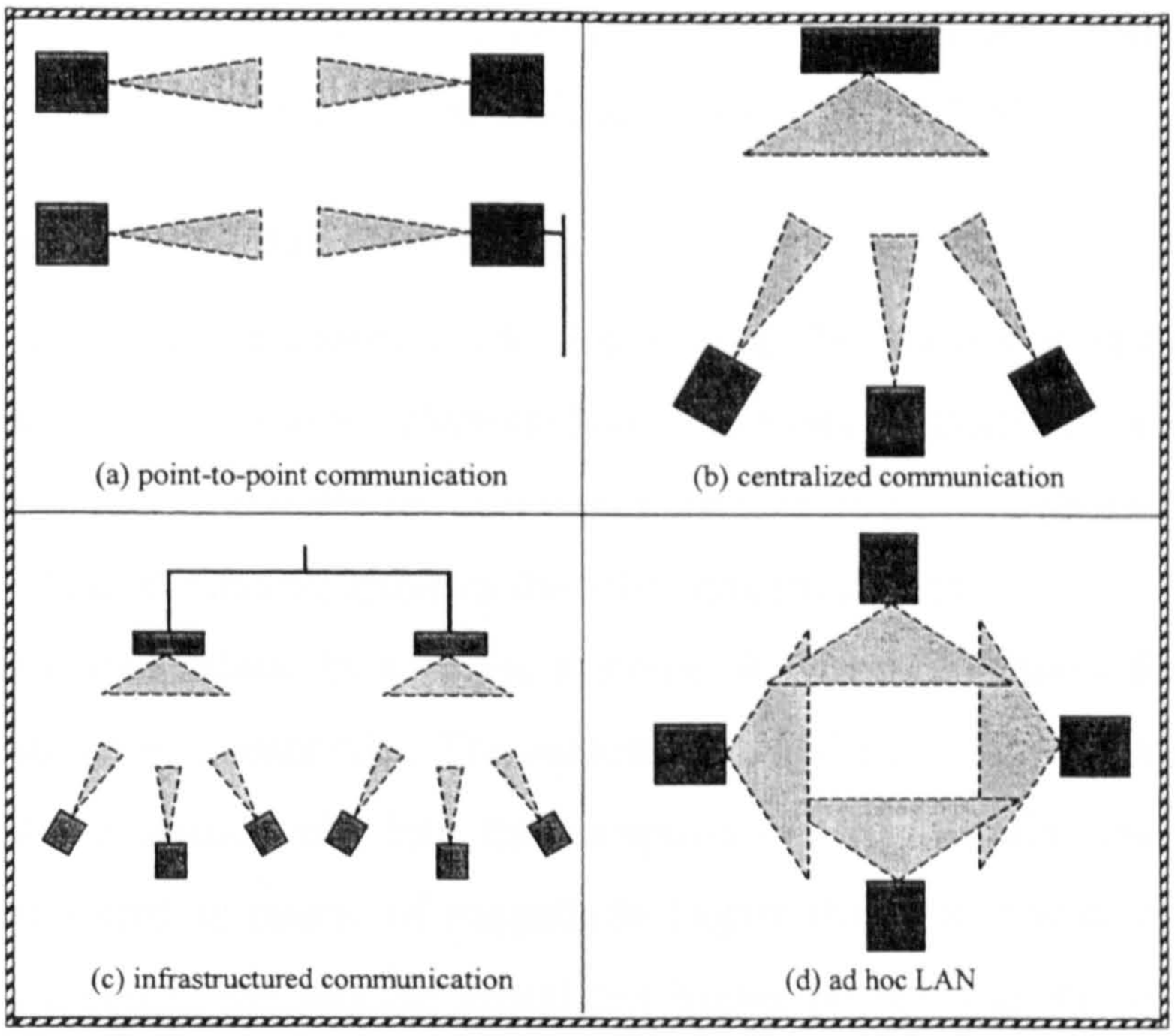

Figure 2.6 Infrared wireless communication systems

exclusively communicate with each other. Typical applications are the information transfer from a portable data-gathering device to a host computer, the printing of pictures from a digital camera and the uploading of music files from a laptop to a portable MP3 player. One of the devices may be fixed and connected to a wired network providing network access to the mobile device.

- **centralised communication** (Fig. 2.6(b)): Multiple narrow angle devices communicate with a wide-angle central node. A laptop computer can be assigned the central node role to form a WPAN. A WLAN is formed if the central node is a hub that echoes the received information to all stations.
- **infrastructured communication** (Fig. 2.6(c)): This is an extension of the centralized communication. In this case, the central hub is connected to a wired backbone providing network access to mobile stations.
- **ad hoc communication** (Fig. 2.6(d)): Multiple wide-angle devices from an ad hoc WLAN. There is no central WLAN coordinator as all stations are allowed to join or leave the network at any time. A typical example is a WLAN formed by laptop computers around a meeting table.

IrDA 1.x connections may be utilized in the first three categories. In the case of centralized and infrastructure IrDA 1.x communications, the central hub must

implement a wide-angle instead of a narrow angle IR port. Infrared devices complying with the AIr protocol standard may be utilized for an ad hoc WLAN.

2.5 Challenges in IR link layer design

Many issues in the protocol stack design must be addressed differently if the infrared medium is utilized at the physical layer. Data rate adaptation to channel quality, medium access and retransmission techniques must consider the characteristics of IR transmissions. The IR medium exhibits the following properties:

a) **half duplex operation.** In wireless systems, it is very difficult for a station to receive data when it transmits. The reason is that when a station transmits, a large fraction of the signal leaks into the reception circuit. Usually, the power of the transmitted signal is orders of magnitude higher than the power of the received signal. As a result, the leakage signal has higher power than the received signal, making remote signal detection impossible while transmitting. Half-duplex operation degrades the performance of infrared wireless links.

b) **collision avoidance.** The inability to detect remote transmissions while transmitting results in another implication if many stations compete for medium access; a station can not determine a collision by monitoring channel activity while transmitting, as in Ethernet type protocols. As a result, all stations competing for medium access must implement another collision detection mechanism and employ collision avoidance techniques to minimize the collision probability.

c) **minimum turn around time.** When a station transmits, the leakage signal blinds its own receiver such that it can not receive remote infrared pulses. After the transmission ends, the receiving circuitry needs a minimum Turn Around Time (TAT) to recover. Thus, a transmitting station is able to receive a TAT time period after its transmission ends. As a result, all participating stations must wait a TAT delay after a transmission finishes before initiating a new frame transmission to ensure that all stations (including the station that transmitted the previous frame) will be able to receive the new frame. The TAT delay is high in infrared ports and should be taken into account in the design of medium access and retransmission protocols.

d) **channel errors.** Transmission errors are more likely in wireless IR transmissions. In wired networks, the probability of errors is very small, a small bit error rate (BER)

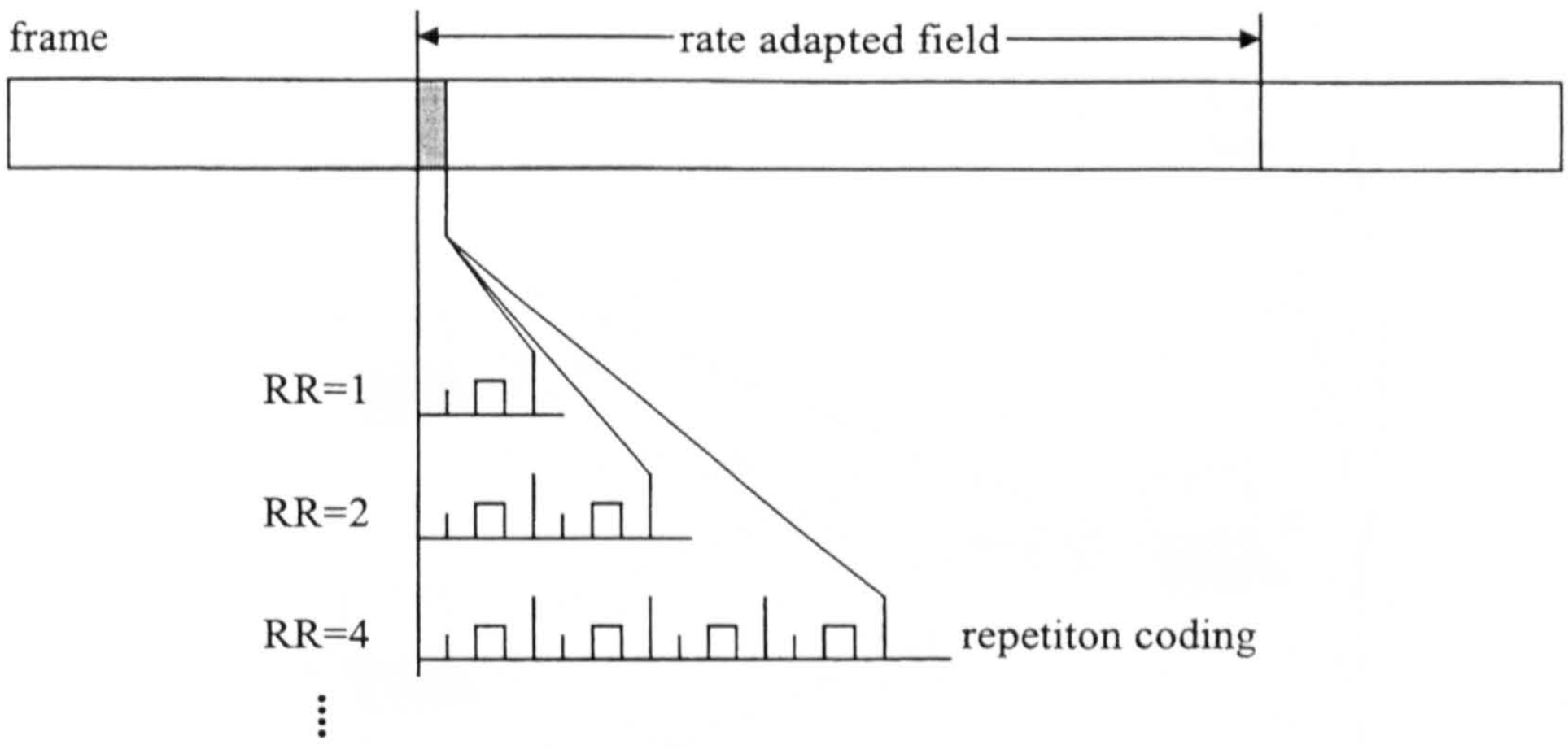

Figure 2.7 RR-coding in 4-PPM transmission

is expected and an immediate frame acknowledgment is meaningless. In contrast, IR wireless channels may have a high BER, resulting in a much higher frame error probability. To cope with frame errors, IR and radio wireless link layer protocols may utilize an immediate acknowledgement (ACK) frame, which follows every data frame transmission. If the ACK frame is not received, the transmitter reschedules the data frame for retransmission. ACK frames may result in significant overhead, especially when followed by considerable TAT delays, as in IR systems.

In order to minimize the ACK frame overhead, infrared wireless link layer protocols may choose to acknowledge a number of data frames using a single ACK frame. They may also employ smaller frame sizes to decrease the frame error probability [31]. Another alternative is the implementation of Forward Error Correcting (FEC) codes or RR coding. Infrared link layer protocols should be efficiently designed to minimize the total delay of data frame retransmissions, ACK frames, frame overheads, TAT delays and FEC or RR coding.

e) **RR-coding.** A power efficient transmission scheme for infrared links is the L-slot Pulse Position Modulation (L-PPM). A transmitted symbol consists of L slots; a pulse is transmitted in one slot and the remaining L-1 slots are empty. To cope with transmission errors in communicating with distant stations with low Signal-to-Noise Ratio (SNR), Repetition Rate (RR) coding may be employed. RR coding advises that every transmitted symbol should be repeated RR times in order to increase the symbol capture probability at the receiver (Fig. 2.7). RR coding utilizes the same symbol rate and virtually improves the SNR by employing redundancy [30]. RR

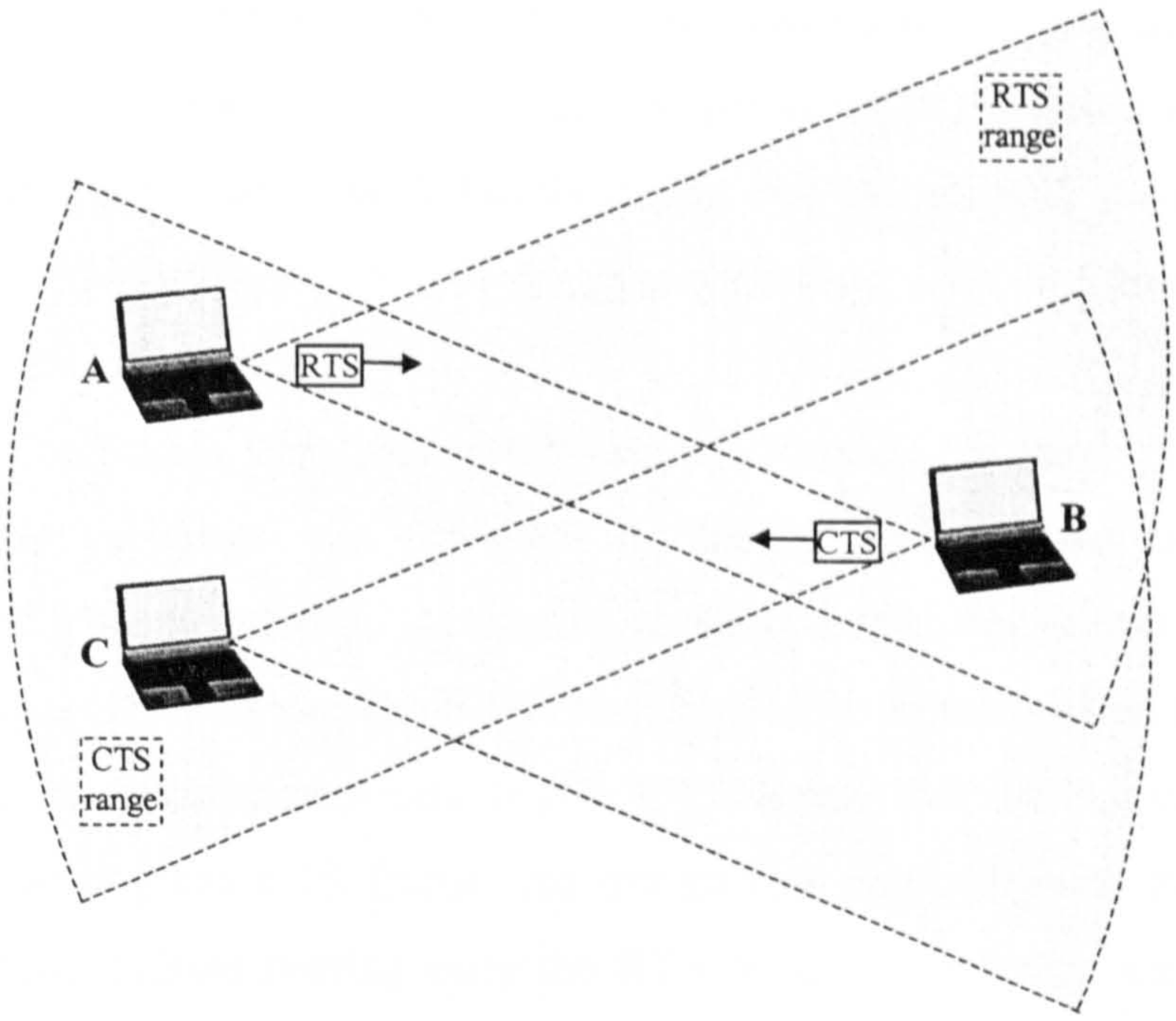

Figure 2.8 The hidden station problem and the RTS/CTS frame exchange

coding results in a better link quality at the expense of a lower link data rate. The receiver may monitor channel quality and advise the transmitter of the suitable RR to be implemented [79][73]. RR coding is a way of adapting the link rate to channel conditions.

RR-coding may be employed on a data frame if the intended receiver has a low SNR. It may also be employed only on the portion of the data frame that contains essential MAC information to ensure that all stations in range will receive this information of the data frame. RR-coding may also be utilized in control frames, such as the RTS and CTS frames. In this way, the reservation information reaches a larger area and the hidden station problem (which is explained next) is minimized.

f) **location dependent carrier sensing (hidden stations).** Infrared signal strength decays with link distance increase. Stations far away from the transmitter may not be able to detect the presence of an infrared transmission. In addition, infrared transmissions are directed; only stations in the reception cone may be able to detect an on-going infrared transmission if adequate reflecting surfaces are not present. The location dependent reception status of an infrared transmission results in the hidden station problem. A hidden station is one that is within the range of the receiver but out of range of the transmitter [34][31][61]. Let's consider the scenario

shown in Fig. 2.8. Station A transmits to station B and station C can not hear the on-going transmission because it is out of the reception range of station A. If station C wishes to transmit to station B, it falsely thinks that the channel is idle, it initiates transmission and interferes with the transmission from A to B. In this case, station C is a hidden station to station A.

To minimize collisions from hidden stations, the Request To Send / Clear To Send (RTS/CTS) frame exchange was proposed in the Multiple Access with Collision Avoidance (MACA) protocol [60]. According to MACA, the transmitter first reserves the medium using an RTS frame. The RTS frame contains the reservation time period in a special field. The receiver responds with a CTS frame that echoes the reservation period. Upon receiving the CTS frame, the transmitter proceeds with the data frame transmission. Thus, stations hearing only the RTS or the CTS frame are aware of the medium busy condition and remain silent for the entire data transmission period even if they are not able to hear the data frame [60]. Using the RTS/CTS frame exchange, hidden stations do not result in data frame collisions; collisions can occur only on the short RTS frames if two (or more) stations try to reserve the medium at the same time.

An extension to MACA, MACAW [11], proposed that the reservation time should be extended to include the link layer ACK frame that copes with transmission errors, as discussed in case (d). IEEE 802.11 protocol utilizes the RTS-CTS-DATA-ACK frame exchange and a Stop-and-Wait ARQ scheme.

AIr protocol addresses the hidden station problem by using variable RR coding and the RTS/CTS control frame exchange. Both RTS and CTS frames are transmitted using the maximum Repetition Rate to increase their transmission range and cope with potential hidden nodes. To minimize the RTS/CTS/TAT overhead, every successful medium reservation may include the transmission of a number of data frames. As the data frames may be transmitted using different RR to match varying channel quality, the reservation time duration is not known when the RTS frame is transmitted. As a result, a reservation is terminated using an End Of Burst / End Of Burst Confirm (EOB/EOBC) control frame exchange. AIr utilizes an RTS-CTS-$DATA_0$-$DATA_1$-...-$DATA_n$-EOB-EOBC frame exchange.

2.6 Modeling of communication systems

Many factors affect the performance of wireless IR links. The significance of

system parameters to link utilization can be evaluated by studying models of the considered IR scenario. Modeling is very useful in communication systems because it:

- provides a detailed understanding of the system performance in specific load conditions without physically implementing and testing a real system
- analyzes protocol operation and leads to protocol design improvements
- evaluates the effectiveness of all parameter values on system performance
- can by employed to derive optimum parameter values
- evaluates the performance increase of implementing optimum parameter values

There are two types of models that can be used to evaluate the performance of communication systems [36]:

a) **Computer simulation modeling.** Computer simulation involves developing models in software that mimic the operation of an information exchange system. The software model is employed to produce performance results when one or more system parameters are varied. The computer program emulates the behavior of every station independently and produces very accurate results because it replicates the behavior of a real system. Simulation models usually involve a few or no assumptions. The main advantage of simulation models is that they can evaluate the performance of very complex communication systems. The main disadvantage of simulation techniques is that, depending on the system complexity, simulation runs may take a considerable amount of computing time.

b) **mathematical modeling.** A mathematical model provides one or more equations that express system performance as a function of protocol parameters, system load and the number of communicating devices. Probability theory, statistical mathematics, queuing theory and stochastic process modeling are often used to develop an analytical model for an information exchange system. The mathematical model is used to produce computer graphs that show how system performance changes when one or more system parameters are varied. These graphs are very useful for protocol designers and are easily produced once the mathematical model is developed. The disadvantage of analytical modeling is that a number of assumptions are usually necessary to develop an analytical model. As simulation modeling accurately predicts system performance; analytical models are usually validated by comparing analytical with simulation results.

2.7 Performance measures

The measures that are helpful to evaluate the performance of an information exchange system depend on the system in question and on the characteristics of the traffic the system is expected to carry. The traffic presented to the system is usually called the offered load. If the offered load contains time sensitive data, such as human speech and video, the communication system must minimize the delay in delivering the time sensitive data to the destination. More important, significant variations of the delay in delivering various frames with time sensitive data are not acceptable. The reason is that the resulting output will be of low quality or not understandable. In this case, the average and the maximum frame delays are of prime importance. If the offered load contains time insensitive data, such as file transfer, e-mail and web browsing, the communication system must maximize the rate at which data can be sent through the system.

There are two fundamental quantitative measures of an information exchange system:

a) Delay. The delay of a system specifies the time needed for information data to travel from the source to the destination station. Users are particularly interested in the delay in which the system delivers their information data to the destination. Delays are more important on time sensitive data. Types of delays in communication systems are [25]:

i) propagation delay arises from the time needed for the signal to travel between two stations. This work considers short-distance indoor links that have very small propagation delays, which are safely neglected.

ii) switching delay arises from electronic devices in a network, such as hubs and bridges. This work does not analyse links that include such electronic devices and does not consider switching delays.

iii) access delay occurs when several devices access the same shared medium and stands for the time needed until the medium is available to a station. IrDA 1.x WPAN implements centralized control and access delays do not affect the considered link scenario. This work analyses the access delay of the collision avoidance procedures of infrared WLANs in chapter 6.

iv) queuing delay occurs in packet switched WANs. When a packet reaches a

packet switching device, it may have to wait on a queue if more packets wait for the intended destination. Queuing delay accounts for the time a packet spends on a queue in a packet switching device. This work does not consider queuing delays.

v) retransmission delay arises when a transmitted frame is not correctly received at the destination due to a transmission error. Transmission errors are more likely when a wireless medium is utilized and may significantly degrade performance. This work considers retransmission delays for point – to-point infrared links in chapters 3 and 4 and for multipoint infrared links in chapter 7.

b) Throughput/utilization

Throughput (D) is the rate at which information data can be sent through the communication system and it is usually specified in bits per second (bit/s). For time insensitive data, network and link designers and implementers aim to increase system throughput in order to achieve a better performance; delays in delivering specific data are of secondary importance. Most technologies deliver the offered load in frames and frame headers do not contribute to throughput. In addition, access and retransmission delays result in throughput degradation.

Throughput usually expresses the performance of a particular information exchange system. Throughput is more useful than the data rate because it specifies the actual performance of the system by evaluating all delays introduced by the communication system. It is usually compared to the link data rate to express the performance degradation introduced by the communication technology, such as frame headers, access delays and transmission errors. This work examines the performance of point-to-point and WLAN communication systems by evaluating the utilization (U) figure, which is defined as

$$U = \frac{D}{C} \tag{2.1}$$

where C is the medium data rate. U expresses the time portion of the total time that the system delivers offered load to destination at the medium data rate. As an example, if U=0.75 for C=4Mbit/s, the system delivers the offered load at 3Mbit/s (D=3Mbit/s) to the destination. It also delivers offered load during the 75% of the time; the remaining

25% is utilized in other communication system tasks, such as medium access delays and transmitting frame headers. Utilization is also referred to as throughput efficiency.

2.8 Research in IR wireless systems

The performance of infrared point-to-point and multipoint connectivity can be measured by the utilization, which can be drawn at the link layer. IrDA 1.x IrLAP is based on the widely used HDLC protocol and utilizes a GBN ARQ scheme. The performance of the GBN ARQ scheme is studied in [9][66]. An analytical model that evaluates HDLC performance using the concept of a frame's virtual transmission time (VTT) is presented in [19][20]. The VTT concept is needed due to the full duplex operation of HDLC. Using the VTT concept, an analytical model for the IrLAP performance is developed in [4][5]. The VTT IrLAP model is employed to study the effect of minimum turn around time as related to link data rate and window size in [6]. An IrLAP simulator using OPNET is developed and used to validate the VTT IrLAP analytical model in [3]. A C++ IrLAP simulator is developed in [84]. This simulator is employed to study the effect of minimum turn around time to link rate increase (up to 4Mbit/s) and to window size increase (up to 7 frames) [84]. The performance improvement of replacing the IrLAP GBN ARQ scheme with a Selective Reject (SREJ) ARQ scheme is presented in [74]. This work concludes that the GBN ARQ scheme is good enough for IrLAP due to the significant turn around delays arising from the IR medium implementation. The effects of extending window size to 127 frames for the 16 Mbit/s data rate is studied in [15] using the VTT IrLAP analytical model. This work questions the effectiveness of increasing window size to 127 frames and advises the implementation of lower or optimum window sizes in high BER links. The derivation of optimum window size values as a function of link BER remained an open challenge. In addition, the VTT model is very complicated and does not give insights (a) for the significance of physical layer parameters to utilization and (b) for the optimum control of the infrared link for maximum utilization. By taking advantage of the IrLAP half-duplex operation, this work develops an analytical model that leads to a simple utilization equation for IrLAP performance. This equation permits a complete analysis to study the significance of the link system parameters on IrLAP utilization performance. By taking the first derivative of the utilization equation, this work derives equations which eventually simplify and allow easy calculation of the optimum values

for the IrLAP window size and frame length parameters. Results indicate that significant utilization increase is observed if the optimum values are implemented at high BER links. The achieved practical utilization increase for optimum parameter implementation by the transmitter is also confirmed by means of simulation.

Design challenges in IR WLANs have also drawn the attention of the research community. The effectiveness of implementing RR on *L*-PPM infrared links is studied in [28][79][83]. Presented results indicate that RR is suitable on *L*-PPM links as it significantly reduces error rate in hostile medium conditions. Infrared WLANs utilize the RTS/CTS frame exchange to address the hidden station problem. To ensure that the RTS/CTS scheme operates efficiently, it is essential to maintain reciprocity, which means that the SNR should be symmetric in every pair of stations. The effect of non-reciprocity on various station configurations when the Stop-and-Wait ARQ scheme is implemented at the MAC layer is presented in [23][24] using AIr PHY and AIr MAC simulators. Results indicate that non-reciprocity depends on physical location and on ambient light level and may result in significant performance degradation. When hidden stations are present in WLANs, some stations may not get an equal chance to access the infrared medium. This fairness problem for AIr LANs and the suitable improvements for the AIr medium access scheme are presented in [75][78]. The effectiveness of implementing the Stop-and-Wait (SW) ARQ scheme at the AIr MAC layer when two stations are communicating in an AIr LAN is presented in [77][89][90]. These results are not complete, as they consider only two ARQ schemes, and incorporate the fixed and significant collision avoidance delays arising when only one station competes for medium access. AIr MAC and LC performance for LANs with many simultaneously transmitting stations has not been studied yet. In addition, the performance of the AIr MAC collision avoidance procedures and of the AIr MAC Go-Back-N ARQ scheme has not been studied in the literature. This is addressed by research presented in this thesis. This work develops mathematical models that evaluate (a) the collision avoidance delay as a function of the number of stations and (b) the performance of all AIr LC ARQ schemes, assuming LANs that maintain reciprocity, that consist of a fixed number of stations and that have no hidden stations. We also propose protocol modifications that improve AIr performance for the considered scenarios.

CHAPTER 3

Performance of Infrared Data Link Layer

The performance of indoor infrared point-to-point links is affected by the half-duplex operation, by the time required to reverse link direction and by transmission errors introduced by the wireless medium. Infrared noise at the receiver arising from the sun and artificial lighting may degrade link quality. The required alignment and link distance can not be always met. In addition, the obstruction of the line of sight path between the transmitter and the receiver reduces the performance of the infrared link.

IrLAP, which drives the infrared hardware, implements a Go-Back-N retransmission scheme to cope with transmission errors. To reduce delays arising from frame overheads, IrLAP may implement large frame sizes. The transmitter may also transmit a window of frames before reversing link direction and soliciting an acknowledgment form the receiver in order to reduce delays arising from frequent link turn around. This chapter considers design issues for efficient operation of the IrLAP layer. It develops a mathematical model that reaches a simple closed form equation for the IrLAP utilization. This formula allows easy calculation of IrLAP utilization and allows a better intuitive understanding of IrLAP performance.

The outline of this chapter is as follows. Section 3.1 presents the IrDA 1.x protocol stack and section 3.2 describes the IrLAP layer, the parameters it negotiates for efficient link operation and the IrLAP frame structure. Section 3.3 presents the considered information exchange model. A mathematical model that evaluates IrLAP utilization by calculating the average window transmission time is developed in section 3.4 and section 3.5 validates the proposed model. Section 3.6 presents an IrLAP performance evaluation focusing on the proposed 16 Mbit/s data rate. Finally, section 3.7 discusses physical and link layer parameter selection for the predicted future increases in IrDA 1.x data rates.

3.1 IrDA 1.x protocol stack

The IrDA architecture is presented in Fig. 3.1. IrPHY ver. 1.0 Serial Infrared (SIR) [50] defines hardware specifications for 2.4 Kbit/s to 115.2 Kbit/s data rates using conventional serial UART chips. It employs RZI modulation scheme and a '0' is

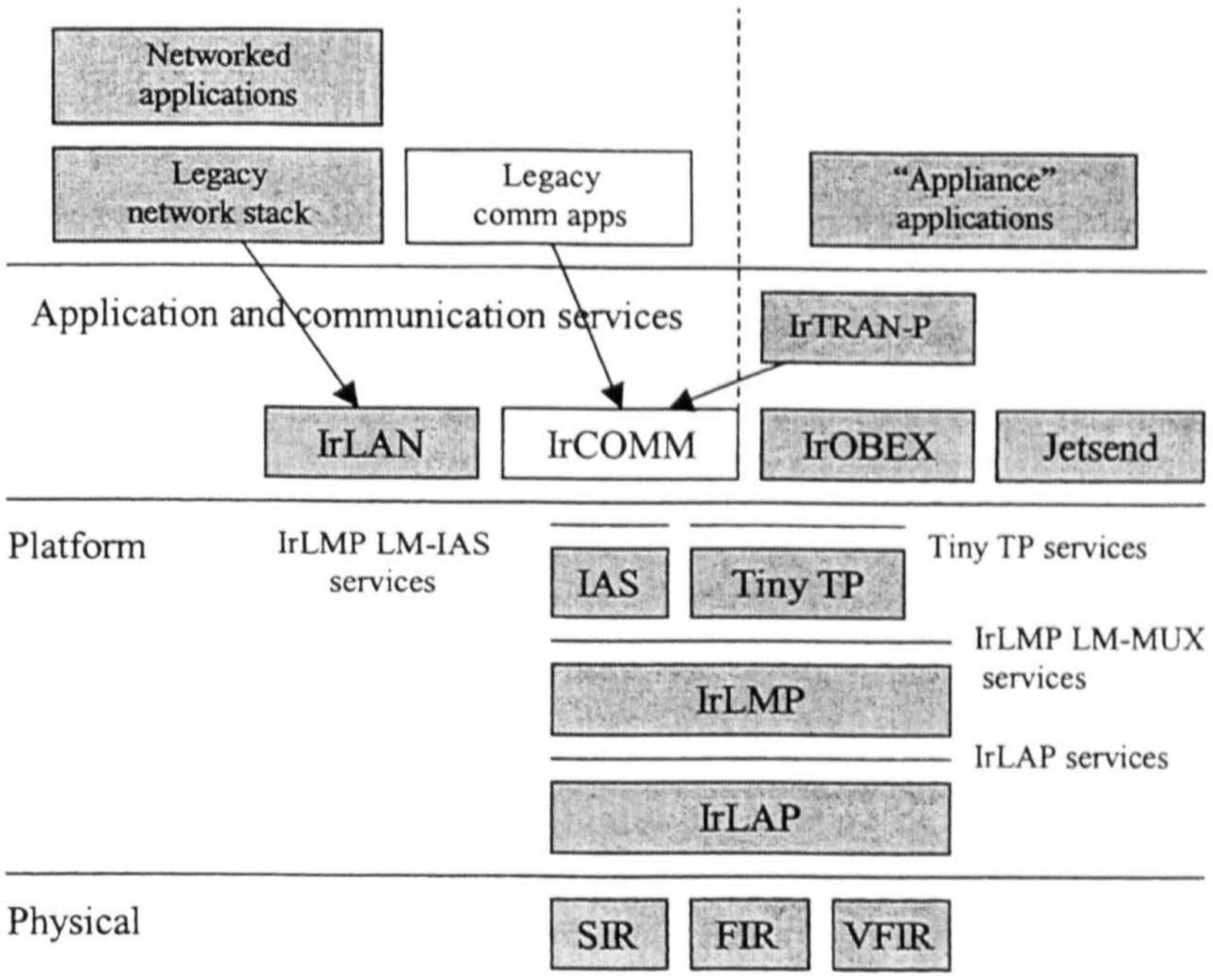

Figure 3.1 The IrDA protocol architecture

represented by a light pulse. The optical pulse duration is nominally 3/16 of a bit duration and the maximum receiver latency allowance is 10ms. The bit error rate (BER) must be less than 10^{-9}. IrPHY ver. 1.1 Fast Infrared (FIR) [51] introduced the 0.576 Mbit/s and 1.152 Mbit/s data rates employing RZI modulation and the 4Mbit/s data rate employing 4PPM modulation scheme. It also allowed higher link error rates by specifying that the link BER should be less than 10^{-8}. Very fast Infrared (VFIR) specification [53] added the 16Mbit/s data rate by using a newly developed HHH(1,13) code [37] and reduced the allowable receiver latency to 0.1ms. IrPHY specifies a link distance of at least 1m and an off axis angle of ±15 to ±30 degrees [67][52]. The IrDA Link Access Protocol (IrLAP) is the data link layer of the IrDA protocol stack [49]. It provides a fixed rate (9,600 bit/s) slotted contention mode for device discovery and parameter negotiation. After initial contact, it defines contention-free access to the IR medium by using master station control. The Link Management Protocol consists of the Link Management Multiplexer (LM-MUX) and the Link Management Information Access Service (LM-IAS) [48]. LM-MUX is a connection oriented multiplexer that allows multiple applications in an IrDA device to communicate over a single IrLAP connection and LM-IAS facilitates discovery of services available by the communicating device. An IrDA service claims an LM-MUX port and advertises itself to the communicating device by placing its service information and necessary

parameters in a lookup table. Implementation of IrPHY, IrLAP and IrLMP is required from all IrDA-compliant devices. TinyTP is a useful light-weight transport protocol for segmentation and reassembly operations and for application level flow control. IrCOMM is the cable replacement of the IrDA stack. IrCOMM is a serial and parallel port emulation protocol, enabling all applications designed to operate over serial or parallel ports to operate unchanged over the infrared medium. IrCOMM allows both DTE-DTE (null modem) and DTE-DCE connections. IrLAN allows station LAN access over an IrDA link and IrOBEX is the IrDA HTTP protocol, facilitating simple data object (business card, phone list) exchange. IrTRAN-P allows the exchange of images between digital cameras, photo printers and PCs while IrJetSend allows IrDA binding to Hewlett-Packard Jetsend protocol [5][67][101].

3.2 IrLAP layer

IrLAP design is based on the pre-existing HDLC and SDLC protocols [101]. The functions of IrLAP include device discovery, link establishment, data exchange and error recovery [49]. IrLAP stations operate in two modes; in the Normal Disconnect Mode (NDM) during the contention period and in the Normal Response Mode (NRM) during the connection period. During the contention period, a station advertises its existence to all stations within its transmission range along with the physical and link layer parameters it supports and wishes to use during the information exchange procedure. IrLAP assigns primary and secondary roles in NDM; one of the participating stations is assigned the primary role and all remaining stations are assigned the secondary role. Any station may claim to become the primary station but only one wins the contention. In NRM mode (connection period), only transmissions to or from the primary station are permitted. If a secondary station wishes to communicate with another secondary station, it does so through the primary station. In NDM mode, communicating stations also determine the best connection capability that can be supported by both stations; they negotiate and agree on the following parameters to be used in NRM mode (connection period):

a) *Data rate (C)*. This parameter specifies the station's transmission rate.

b) *Maximum turn around time (T_{max})*. This parameter specifies the maximum time period a station can hold transmission control. IrLAP specifies that T_{max}=500ms for data rates less than 115.2 Kbit/s but smaller values may be agreed for the 115.2

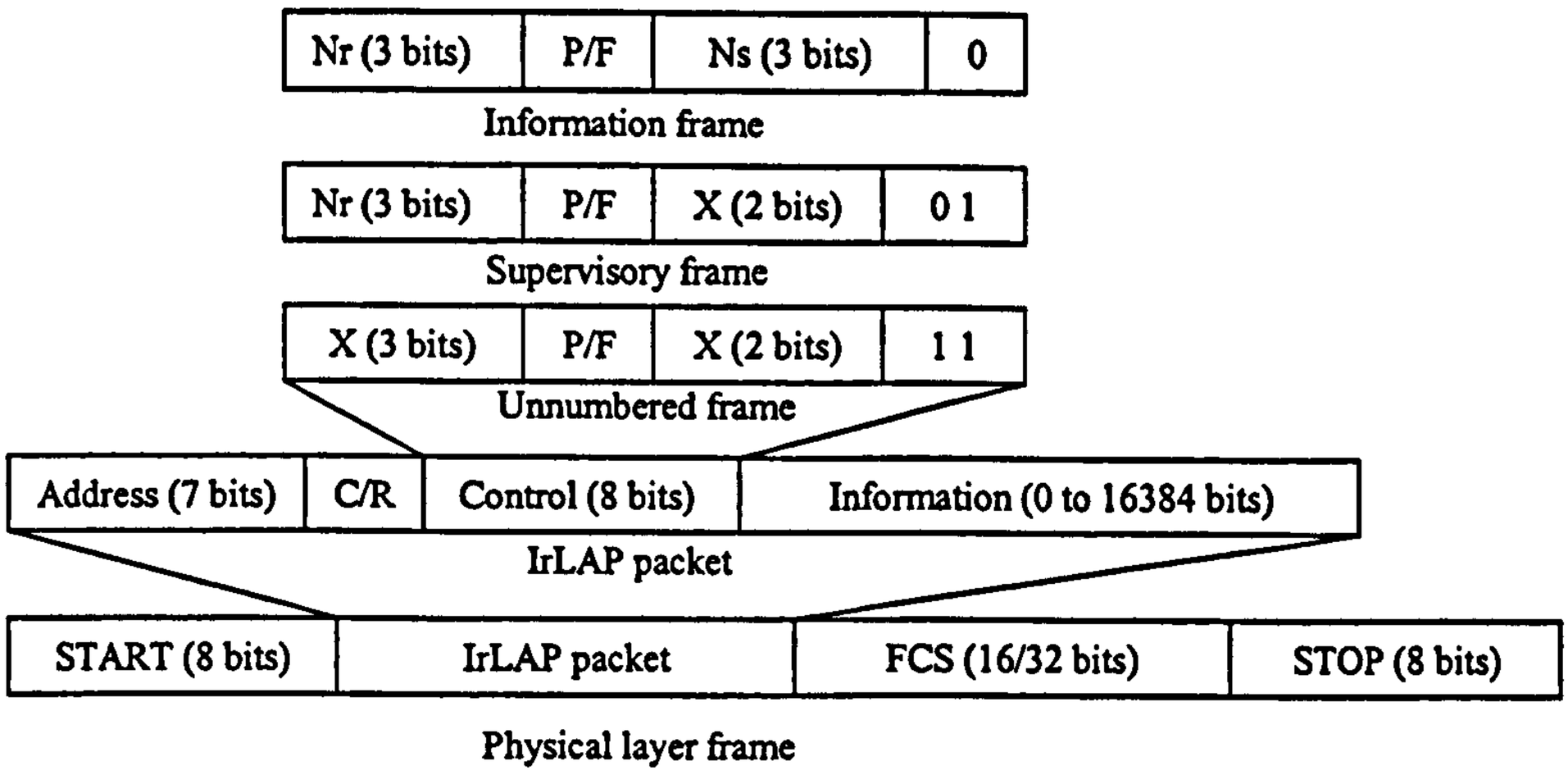

Figure 3.2 IrDA SIR and FIR frame structure

Kbit/s or higher data rates.

c) *Data size (l)*. This parameter specifies the maximum size of the data field of any received Information frame (I-frame). IrLAP supports a maximum data size value of 2,048 bytes (16Kbits).

d) *Window size (W_{max})*. This is the maximum number of unacknowledged I-frames a station can receive before it has to transmit an acknowledgement. The transmitting station may request an acknowledgement before the window size is reached. IrLAP specifies that W_{max} has an upper limit of 7 for data rates up to 4Mbit/s and 127 for the 4Mbit/s and 16Mbit/s data rates [49][53].

e) *Minimum turn around time (t_{ta})*. This is the time period needed by the receive circuit to recover after the end of a transmission originated from the same station, as explained in section 2.5(c). This is the time required to reverse link direction.

Parameters (b), (c), (d) and (e) are negotiated and agreed independently for each station. However, both stations must agree and use the same data rate (parameter (a)).

Fig. 3.2 presents the IrDA 1.x frame structure. A frame consists of the START flag, the IrLAP packet, the frame check sequence (FCS) field and the STOP flag. The FCS field contains a 16-bit CRC for data rates lower than 4Mbit/s and a 32-bit CRC for the 4Mbit/s and higher data rates.

IrLAP specification defines the following frame types (Fig. 3.2):

a) Unnumbered frames (U-frames): U-frames are employed for link management. They are used to exchange connection data, to discover and initialize secondary

stations and to report procedural errors that can not be recovered by retransmissions.

b) Supervisory frames (S-frames): S-frames contribute in the information exchange procedure although they never carry information data themselves. S-frames are used to report frame sequencing errors, to acknowledge correctly received frames and to request an acknowledgement from the remote station.

c) Information frames (I-frames): I-frames carry information data to the remote station during the connection period. I-frames are sequenced to ensure that they are received in the correct order by the receiver.

Every frame has a control field. The control field always contains a frame identifier, which determines the frame type and the P/F bit, which is used to pass transmission control. The control field of I-frames (Fig. 3.2) contains a send sequence number, N_s, used to number the transmitted I-frames. I-frame and S-frame control field contains a receive sequence number, N_r, which is used to indicate the expected sequence number of the next I-frame. S-frame and U-frame control field contains the command/response code, X, of the frame. SIR and FIR specifications define an 8-bit control field (Fig. 3.2). N_s and N_r occupy 3 bits each, N_s and N_r cycle through values from 0 to 7 and maximum window size is 7. VFIR specification extended the length of the control field to 16 bits for the 4 Mbit/s and 16 Mbit/s data rates. In 16-bit control fields, N_s and N_r are 7 bits each, they cycle through values 0 to 127 and a maximum window size of 127 is supported.

The control field always contains the P/F bit, which implements token passing between the communicating stations. When it is set by the primary station, it is the poll (P) bit. When it is set by the secondary, it is the final (F) bit. When the P/F bit is set, the link direction is reversed. Primary sets the P-bit to solicit a response or sequence of responses from the secondary. When the secondary receives a frame with the P-bit set, it responds by transmitting one or more frames. The secondary also sets the F-bit of the last frame it transmits to reverse link direction and return transmission control to the primary station. Thus, the secondary stations have transmission control only when they are transmitting frames to the primary [49].

IrLAP stations also employ the P-timer. The P-timer is assigned with the maximum turn around time (T_{max}) agreed between the two stations during the contention period

(NDM mode). As T_{max} stands for the maximum time the station can hold transmission control, the station starts the P-timer when it receives a frame with the P/F bit set and stops the P-timer when it transmits a frame with the P/F bit set. If P-timer expires, meaning that the station has already held transmission control long enough, it immediately transmits a Receive Ready (RR) S-frame with the P/F bit set to pass transmission control.

The primary station also employs an F-timer to limit the time a secondary station can hold transmission control. The primary starts the F-timer upon transmission of a frame with the P-bit set and stops the F-timer upon reception of a frame with the F-bit set. F-timer expiration means that the secondary failed to return transmission control within the agreed time period. Since the secondary's P-timer operation guarantees that this never happens, F-timer expiration can only be explained by the loss of either the frame that contained the P-bit or the frame that contained the F-bit. The primary resolves this situation by transmitting a RR frame with the P-bit set when the F-timer expires.

3.3 Functional model description

This work considers the transmission of a large amount of information data between two stations because IrDA links are usually employed for information transfer from one device to another. The saturation case is studied, in which the transmitter always has information data ready for transmission. Typical practical examples of the considered scenario are (a) the picture downloading form a digital photo camera to a laptop computer for processing, (b) the downloading of data from a portable information gathering appliance to a host computer, (c) the transferring of a phone list from a mobile phone to a computer or to another mobile phone and (d) the printing from a laptop to a (usually inkjet) printer.

In the considered scenario, only two stations form the infrared WPAN, the primary station and only one secondary station. It is assumed that the transmitting station claimed and was finally granted the primary role during the contention period. It is also assumed that transmission errors follow a random distribution.

The parameters used in the current model are shown in Table 3.1. In the contention period (negotiation stage), the primary station determines the window size N it will employ. N represents the maximum number of I-frames the primary can transmit before

Parameter	Description	Unit
C	Link data bit rate	bits /sec
p_b	Link bit error rate	-
p	Frame error probability	-
l	I-frame message data length	bits
l'	S-frame length / I-frame overhead	bits
t_I	Transmission time of an I-frame	sec
t_{Imax}	Transmission time of an I-frame with l=16Kbits	sec
t_S	Transmission time of an S-frame	sec
t_{ta}	Minimum turn-around time	sec
t_{ack}	Acknowledgement time	sec
T_{max}	Maximum turn-around time	sec
t_{Fout}	F-timer time-out period	sec
W_{max}	Maximum window size	frames
N	Window size	frames
D_f	Frame throughput	frames/sec
U	Utilization	-

Table 3.1: Parameters used in modeling IrLAP utilization

soliciting an acknowledgement. Maximum window size parameter W_{max} is negotiated and agreed between the two stations in the contention period. However, the maximum time a station can hold transmission control, T_{max}, must always be obeyed and, according to IrLAP specification [49], T_{max} has a higher priority than W_{max}. T_{max} combined with the implemented frame size and link data rate may limit the window size applied. In other words, if the time needed for transmitting W_{max} frames carrying 'frame size' information bytes at the link data rate exceeds T_{max}, then a smaller window size must be implemented. Thus, N is given by

$$N = min\left\{W_{\max}, floor\left(\frac{T_{max}}{t_I}\right)\right\} \tag{3.1}$$

where *min* is 'the lesser of' and *floor* is 'the largest integer not exceeding'. In this work, T_{max} is always fixed at 500 ms.

IrLAP utilizes a Go-Back-N retransmission scheme and retransmits the correctly received frames that follow an error frame in a window transmission. The information transfer procedure used in the current model is presented in Fig. 3.3. Each node holds three variables, V_s for counting the transmitted frames, V_r for counting the received frames and w indicating the number of the remaining I-frames the station can transmit before reversing link direction [91]. The primary also employs an F-timer that limits the secondary's transmission period.

The primary station acts as follows. When it prepares an I-frame, the N_s sub-field of the frame's control field is assigned the current V_s value and V_s is increased by 1

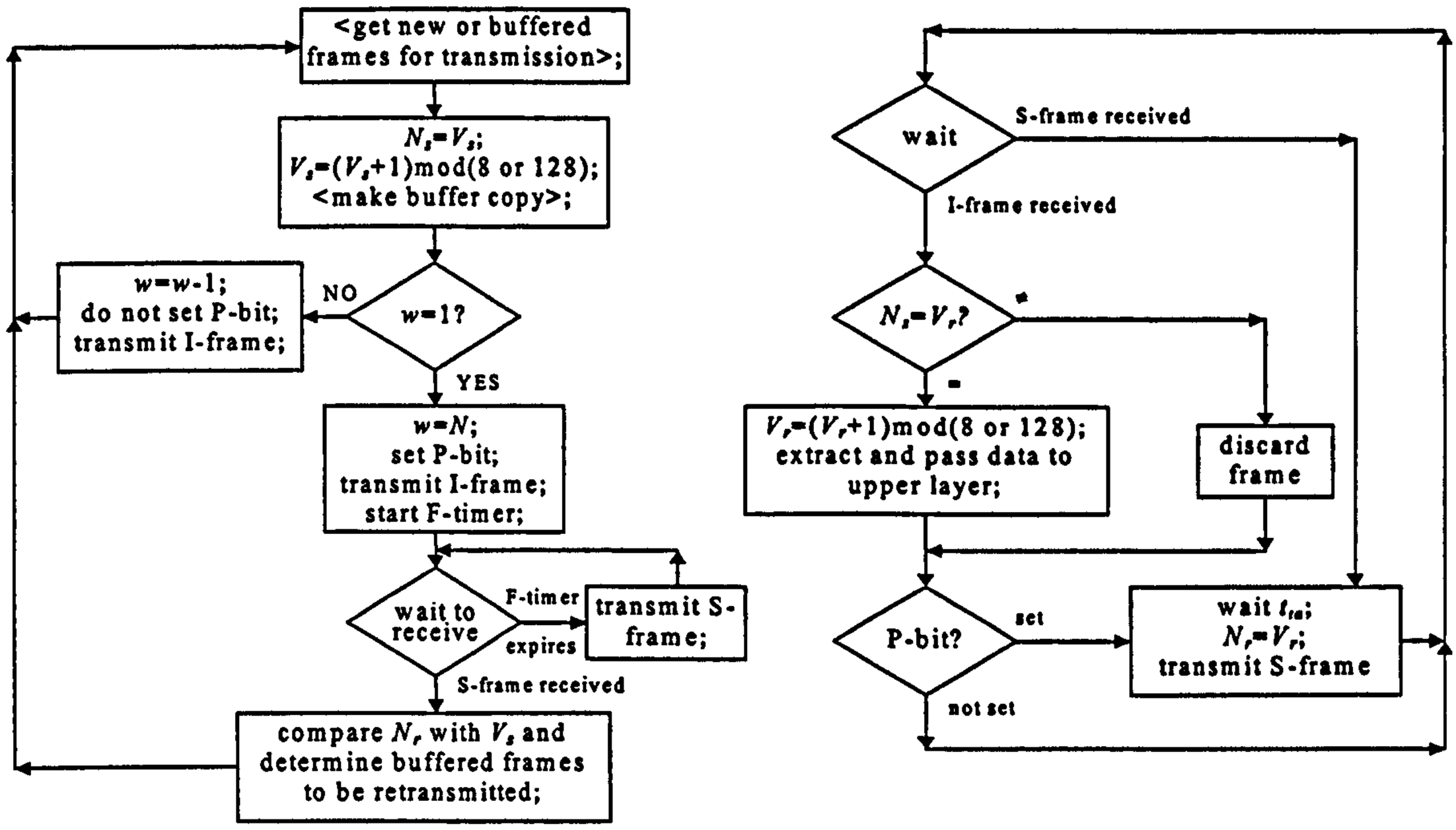

Figure 3.3 Information transfer procedure

(modulo 8 or 128 depending on control field size employed). The primary also makes a buffer copy of the frame for possible retransmissions. Since the primary always has I-frames ready for transmission, it immediately checks the w value. If w is not equal to 1, primary reduces w by 1, transmits the I-frame with the P-bit not set and repeats the actions previously described. When w reaches 1, indicating that the next I-frame should be the last frame in the window transmission, the primary sets the P-bit to poll the secondary and transmits the I-frame. The primary also assigns N to w for the next N window frame transmission and starts the F-timer.

The secondary node acts as follows. When it receives an I-frame, it compares the received frame sequence N_s value with station's expected V_r value. If N_s equals V_r (the received frame is in sequence), V_r is increased by 1 (modulo 8 or 128) and information data is extracted and passed to the upper layer. If the received frame is not in sequence (one of the previous I-frames in current window transmission was lost due to a CRC detected error), the frame is discarded and V_r remains unchanged. The secondary also checks the P-bit. If the P-bit is set and as the current model assumes that the secondary station never has information data for transmission, it awaits a *minimum turn around time* t_{ta} to allow for the primary's hardware recovery latency and transmits an S-frame with the F-bit set. The S-frame's N_r field is assigned the V_r value informing the primary

of the number of I-frames received correctly and in sequence in the previous window transmission. When the primary receives the S-frame, it resumes I-frame transmission as transmission control was returned to the primary by means of the F-bit. The primary first compares the received S-frame's N_r with current V_s value. If N_r equals to V_s (all I-frames in the previous window transmission were received correctly by the secondary), the primary transmits I-frames containing new information data to the secondary. If N_r is not equal to V_s, one or more I-frames in the previous window transmission are lost. The primary retransmits buffered I-frames starting from the indicated N_r position before transmitting new I-frames.

If the last I-frame that contains the P-bit is lost, the secondary station fails to respond, as it does not realize that it has transmission control. The situation is resolved by primary's F-timer expiration. The primary realizes that the secondary failed to respond during the agreed time period and transmits an S-frame forcing the secondary to respond. In the current model, S-frames are considered small enough to be always received error free.

The saturation model considered in this work can be summarized as follows. The transmitting station always has information ready for transmission. As a result, it transmits a window of N consecutive I-frames and reverses the link direction by setting the P-bit in the last I-frame. The receiver awaits a minimum turn around time (t_{ta}) and responds with a Receive Ready (RR) S-frame indicating the next frame expected. The RR frame always has the F-bit set. The transmitter determines the number of frames correctly received before any error(s) occurred and repeats the erred frame and the frames following it, in the next window, followed by new frames to form a complete N frame transmission. If the last frame in a window transmission is lost, the receiver fails to respond as the P-bit is lost. When the F-timer expires, the primary station sends a RR S-frame with the P-bit set forcing the secondary station to acknowledge correctly received frames [92].

3.4 IrLAP mathematical model

The values for t_S, t_I, t_{ack}, p and U are given by (Fig. 3.4):

$$t_S = \frac{l'}{C} \tag{3.2}$$

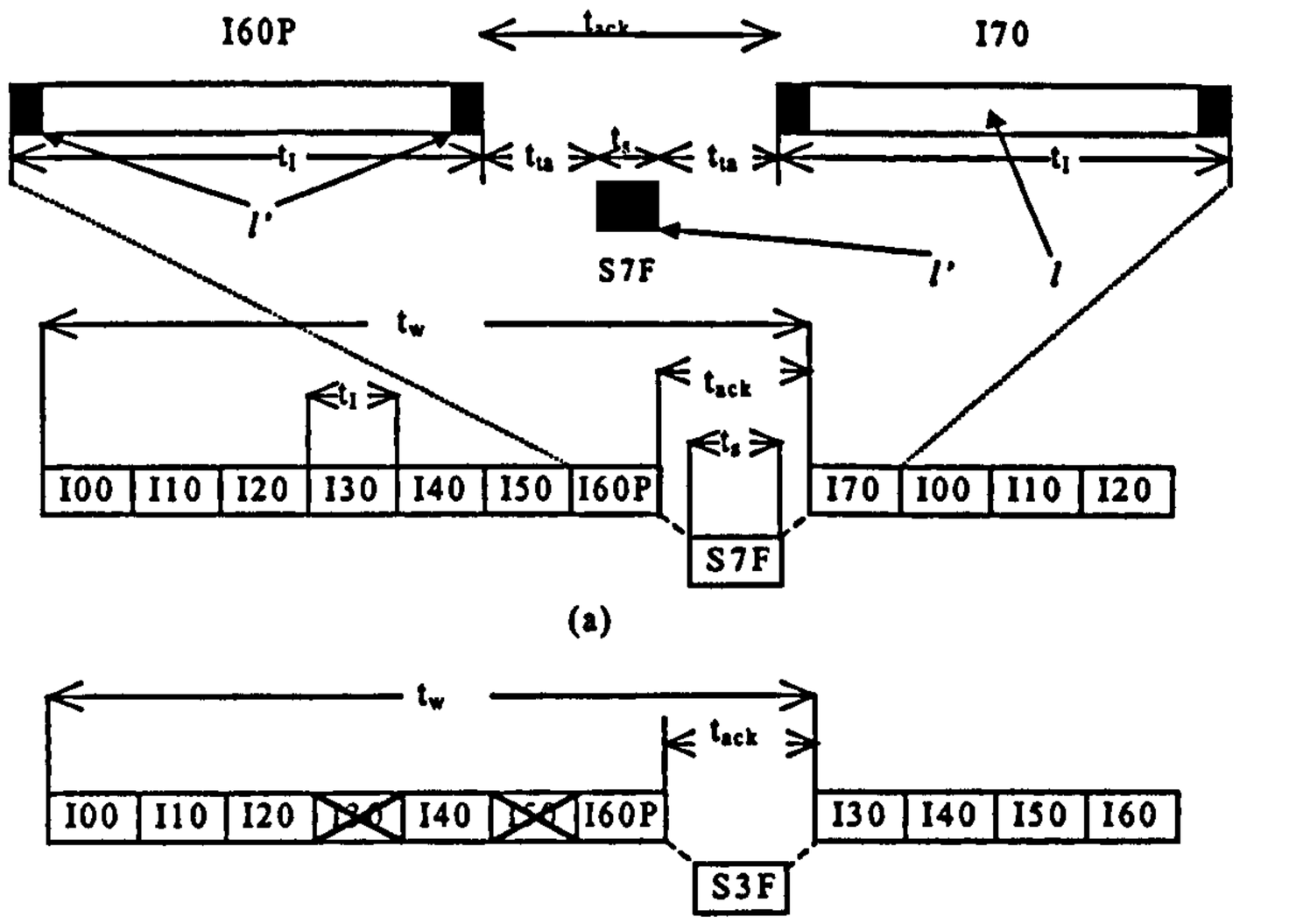

Ixy : *I-frame with N_s=x and N_r=y*
IxyP : *I-frame with N_s =x, N_r =y and P-bit set*
SxP : *S-frame with N_r =x and P-bit set*
SxF : *S-frame with N_r =x and F-bit set*
(a) Window error free transmission
(b) Retransmitted frames due to error frame with N_s =3 and N_s =5
(c) Retransmitted frames and F-timer delay due frame error at N_s =3 and N_s =6

Figure 3.4 Determination of window transmission time t_w

$$t_I = \frac{l + l'}{C} \tag{3.3}$$

$$t_{ack} = 2t_{ta} + t_s \tag{3.4}$$

$$p = 1 - (1 - p_b)^{l+l'} \tag{3.5}$$

$$U = \frac{l}{C} D_f \tag{3.6}$$

This model uses the term "window transmission time" (WTT) to denote the average time needed for a complete window frame transmission and for the acknowledgments and delays concerning this transmission. WTT accounts for the time taken from the start of the first frame in a window transmission to the start of the first frame in the next window transmission. WTT incorporates time utilized in I-frame transmissions, in acknowledgments, in reversing link direction and in possible timer time out delays.

As shown in Fig. 3.4, the key issue that determines WTT is the reception status of the last I-frame in the window, the frame that contains the P-bit. If this frame is correctly received and regardless of the existence of previous errors, (Fig. 3.4(a)&(b)), WTT t_w is given by

$$t_w = Nt_I + t_{ack} \tag{3.7}$$

If the last I-frame that contains the P-bit is lost, an additional delay for the F-timer expiration and S-frame transmission t_s is introduced and WTT is independent of possible additional I-frame errors. This situation is shown in Fig. 3.4(c) and WTT is given by

$$t_w = Nt_I + t_{Fout} + t_s + t_{ack} \tag{3.8}$$

As an I-frame is incorrectly received with probability p, the average WTT is given by

$$t_w = Nt_I + p\left(t_{Fout} + t_s\right) + t_{ack} \tag{3.9}$$

Considering that all I-frames, that follow an I-frame incorrectly received in an N window frame transmission, are considered as out of sequence and are discarded by the receiver, the probability $p_c(w)$ that exactly w frames at the beginning of a window transmission are correctly in sequence received and are followed by an error frame in position (w+1) is

$$p_c(w) = (1-p)^w p\,,\ w=0,1,2,\ldots,N\text{-}1 \tag{3.10}$$

The probability that all I-frames in a window transmission are correctly received is

$$p_c(N) = (1-p)^N \tag{3.11}$$

The expected number of correctly received frames, p_{all}, at the beginning of an N I-frame window transmission is

$$p_{all} = \sum_{w=0}^{N} w p_c(w) \tag{3.12}$$

Frame throughput D_f can now be found by dividing the expected number of frames correctly received in a window transmission, p_{all}, by the average WTT required for the window transmission

$$D_f = \frac{\sum_{w=0}^{N} w p_c(w)}{Nt_I + p\left(t_{Fout} + t_s\right) + t_{ack}} \tag{3.13}$$

After some algebra, (3.13) reduces to

$$D_f = \frac{1-p}{p} \cdot \frac{1-(1-p)^N}{Nt_I + p(t_{Fout} + t_s) + t_{ack}} \tag{3.14}$$

and by combining (3.6) with (3.14), link utilization is given by

$$\boxed{U = \frac{l}{C} \cdot \frac{(1-p)}{p} \cdot \frac{1-(1-p)^N}{Nt_I + p(t_{Fout} + t_s) + t_{ack}}} \tag{3.15}$$

An intuitive explanation of (3.14) is as follows. Term $(1-p)/p$ represents the expected number of frames correctly received before a frame error occurs. It counts for the frames from the first frame in a window transmission that follows a window containing an error to the next frame in error. Term $\left(1-(1-p)^N\right)$ is the probability that there is at least an error in a window transmission and term $Nt_I+p(t_{Fout}+t_s)+t_{ack}$ stands for the average WTT.

This analysis allows the evaluation of all component tasks affecting the IrLAP utilization. Such an evaluation reveals the main factors resulting in utilization degradation when IrLAP operates over high BER infrared links. Equation (3.15) can be rewritten as

$$U = \frac{l}{C} \cdot \frac{(1-p)}{p} \cdot \frac{1-(1-p)^N}{N\frac{l+l'}{C} + p(t_{Fout} + t_s) + t_{ack}} \tag{3.16}$$

Time portion attributed to acknowledgments T_{tack} is given by

$$T_{tack} = \frac{t_{ack}}{N\frac{l+l'}{C} + p(t_{Fout} + t_s) + t_{ack}} \tag{3.17}$$

Time portion used on P-bit loss and F-timer expiration T_{Fout} is given by

$$T_{Fout} = \frac{p(t_{Fout} + t_s)}{N\frac{l+l'}{C} + p(t_{Fout} + t_s) + t_{ack}} \tag{3.18}$$

Time portion taken on transmitting frame overheads l' is given by

$$T_{l'} = \frac{\frac{Nl'}{C}}{N\frac{l+l'}{C} + p(t_{Fout} + t_s) + t_{ack}} \tag{3.19}$$

As the expected number of error frames in a window transmission is pN, time portion spent on retransmission of error frames T_{error} is

$$T_{error} = \frac{\frac{pNl}{C}}{N\frac{l+l'}{C} + p(t_{Fout} + t_s) + t_{ack}} \tag{3.20}$$

The expected number of correctly transmitted frames following an error frame in a window transmission can be found if from the total number of frames in a window N, we subtract the error frames pN and the correct in sequence frames $\frac{(1-p)}{p}\left(1-(1-p)^N\right)$.

Thus the time portion spent on retransmitting correctly received out of sequence frames is given by

$$T_{corr} = \frac{\left(N(1-p) - \frac{(1-p)}{p}\left(1-(1-p)^N\right)\right)\frac{l}{C}}{N\frac{l+l'}{C} + p(t_{Fout} + t_s) + t_{ack}} \tag{3.21}$$

As all component tasks that affect IrLAP utilization are considered, equation

$$U + T_{tack} + T_{Fout} + T_f + T_{error} + T_{corr} = 1 \tag{3.22}$$

always holds true. Eq. (3.22) can be easily verified from eq. (3.16)-(3.21).

3.5 Model validation

3.5.1 Comparison with simulation

To validate the above mathematical model, a set of simulation runs was performed using the OPNET™ simulation package [71]. The OPNET simulator emulates IrLAP station behavior as close as possible, including transmission times, turn around delays, transmission errors and timer expiration.

Fig. 3.5 plots utilization versus window size for different bit error rate (BER) p_b values. The analytical model is validated as its calculated utilization (lines) practically coincides with simulation results (points). Simulation results are obtained with a confidence interval of 98%.

3.5.2 Comparison with existing analytical models

The proposed analytical model is also validated using the existing analytical model presented in [4],[6]. This analytical model evaluates the IrLAP performance for the same information exchange scenario using the concept of a frame's virtual transmission time (VTT). However, the VTT concept leads to very complex algebraic expressions

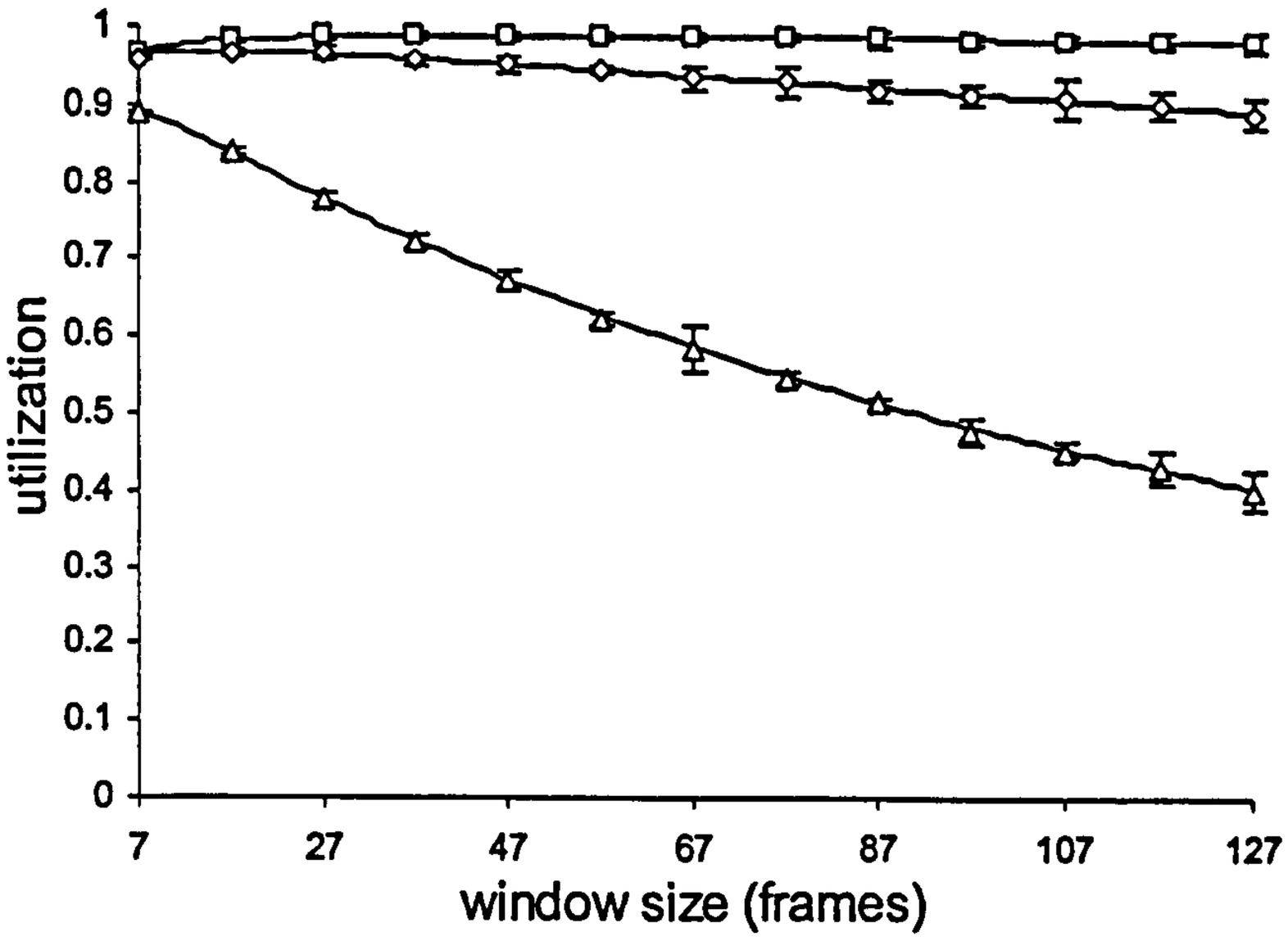

□ $p_b=10^{-8}$ ◇ $p_b=10^{-7}$ △ $p_b=10^{-6}$

Figure 3.5 Analysis versus simulation: Utilization against window size, C=16Mbit/s, I=16Kbits, T_{max}=500ms, t_{ta}=0.1ms. Simulation confidence interval=98%

that calculate IrLAP utilization [6]. After considerable algebraic calculations, the existing model simplifies and reaches the same simple equation (3.15), thus validating the mathematical model developed in this work. An extensive discussion on IrLAP mathematical models can also be found at [99].

3.6 IrLAP performance evaluation

Equation (3.15) allows us to get an intuitive understanding of IrLAP performance. Three factors contribute to average WTT given in (3.9). Factor Nt_I stands for user data transmission, factor $p(t_{Fout}+t_s)$ stands for lost P/F bit overhead and t_{ack} stands for delays introduced by reversing link direction. It is clear that for very low BERs, factor $p(t_{Fout}+t_s)$ introduces negligible overhead as the P/F bit is seldom lost. Table 3.2 shows

specifi-cation	data rate	year	W_{max}	N	Nt_I (ms)	t_{ta} (ms)	t_{ack} (ms)
SIR	115.2 Kbit/s	1994	7	3	427.9	10	20.00
FIR	576 Kbit/s	1995	7	7	199.7	10	20.00
FIR	1.152 Mbit/s	1995	7	7	99.8	10	20.00
FIR	4 Mbit/s	1995	7	7	28.8	10	20.00
VFIR	4 Mbit/s	1999	127	121	497.8	10	20.00
VFIR	16 Mbit/s	1999	127	127	130.6	0.1	0.20

Table 3.2: Factors Nt_I and t_{ack} that contribute to t_w for SIR and FIR data rates

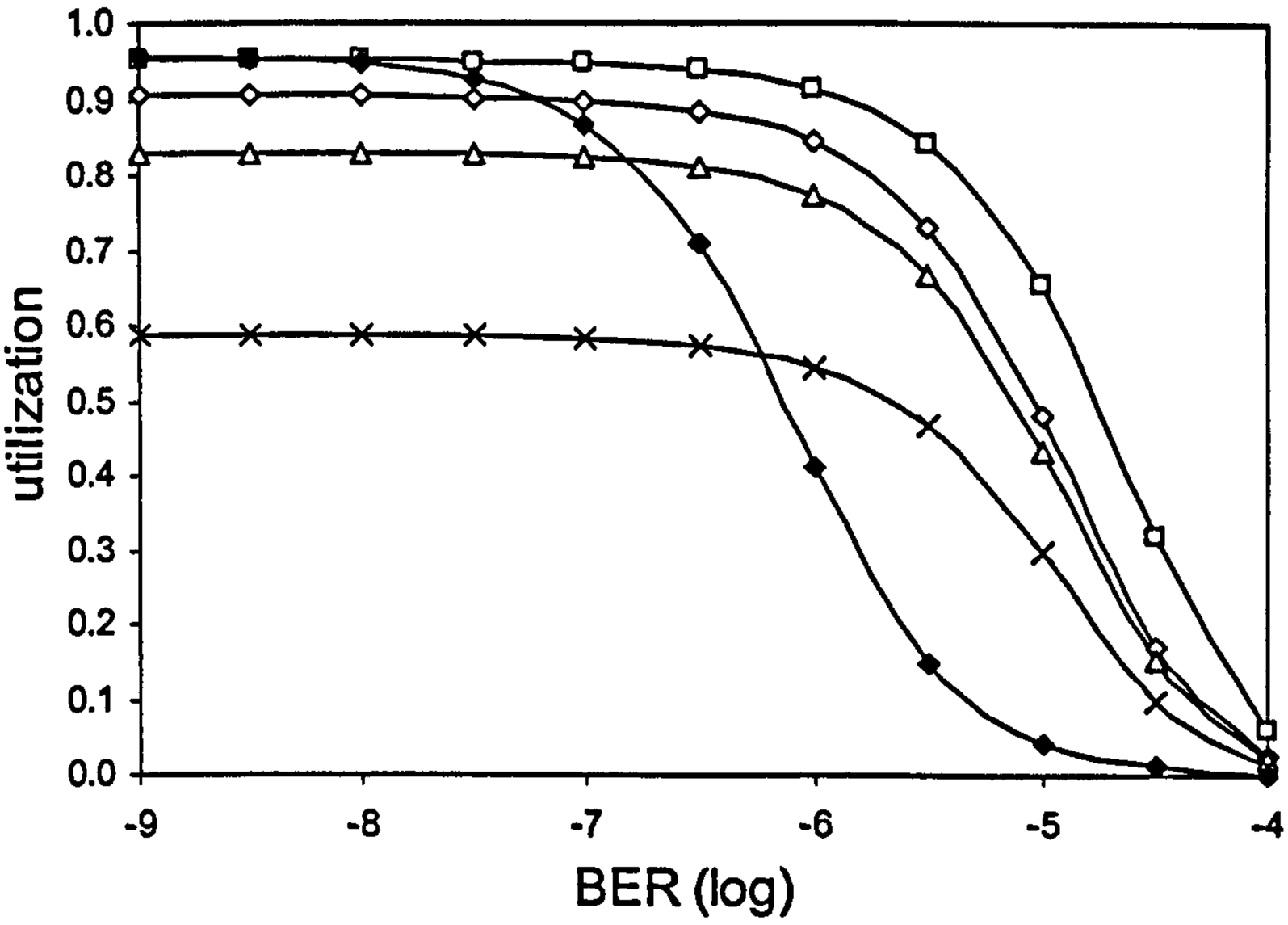

□ *C=115.2 Kbit/s, W_{max}=7* ◇ *C=576 Kbit/s, W_{max}=7* △ *C=1.152 Mbit/s, W_{max}=7*
x *C=4 Mbit/s, W_{max}=7* ◆ *C=4 Mbit/s, W_{max}=127*

Figure 3.6 Utilization versus BER for t_{ta}=10ms, l=16Kbits, $t_{Fout}=t_{Imax}+2t_{ta}$

the remaining two factors for IrPHY data rate evolution. IrPHY ver. 1.0 Serial Infrared (SIR) specification [50] supported data rates up to 115.2 Kbit/s using standard serial hardware, IrPHY ver. 1.1 Fast Infrared (FIR) [51] extended data speed to 4Mbit/s and finally IrPHY ver. 1.3 Very Fast Infrared (VFIR) [53] specification added the 16Mbit/s link rate. Table 3.2 presents the data rates introduced by new specifications, the year a specification was introduced, specification's maximum window size, maximum window size that can be enforced for 16Kbit frames within T_{max} (denoted by N), specification's t_{ta} and the two factors that contribute to WTT. Table 3.2 reveals that although FIR introduced much higher speeds (up to 4Mbit/s), it did not change the maximum t_{ta} value allowed for FIR IrDA ports. As a result, time utilized on user data transmission dropped from 427.9 ms to 28.8 ms while time utilized on reversing link direction twice, was steady at 20 ms as the t_{ta} value was not changed [92]. As a result, 4Mbit/s IrDA links employing the maximum allowed t_{ta}=10ms spend 20ms for acknowledgments for every 28.8ms of data transmission! Fig. 3.6 plots utilization versus BER for SIR and FIR link rates with t_{ta}=10ms, W_{max}=7 and l=16Kbits. Utilization decreases with data rate increase as the link turn around frequency is increased. As a result a maximum utilization of 0.59 can be achieved for 4 Mbit/s links.

VFIR specification, along with introducing the higher 16Mbit/s rate, addressed the

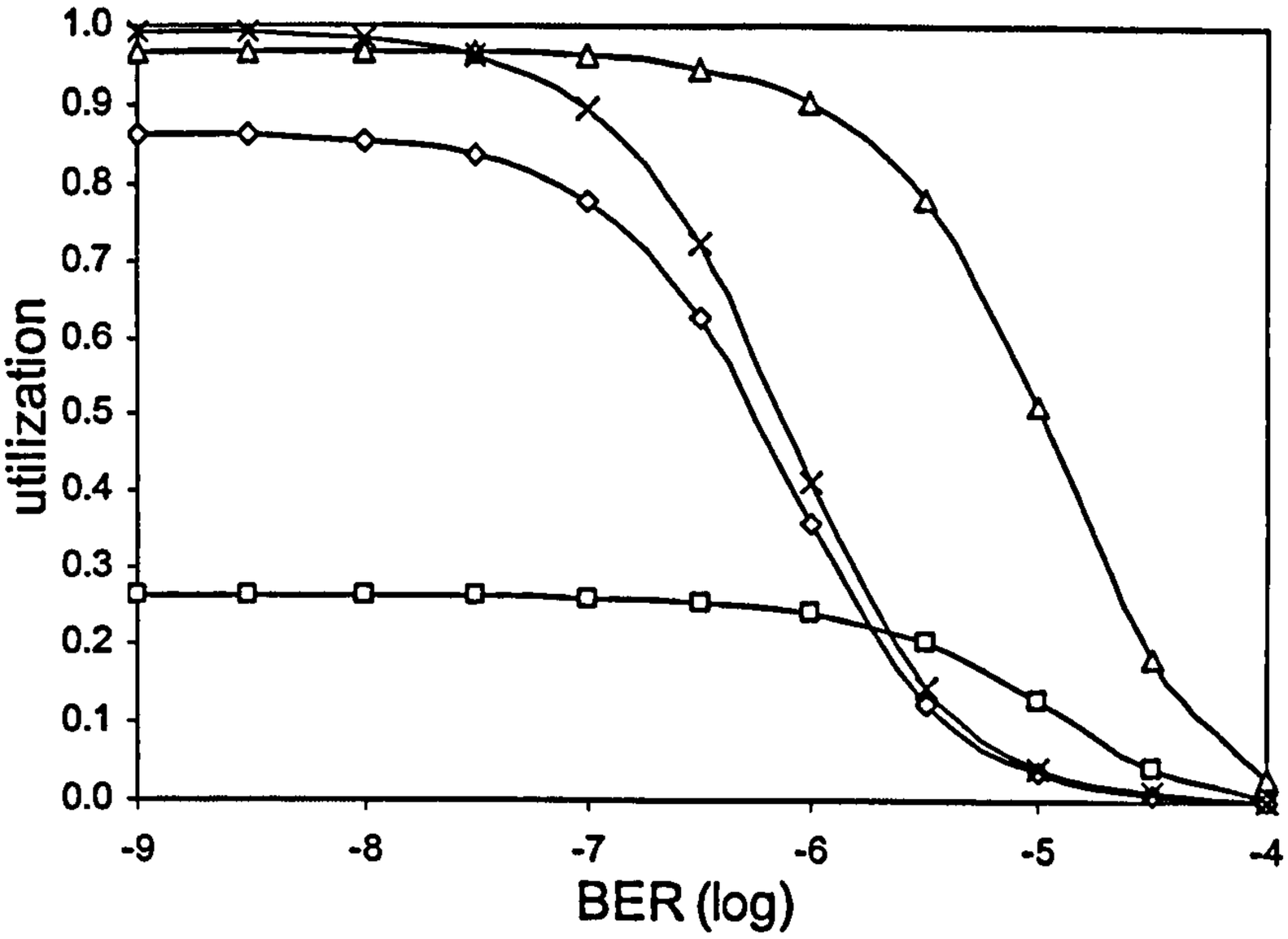

□ W_{max}=7, t_{ta}=10ms
◇ W_{max}=127, t_{ta}=10ms
△ W_{max}=7, t_{ta}=0.1ms
× W_{max}=127, t_{ta}=0.1ms

Figure 3.7 Utilization versus BER for C=16Mbit/s, l=16Kbits, $t_{Fout}=t_{Imax}+2t_{ta}$

problem by reducing t_{ta} to 0.1 ms and by optionally increasing window size to 127 frames for 16Mbit/s links [53]. The specification also introduced an optional window size increase to 127 frames for the existing 4Mbit/s links in an effort to solve the existing problem. Fig. 3.6 plots utilization versus link BER for 4 Mbit/s links with t_{ta}=10ms, l=16Kbits and a window size of 127 frames. Utilization significantly increases with the 127 window size employment and reaches the acceptable value of 0.96 at low BER.

Fig. 3.7 plots utilization versus link BER. It examines the effect in utilization of reducing t_{ta} and/or increasing window size for a 16 Mbit/s link. Utilization for t_{ta}=10ms and W_{max}=7 shows that the increased turnaround frequency results in poor performance. Reducing acknowledgement time portion by only increasing window size (t_{ta}=10ms and W_{max}=127) results in a significant increase but yet a questionable performance. By reducing only t_{ta} (t_{ta}=0.1ms and W_{max}=7) an excellent performance is observed. Taking further advantage of the optional window size increase (t_{ta}=0.1 ms and W_{max}=127) results a slightly better performance for low BER but renders the link vulnerable to BER increase as it requires a link BER of 10^{-8} to achieve an excellent performance as opposed to a 10^{-7} BER requirement for W_{max}=7. As a conclusion, t_{ta} adjustment is a necessity while the effectiveness of window size increase is debatable.

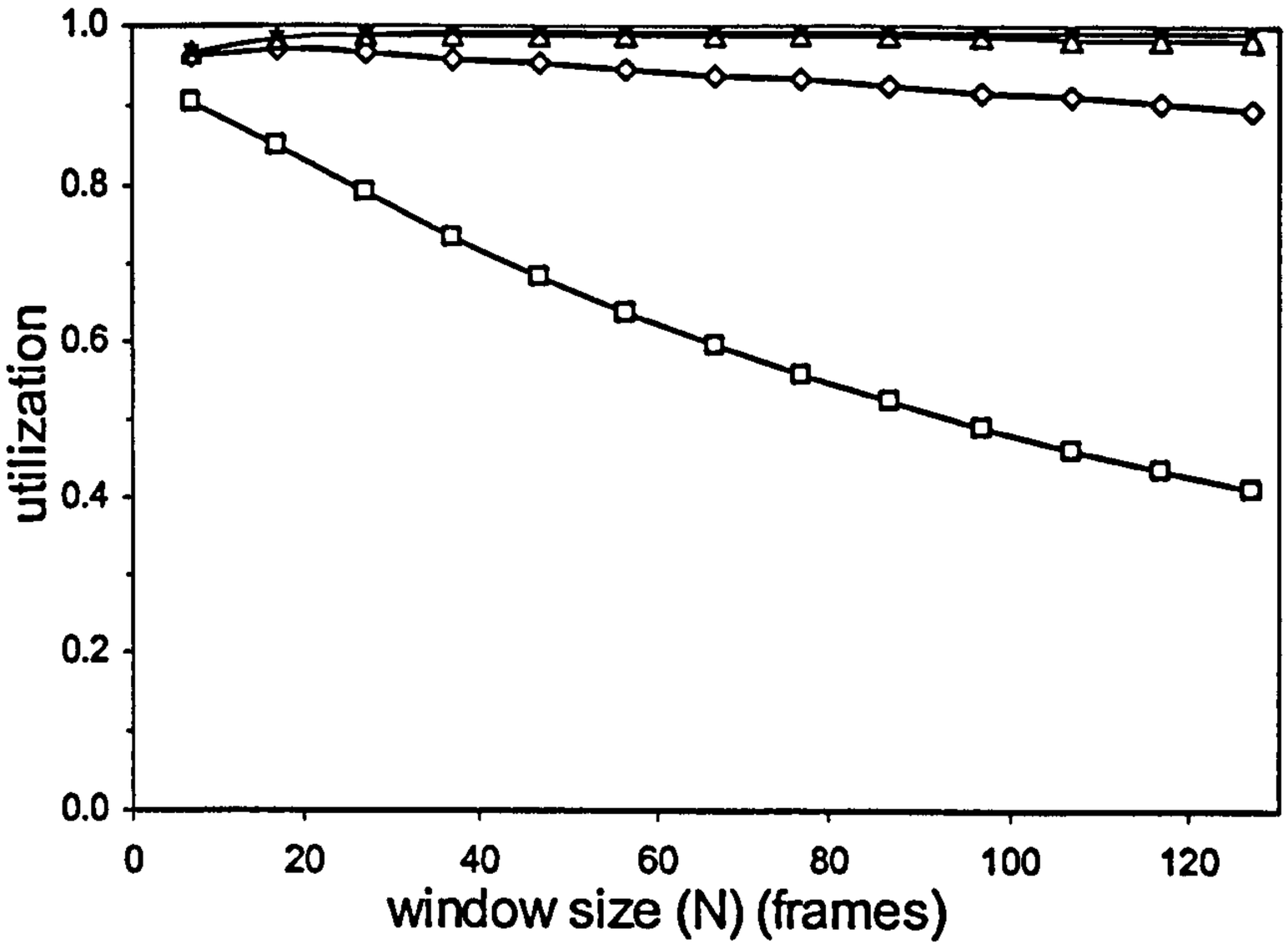

□ $p_b=10^{-6}$
◇ $p_b=10^{-7}$
△ $p_b=10^{-8}$
× $p_b=10^{-9}$

Figure 3.8 Utilization versus window size for C=16Mbit/s, t_{ta}=0.1ms, l=16Kbits, $t_{Fout}=t_{lmax}+2t_{ta}$

Fig. 3.8 plots utilization versus window size for different link BERs for 16Mbit/s links with t_{ta}=0.1 ms. Window size increase results in slight utilization increase for low BERs and significant decrease for high BERs. Fig. 3.9 plots utilization versus window size for 4Mbit/s links with t_{ta}=10ms. A much different behavior is observed due to the large link turnaround time value as related to data rate. A significant utilization increase with window size increase for low BER is observed as the link turnaround frequency is decreased. This also applies for high BER (10^{-6}) but when window size becomes very large, a utilization decrease is observed caused by the increased number of retransmitted frames following an error frame in a window transmission. Fig. 3.10 shows the % time consumed for different IrLAP tasks for a 16Mbit/s link with W_{max}=127 and t_{ta}=0.1 ms. It reveals that for high window size values (W_{max}=127), the key factor that reduces utilization for a wide range of BER (from 10^{-8} to 10^{-4}) is the retransmission of correctly received out of sequence frames. This is a limitation of the IrDA IrLAP protocol when non-optimum window size is used, especially for high BER [18]. As a conclusion, high window size employment increases utilization by reducing the link turn around frequency. The price we pay for using high window sizes is that utilization becomes sensitive to an increase in BER.

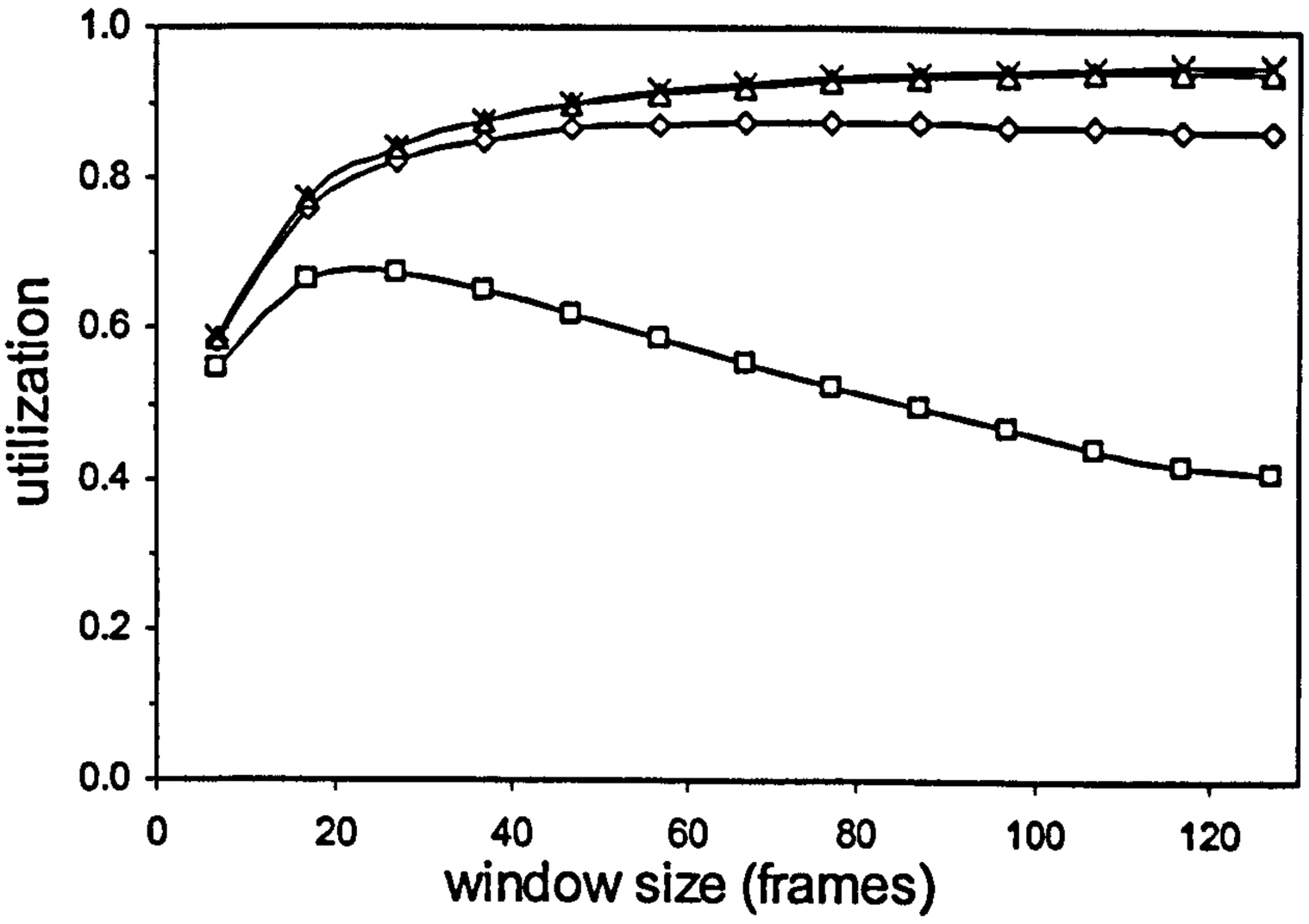

□ $p_b=10^{-6}$
◇ $p_b=10^{-7}$
△ $p_b=10^{-8}$
× $p_b=10^{-9}$

Figure 3.9 Utilization versus window size for C=4Mbit/s, t_{ta}=10ms, l=16Kbits, $t_{Fout}=t_{Imax}+2t_{ta}$

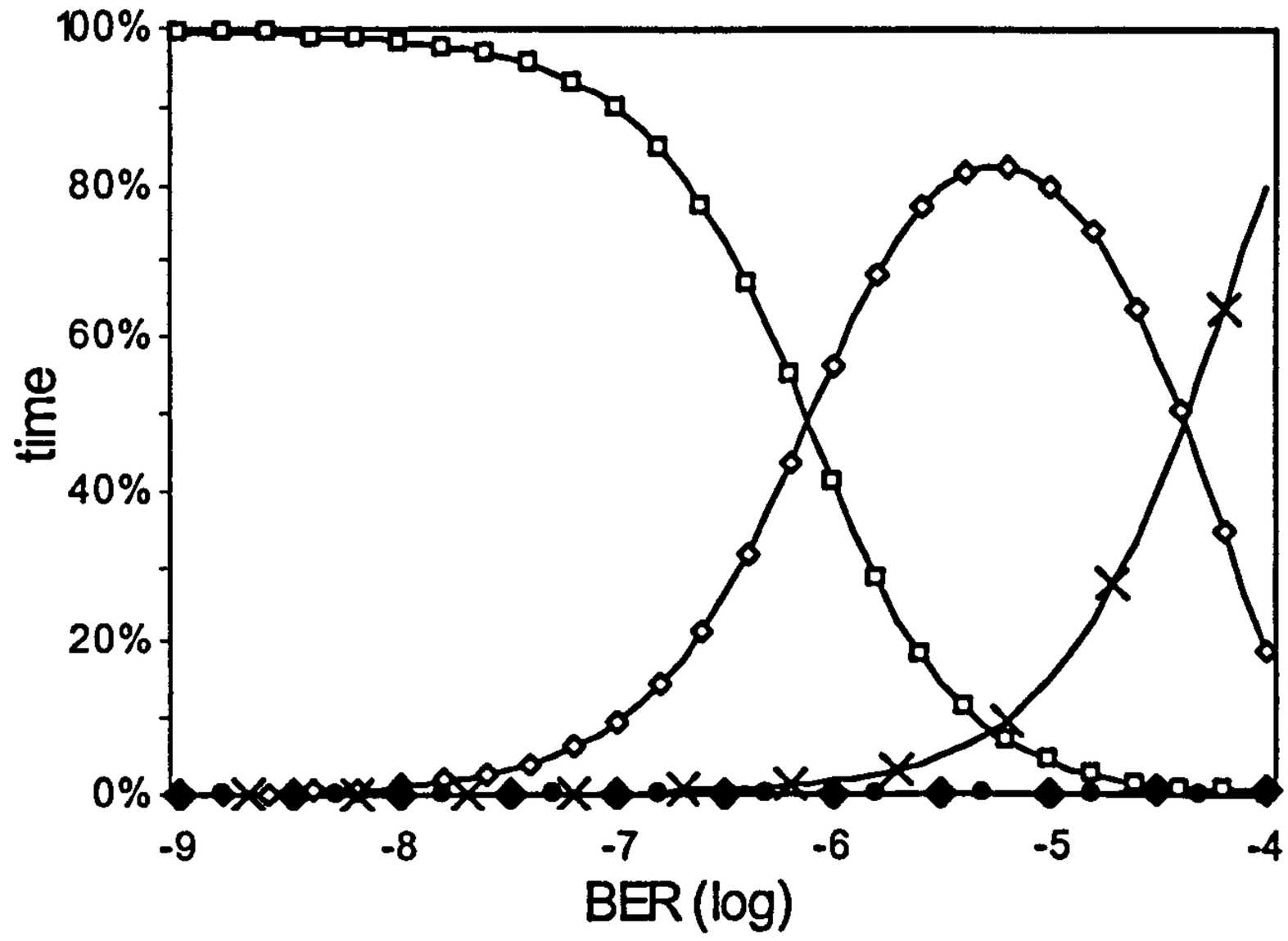

□ *useful data transmission (utilization)*
◇ *retransmission of correctly received out of sequence frames*
× *retransmission of error frames*
◆ t_{Fout} *timer expiration*
● *reversing link direction (hardware latency)*

Figure 3.10 Time allocation of various IrLAP tasks versus BER, C=16Mbit/s, l=16Kbits, W_{max}=127 frames, t_{ta}=0.1ms, $t_{Fout}=t_{Imax}+2t_{ta}$

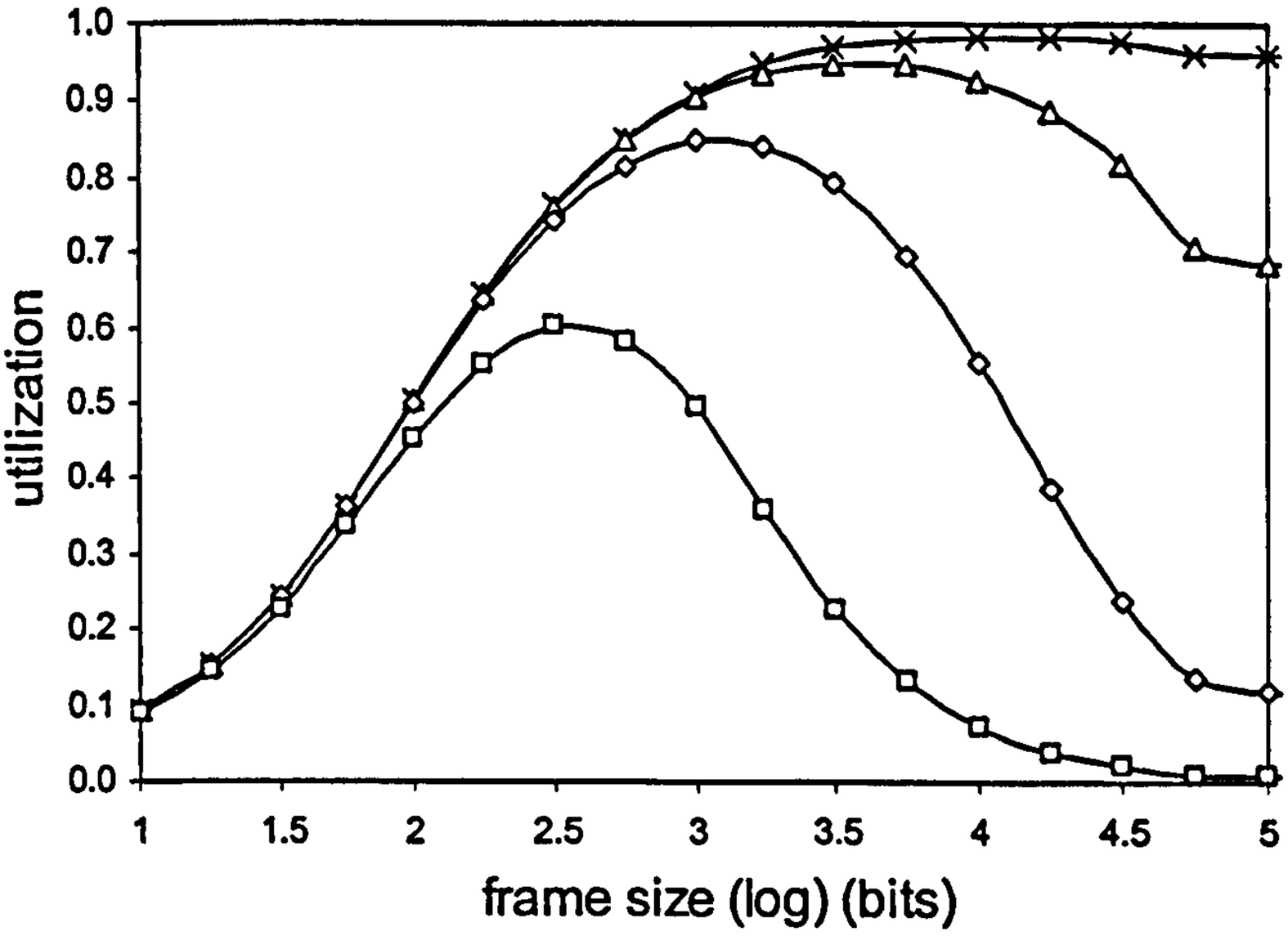

□ $p_b=10^{-5}$
◇ $p_b=10^{-6}$
△ $p_b=10^{-7}$
× $p_b=10^{-8}$

Figure 3.11 Utilization versus frame size for C=16Mbit/s, t_{ta}=0.1ms, W_{max}=127 frames, $t_{Fout}=t_{Imax}+2t_{ta}$

Fig. 3.11 plots utilization versus frame size for 16Mbit/s links with t_{ta}=0.1 ms and W_{max}=127. It shows that, although for low BER the maximum frame size should be used, a much different frame size value should be implemented at high BER for maximum utilization. Thus, optimum window size and frame size parameters are of great importance for IrLAP performance.

3.7 IrLAP performance for future high data rates

IrDA is expected to develop new IrPHY specifications that will support higher data rates to meet user needs for faster information transfers [47][17]. This section examines how well the IrLAP protocol fares with predicted future increases of IrPHY data rates if optimum window and frame size values are not implemented. It focuses on whether the new IrPHY specification should decrease or not the maximum t_{ta} value defined in the current IrPHY ver. 1.3 VFIR specification (t_{ta}=0.1ms) [53] as related to the window size that IrLAP utilizes for efficient data transfers.

Fig. 3.12 plots utilization versus BER for C=40 Mbit/s and different window size and t_{ta} values. It shows that for W_{max}=127 frames, reducing t_{ta} to 0.01ms is not beneficial because no utilization increase is observed. For W_{max}=127 frames, IrLAP performance is

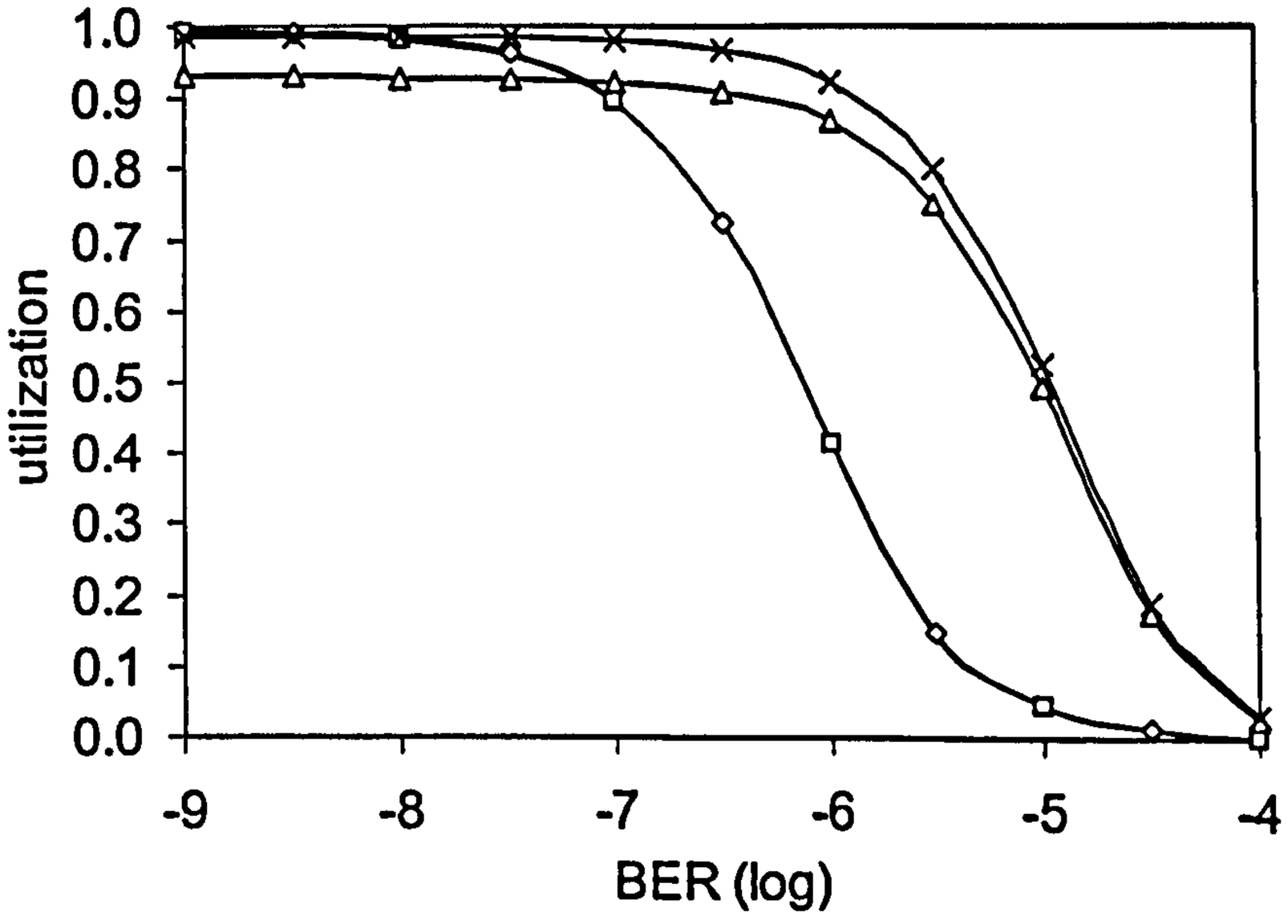

□ W_{max}=127, t_{ta}=0.1ms
◇ W_{max}=127, t_{ta}=0.01ms
△ W_{max}=7, t_{ta}=0.1ms
x W_{max}=7, t_{ta}=0.01ms

Figure 3.12 Utilization versus BER for C=40Mbit/s, l=16Kbits, $t_{Fout}=t_{lmax}+2t_{ta}$

vulnerable to BER increase. If IrLAP utilizes a window size of 7 frames (W_{max}=7), reducing t_{ta} to 0.01 results in utilization improvement for low BER. In addition, the low window size value renders the link more robust to BER increase. Fig. 3.13 plots the same results for C=100Mbit/s. Reducing t_{ta} to 0.01 ms is not again beneficial for W_{max}=127. However, if W_{max}=7 frames, reducing t_{ta} to 0.01ms highly improves utilization for low BER. As a conclusion, the t_{ta} value defined in the future IrPHY specification should not be reduced if future high speed (40 Mbit/s or 100 Mbit/s) IrDA links are expected to operate in good quality links that have a low BER. If it is desired that the future high speed links should be more robust to BER increase, a lower t_{ta} of 0.01 ms should be defined and the IrLAP should utilize low (or optimum) window sizes in low quality infrared links.

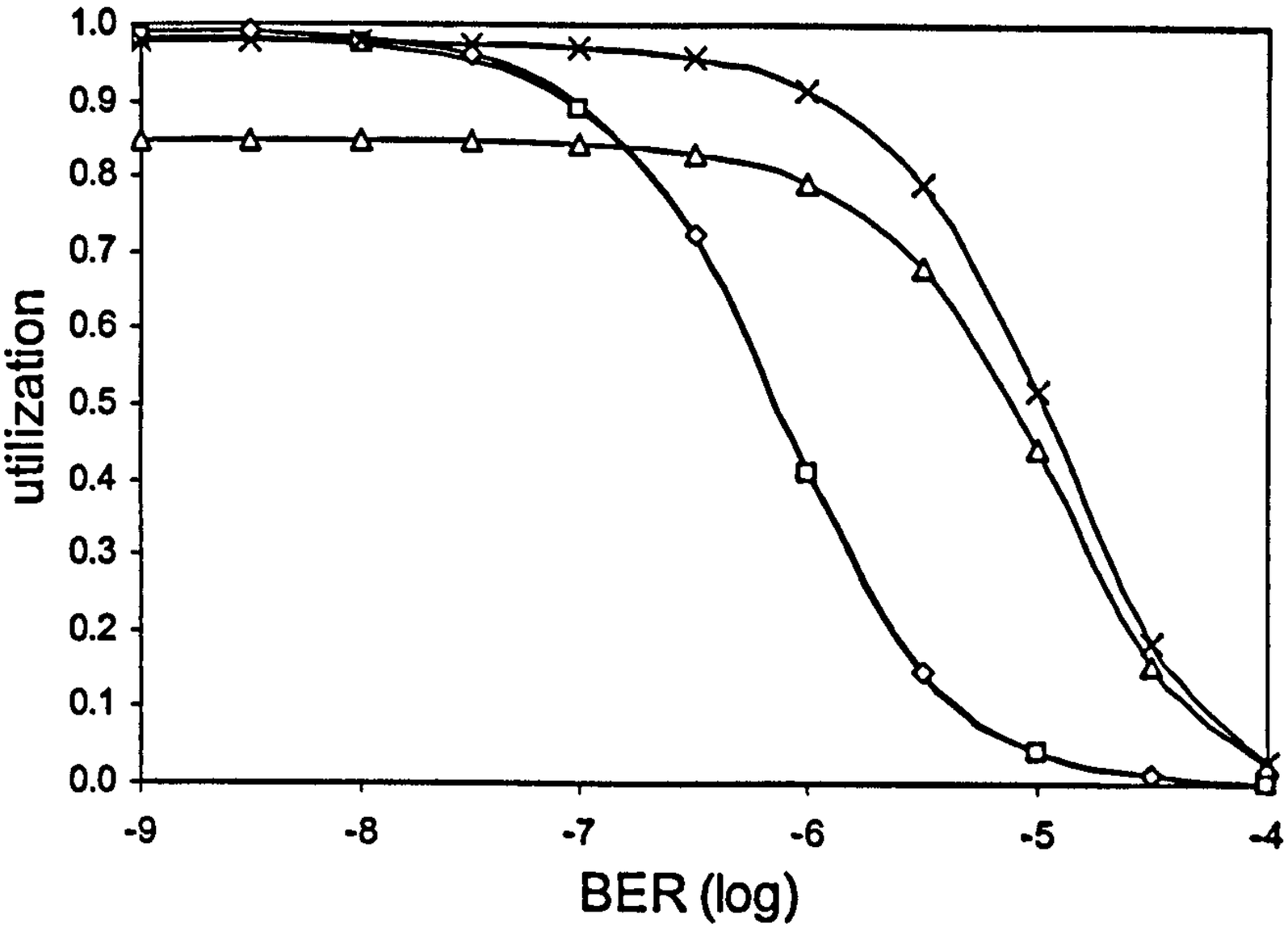

□ $W_{max}=127$, $t_{ta}=0.1ms$

◇ $W_{max}=127$, $t_{ta}=0.01ms$

△ $W_{max}=7$, $t_{ta}=0.1ms$

× $W_{max}=7$, $t_{ta}=0.01ms$

Figure 3.13 Utilization versus BER for C=100Mbit/s, l=16Kbits, $t_{Fout}=t_{Imax}+2t_{ta}$

CHAPTER 4

Optimization of Infrared Data Link Layer

The IrLAP performance evaluation presented in chapter 3 revealed that utilization significantly degrades if unsuitable values for the window and frame size parameters are implemented. If a high window size value is used in links with high BER, an error frame is followed by many frames in the same window transmission. As IrLAP utilizes a Go-Back-N retransmission scheme, all these frames will be eventually retransmitted. If a low window size value is utilized, the increased link turn around frequency may significantly affect performance. If a large frame size is used as related to link BER, the resulting high frame error probability degrades utilization because a single bit error causes the retransmission of the entire frame. If a small frame size is used, the constant frame overhead degrades performance.

This chapter employs the mathematical model developed in the previous chapter for IrLAP performance to derive optimum values for window and frame size parameters for maximum performance. To find the utilization maximum, the first derivative of the utilization equation versus window and frame size is set to zero to derive simple equations for optimum window and frame size values. However, the communicating stations can only estimate the link BER based on the number of error frames. An algorithm is developed for the transmitting station that estimates link BER and implements optimum values based on frame rejections by the receiver. The effectiveness of the proposed algorithm is explored using simulation techniques.

The outline of this chapter is as follows. Section 4.1 presents the importance of the F-timer time out period when optimum window and frame size values are implemented. It also proposes an S-frame improvement to IrLAP operation that eliminates delays arising from the F-timer expiration. Section 4.2 derives (a) optimum window size values for fixed frame size, (b) optimum frame size values for fixed window size and (c) simultaneously optimal window and frame size values. Section 4.3 presents the improvement in IrLAP performance when optimum window and/or frame size values are employed. Section 4.4 presents the effectiveness of the proposed (in section 4.1) S-frame improvement in IrLAP operation combined with optimum window and frame size employment. The implementation issues of optimum values are addressed in section 4.5

by developing a simple and effective algorithm for the transmitting station that estimates link BER and implements optimum window and frame size values.

4.1 Significance of F-timer time out period

Equation (3.5) shows that if the link BER p_b is increased, frame error probability p is significantly increased. In such a case, the time spent on the primary's F-timer expiration, represented in (3.9) by term pt_{Fout}, may significantly increase the average WTT resulting in utilization degradation. IrLAP specification [49] poses only an upper limit of 500ms for the t_{Fout} value and allows the implementation of smaller values. According to IrLAP specification [49], if the secondary has information ready for transmission, it sets the F-bit in the last I-frame it transmits. Otherwise, upon gaining transmission control, it immediately transmits an S-frame with the F-bit set, thus acknowledging correctly received I-frames and reversing link direction. Thus, the secondary station never holds transmission control without transmitting I-frames. As a result, the t_{Fout} value may be safely reduced from 500ms to the smaller time period required for the secondary to transmit a full window (N) of full payload (16Kbits) I-frames plus the time required to reverse the link direction twice, $t_{Fout} = Nt_{Imax} + 2t_{ta}$. This value assumes that the secondary has transmitted a full window of I-frames and the primary did not manage to correctly receive a single I-frame.

In the saturation case considered in this work, the secondary station never transmits I-frames to the primary and immediately acknowledges I-frames correctly received by means of an S-frame transmission. As a result, a smaller t_{Fout} value of $t_{Fout} = t_{Imax} + 2t_{ta}$ may be safely implemented in the current information exchange scenario. This value allows the secondary station to transmit an S-frame or an I-frame if it wishes to transmit data at the end of considered information transfer from the primary. This t_{Fout} value is valid since it corresponds to a maximum window size parameter of one for the primary station negotiated and agreed during link establishment.

The t_{Fout} value becomes of key importance for maximum utilization at high BER if optimum link layer parameter values are implemented by the primary station. Fig. 4.1 shows the time allocation of various IrLAP tasks versus BER when optimum window size N values are implemented for t_{Fout}=500ms. At high BER, a significant amount of time is spent on F-timer expiration causing serious utilization degradation. It can be

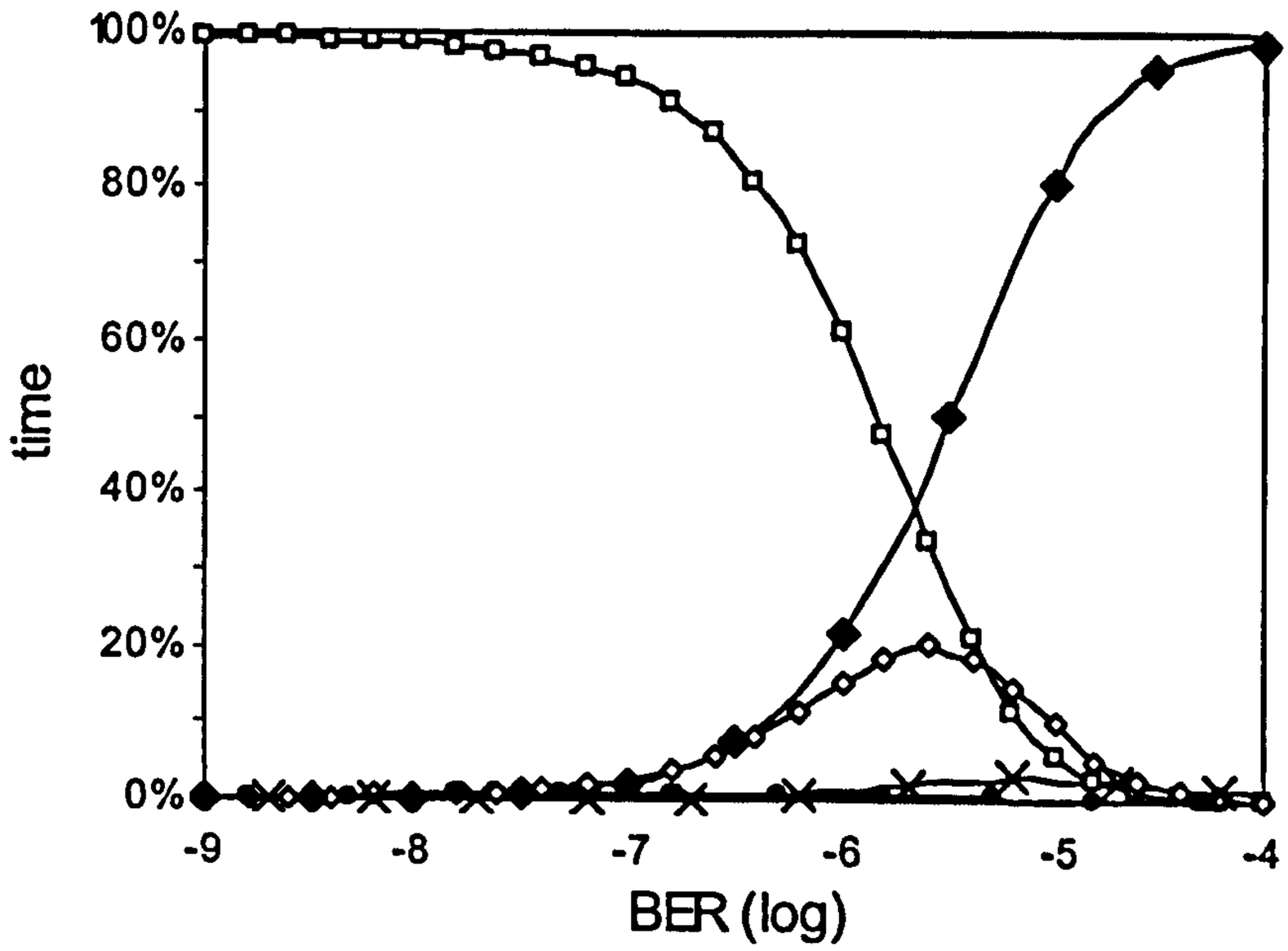

□ *useful data transmission (utilization)*
◇ *retransmission of correctly received out of sequence frames*
x *retransmission of error frames*
◆ *F-timer expiration*
● *reversing link direction (hardware latency)*

Figure 4.1 Time allocation of various IrLAP tasks against BER for N optimum, t_{Fout}=500ms, C=16Mbit/s, I=16Kbits, t_{ta}=0.1ms

easily observed that time portion utilized on F-timer expiration is much larger than the time portion utilized on other IrLAP tasks, such as retransmitting error frames, retransmitting correctly received out of sequence frames and reversing link direction. The situation is explained by considering that a single I-frame transmission error results in a significant 500ms delay if the lost I-frame contains the P-bit. For the saturation case considered, if the maximum window size allowed for the primary is agreed to be equal to one and $t_{Fout} = t_{Imax} + 2t_{ta}$, a much different behavior is shown in Fig. 4.2. A significant utilization improvement is observed over a wide BER range (10^{-7} to 10^{-4}) mainly by taking advantage of time otherwise wasted on F-timer expiration [98]. Unless otherwise specified, the t_{Fout} value implemented in this work is given by

$$t_{Fout} = t_{Imax} + 2t_{ta} \tag{4.1}$$

A different approach to address the significant delays arising from the F-timer expiration is to reduce the probability of P-bit loss rather than reducing the time wasted for every P-bit loss. According to the IrLAP specification state charts [49], the primary station sets the P-bit of the last I-frame in a window transmission. This decision

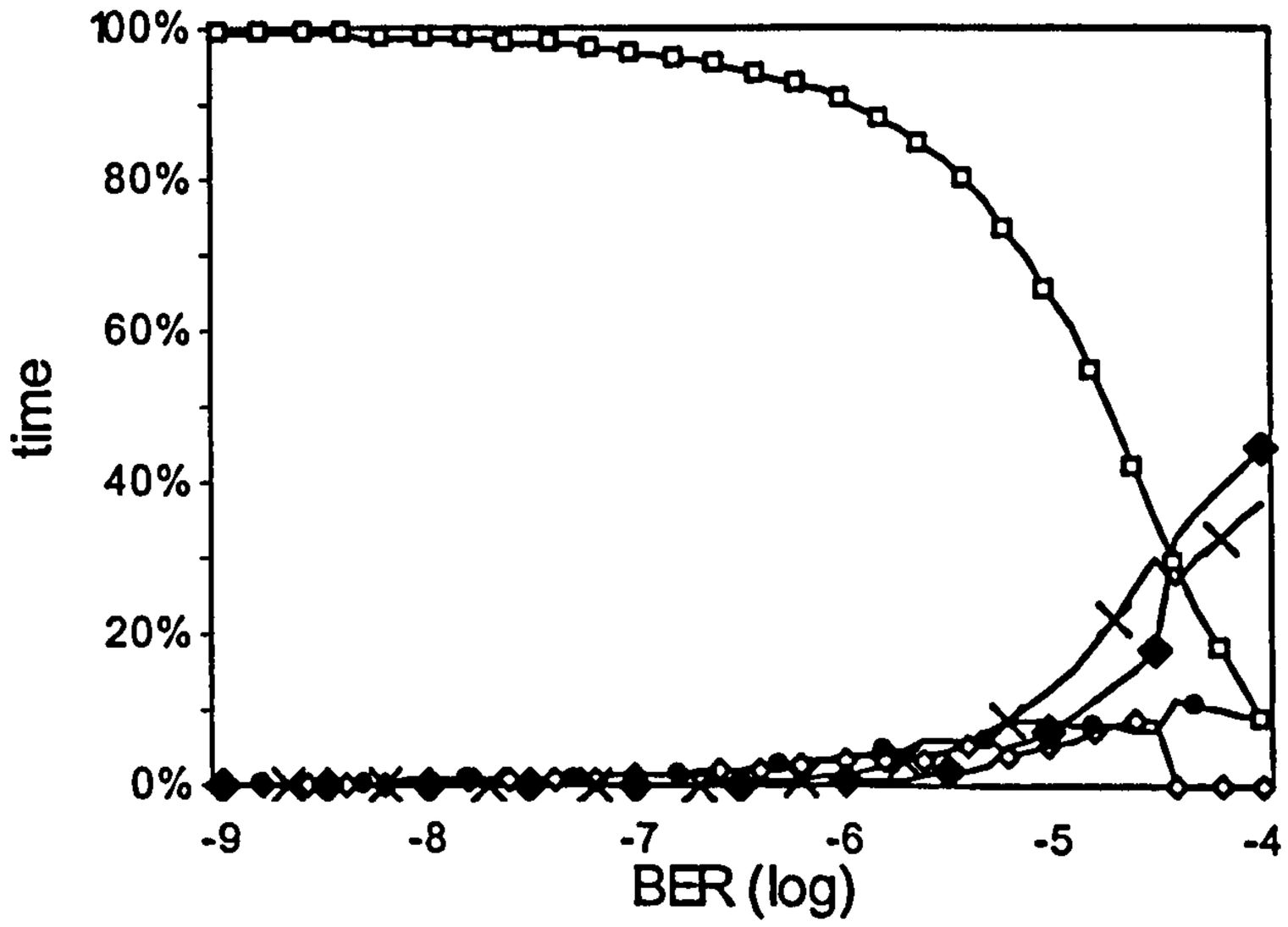

□ *useful data transmission (utilization)*
◇ *retransmission of correctly received out of sequence frames*
x *retransmission of error frames*
◆ *F-timer expiration*
● *reversing link direction (hardware latency)*

Figure 4.2 Time allocation of various IrLAP tasks against BER for N optimum, $t_{Fout}=t_{Imax}+2t_{ta}$, *C=16Mbit/s, l=16Kbits,* $t_{ta}=0.1ms$

assumes that link BER is very low and frame error probability p is very small. Thus, the P-bit is seldom lost and time spent on F-timer expiration is negligible. However, if link BER is relatively high, p is significantly increased as it usually refers to an I-frame with 16Kbits of user data. To reduce the probability of P-bit loss, an IrLAP modification is proposed. The primary should not set the P-bit in the last I-frame it transmits, but transmit the P-bit in a new Receive Ready (RR) S-frame that follows the last I-frame transmission. As S-frames are very small, they introduce negligible additional delays. As S-frames have very small frame error rates, delays on F-timer expiration are significantly reduced. The mathematical model presented in this work can be easily altered to calculate the utilization performance for the proposed IrLAP improvement. S-frame modification is presented in Fig. 4.3(a)(b) and WTT becomes

$$t_{w-RR} = Nt_I + t_s + t_{ack} \tag{4.2}$$

independent of the number of frame errors in the window transmission. The assumption that S-frames are always transmitted error free holds true because the S-frame error rate is well below 0.01 at the highest BER value considered in this work. Utilization is given

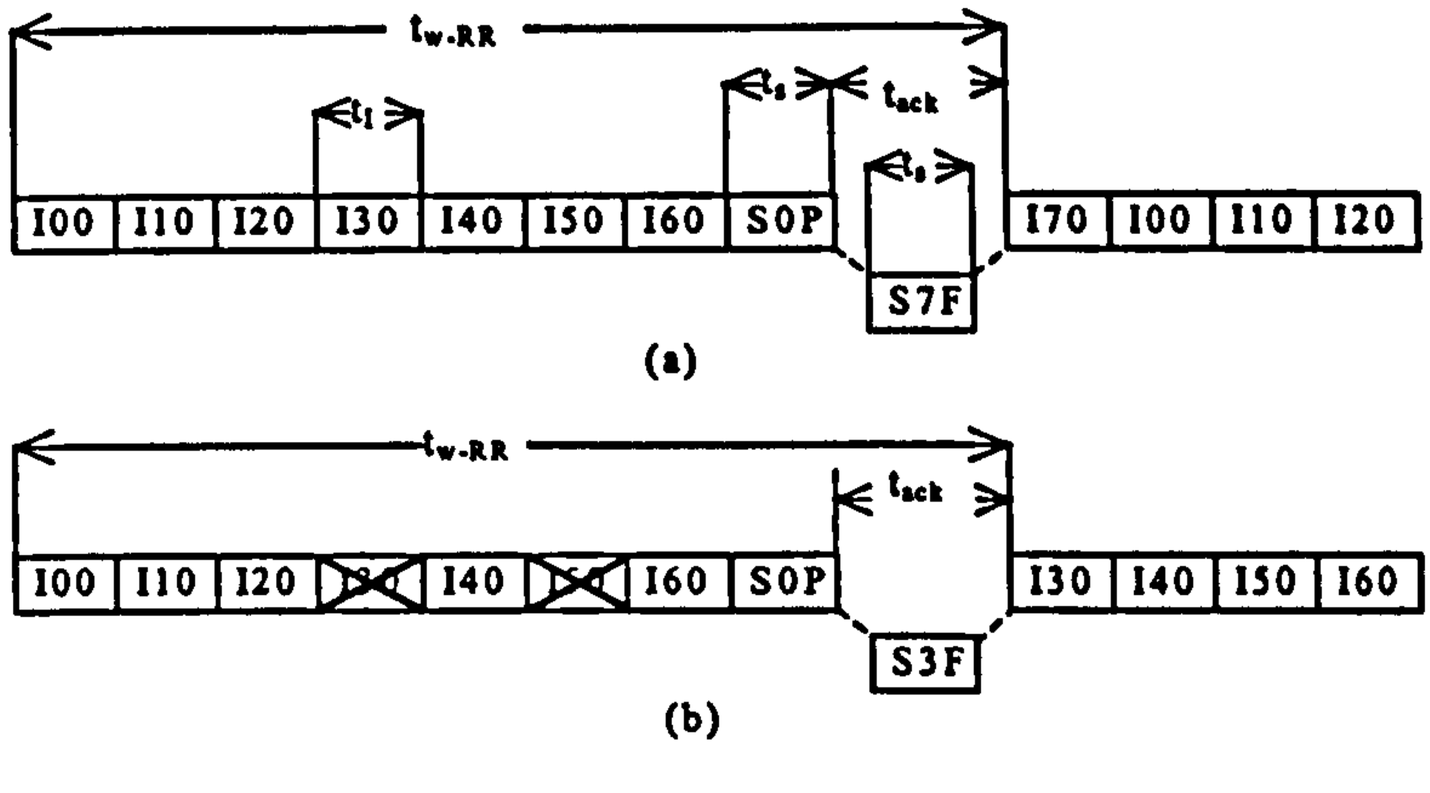

Ixy : *I-frame with N_s=x and N_r=y*
SxP : *S-frame with N_r =x and P-bit set*
SxF : *S-frame with N_r =x and F-bit set*
a) Window error free transmission (P-bit in S-frame)
b) Retransmitted frames due to error frame with N_s =3 and N_s =5 (P-bit in S-frame)

Figure 4.3 Determination of window transmission time $t_{w\text{-}RR}$

by

$$U_{RR} = \frac{l}{C} \cdot \frac{1-p}{p} \cdot \frac{1-(1-p)^N}{Nt_I + t_s + t_{ack}} \tag{4.3}$$

The following analysis for deriving optimum values for window and/or frame size parameters is derived for links not employing the S-frame modification and using small t_{Fout} values, such as the value given in (4.1). Identical formulae have been derived for the S-frame modification (which eliminates F-timer delays) by taking the first derivative of utilization equation (4.3). Hence the following results and conclusions apply to both cases.

4.2 Derivation of optimum values

4.2.1 Optimum window size for fixed frame size

Due to the half duplex nature of the IrLAP protocol, window size is a very important and easily adjustable parameter. If a small window size value is implemented, the increased link turn around frequency results in significant delays and decreases utilization. If a high window size value is implemented for high BERs, a large number of frames following an error frame may be transmitted. Even if these frames are correctly received, they are considered as out of sequence and are discarded by the receiver. These frame transmissions essentially delay reversing link direction, acknowledging correctly received frames and retransmitting the erred frame. Time

needed for such frame transmissions is simply wasted.

To derive optimum window size values that result in maximum utilization, the first derivative of (3.15) against N must be set to zero. First considering the valid approximation for small p,

$$(1-p)^N \approx 1-Np+\frac{N(N-1)}{2}p^2 \tag{4.4}$$

the derivative of (3.15) becomes

$$\frac{\partial U}{\partial N}=\frac{l(1-p)}{2C}\cdot\frac{\partial}{\partial N}\left\{\frac{2N-N(N-1)p}{Nt_1+2pt_{ta}+pt_{Imax}+pt_s+t_{ack}}\right\}=0 \tag{4.5}$$

After some algebra and assuming $2pt_{ta}+pt_{Imax}+pt_s+t_{ack}\approx t_{ack}$

$$(-pt_1)N^2+(-2pt_{ack})N+2t_{ack}+pt_{ack}=0 \tag{4.6}$$

Assuming $pt_{ack}<<2t_{ack}$ and $-2pt_{ack}<-pt_1$, (4.6) becomes

$$(-pt_1)N^2+2t_{ack}=0 \tag{4.7}$$

and

$$N_{opt}=\sqrt{\frac{2t_{ack}}{pt_1}} \tag{4.8}$$

Considering the valid approximations for small p_b and $l>>l', p\approx lp_b$ and $t_1\approx\frac{l}{C}$, optimum window size value is given by

$$N_{opt}=\sqrt{\frac{2t_{ack}C}{l^2p_b}} \tag{4.9}$$

The optimum window size values versus BER for fixed frame size are shown in Fig. 4.4. Window size should be decreased with the increase of BER for maximum utilization. Note that at very low BER, the optimum window size values should be greater than the maximum window size value of 127 frames allowed by the IrLAP specification. Fig. 4.4 compares N_{opt} values derived from (4.9) with optimum window size values obtained using exact numerical methods in (3.15) for a 16Mbit/s link with t_{ta}=0.1ms and for a 4Mbit/s link with t_{ta} =1 ms. An exact match is observed validating the approximations used to derive (4.9).

4.2.2 Optimum frame size for fixed window size

A different approach for reducing the data transmitted in a window transmission is

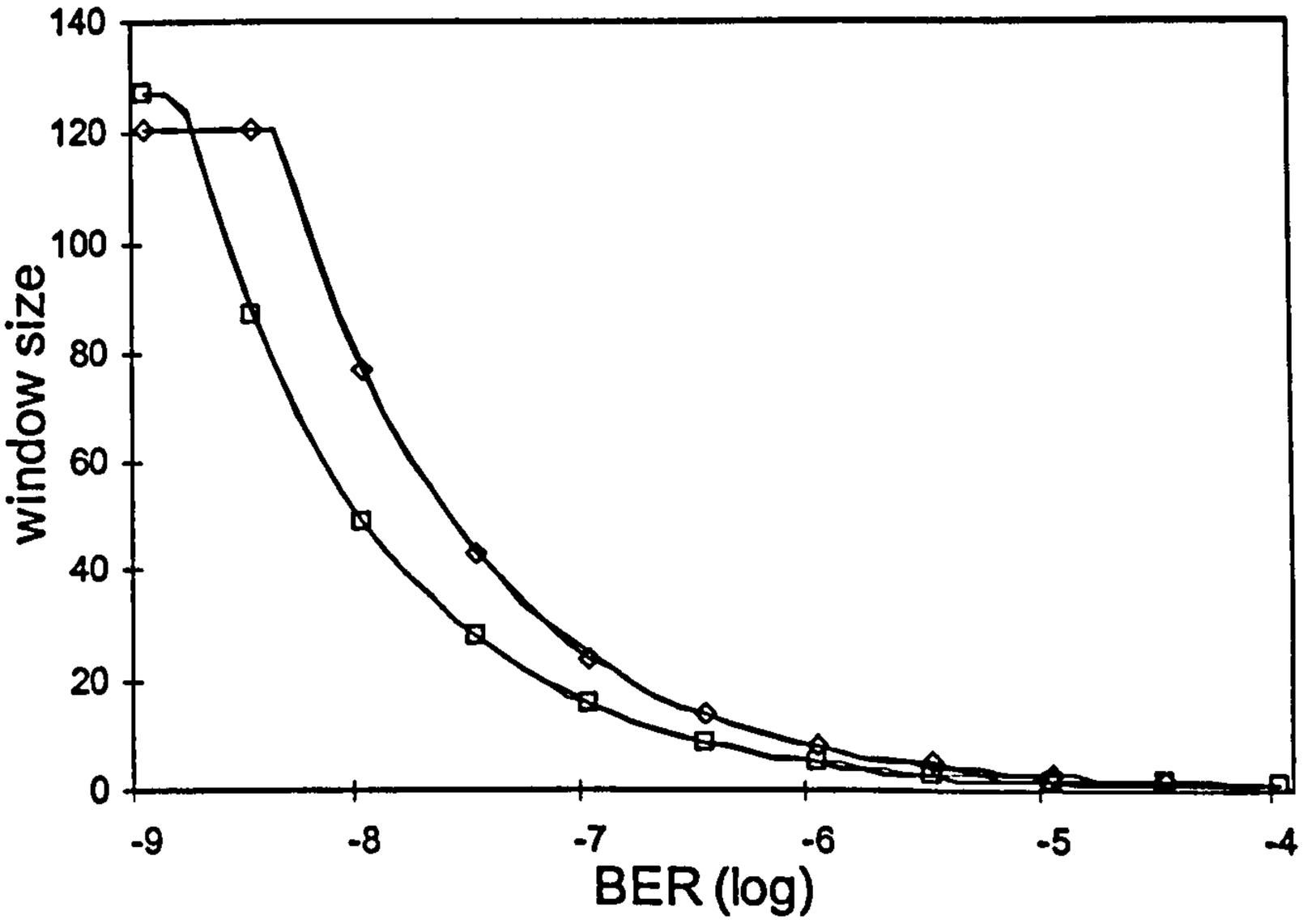

- *optimum N (analysis), C=16Mbit/s, t_{ta}=0.1ms*
□ *optimum N (numerical), C=16Mbit/s, t_{ta}=0.1ms*
- *optimum N (analysis), C=4Mbit/s, t_{ta}=1ms*
◇ *optimum N (numerical), C=4Mbit/s, t_{ta}=1ms*

Figure 4.4 Optimum window size validation, l=16Kbits, $t_{Fout}=t_{lmax}+2t_{ta}$

by decreasing frame size. A small frame size reduces frame error probability and the necessity for retransmissions. However, as each frame transmission requires the transmission of flags, address field, control field and FCS, employing small frame sizes results in relative increase of overheads. Frame size adjustment may require buffer reorganisation if adjustment on frame retransmissions is implemented. Thus, optimum frame size implementation is more difficult than optimum window size implementation but it may also be employed for increasing utilization performance.

The following approximations are considered for small p_b

$$p = 1-(1-p_b)^{l+l'} \approx (l+l')p_b \tag{4.10}$$

$$\frac{1-p}{p} = \frac{1}{p} - 1 \approx \frac{1}{p} \tag{4.11}$$

$$(l+l')p_b t_{Fout} = 0 \tag{4.12}$$

$$(l+l')p_b t_s = 0 \tag{4.13}$$

$$1-(1-(l+l')p_b)^N \approx N(l+l')p_b - \frac{N(N-1)}{2}(l+l')^2 p_b^2 \tag{4.14}$$

and U is given, to a good approximation, by

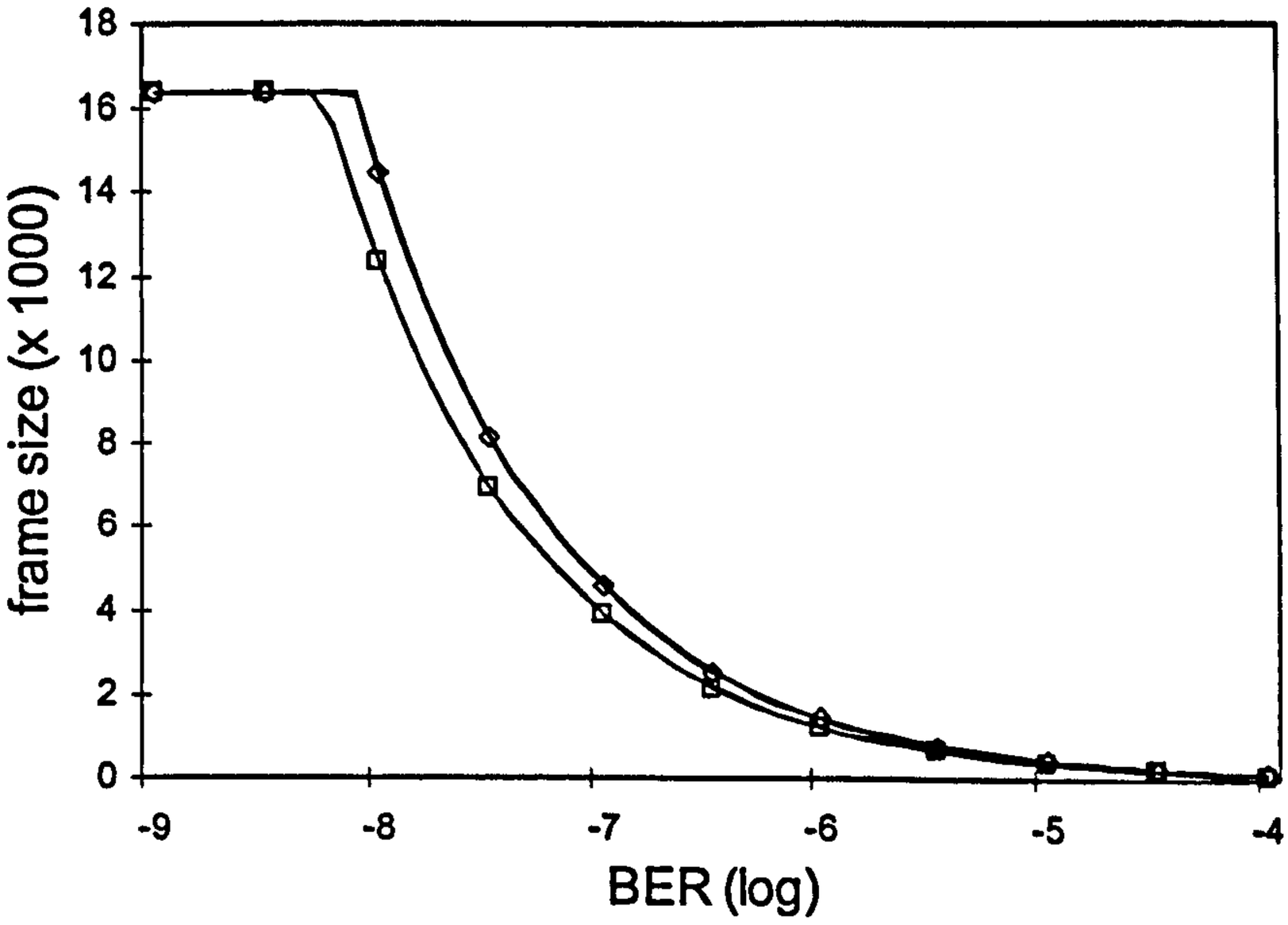

- optimum l (analysis), C=16Mbit/s, t_{ta}=0.1ms
□ optimum l (numerical), C=16Mbit/s, t_{ta}=0.1ms
- optimum l (analysis), C=4Mbit/s, t_{ta}=1ms
◇ optimum l (numerical), C=4Mbit/s, t_{ta}=1ms

Figure 4.5 Optimum frame size validation, N=127, $t_{Fout}=t_{Imax}+2t_{ta}$

$$U=\frac{l}{2Np_b}\cdot\frac{2Np_b-N(N-1)(l+l')p_b^2}{(l+l')+\frac{t_{ack}C}{N}} \tag{4.15}$$

The derivative against *l* is taken, set equal to zero and after some algebra, we derive that optimum frame size values are given to a good approximation by

$$l_{opt}=\sqrt{\frac{2(Nl'+t_{ack}C)}{N^2p_b}} \tag{4.16}$$

The optimum frame size values versus BER for a fixed window size of 127 are shown in Fig. 4.5. As expected, frame size should be decreased for high BER in order to increase utilization. Note that at very low BER, the optimum frame size values should be greater than the maximum frame size value of 16Kbits allowed by the IrLAP specification. As in the case of optimum window size values, all approximations considered in deriving (4.16) are validated by comparing optimum values given from (4.16) with optimum values derived by employing numerical methods in (3.15) for a 16Mbit/s link with t_{ta}=0.1ms and for a 4Mbit/s link with t_{ta}=1 ms.

An important conclusion can be extracted by observing that (4.9) and (4.16) for optimum values can be rewritten as

$$Nlp_b \frac{Nl}{2} = t_{ack}C + Nl' \tag{4.17}$$

Equation (4.17) reveals that maximum utilization is achieved when the probability of a bit error in a window frame transmission ($\approx Nlp_b$), times the number of bits that have to be retransmitted due to the error occurred, which on average is half the window transmission $Nl/2$, is equal to the acknowledgement time in bits $t_{ack}C$ plus the number of overhead bits in the window transmission Nl'.

The term Nl' is missing from (4.9) because, if optimum window size values are implemented, optimum N becomes relatively small for high BER, so term Nl' can be safely neglected [92].

4.2.3 Simultaneous optimal window and frame sizes

If the window and frame size parameters can be simultaneously adjusted, maximum utilization performance can be achieved. Optimum N and l values are derived by taking $\frac{\partial U}{\partial N} = \frac{\partial U}{\partial l} = 0$ [98]. First, the derivative versus N can be taken following the analysis in section 4.2.1. Optimum N values derived by setting the derivative equal to zero can be substituted to utilization equation. Utilization U is now a function of frame size l for optimum N values. The derivative versus l can now be taken and set equal to zero to derive optimum l values. N_{opt} given by (4.8) should be used as the assumption $l>>l'$ is no longer valid as optimum l values may be significantly small.

$$N_{opt} = \sqrt{\frac{2t_{ack}}{pt_l}} \approx \sqrt{\frac{2t_{ack}}{(l+l')p_b \frac{l+l'}{C}}} = \sqrt{\frac{2t_{ack}C}{(l+l')^2 p_b}} \tag{4.18}$$

and

$$N_{opt}(l+l') = \sqrt{\frac{2t_{ack}C}{p_b}} = c \tag{4.19}$$

Considering (3.5), utilization equation (3.15) can be rewritten as

$$U = \frac{l(1-p)}{pC} \cdot \frac{1-(1-p_b)^{N(l+l')}}{N\frac{l+l'}{C} + p(t_{Fout} + t_s) + t_{ack}} \tag{4.20}$$

Considering (4.19), (4.20) becomes

$$U=\frac{l(1-p)}{pC}\cdot\frac{\left(1-(1-p_b)^c\right)}{\left(\frac{c}{C}+p\left(t_{Fout}+t_s\right)+t_{ack}\right)} \tag{4.21}$$

Assuming the valid approximation $p\approx(l+l')p_b$ then

$$U=\frac{\left(1-(1-p_b)^c\right)}{c}\cdot\frac{l\left(1-(l+l')p_b\right)}{(l+l')p_b\left(1+(l+l')p_b\frac{\left(t_{Fout}+t_s\right)C}{c}+\frac{t_{ack}C}{c}\right)} \tag{4.22}$$

Denoting $s=\frac{\left(t_{Fout}+t_s\right)C}{c}$, taking the first derivative versus l and by setting it to zero

$$\left(-2lp_b-(l'p_b-1)\right)\left((l+l')^2p_b^2s+(l+l')p_b\left(1+\frac{t_{ack}C}{c}\right)\right)+\left(l^2p_b+l(l'p_b-1)\right)\left(2(l+l')p_b^2s+p_b\left(1+\frac{t_{ack}C}{c}\right)\right)=0 \tag{4.23}$$

Considering the valid approximation $l'p_b\approx 0$, we reach, after some algebra

$$-l^2p_b\left(s+2l'p_bs+1+\frac{t_{ack}C}{c}\right)+p_bl\left(-2l'^2p_bs-2l'\left(1+\frac{t_{ack}C}{c}\right)\right)+l'^2p_bs+l'\left(1+\frac{t_{ack}C}{c}\right)=0 \tag{4.24}$$

As $-2l'^2p_bs-2l'\left(1+\frac{t_{ack}C}{c}\right)\approx 0$

$$l_{opt}^2=\frac{l'\left(l'p_bs+1+\frac{t_{ack}C}{c}\right)}{p_b\left(s+2l'p_bs+1+\frac{t_{ack}C}{c}\right)} \tag{4.25}$$

and, to a very good approximation,

$$l_{opt}\approx\sqrt{\frac{l'}{p_b}} \tag{4.26}$$

By substituting (4.26) into (4.9), we obtain

$$N_{opt}\approx\sqrt{\frac{2t_{ack}C}{l'}} \tag{4.27}$$

Fig. 4.6 plots simultaneously optimal window and frame sizes for 4Mbit/s links with t_{ta}=0.1ms. It is observed that for a high range of BERs (less than $10^{-6.5}$), (4.26) suggests that frame size values greater than 16Kbits (the maximum allowed by IrLAP) should be employed. For this range, optimum N values are given by (4.9) instead of (4.27) since frame size values are constant (l=16Kbits) and not optimum. As a very good match between values given by (4.9)(4.26) and (4.27) and optimum values derived by using numerical methods in (3.15) is observed, approximations made to derive (4.26) and (4.27) are validated. Slight differences are observed mainly for high BER because

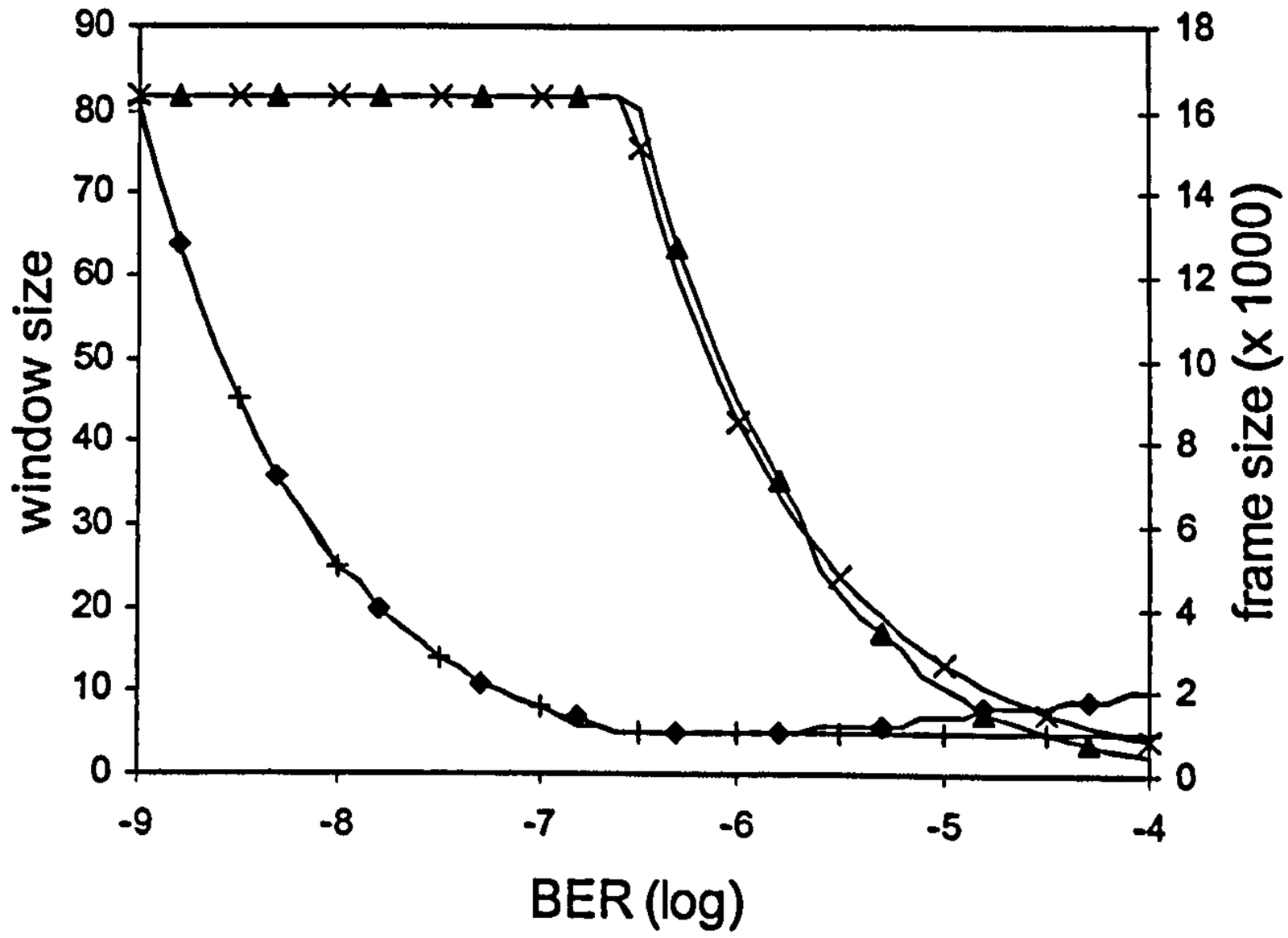

+ *optimum N (analysis)*
◆ *optimum N (numerical)*
x *optimum l (analysis)*
▲ *optimum l (numerical)*

Figure 4.6 Optimum window and frame size validation for C=4Mbit/s, t_{ta}=0.1ms, $t_{Fout}=t_{Imax}+2t_{ta}$

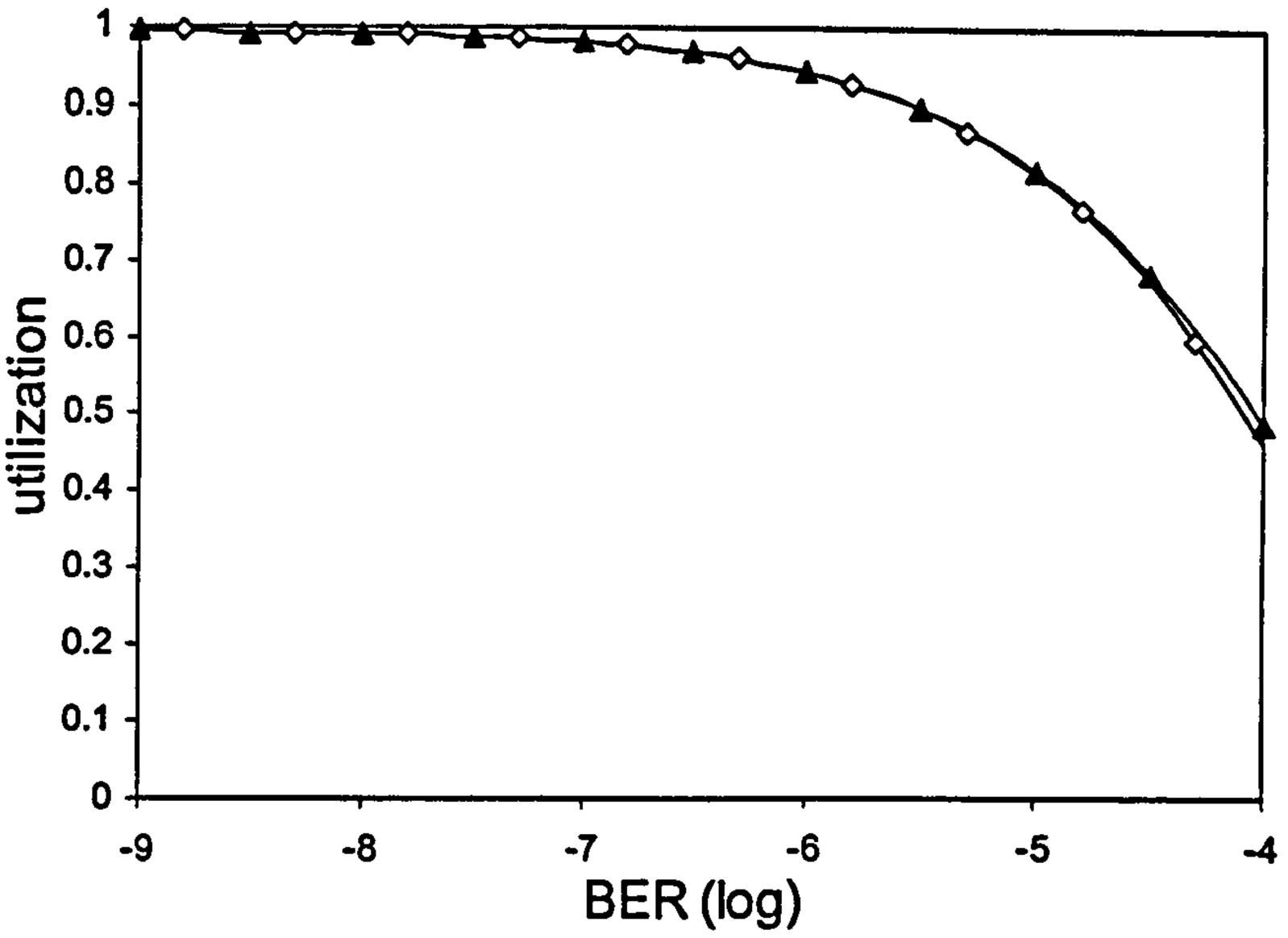

◇ *maximum utilization for optimum N and l values (analysis)*
▲ *maximum utilization for optimum N and l values (numerical)*

Figure 4.7 Utilization for simultaneous optimal N and l, C=4Mbit/s, t_{ta}=0.1ms, $t_{Fout}=t_{Imax}+2t_{ta}$

optimum *N* values given by the mathematical analysis and (4.27) are real values and have to be rounded as *N* can, of course, take only integer values. These differences result in negligible difference in maximum utilization as shown in Fig. 4.7.

An important conclusion can be extracted by observing that (4.9) and (4.26) for optimum values can be rewritten as

$$N_{opt} l_{opt} p_b \frac{N_{opt} l_{opt}}{2} = t_{ack} C \tag{4.28}$$

$$l_{opt} l_{opt} p_b = l' \tag{4.29}$$

Equation (4.29) reveals that maximum utilization is achieved when the probability of a bit error in the optimum frame length ($\approx l_{opt} p_b$), times the number of bits that have to be retransmitted due to this error ($\approx l_{opt}$) must be equal to the frame bit overhead l'. This equation shows that optimum frame size values should balance between time consumed on retransmitting error frames and time consumed on transmitting overheads. Equation (4.28) shows that maximum utilization is achieved when the probability of a bit error in the optimum window frame transmission ($\approx N_{opt} l_{opt} p_b$), times the number of bits that have to be retransmitted in the following frames due to this error, which on average is half the window transmission $N_{opt} l_{opt}/2$, is equal to the acknowledgement time in bits $t_{ack} C$. In other words, the bits transmitted in the optimum window transmission, $N_{opt} l_{opt}$, should balance the time utilized in retransmitting out of sequence frames and the time utilized on acknowledgments.

4.3 IrLAP Performance for optimum value implementation

Fig. 4.8 compares the utilization of a 16Mbit/s link with t_{ta}=0.1ms employing N=127 frames and l=16Kbits with the utilization achieved by implementing optimum window or frame size values given by (4.9) and (4.16) respectively. It shows that utilization is significantly improved for a wide range of BER (from 10^{-7} to 10^{-4}) if optimum window or frame size values are employed. For low BER, utilization for optimum N values is higher than utilization for optimum l values because as window size decreases, fewer frame overheads l' are utilized in a window transmission. The situation is reversed for high BER because the optimum window size implementation always utilizes large frame sizes (l=16Kbits), has a high frame error probability in high BER links and often the P-bit is lost. Fig. 4.8 also shows that applying optimum window and frame size values simultaneously (given by 4.9, 4.26 and 4.27) results in better performance overall. Fig. 4.9 shows the % time portion utilized on various IrLAP tasks for simultaneously optimal N and l values for the same link parameters. It reveals

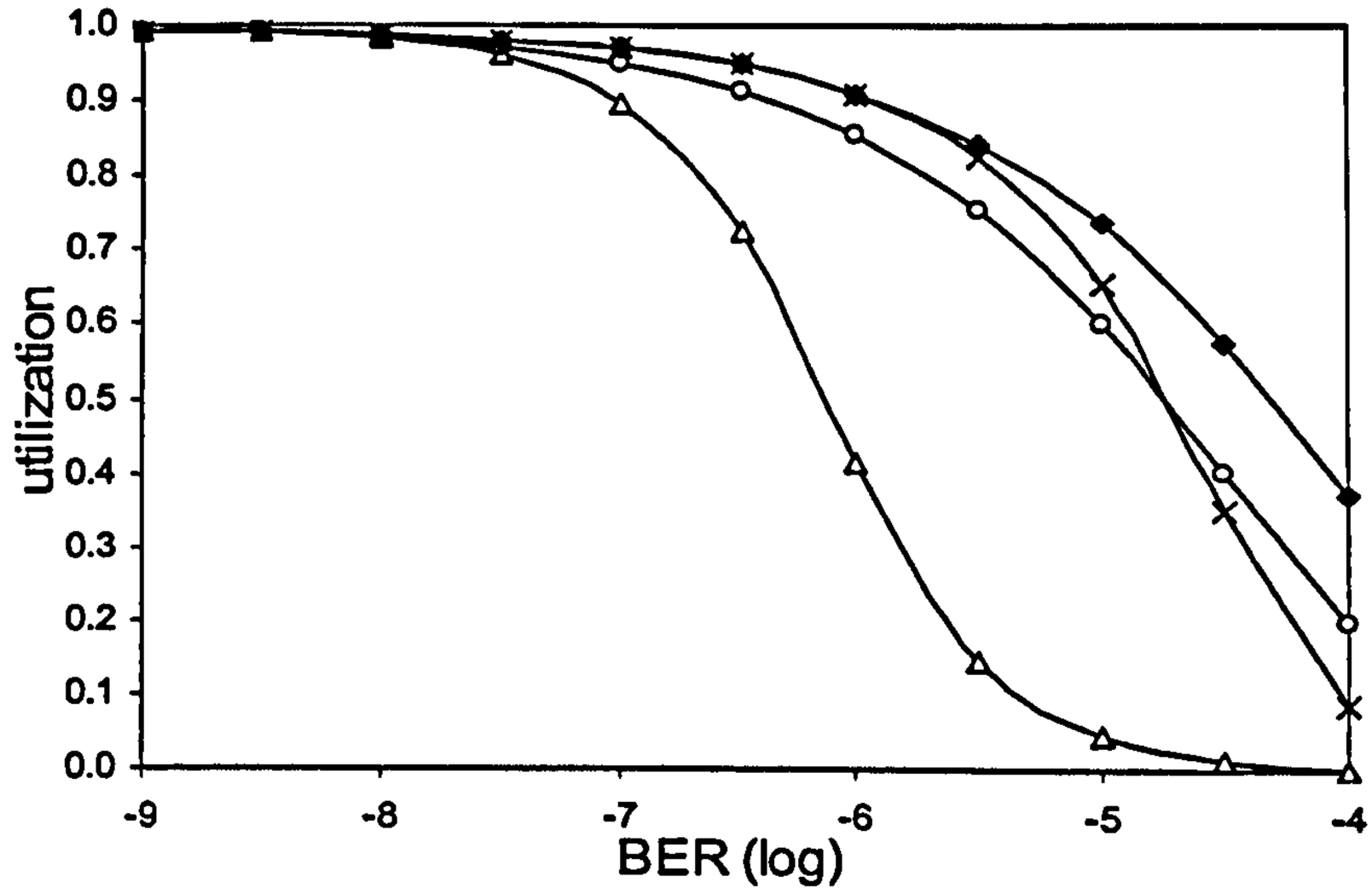

△ *N=127, l=16Kbits*
∘ *optimum l, N=127*
x *optimum N, l=16Kbits*
◆ *optimum N and optimum l*

Figure 4.8 Utilization against BER, C=16Mbit/s, t_{ta}=0.1ms, $t_{Fout}=t_{Imax}+2t_{ta}$

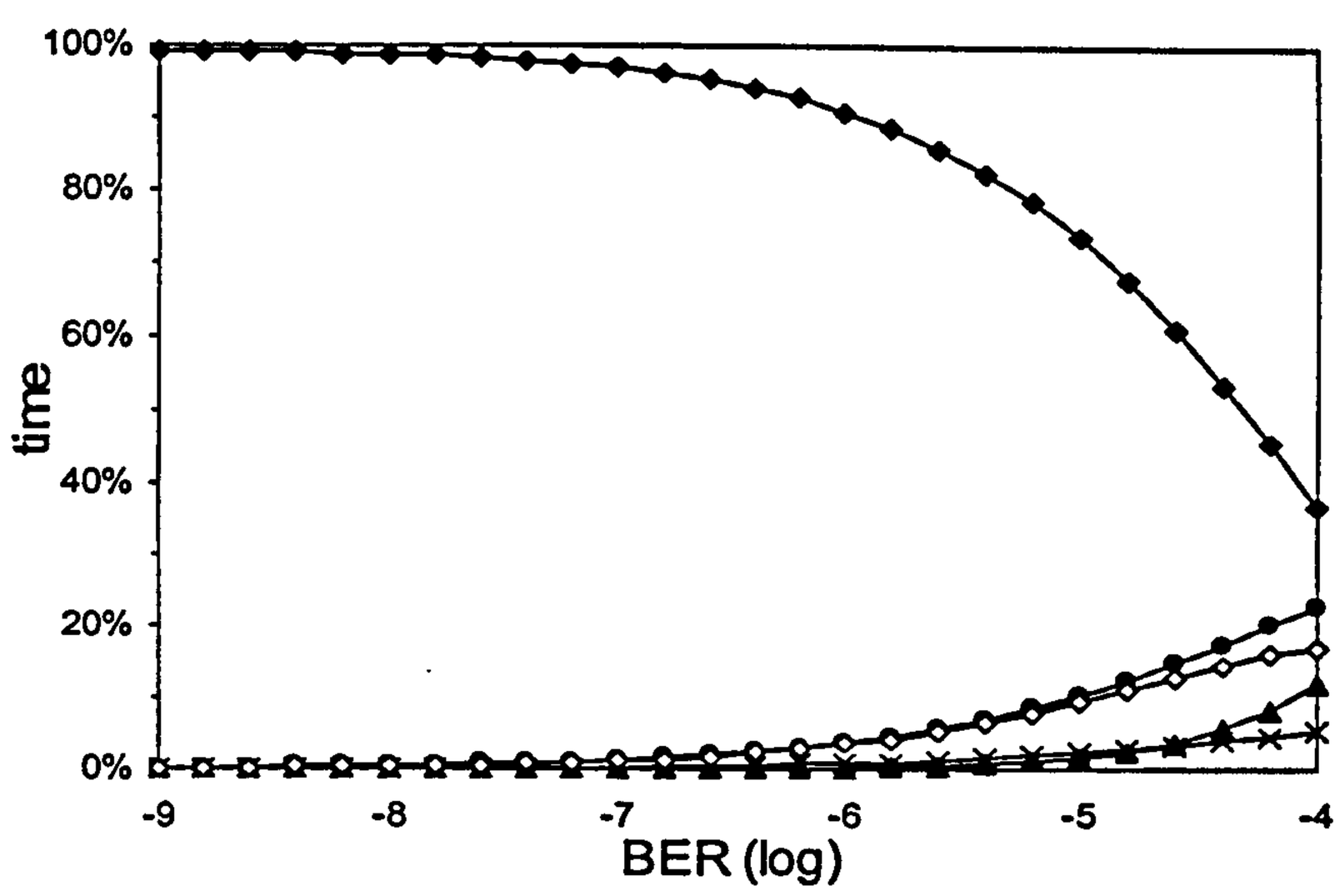

◆ *useful data transmission (utilization)*
◇ *retransmission of correctly received out of sequence frames*
x *retransmission of error frames*
▲ *F-timer expiration*
● *reversing link direction (hardware latency)*

Figure 4.9 Time allocation of various IrLAP tasks against BER for simultaneous optimal N and l, C=16Mbit/s, t_{ta}=0.1ms, $t_{Fout}=t_{Imax}+2t_{ta}$

that the retransmission of correctly received out of sequence frames is of no importance any more as optimum window and frame size employment reduced the probability of transmitting out of sequence frames. The main factor that results in utilization degradation is the hardware latency arising from the frequent link turn around.

Figures 4.10 and 4.11 show the effect of reducing t_{ta} in 16Mbit/s links by plotting the same results as figures 4.8 and 4.9 for t_{ta}=0.01ms. Comparison of figures 4.8 and 4.10 shows that reducing t_{ta} significantly improves only the simultaneously optimal N and l implementation because the link has a high turn around frequency in this case. For high BER, Fig. 4.11 shows that the main detrimental factor to utilization in this case is the F-timer expiration; IrLAP utilizes 36% of the time on F-timer expiration and 46% of the time on transferring payload data (U=0.46) for BER=10^{-4}.

This analysis leads to the conclusion that the implementation of optimal window size (N) and frame size (l) values simultaneously results in significant utilization improvement. The minimum turn around time (t_{ta}) and F-timer time-out period (t_{Fout}) are the main detrimental factors to utilization if optimal N and l values are implemented. Reducing t_{ta} (a physical layer parameter) significantly improves utilization.

4.4 IrLAP S-frame modification combined with optimum values

Analysis in the previous section revealed the importance of t_{ta} and t_{Fout} to IrLAP performance when optimal N and l values are employed. If t_{ta} is adequately decreased, time utilized on F-timer becomes of prime importance. This section discusses IrLAP performance when optimal N and/or l values are implemented for the S-frame modification (proposed in section 4.1) that minimizes delays on F-timer.

Fig. 4.12 compares the utilization of a 16Mbit/s link with t_{ta}=0.1ms employing N=127 frames and l=16Kbits with the utilization achieved by implementing optimum window or frame size values given by (4.9) and (4.16) respectively. Utilization for optimum N values is usually higher than utilization for optimum l values because the optimum window size implementation utilizes fewer frame overheads l' in a window transmission and delays from F-timer are minimized in the S-frame modification case. Simultaneous implementation of optimal window and frame size values always results in better performance. Fig. 4.13 shows the % time portion utilized on various IrLAP tasks for simultaneously optimal N and l values for the same link parameters. The main detrimental factor to utilization is again the hardware latency arising from the frequent link turn around.

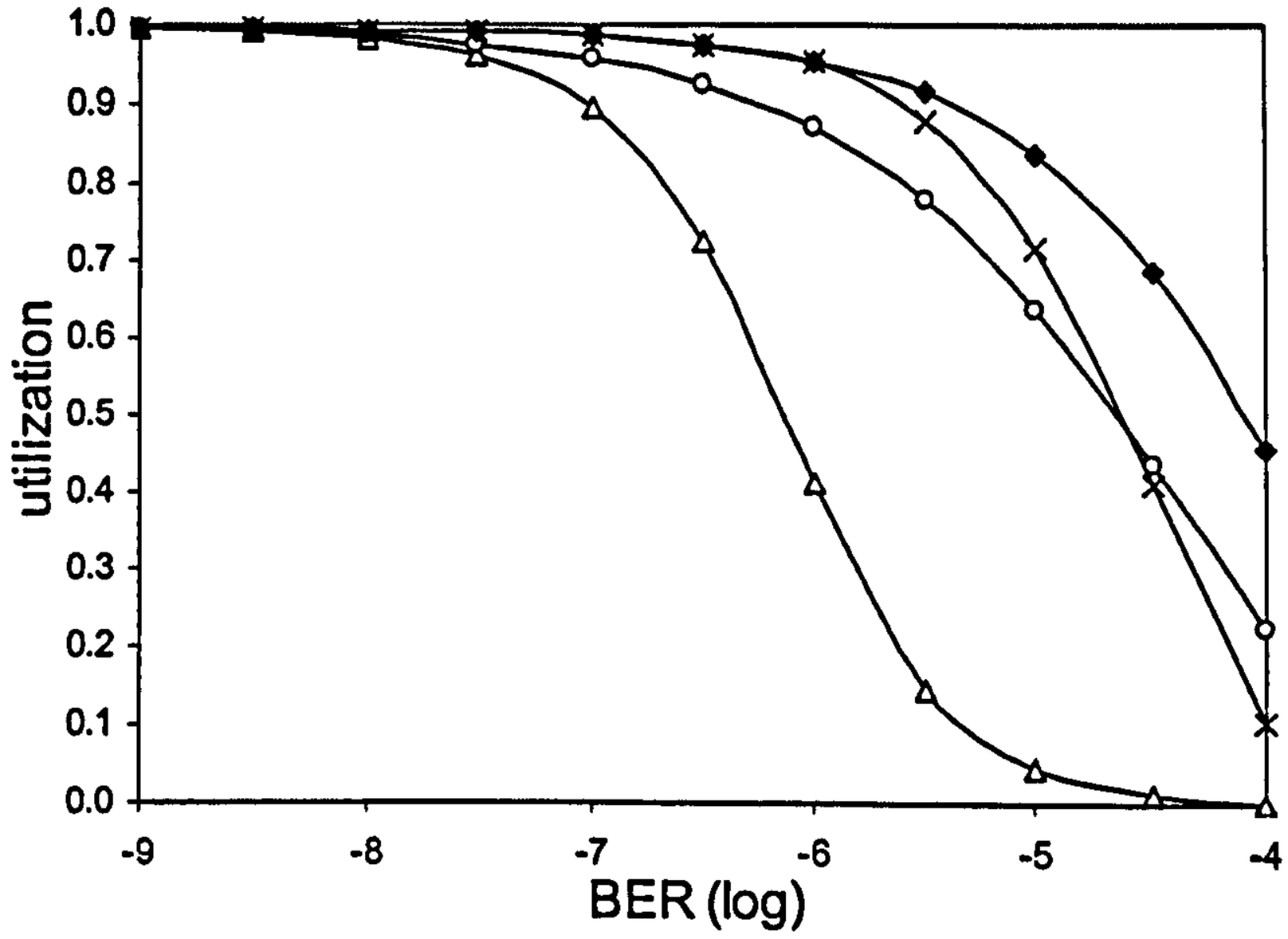

△ *N=127, l=16Kbits*
× *optimum N, l=16Kbits*
○ *optimum l, N=127*
◆ *optimum N and optimum l*

Figure 4.10 Utilization against BER, C=16Mbit/s, t_{ta}=0.01ms, $t_{Fout}=t_{Imax}+2t_{ta}$

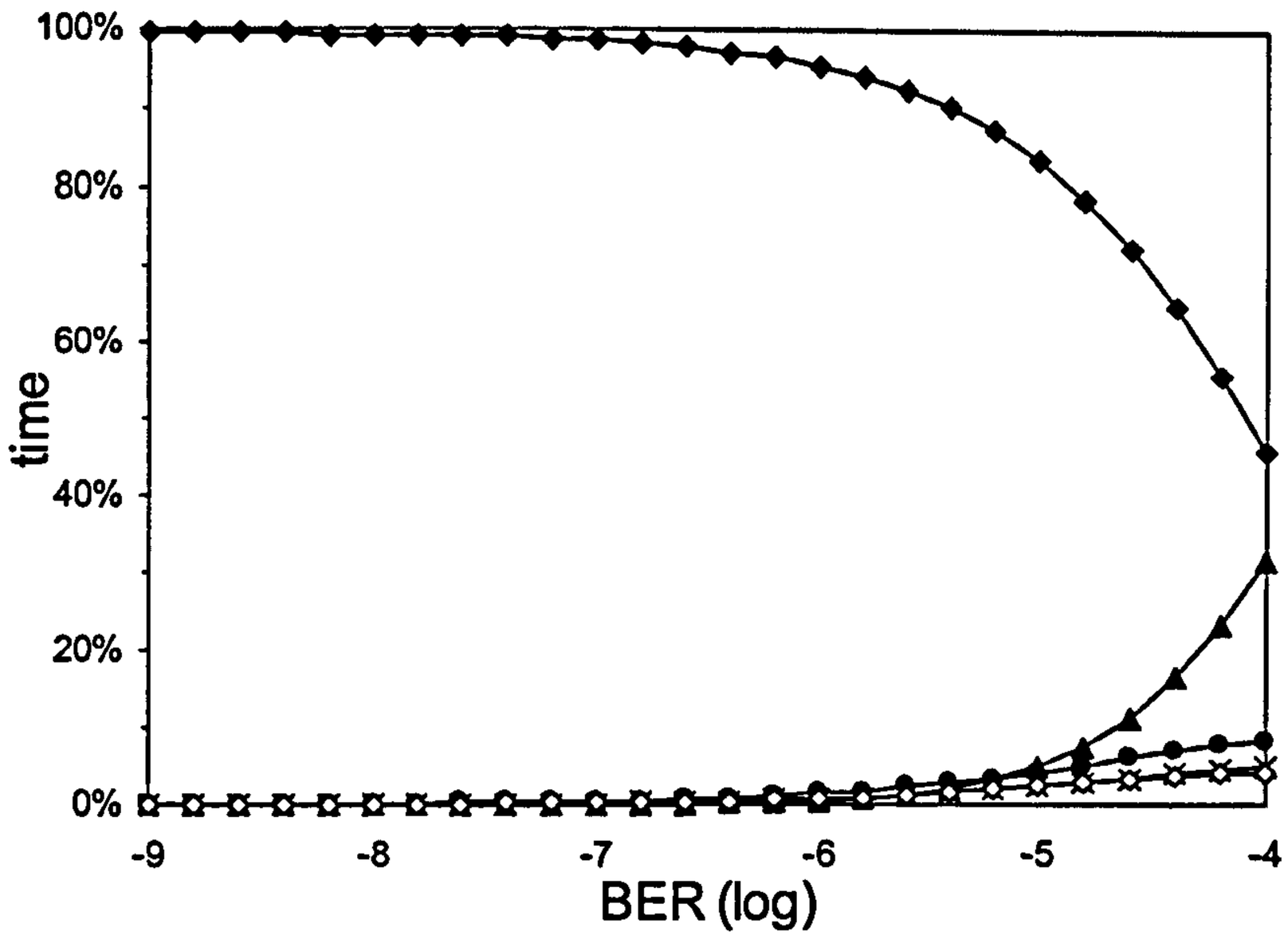

◆ *useful data transmission (utilization)*
◇ *retransmission of correctly received out of sequence frames*
× *retransmission of error frames*
▲ *F-timer expiration*
● *reversing link direction (hardware latency)*

Figure 4.11 Time allocation of various IrLAP tasks against BER for simultaneous optimal N and l, C=16Mbit/s, t_{ta}=0.01ms, $t_{Fout}=t_{Imax}+2t_{ta}$

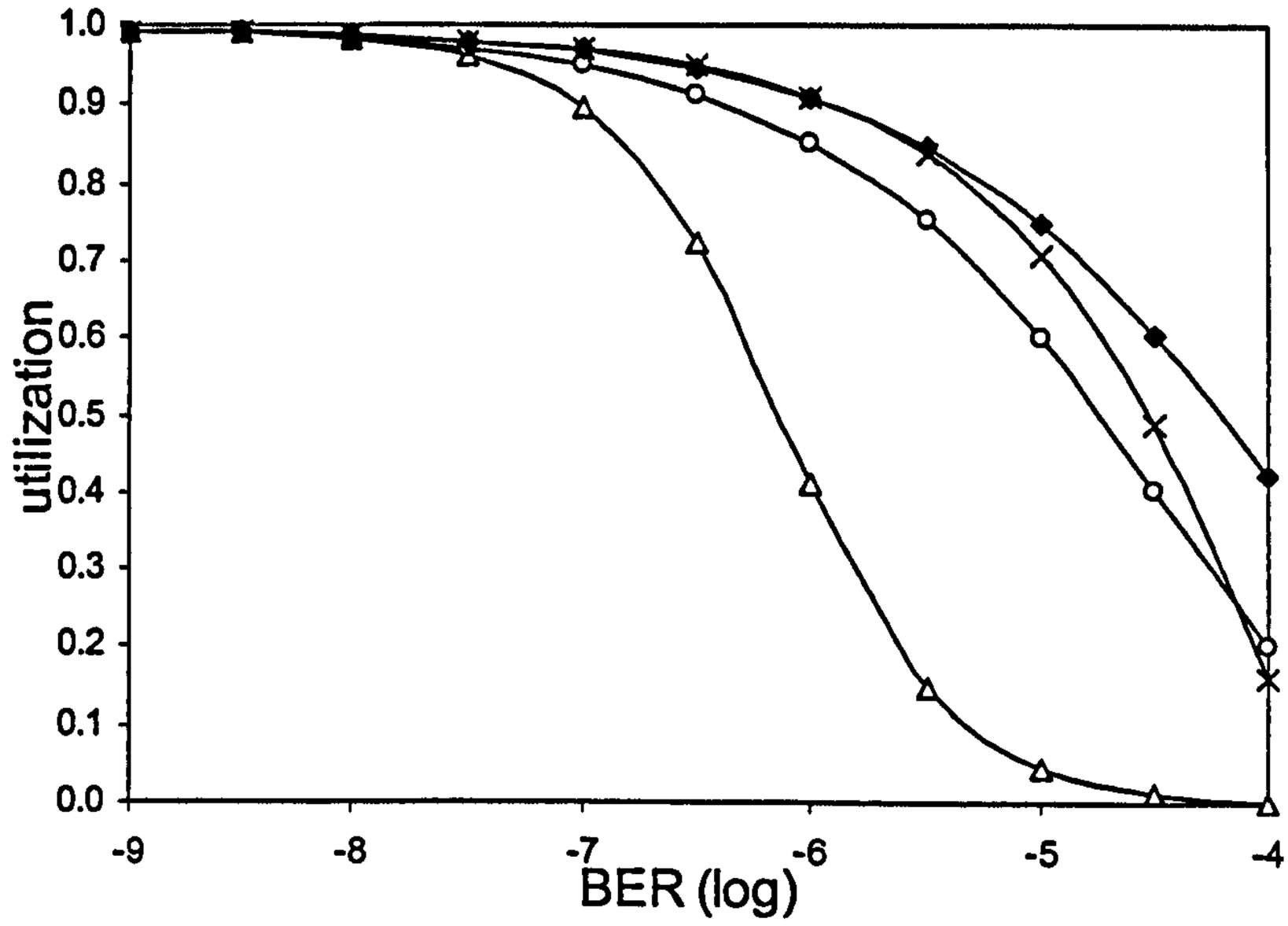

△ *N=127, l=16Kbits*
∘ *optimum l, N=127*
× *optimum N, l=16Kbits*
◆ *optimum N and optimum l*

Figure 4.12 Utilization against BER, C=16Mbit/s, t_{ta}=0.1ms, P-bit in S-frame

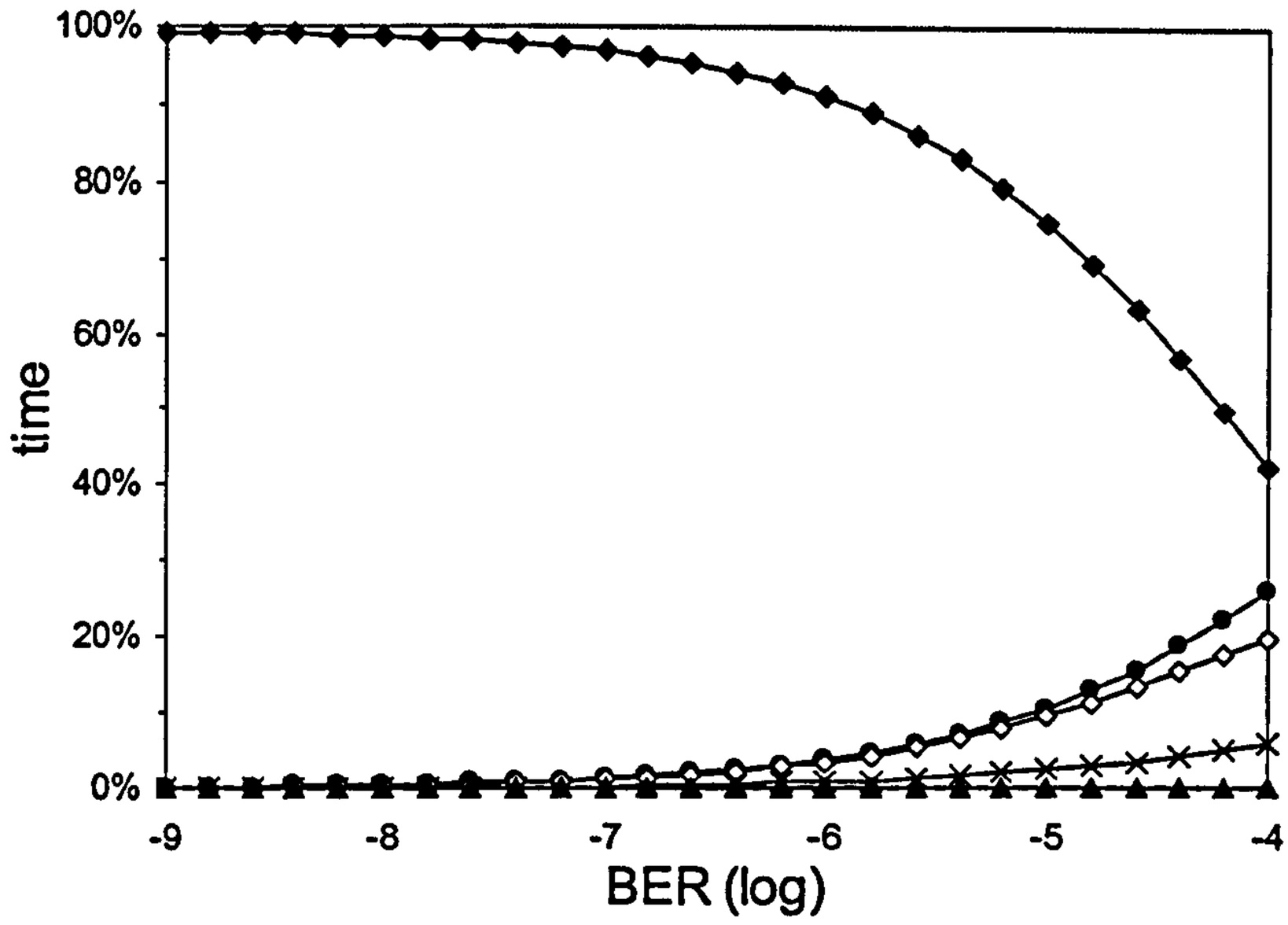

◆ *useful data transmission (utilization)*
◇ *retransmission of correctly received out of sequence frames*
× *retransmission of error frames*
▲ *F-timer expiration*
● *reversing link direction (hardware latency)*

Figure 4.13 Time allocation of various IrLAP tasks against BER for simultaneous optimal N and l, C=16Mbit/s, t_{ta}=0.1ms, P-bit in S-frame

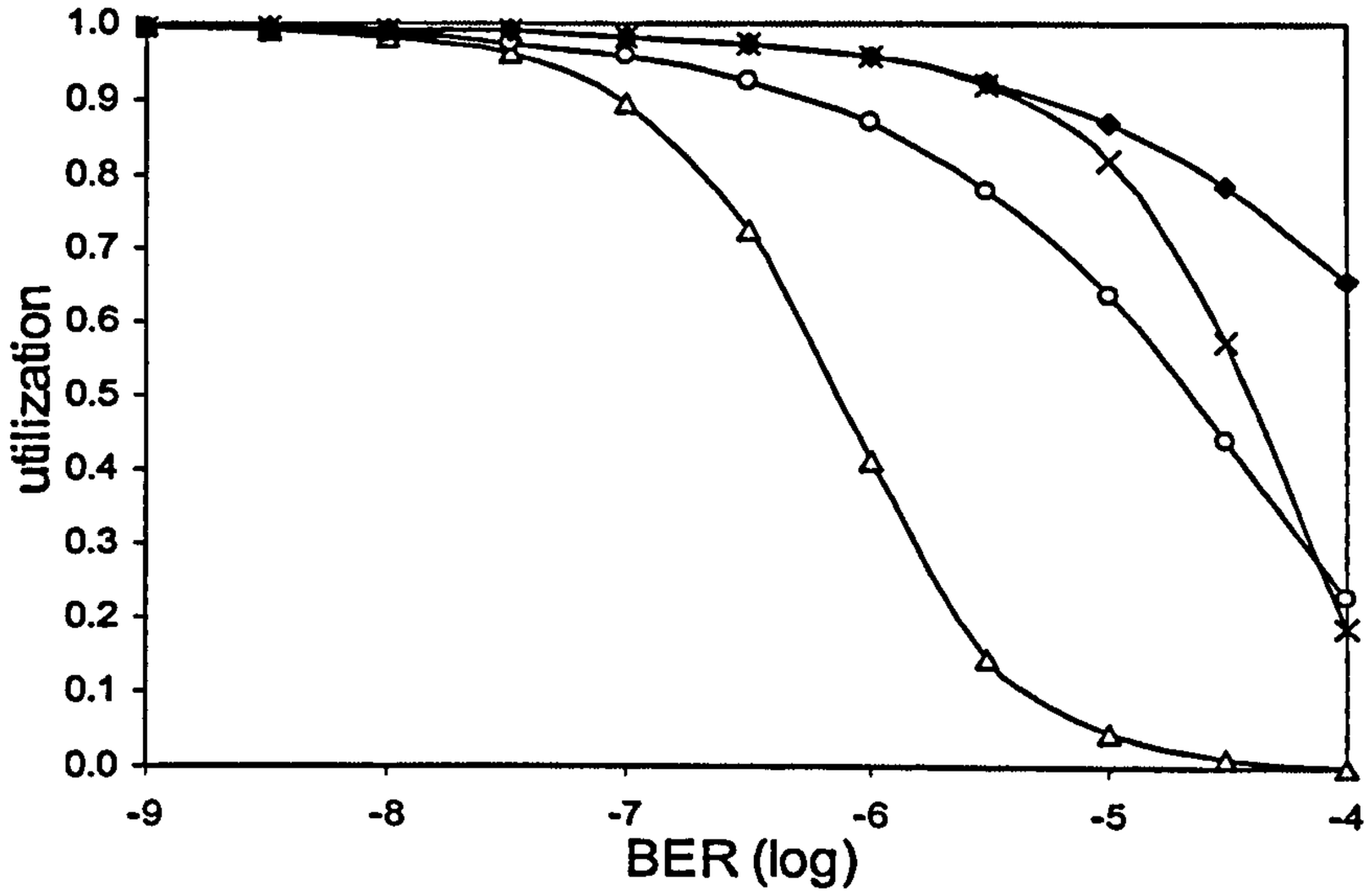

△ *N=127, l=16Kbits*
∘ *optimum l, N=127*
x *optimum N, l=16Kbits*
◆ *optimum N and optimum l*

Figure 4.14 Utilization against BER, C=16Mbit/s, t_{ta}=0.01ms, P-bit in S-frame

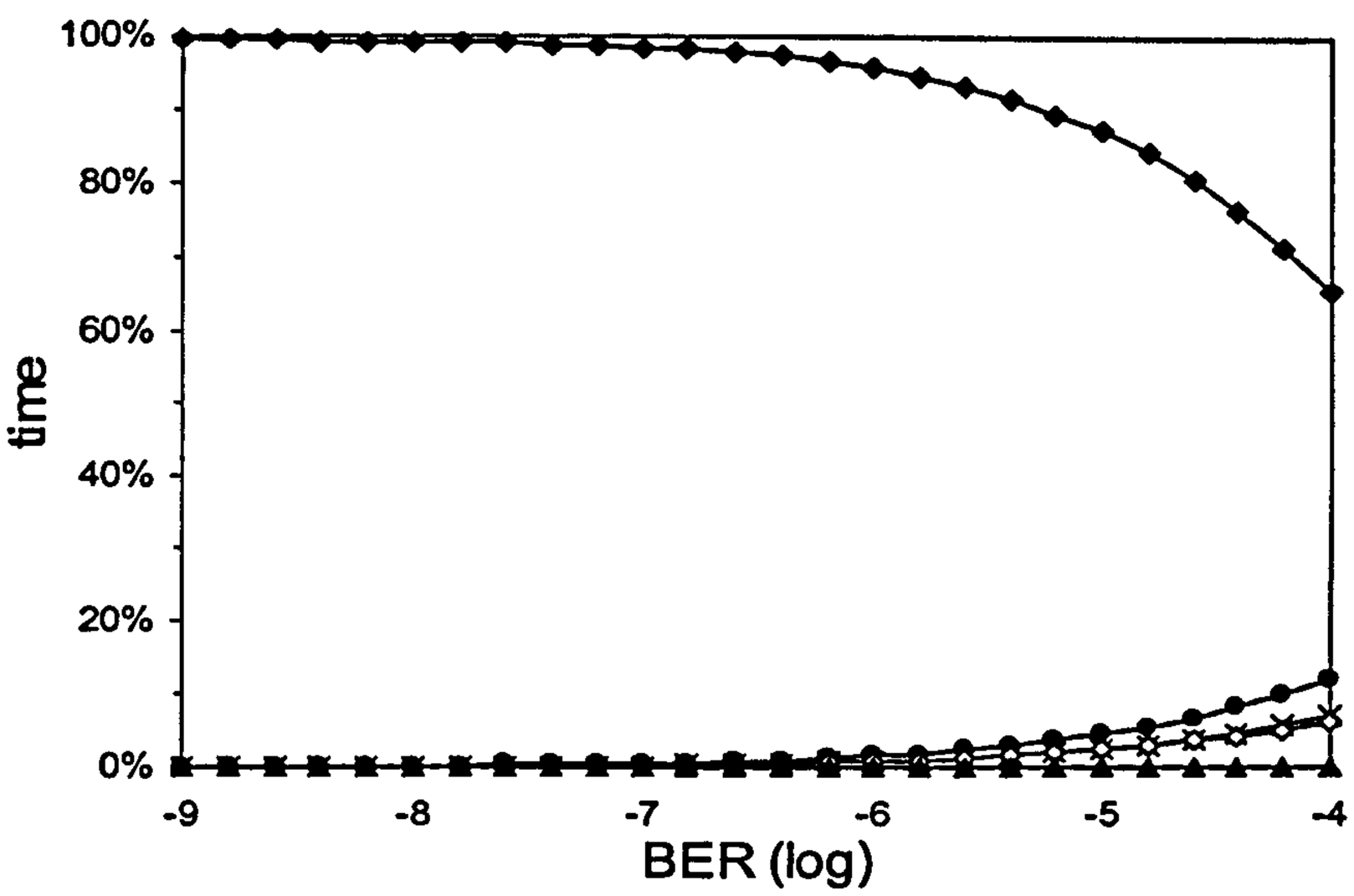

◆ *useful data transmission (utilization)*
◇ *retransmission of correctly received out of sequence frames*
x *retransmission of error frames*
▲ *F-timer expiration*
● *reversing link direction (hardware latency)*

Figure 4.15 Time allocation of various IrLAP tasks against BER for simultaneous optimal N and l, C=16Mbit/s, t_{ta}=0.01ms, P-bit in S-frame

Figures 4.14 and 4.15 show the same results when reducing t_{ta} to 0.01ms. Fig. 4.14 shows that the t_{ta} reduction significantly improves the utilization for the optimum N and the simultaneous optimal N and l cases. Fig. 4.15 shows that all IrLAP tasks affecting utilization are kept to minimum. As a result, 16 Mbit/s links employing a small t_{ta} of

0.01ms and the proposed S-frame modification achieve a utilization of 0.66 (U_{RR}=0.66) even for a 10^{-4} BER by employing optimum window and frame size values.

This analysis concludes that the implementation of simultaneous optimal window and frame size values, combined with the S-frame modification and a small minimum turn around time results in significant utilization figures in high BER links.

4.5 Practical implementation of optimum values

This section examines the practical utilization improvement that can be achieved if the transmitter implements the optimum values for window and/or frame size parameters derived in the previous section. The OPNET simulator presented in section 3.5.1 is altered to implement window and frame size adaptivity to link BER. The transmitter can estimate the link BER based on the frame acknowledgments provided by the receiving station [100]. Based on this estimation, the transmitter calculates the window and frame size values it implements using equations (4.9)(4.16)(4.26) and (4.27) for optimum values.

According to the IrLAP analysis presented in section 4.3, maximum window and frame size values should be implemented at link BERs less than 10^{-9}. The analysis also shows that if the link BER is higher that 10^{-4}, the low link quality at the physical layer renders the link unoperational and optimum value implementation is unprofitable. Thus, only the BER range [10^{-9}, 10^{-4}] is considered. Simulation results are obtained by varying link BER using a step of 0.1 in the logarithmic scale in the above range. Simulations run for 15 sec after a 'warm-up' period of 1 sec.

An algorithm is presented in [68] for optimizing frame size for full duplex "optimal" ARQ protocols, i.e. protocols that retransmit only error frames. The presented algorithm estimates optimum frame size based on the number of frame retransmission requests R out of the last M frame transmissions. Analysis presented in [68] concludes that an accurate estimate of the link BER is not necessary in order to choose the optimum frame size for nearly maximum performance; an approximate estimate is usually sufficient. In the IrLAP information transfer procedure, as the receiver rejects frames not received correctly, the transmitter receives information about bit errors occurring on its transmission. Despite the fact that the bit error position in an error frame is not known, an approximate bit error evaluation can be made by the transmitter, as it knows the frame containing the error bit. This section proposes a model in which

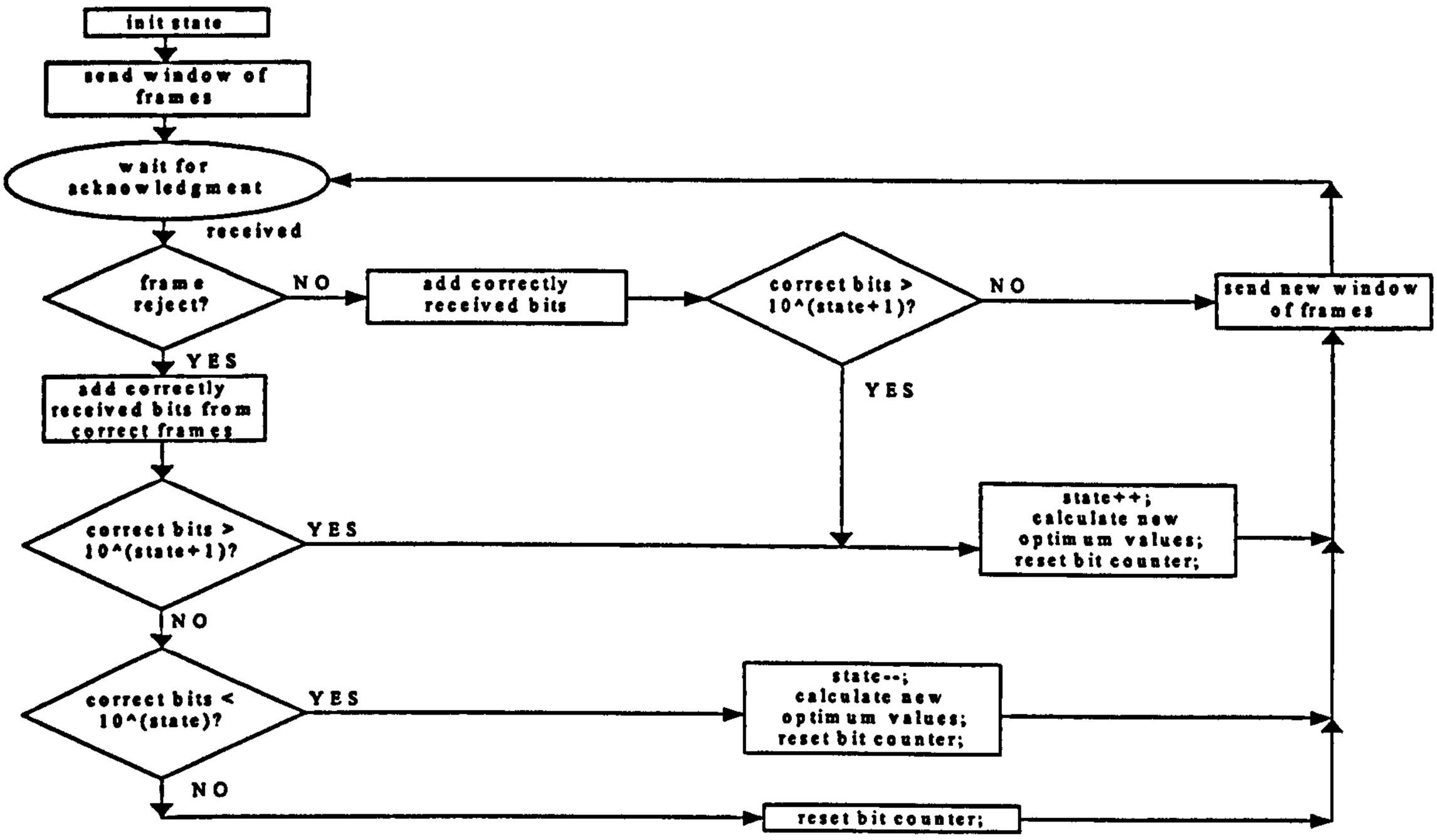

Figure 4.16 Adaptive window and/or frame size scheme based on link BER evaluation

the transmitter approximately estimates link BER by counting correct frame transmissions before a frame is rejected. Based on this estimation of the number of correctly transmitted bits between two error bits, the transmitter adjusts window and/or frame size, according to eq. (4.9)(4.16)(4.26) and (4.27).

This model assumes that retransmitting buffered copies of error frames using different frame and window sizes does not result in significant processing delays. The transmitter's decisions are based on instant evaluations of link BER. This model may enforce different window and/or frame size values after a bit error assuming that the old values are not suitable. In the proposed adaptive model, the BER range $[10^{-9},10^{-4}]$ is divided to a small number of sub-ranges and optimum values suitable for each subrange are calculated and implemented. Implementation of this model is simple as the transmitter only needs to hold information about its current evaluation of link BER and of the number of sub-ranges implemented in the above BER range.

The transmitter's adaptive model for implementing optimum values is shown in Fig. 4.16. The following example assumes that the BER range $[10^{-9}, 10^{-4}]$ is divided into five subranges, the transmitter's current evaluation of link BER is 10^{-6} (state=6) and that optimum values from eq. (4.9)(4.16)(4.26)(4.27) have been calculated and implemented for $p_b=10^{-6}$. It is also assumed that these values are suitable for the third BER subrange of $[10^{-7},10^{-6}]$. The transmitter then counts the frames acknowledged correctly by the

receiver and multiplies the number of frames correctly received with the frame size it implements. The product represents the number of correctly transmitted bits. If 10,000,000 (10^7) bits are correctly transmitted before an error occurs, the transmitter assumes that link BER is less that 10^{-7}, it changes its current BER evaluation to 10^{-7} (state=7) and calculates new window and/or frame size values from eq. (4.9)(4.16)(4.26)(4.27) for p_b=10^{-7}. The transmitter implements these values in future transmissions and resets counters. If a bit error occurs before 10,000,000 (10^7) but after 1,000,000 (10^6) correctly transmitted bits, the transmitter assumes that its current BER evaluation of 10^{-6} is correct, it continues to implement current optimum values and resets counters. If a bit error occurs before 1,000,000 (10^6) correct bits, the transmitter assumes that link BER is now higher that 10^{-6}. It changes its current BER evaluation to 10^{-5} (state=5), calculates and implements new window and/or frame size values suitable for p_b=10^{-5} and resets counters.

The above set of rules for BER estimation and optimum value adjustment were chosen due to their simplicity. As IrLAP procedures are implemented at low level, simple and easily implemented at run time adaptive rules are needed. Simulation results presented in this section always divide the BER range [10^{-9},10^{-4}] into ten subranges, thus employing eleven different window and/or frame size values.

Fig. 4.17 plots the optimum window size values and the corresponding utilization versus link BER derived by applying numerical methods to eq.(3.15) for a 16Mbps link with t_{ta}=0.1ms and l=16Kbits. It also plots the implemented window sizes in simulation and the resulting utilization. An almost exact match between simulation and maximum utilization is observed. Results show that the implementation of exact optimum window size values for link BER is not necessary. The implementation of window size values close to the optimum value based on estimations of link BER result in a utilization figure very close to the maximum for the specific BER.

Fig. 4.18 plots optimum l values for fixed N=127 frames and the corresponding maximum utilization versus BER by employing numerical methods to eq. (3.15) for a 16Mbps link with t_{ta}=0.1ms. It also plots the implemented frame sizes by the simulator and the resulting utilization. A very close match between simulation and maximum utilization is observed. As a conclusion, an almost optimum IrLAP performance is achieved by implementing ten subranges.

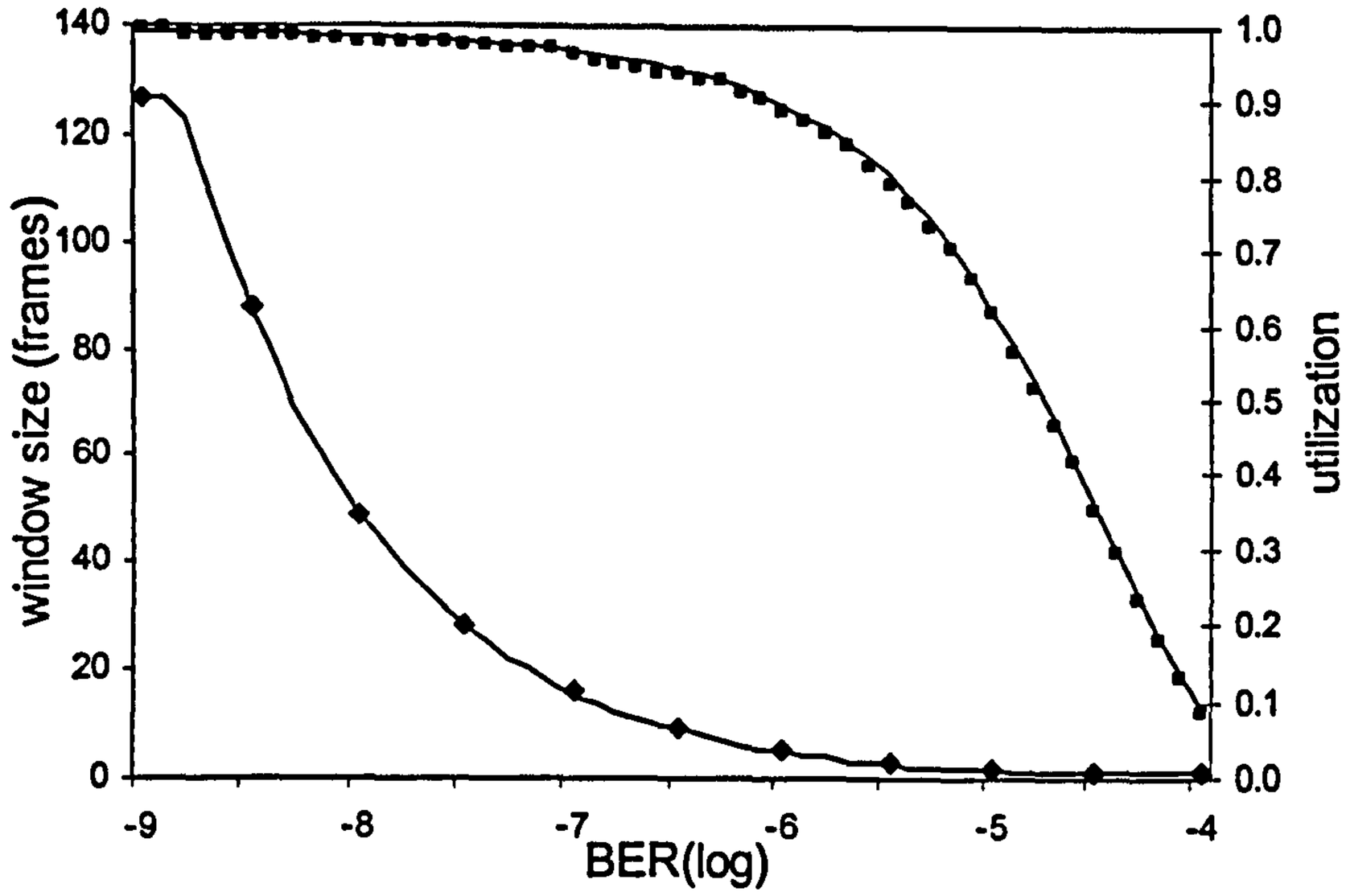

— N optimum (numerical)

◆ N values implemented by primary station in simulation

— optimum utilization (numerical)

■ simulation utilization

Figure 4.17 Utilization comparison for implementing 11 window size values, C=16Mbit/s, t_{ta}=0.1ms, l=16Kbits, $t_{Fout}=t_{lmax}+2t_{ta}$

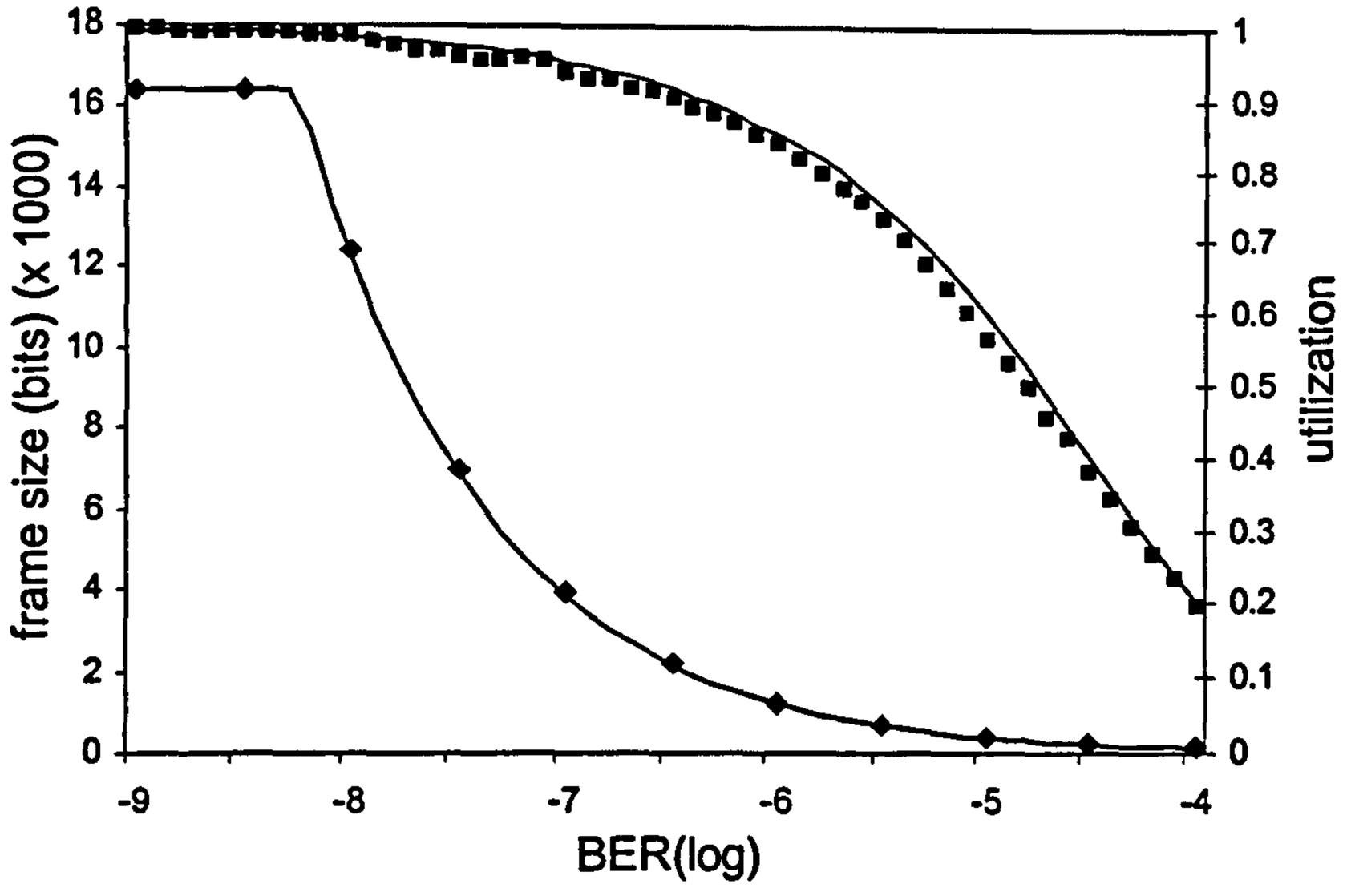

— l optimum (numerical)

◆ l values implemented by primary station in simulation

— optimum utilization (numerical)

■ simulation utilization

Figure 4.18 Utilization comparison for implementing 11 frame size values, C=16Mit/s, t_{ta}=0.1ms, N=127, $t_{Fout}=t_{lmax}+2t_{ta}$

Fig. 4.19 plots simultaneous optimum window and frame size values derived numerically from eq. (3.15) for maximum utilization for a 16Mbps link with t_{ta}=0.1ms. It also plots the optimum values implemented in simulations and derived from eq. (4.9)(4.26)(4.27) for the same link parameters. The simulation utilization is very close to the maximum utilization as presented in Fig. 4.20. As a conclusion, the proposed simple model for BER estimation and implementation of optimum values is very effective. If the primary station implements (a) only eleven different sets for both optimum window and frame size values, (b) simple rules for estimating BER and (c) both optimum window and frame size values, a significant IrLAP increase can be achieved.

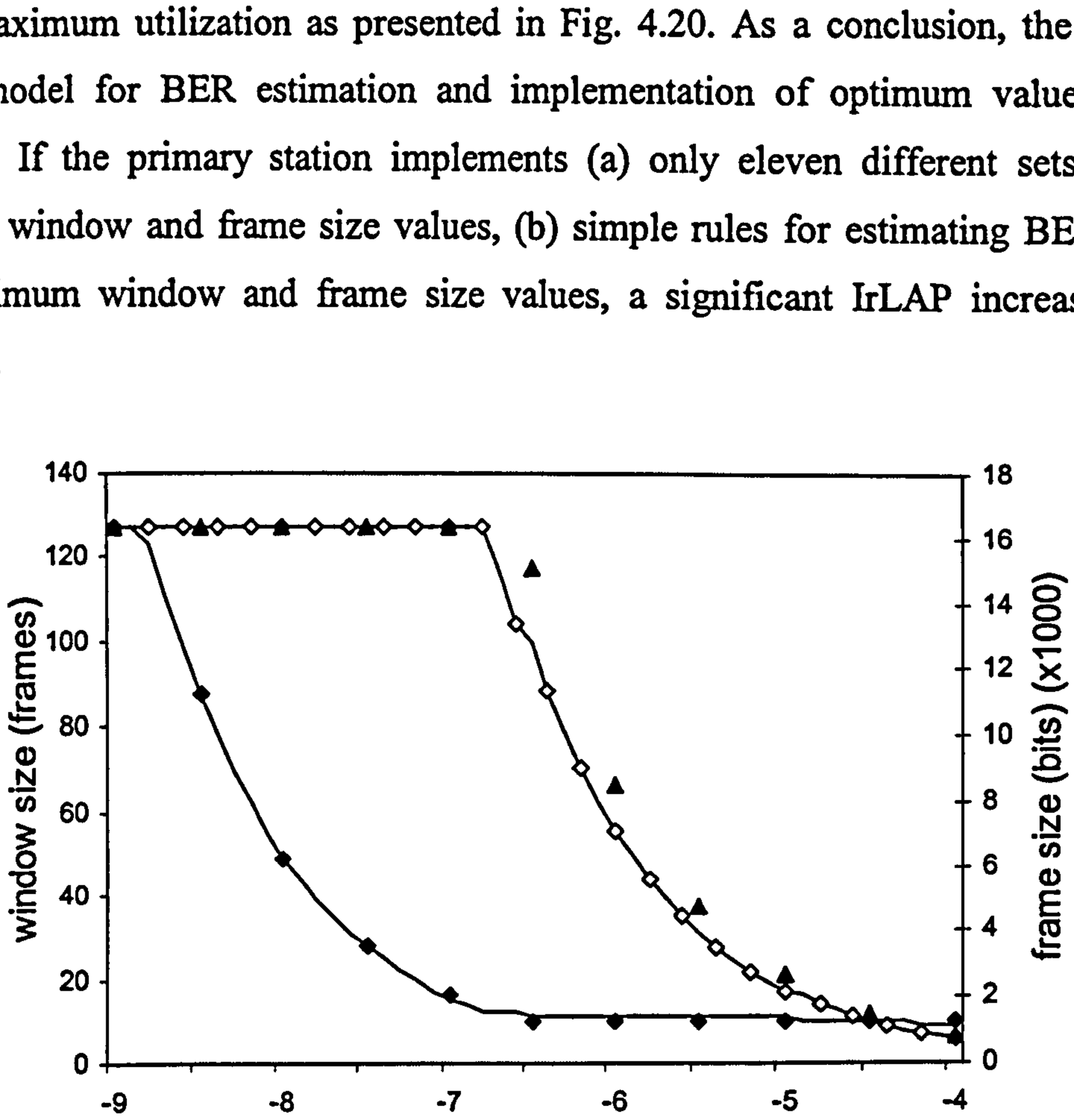

◇ *l optimum (numerical)*
▲ *l values implemented by primary station in simulation*
— *N optimum (numerical)*
◆ *N values implemented by primary station in simulation*

Figure 4.19 Optimum value comparison for implementing 11 window and frame size values, C=16Mbit/s, t_{ta}=0.1ms, $t_{Fout}=t_{Imax}+2t_{ta}$

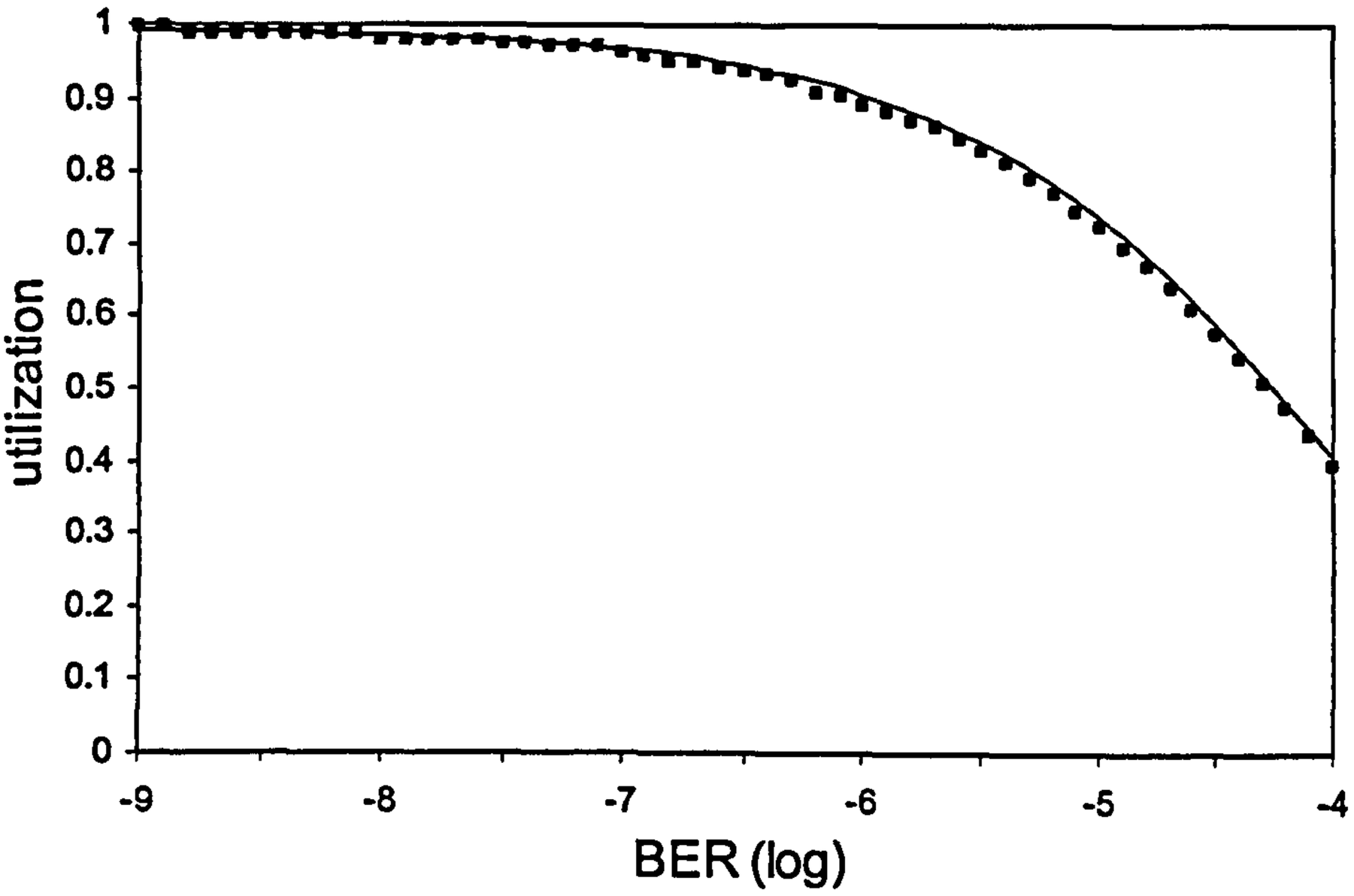

—*maximum utilization (numerical)*

■ *simulation utilization*

Figure 4.20 Utilization comparison for implementing 11 window and frame size values, C=16Mbit/s, t_{ta}=0.1ms, $t_{Fout}=t_{Imax}+2t_{ta}$

CHAPTER 5

Advanced Infrared Medium Access Control Layer

The IrDA 1.x protocol has been proven very popular and millions of devices are equipped with an IrDA 1.x infrared port. However, IrDA 1.x specifications are addressing the 'point and shoot' user model; only one pair of devices can communicate in the same infrared space and the link range is limited. The significant increase on the number of mobile devices on the market today and recent advances in infrared technology have led to the decision to address the communication requirements of a pool of users.

IrDA proposed the Advanced Infrared (AIr) protocol specifications for indoor, high-speed, low cost and multipoint wireless communications. This chapter describes the AIr protocol and evaluates AIr performance by using simulation results. The outline of this chapter is as follows. Section 5.1 introduces the AIr protocol architecture and section 5.2 presents the frame formats supported by the AIr MAC layer. Section 5.3 discusses the AIr MAC transfer schemes including the Reserved and Unreserved transfer modes of the protocol. Section 5.4 presents the collision avoidance procedures of the AIr protocol and section 5.5 explains the interface between the MAC and PHY layers. Section 5.6 presents an OPNET simulator developed for the AIr protocol. Finally, sections 5.7 and 5.8 evaluate, using simulation results, the performance of the Unreserved and of the Reserved transfer modes respectively.

5.1 Architecture overview

The primary goal in developing AIr specifications was to introduce multipoint connectivity and, at the same time, preserve the investment in upper layer applications by making certain that existing IrDA 1.x applications will be able to utilize the proposed extensions in lower layers [101]. Fig. 5.1 presents the OSI standards level overview of the AIr protocol architecture. A new physical layer, AIr PHY [46], is introduced and the IrDA 1.x IrLAP layer [49] is split into three sub-layers, the AIr Medium Access Control (MAC) [45], the AIr Link Manager (LM) [42] and the AIr Link Control (LC) [43] sub-layers. IrDA 1.x and AIr LC procedures for establishing device-to-device connections is transparent to network layer entities.

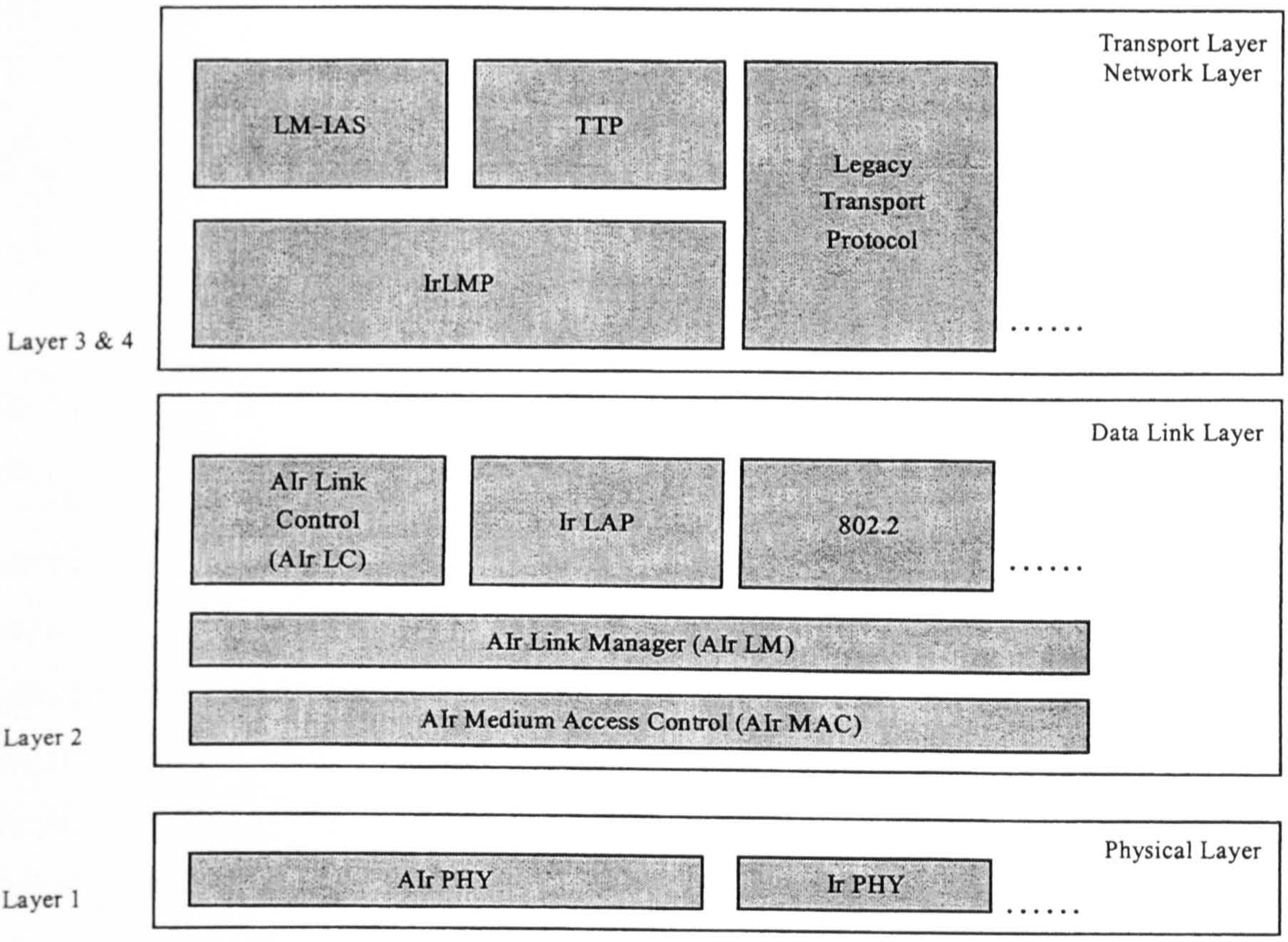

Figure 5.1 AIr architecture overview

AIr PHY supports wide-angle ports operating at ±60 to ±75 degrees, compared to narrow-angle ±15 to ±30 degrees for the IrDA 1.x, in order to achieve multipoint connectivity. AIr utilizes one common modulation format for all supported data rates. This format is defined as four slot Pulse Position Modulation with Variable Repetition Rate (RR) encoding (4PPM/VR). The base rate is 4 Mbit/s. Lower data rates (up to 256Kbit/s) may be utilized by repeating the transmitted symbols RR times at the base rate. The introduced redundancy improves link signal to noise ratio (SNR) at the expense of a lower data rate. It is expected that halving the data rate results in a 19% range increase at each reduction step [101]. Variable rate coding is introduced in [30] and physical layer issues for achieving the required channel symmetry are discussed in [29][14]. AIr physical characteristics with experimental results can be found in [28]. Standard range (S-class) AIr transceivers are expected to provide a transmission distance from 1m to 2.5m at 4Mbit/s. At 256 Kbit/s, a range from at least 2m to at least 5m is achieved. Long-range (L-class) AIr transceivers accomplish a transmission range from 2.5m to 6m at 4 Mbps and a range of at least 5m to at least 12m at 256 Kbit/s [46]. An AIr prototype port on a US quarter dollar presented by IBM is shown in Fig. 5.2.

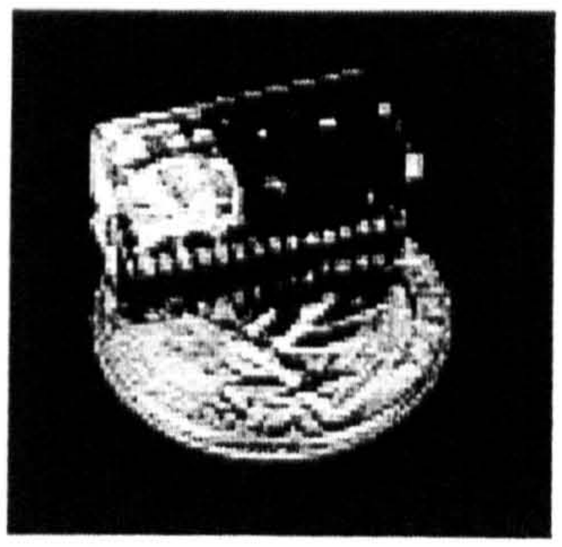

Figure 5.2 AIr prototype port on a US quarter dollar presented by IBM

The AIr MAC sub-layer allows upper layers to cope with the relaxing of restrictions on the angle and range of AIr PHY ports. AIr MAC is responsible for coordinating the access to the infrared medium among AIr and IrDA 1.x devices. AIr MAC supports reservation based media access control, reliable and unreliable data transfer, data sequencing and data rate adaptation. AIr MAC coordinates medium access by employing Carrier Sense Multiple Access with Collision Avoidance (CSMA/CA) techniques [45]. AIr LM is a 'thin' layer that allows multiplexing of multiple different client protocols. It also provides dynamic addressing, station grouping and priority and non-priority data channels [42]. Dynamic addressing is used to cope with MAC address conflicts and station grouping is utilized to enable multicast transmissions. AIr LC supports connections to multiple devices. AIr LC is a derivative of the widely used HDLC protocol operating at the Asynchronous Balanced Mode of the protocol. AIr LC does not assign primary and secondary roles to communicating devices. It supports error detection and recovery services, address conflict resolution procedures and guaranteed data delivery services.

5.2 AIr MAC frame formats

The following Repetition Rate (RR) values are supported by AIr PHY and MAC layers:

Repetition Rate	Data rate
RR=1	4 Mbit/s
RR=2	2 Mbit/s
RR=4	1 Mbit/s
RR=8	512 Kbit/s
RR=16	256 Kbit/s

AIr MAC utilizes 12 frame types in total. Two general classes are defined; the

reservation control frames and the data transfer frames. The following reservation control frames are used to contend, initiate and terminate reservations:

Type	Description
RTS	Request To Send
CTS	Clear To Send
SOD	Start Of Data
EOB	End Of Burst
EOBC	End Of Burst Confirmed

The following data transfer frames are use to transfer payload data:

Type	Description
DATA	Reserved data frame
ADATA	Reserved data frame with acknowledgment
UDATA	Unreserved data frame
SDATA	Reserved data frame with sequencing
ACK	Acknowledgment frame
SPOLL	Sequenced poll frame
SACK	Sequenced acknowledgment

The AIr MAC frame format definitions are shown in Fig. 5.3. Three major elements are defined:

a) The *initialisation* element consists of the Preamble (PA) and the synchronisation (SYNC) fields. These two fields allow the receiver to detect an incoming frame. The PA field consists of a predefined sequence that helps the Phase Locked Loop (PLL) to lock on to and detect the start of an incoming transmission. PA provides an early form of carrier sense and lasts for 64 μsec (TT_{PA}=64 μsec). The SYNC field qualifies the carrier detection and allows exact identification of the beginning of the robust header element. SYNC lasts for 40 μsec (TT_{SYNC}=40 μsec).

b) The *robust header* (RH) element contains the essential information required by the PHY and MAC layers to co-ordinate medium access. It is always transmitted using maximum RR=16 to allow reception of this essential information by all stations in range. Thus, all stations capable of interfering with the current transmission refrain from transmitting. RH contains 32 bits and lasts for 128 μsec (TT_{RH}=128 μsec).

c) The *main body* (MBR) element, which includes the Cyclic Redundancy Check (CRC). MBR contains non-essential MAC protocol information and is transmitted using variable RR. MBR contains payload data and has a variable length.

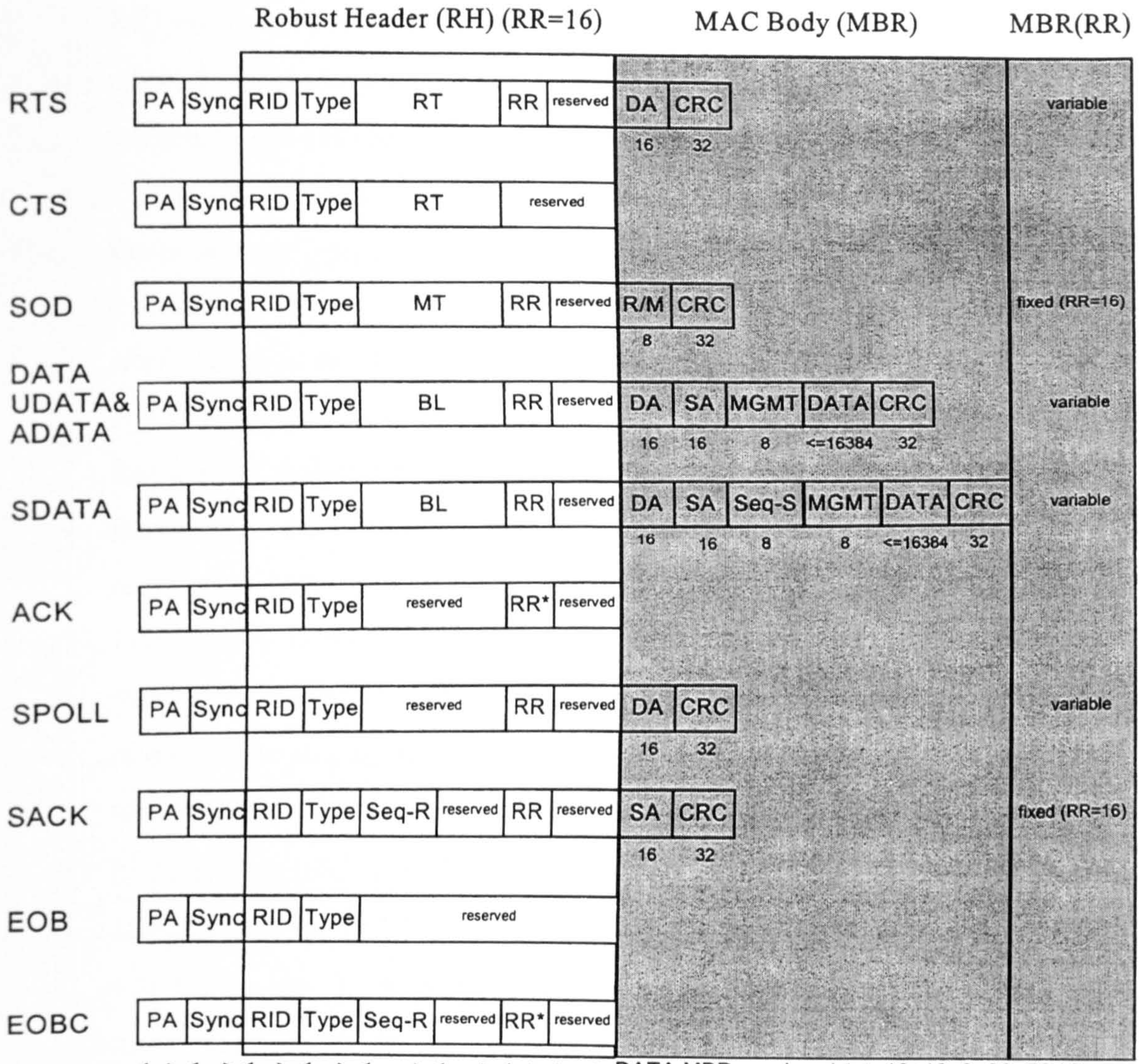

Figure 5.3 AIr MAC frame definitions

PA, SYNC and RH fields are present in all AIr MAC frame types. However, MBR is not present in some frame types. In this case, the RH field is not protected by a CRC because it is transmitted using maximum RR=16. The transmission time of frames with no MBR field is $T_{RH}=TT_{PA}+TT_{SYNC}+TT_{RH}=232$ μsec.

5.2.1 Robust Header (RH) fields

The RH fields contain all the PHY and MAC information needed by all stations in order to operate efficiently in accessing the infrared medium.

- Reservation Identifier (RID) field: This field specifies the Reservation Identifier of a reservation attempt or an on-going reservation. A station randomly selects a

RID value every time it attempts to reserve the infrared medium. RID associates AIr MAC frames with a specific reservation and acts as a shorthand notation for the source and destination addresses for the entire reservation duration.

- TYPE field: This field defines the type of frame. The frame type specifies the frame structure, which is used by all receiving stations to extract the information carried in the frame fields. It is also used to determine the suitable response (if any). There is no difference in the frame structure of DATA, UDATA and ADATA frames but different frame types are assigned to these frames because they require different actions from the receiver.
- Reservation Time (RT) field: This field specifies the length of the time that a reservation will last. It is present in both RTS and CTS frame types. Although EOB and/or EOBC frames normally inform all stations in range that current reservation is over, the RT field ensures that a reservation will terminate even in cases where overlapping reservations and collisions will prevent a normal reservation termination.
- Block Length (BL) field: The BL field defines the length of the frame in bytes.
- Modulation Time (MT) field: This field specifies the time duration a modulation will be in use. It is present only in SOD frames that support IrDA 1.x communications.
- Repetition Rate (RR) field: This field specifies the Repetition Rate used in the MBR field of the frame. It is present only in frames that have an MBR field (i.e. RTS, SOD, DATA, UDATA, ADATA, SDATA, SPOLL and SACK frame types).
- Sequenced Receive (SEQ-R) field: This field carries MAC sequencing information. It is present only in SACK and EOBC frame types and carries the next sequence number expected by the receiving station.
- Recommended Rate (RR*) field: This field is similar to RR field except that it specifies recommendations for the RR in the reverse direction based on the receiver's evaluation of the link quality. The RR* field is present only in ACK and EOBC frames.

5.2.2 Main Body (MBR) fields

The MBR field contains upper layer and non-essential AIr MAC protocol information. When present, it contains a CRC field that protects both RH and MBR fields.

- Rate/Modulation (R/M) field: This field specifies the rate and modulation format of the IrDA 1.x transmission
- Source and Destination Address (SA & DA) fields: These fields specify the Source Address (SA) and Destination Address (DA) of the communicating stations. When appropriate, the DA address can be a multicast or the broadcast (i.e. all stations) address.
- MGMT field: This field carries upper layer control information in frames with payload data.
- Sequenced Send (SEQ-S) field: This field carries the MAC generated sequence numbers on SDATA frames. The first SDATA frame in a reservation always has sequence number 0.
- DATA field: This is a variable length field that carries information data provided by the upper layers. The maximum field length is 16Kbits.
- CRC field: This field carries the CRC of the frame.

5.3 AIr MAC transfer modes

When the transmitter is sending a frame, it 'blinds' its own receiver such that it can not receive remote infrared pulses. The transmitter's receive circuitry needs a minimum Turn Around Time (TAT) to recover. As a result, when a frame reception is completed, the receiving station must always wait a TAT delay before transmitting its response to ensure that the intended station's receive circuitry will have successfully recovered. According to AIr MAC specification, TAT duration is 200μsec. This duration is significantly higher than the TAT period of similar WLAN protocols, such as the IEEE 802.11 [39][95].

AIr MAC supports medium reservation utilizing the Request To Send (RTS) / Clear To Send (CTS) frame exchange. The transmitting station reserves the medium for the duration contained in the Reservation Time (RT) field of the RTS frame it transmits. After a TAT delay, the receiving station echoes the reservation period in the RT field of

the responding CTS frame. Thus, even stations being able to hear only the RTS or only the CTS frame refrain from transmitting for the entire reservation period. The RTS/CTS scheme is used to address the hidden station (a station not being able to hear the transmitter or the receiver) problem [31][60][61] at the expense of the time required for transmitting the RTS and CTS frames. When the CTS frame is successfully received, the transmitter waits a TAT delay and initiates a window frame transmission. After the last data frame is transmitted and before the reservation time expires, the transmitter can request termination of current reservation by transmitting an End Of Burst (EOB) frame. The receiver waits a TAT period and responds with an End Of Burst Confirm (EOBC) frame confirming termination of current reservation. As with RTS/CTS exchange, a station hearing only the EOB or the EOBC frame realizes that the current reservation is over and that it is able to contend for the medium again. AIr MAC implements two timers (EXIT1 and EXIT2) to ensure that stations hearing only the EOB or the EOBC frame will contend for medium access at exactly the correct time.

AIr MAC provides reserved and unreserved transfer modes. AIr transfer modes are shown in Fig. 5.4.

5.3.1 Unreserved transfer mode

Unreserved transfer mode (Fig. 5.4(a)) does not utilize the RTS/CTS exchange and transmits only one UDATA frame to a multicast or broadcast (i.e. all devices) address. Unreserved transfer mode is unreliable because no acknowledgment is received. Protocol specifications suggest that UDATA frames should be transmitted at maximum RR = 16 to ensure maximum coverage.

5.3.2 Reserved transfer modes

5.3.2.1 Reserved transfer mode with DATA frame

Reserved transfer mode with no acknowledgment (Fig. 5.4(b)) reserves the medium using the RTS/CTS frame exchange, transmits a window of DATA frames in a successful reservation, terminates the reservation using the EOB/EOBC frame exchange but it is still unreliable as no acknowledgment is received. When an unreliable data transfer mode is used, (Fig. 5.4(a) & (b)), a MAC successful transmission indication to LM layer means that the frames are sent and not that the frames are correctly received.

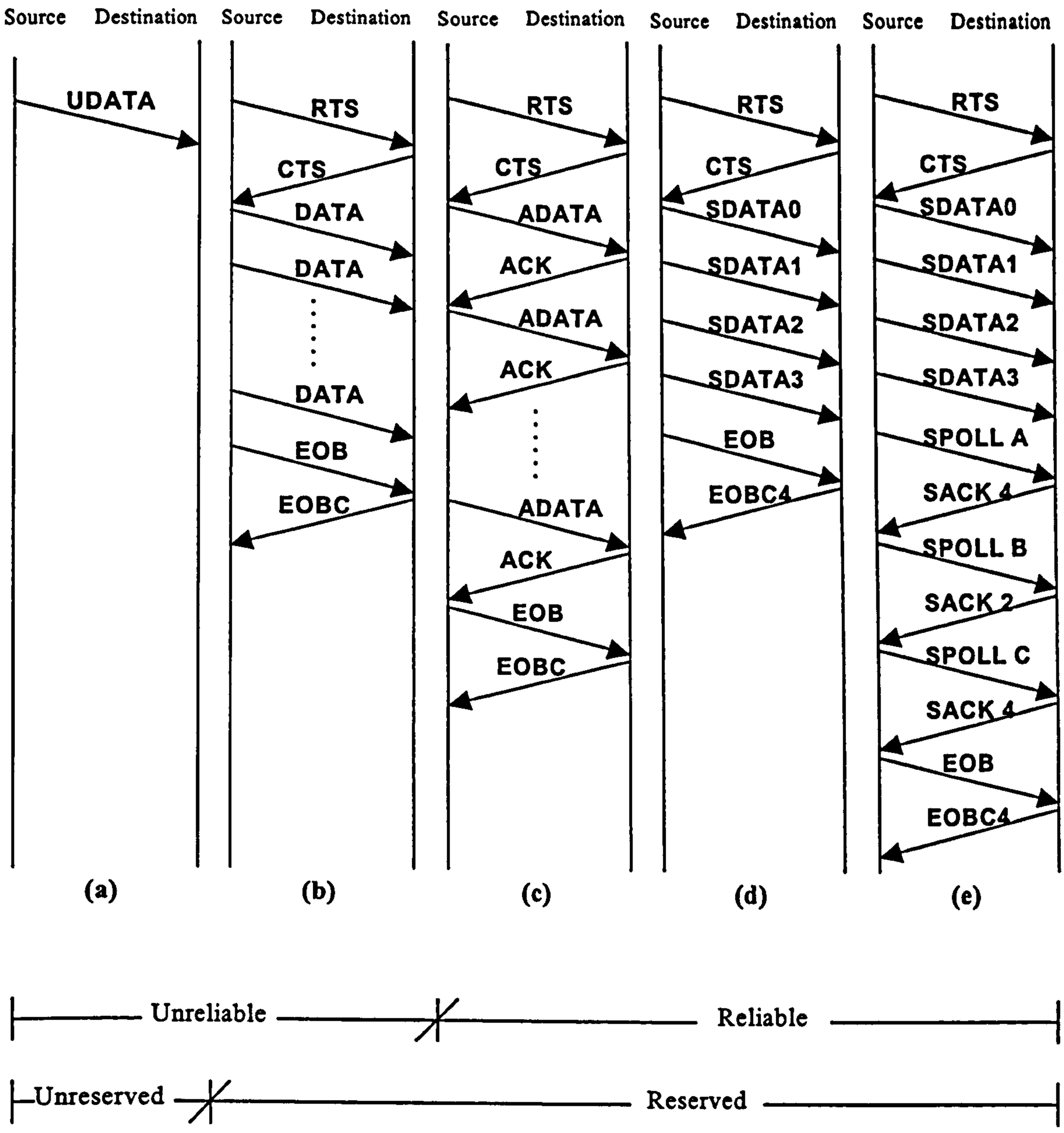

(a) Unreserved transfer mode with UDATA frame
(b) Reserved transfer mode with DATA frame (no acknowledgment)
(c) Reserved transfer mode with Acknowledgment (ADATA frame)
(d) Reserved transfer mode with Sequenced Data (SDATA frame)
(e) Reserved transfer mode with reliable multicast

Figure 5.4 AIr transfer modes

In this case, the LC layer implements a retransmission scheme to handle frame errors.

5.3.2.2 Reserved transfer mode with acknowledgment

Reserved transfer mode with frame acknowledgment (Fig. 5.4(c)) utilizes the RTS/CTS reservation scheme, ADATA frames to carry payload data and transmits a window of frames in a successful reservation. Successful ADATA frame reception is

based on an immediate ACK (acknowledgement) frame transmitted by the receiver. Finally, the reservation is terminated by using the EOB/EOBC control frame exchange.

ACK frames contain RR recommendations based on the receiver's evaluation for the link quality. The transmitter's LM layer specifies when its MAC layer can change the RR it implements during a reservation based on the recommended rates provided by the receiver. Only this transfer mode can quickly adapt the RR to meet varying channel conditions because it includes multiple RR recommendations in ACK frames during a successful reservation.

5.3.2.3 Reserved transfer mode with sequenced data

Reserved transfer mode with sequenced data (Fig. 5.4(d)) uses the RTS/CTS frame exchange and sequences transmitted data using SDATA frames. An SDATA frame contains its sequence number in the Seq-S field. This mode terminates a reservation by using the EOB/EOBC frame exchange but, in this case, the EOBC frame contains the next frame sequence number expected by the receiver in the Seq-R field. Thus, the transmitter is informed of the correctly in-sequence received frames when the reservation terminates.

5.3.2.4 Reserved transfer mode with reliable multicast

Reserved transfer mode with reliable multicast (Fig. 5.4(e)) is similar to reserved transfer mode with sequenced data but transmits data to a multicast address. As a result, each target station must be separately polled at the end of the SDATA frame transmissions. An 'SPOLL *n*' frame is used to poll station *n*, which responds with an SACK frame indicating in the Seq-R field the next frame sequence number expected. When a reliable data transfer mode is used, (Fig. 5.4(c), (d) & (e)), a MAC successful transmission indication to LM layer means that the frames are correctly received.

5.4 Collision avoidance procedures

AIr MAC employs Carrier Sense Multiple Access with Collision Avoidance (CSMA/CA) techniques to minimize collision probability. A station wishing to transmit and regardless of the transfer mode it employs, it first invokes the Collision Avoidance (CA) procedures in an effort to minimize collisions with other stations. Considering the AIr transfer modes presented in the previous section, a contending station always

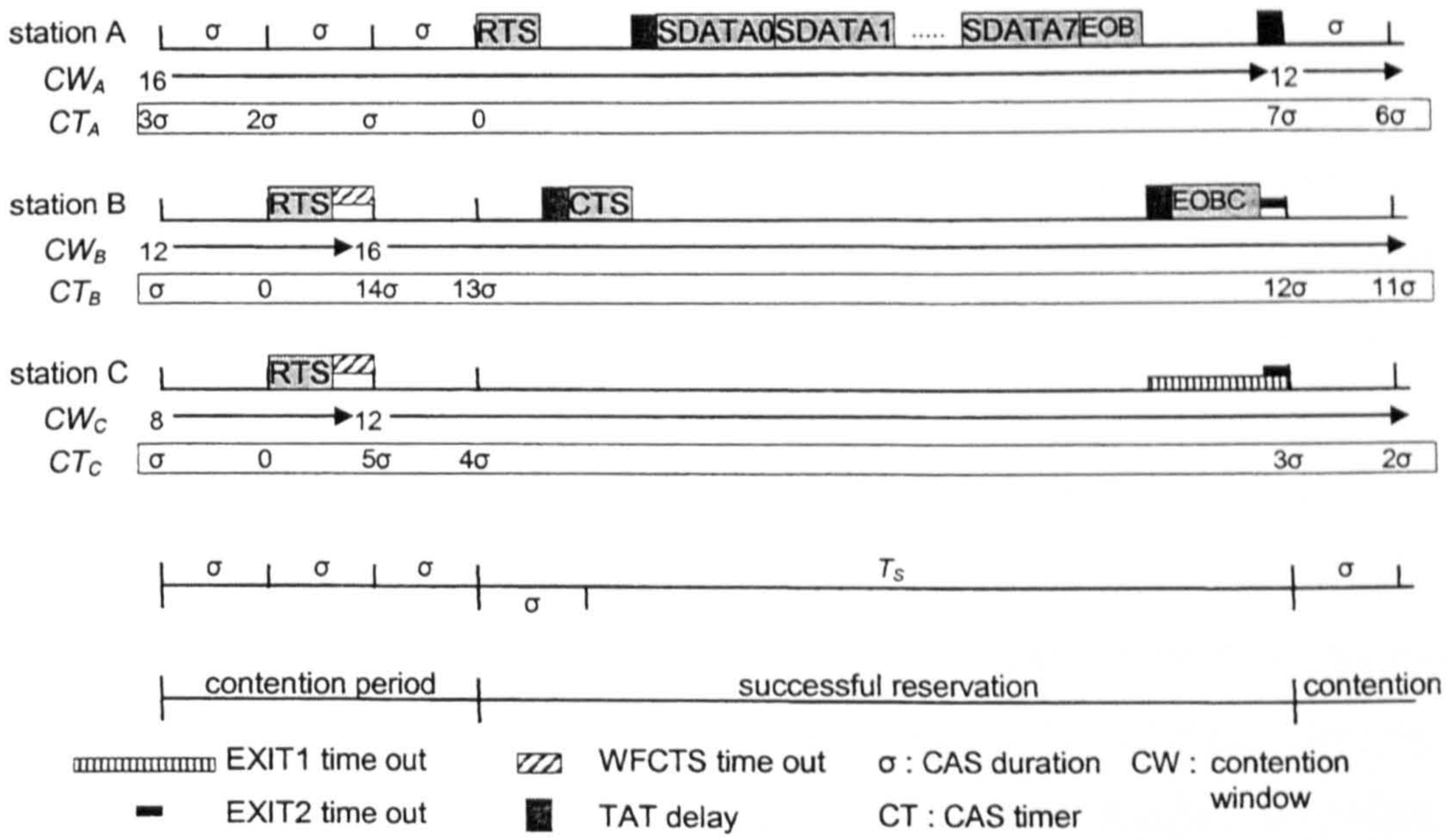

Figure 5.5 Operation of Collision Avoidance procedures

invokes the CA procedures before an RTS and a UDATA frame transmission. If the medium is busy, the contending station first waits until the medium is idle and the next contention period starts. Contention periods start a TAT period after the UDATA or the EOBC frame that terminates a reservation. The TAT delay is required because the station that transmitted the UDATA or EOBC frame should be able to receive the next frame (Fig. 5.5). Contention periods end when a non-colliding RTS or UDATA frame is transmitted. AIr MAC specification ensures that even stations hidden from the transmitter or the receiver are synchronized in contending for the medium at the beginning of the next contention period after a successful RTS/CTS medium reservation. Synchronization is accomplished by means of the EXIT1 and EXIT2 timers. EXIT1 is started when the EOB frame is received. EXIT1 expires at the beginning of the next contention period synchronizing stations not receiving the EOBC frame. EXIT2 is started when the EOBC frame is received and, as it accounts for the TAT delay, it expires when the next contention period starts (Fig. 5.5). Thus, stations hearing only the EOB or the EOBC frame will contend for medium access at exactly the correct time [45].

The contention period is slotted and a station is allowed to transmit only at the beginning of a Collision Avoidance Slot (CAS). The CAS duration (σ) is defined as being greater than the transmission time of the RTS frame plus the TAT delay plus the

time need to detect the PA and SYNC fields of the responding CTS frame ($\sigma > T_{RTS}$+TAT+TT_{PA}+TT_{SYNC}). AIr MAC defines that σ=800 μsec. Such a long CAS duration aims to avoid collisions caused by stations hidden from the transmitter that are not able to hear the RTS frame transmission. These stations will detect the beginning of the CTS frame during the CAS duration, realize that another competing station has selected this CAS and refrain from transmitting [95].

The CAS duration AIr protocol employs is significantly longer than the CAS duration similar CSMA/CA protocols define. These protocols define that the CAS duration should only be long enough for a station to detect the beginning of an incoming RTS frame. For example, the IEEE 802.11 specification [39] defines that the CAS duration accounts for the propagation delay, for the time needed to switch from receiving to transmitting state and for the time needed for the physical layer to signal the channel state to the MAC layer. AIr MAC defines a longer CAS duration that provides a much better hidden station approach at the expense of longer contention periods caused by the longer CAS duration.

As discussed earlier, when the medium is busy, a competing station for medium access first waits for the transmitting station to finish and for the beginning of the next contention period. It then selects a random number of CASs to wait before transmitting and assigns the deferral period to the CAS timer (CT). This integer random number is uniformly chosen in the range (0, *CW*-1), where *CW* is the current Contention Window (CW) size. CW size represents the range the random number is picked from and competing stations may utilize different *CW* values during the contention period. If during the station's deferral period another transmission is observed, the station freezes the CAS timer and restarts it again when the on-going transmission is finished and the next contention period is started. When the CAS timer reaches zero, the station transmits.

If the station employs a Reserved transfer mode scheme, it transmits the RTS frame and starts the Wait For CTS (WFCTS) timer. If another (or more) station has selected the same CAS, as in the second CAS in Fig. 5.5, it transmits its RTS frame at the same time. The resulting collision is determined by the transmitting stations by the WFCTS timer expiration. The colliding stations select a new CAS and continue contending for medium access. To synchronise the colliding stations with the remaining stations, the

WFCTS timer should expire at the end of the current CAS.

The *CW* parameter is of great importance because in the standard a long CAS duration is defined. If a small *CW* value for the specific network size and load is used, a low utilization figure will be reached caused by the increased number of collisions. If a large *CW* value is used, the increased number of empty CAS will result in low medium utilization. A station can only estimate the appropriate *CW* value it should implement based on the experienced successful reservations and collisions. AIr specifications define that the LM layer selects the *CW* value to be used in every reservation attempt and pass it down to the MAC layer [42].

The AIr LM specification defines guidelines for adjusting *CW*. It presents a linear algorithm that increments and decrements *CW* after a collision and a successful reservation respectively. The transmitter 'remembers' the *CW* value used in the previous reservation attempt. If this attempt was successful, *CW* is decreased by 4 (see station A in Fig. 5.5); if it resulted in a collision, *CW* is increased by 4 (stations B and C in Fig. 5.5). A minimum *CW* value of 8 and a maximum *CW* value of 256 are also defined [42].

Fig. 5.5 illustrates the station behavior for a LAN with three contending stations employing the Reserved transfer mode with sequenced data. It is assumed that at the beginning of the first contention period, station A has a current *CW* value of 16 (CW_A=16) and defers transmission for three CAS. The CT of station A has a value of 3σ ($CT_A=3\sigma$), where σ is the CAS duration. We also assume that Station B has CW_B=12, $CT_B=\sigma$ and station C has CW_C=8, $CT_C=\sigma$. As all stations defer transmission, the first CAS is empty. All stations decrease their CTs for the entire CAS duration. As a result, at the beginning of the second CAS, $CT_A=2\sigma$, CT_B=0 and CT_C=0. The deferral period of stations B and C has expired and these stations transmit an RTS frame at the beginning of the second CAS resulting in a collision. As no CTS frames are generated, stations B and C realize the collision by the expiration of their WFCTS timers. As explained earlier, the WFCTS timer expiration occurs at the beginning of the next CAS synchronizing stations B and C with station A. Stations B and C increase their *CW* values (CW_B=16 and CW_C =12) and select new deferral periods. Assuming station B selects 14 and station C selects 5, $CT_B=14\sigma$ and $CT_C=5\sigma$ at the beginning of the third CAS. At this point $CT_A=\sigma$ as station A was decreasing its CAS timer for the entire duration of the second CAS because it did not receive any valid frame. As all stations

PSAP Primitive	abbreviation	type	explanation
AIr PHY Carrier Sense Detect	CSD	indication	Preamble (PA) portion of an incoming frame detected
AIr PHY Carrier Sense Confirm	CSC	indication	Synchronization (SYNC) portion of an incoming frame detected
AIr PHY Robust Header Received	RHR	indication	Robust Header (RH) portion of an incoming frame received
AIr PHY Main Body Received	MBR	indication	Main Body (MBR) portion of an incoming frame received
AIr PHY Frame Transmit	FTX	request	MAC requests a frame transmissi-on
AIr PHY Frame Transmission Completed	FTC	indication	MAC requested frame transmissi-on completed

Table 5.1 AIr Physical layer Service Access Point primitives

defer transmission, the third CAS is empty. Station A transmits an RTS at the beginning of the fourth CAS and successfully reserves the infrared medium. After the RTS/CTS exchange, station A transmits a window of SDATA frames and requests reservation termination by an EOB frame. The receiving station (station B) confirms reservation termination using an EOBC frame. As explained earlier, the next contention period starts a TAT delay after the EOBC frame and all stations are synchronized by the EXIT1 and EXIT2 timers. As station A has successfully reserved the medium, it decreases its *CW* value (CW_A=12), selects a new deferral period (7σ for example) and contention for medium access continues.

5.5 Physical layer service access point

AIr MAC layer uses the service primitives provided by the AIr physical layer through the AIr Physical layer Service Access Point (PSAP) [46]. AIr PHY passes frame reception information to MAC layer by PSAP service primitives called indications. AIr MAC calls for frame transmissions by invoking PSAP primitives called requests. PSAP indications and requests concerning frame transmissions are presented in Table 5.1. Fig. 5.6 (a) and (b) shows the PSAP primitives for a frame reception and a frame transmission respectively. When a station receives an incoming frame, AIr PHY layer indicates reception of PA, SYNC, RH and MBR fields separately by using the CSD, CSC, RHR and MBR indications respectively. AIr MAC requests a frame transmission by invoking a PSAP FTX request; when the frame transmission is completed, AIr PHY invokes a FTC indication.

The remaining sections present an AIr MAC simulator implementing the described

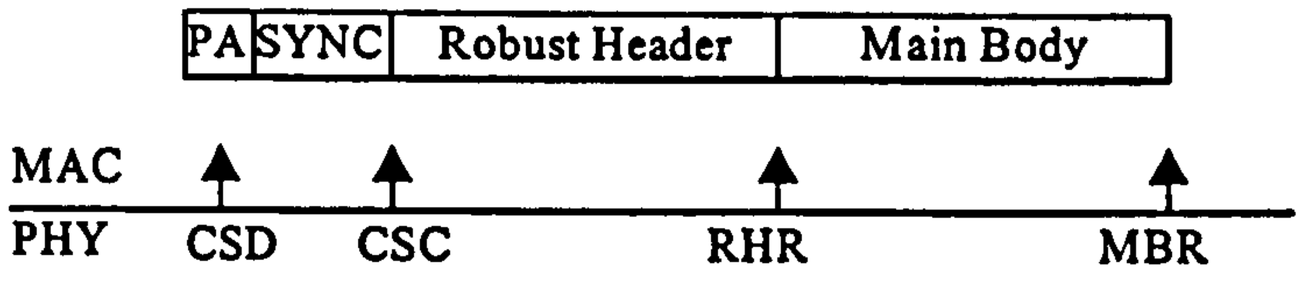

(a)

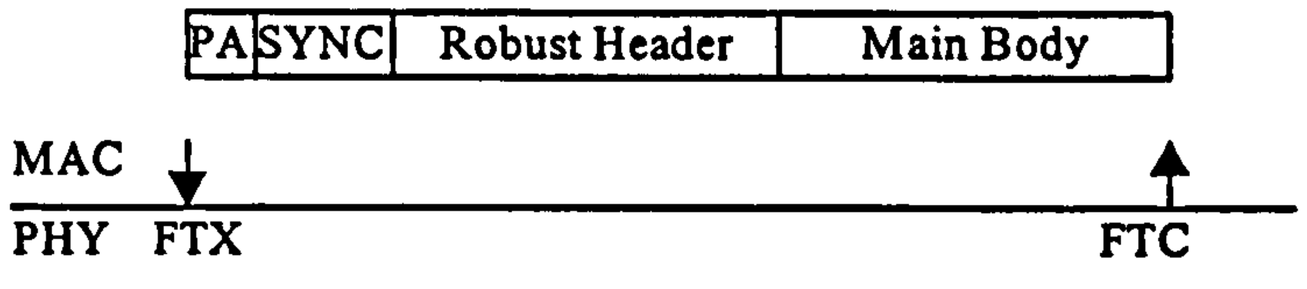

(b)

Figure 5.6. Physical layer Service Access Point primitives (a) frame reception (b) frame transmission

frame types, collision avoidance procedures and PSAP indications and requests. Simulation results are presented for the Unreserved transfer mode and for the Reserved transfer mode with sequenced data in an effort to evaluate the effectiveness of the presented collision avoidance procedures, PSAP primitives and transfer modes.

5.6 AIr simulator using OPNET

A simulator for the AIr protocol is developed using the OPNET™ package from MIL3 Inc. Infrared transmissions are emulated by altering the radio version of the OPNET modeler. Simulation models for the AIr PHY and AIr MAC layer operations are developed. The LM contention window adjustment algorithm is also implemented. The simulator emulates the real operation of a station as closely as possible, by implementing the collision avoidance procedures and all parameters such as frame transmission times and turn around times.

OPNET uses hierarchically linked domains to denote a network design. Stations are defined in the network domain, which is the top-level domain. Each station has a set of processes specified at the lower level, the node domain. Each process can represent a layer in the protocol stack or physical layer transmitters and receivers. A process can be defined by a finite state machine. User written C code to be executed when entering and exiting each state can be defined. Finally, the C code is accumulated and compiled. OPNET is an event driven simulator and provides a powerful graphical tool to display simulation statistics.

The OPNET AIr simulator closely follows all timer values and frame element

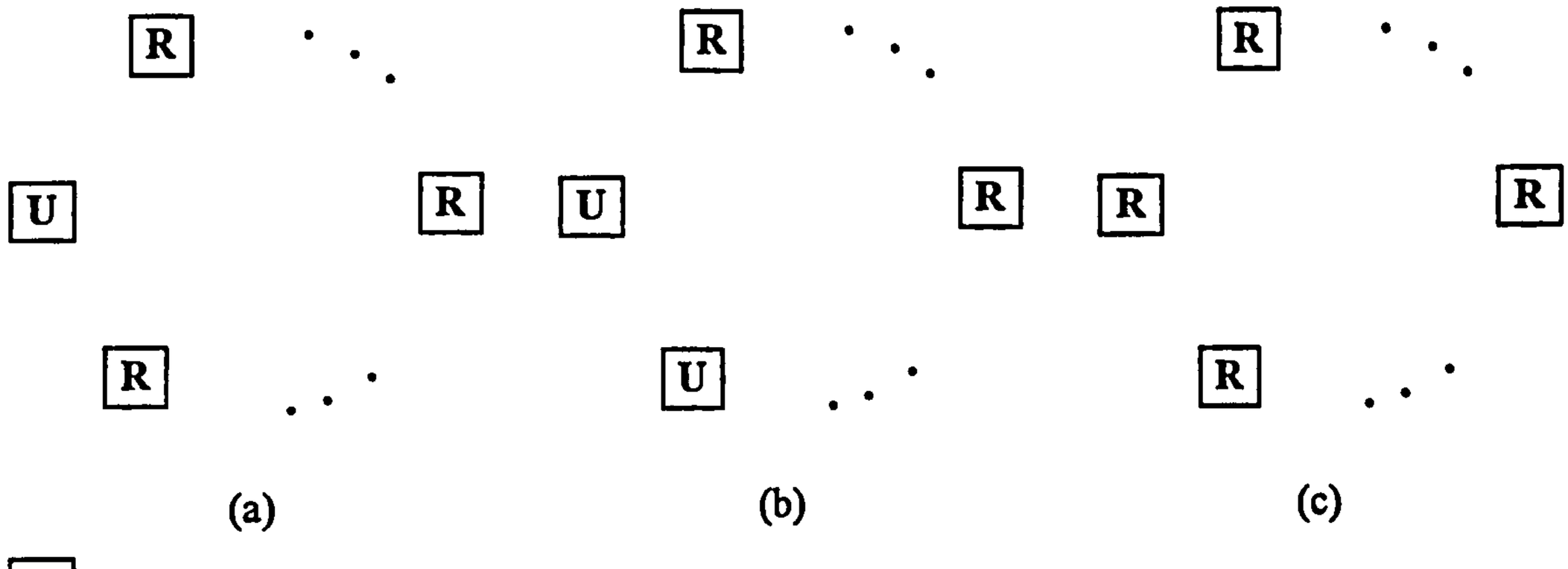

R : station using the Reserved transfer mode with sequenced data

U : station using the Unreserved transfer mode

(a) one station use the Unreserved transfer mode
(b) two stations use the Unreserved transfer mode
(c) no stations use the Unreserved transfer mode

Figure 5.7. LAN simulation scenarios with stations employing the Unreserved transfer mode

transmission times defined by AIr specifications. However, a different value for the Wait For CTS (WFCTS) timer is implemented. WFCTS timer operation is explained in section 5.4. The implemented WFCTS timer value of 556 μsec is different from the protocol proposed value of 632 μsec but still obeys the protocol restriction $T_{WFCTS}>432$ μsec. The implemented value was selected because it directs the colliding stations to contend again for medium access at the beginning of the next CAS [97].

A set of simulation runs was taken [7] to examine the performance of the AIr protocol under ideal channel conditions; an error free medium is assumed and no hidden stations are considered. Simulation runs that examine the performance of the Unreserved transfer mode are presented in section 5.7. The performance of the CA procedures and of the Reserved transfer modes is examined in section 5.8. All simulation runs consider a LAN of n transmitting stations operating at saturation conditions, i.e. all stations always have a frame ready for transmission.

5.7 Simulation results for the Unreserved transfer mode

According to the AIr MAC specification [45], Unreserved mode will be employed only for multicast and broadcast transmissions. Thus, it is expected that only a small number of stations will employ the Unreserved transfer mode in real life scenarios. Two different scenarios are considered; in the first (Fig. 5.7(a)) only one and in the second

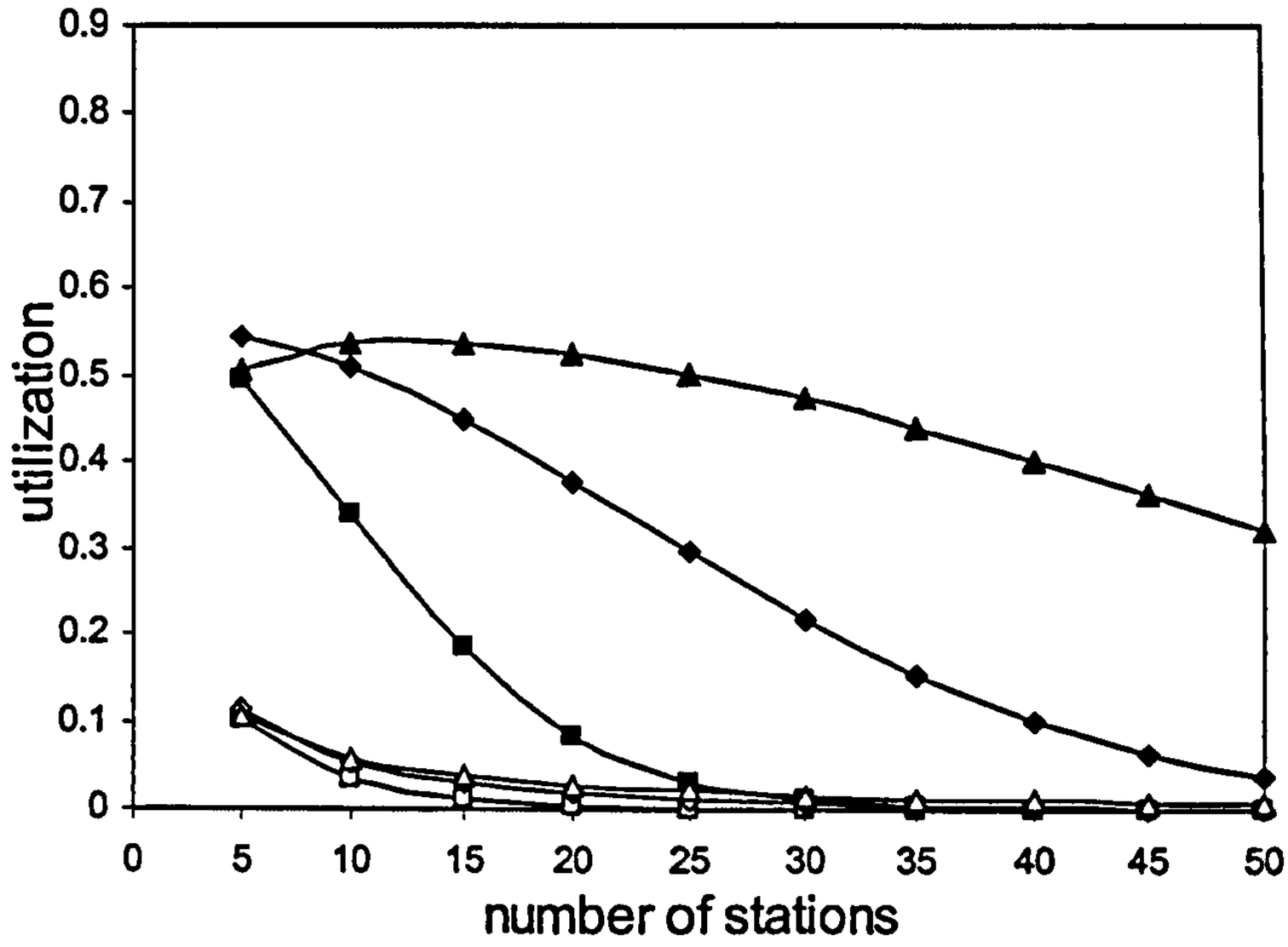

■ *CW=8, total utilization*
◆ *CW=16, total utilization*
▲ *CW=32, total utilization*
□ *CW=8, UDATA utilization*
◇ *CW=16, UDATA utilization*
△ *CW=32, UDATA utilization*

Figure 5.8 Utilization versus n for fixed CW, C=4 Mbit/s, l=16Kbits, 1 UDATA station

(Fig. 5.7(b)) only two stations implement the Unreserved transfer mode. All the remaining stations always employ the Reserved transfer mode with sequenced data. This reservation scheme was chosen because it incurs the least overhead among the AIr MAC reservation schemes and, at the same time, acknowledges frames at the MAC layer. The Unreserved transfer mode transmits only one UDATA frame at every transmission attempt. To allow comparison between UDATA and SDATA frame transmissions, stations employing the Reserved transfer mode transmit only one SDATA frame in every successful reservation. SDATA and UDATA frames always carry 16Kbits of payload data at RR=1 for the 4Mbit/s data rate. Simulations run for 15 sec and calculate utilization as defined in section 2.7. In particular, they calculate total utilization, which is defined as the time portion the medium transfers SDATA and UDATA payload data between stations. They also calculate UDATA utilization, which is defined as the time portion the medium transfers only UDATA payload data between stations.

Fig. 5.8 plots total (SDATA and UDATA) and UDATA utilization versus network size for different fixed *CW* values. The figure shows drastic utilization decrease for large network sizes due to the increased number of collisions. As collisions may involve

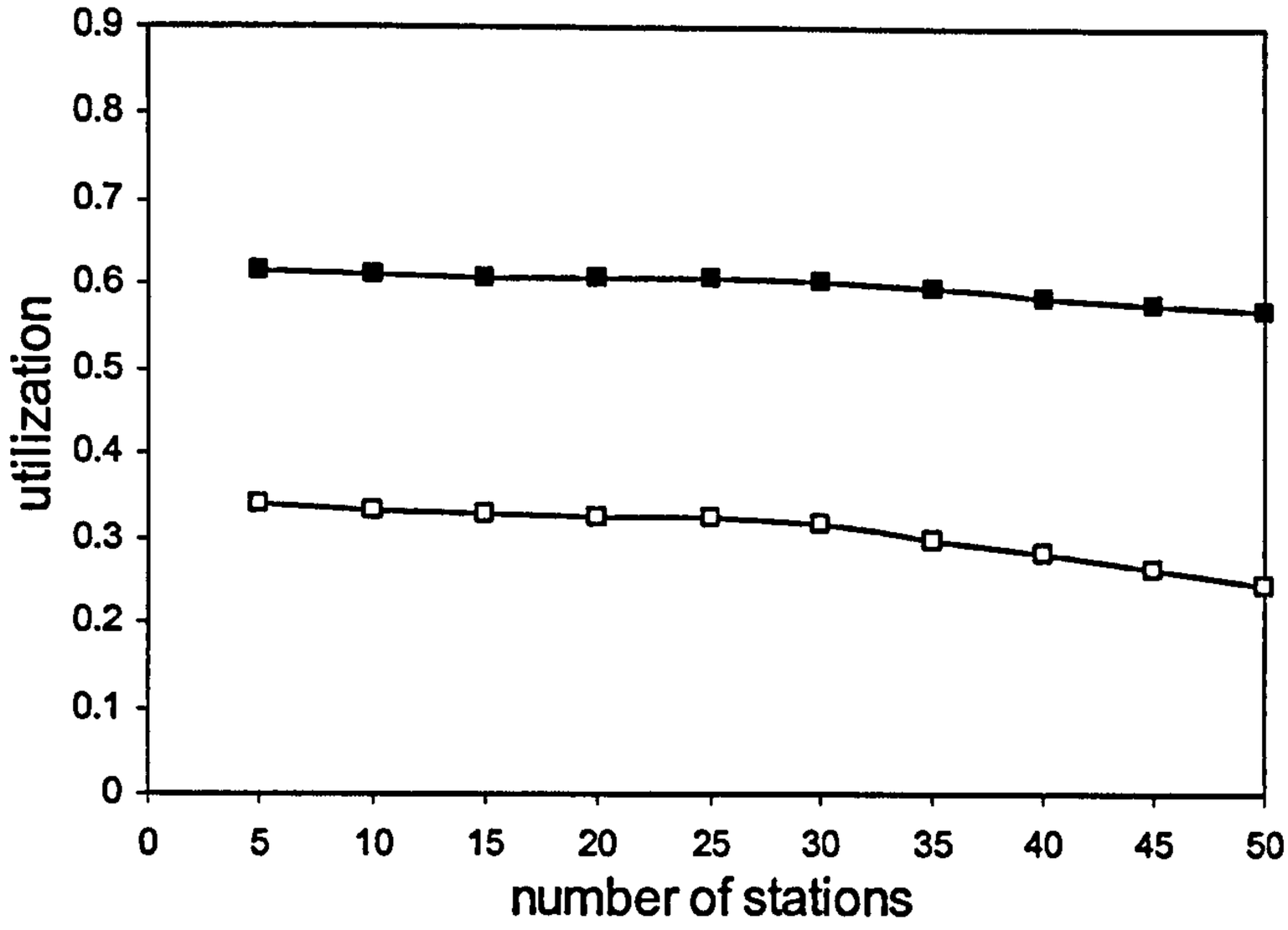

■ *total utilization* □ *UDATA utilization*

Figure 5.9 Utilization versus n, CW_{min}=8, CW_{max}=256, C=4 Mbit/s, l=16 Kbits, 1 UDATA station

a large UDATA frame, collision duration is very long and significantly affects LANs implementing small *CW* values because the collision probability is high in this case. As a conclusion, the selection of 'proper' *CW* value is of great importance when a number of stations employ the Unreserved transfer mode. The degradation of UDATA utilization for large network sizes can be easily explained by considering that the number of SDATA stations increases with network size increase but one station always employs UDATA transmissions.

Fig. 5.9 plots total (SDATA and UDATA) and UDATA utilization versus network size for the CW adjustment algorithm proposed by the protocol as described in section 5.4. Comparison of figures 5.8 and 5.9 indicates that the CW adjustment algorithm significantly increases UDATA utilization, especially for large network sizes where a large number of stations employ the Reserved transfer mode. The situation is explained as follows. When a UDATA frame is involved in a collision, the collision lasts for the time required for the complete UDATA frame transmission. The remaining stations are unaware of the collision existence since the AIr PHY layer, as shown in Table 5.1 and Fig. 5.6, does not send an indication to the MAC layer unless a valid PA portion of an incoming frame is detected. The remaining stations continue contending for medium access resulting in unsuccessful reservation attempts in the collision duration. As the

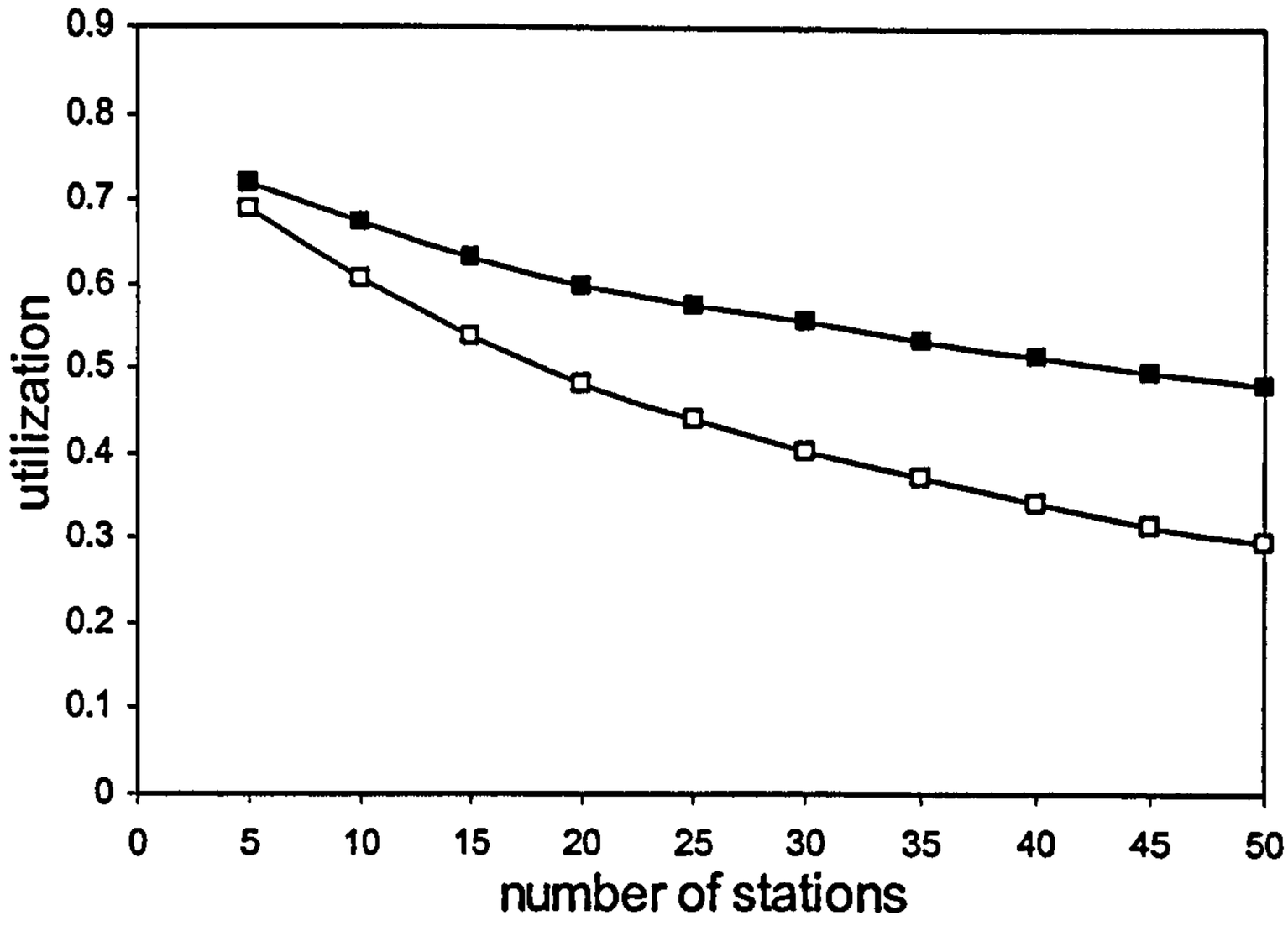

■ *total utilization* □ *UDATA utilization*

Figure 5.10 Utilization versus n, CW_{min}=8, CW_{max}=256, C=4 Mbit/s, l=16 Kbits, 2 UDATA stations

CW is increased after every unsuccessful reservation attempt, the stations employing the Reserved data transfer mode end up using large CW sizes and having a low probability of gaining access to the infrared medium. At the same time, the station employing the Unreserved data transfer mode uses the smallest CW size and transmits a UDATA frame often. The reason is that this station is unaware of whether its UDATA frame collides or not because it does not expect a CTS frame response or a MAC layer acknowledgment. As a result, no CW adjustment takes place. Upper layers are informed of the reception status of the UDATA frames but protocol specifications do not pass this information down to the LM layer, which is responsible for adjusting the CW.

Fig. 5.10 plots the same results when two transmitting stations employ the Unreserved transfer mode (Fig. 5.7(b)). It shows that total utilization is more sensitive to network size increase because the probability of long collisions is increased. It also shows that UDATA utilization is increased and UDATA frame transmissions dominate over SDATA transmissions because the Reserved stations increase their *CW* values more frequently. As a conclusion, an unexpected behavior is observed when the Unreserved transfer mode is employed because the PSAP does not include an indication to the MAC layer that the medium is busy. As a result, when a UDATA frame collides, the remaining stations contend for medium access during the collision. The resulting

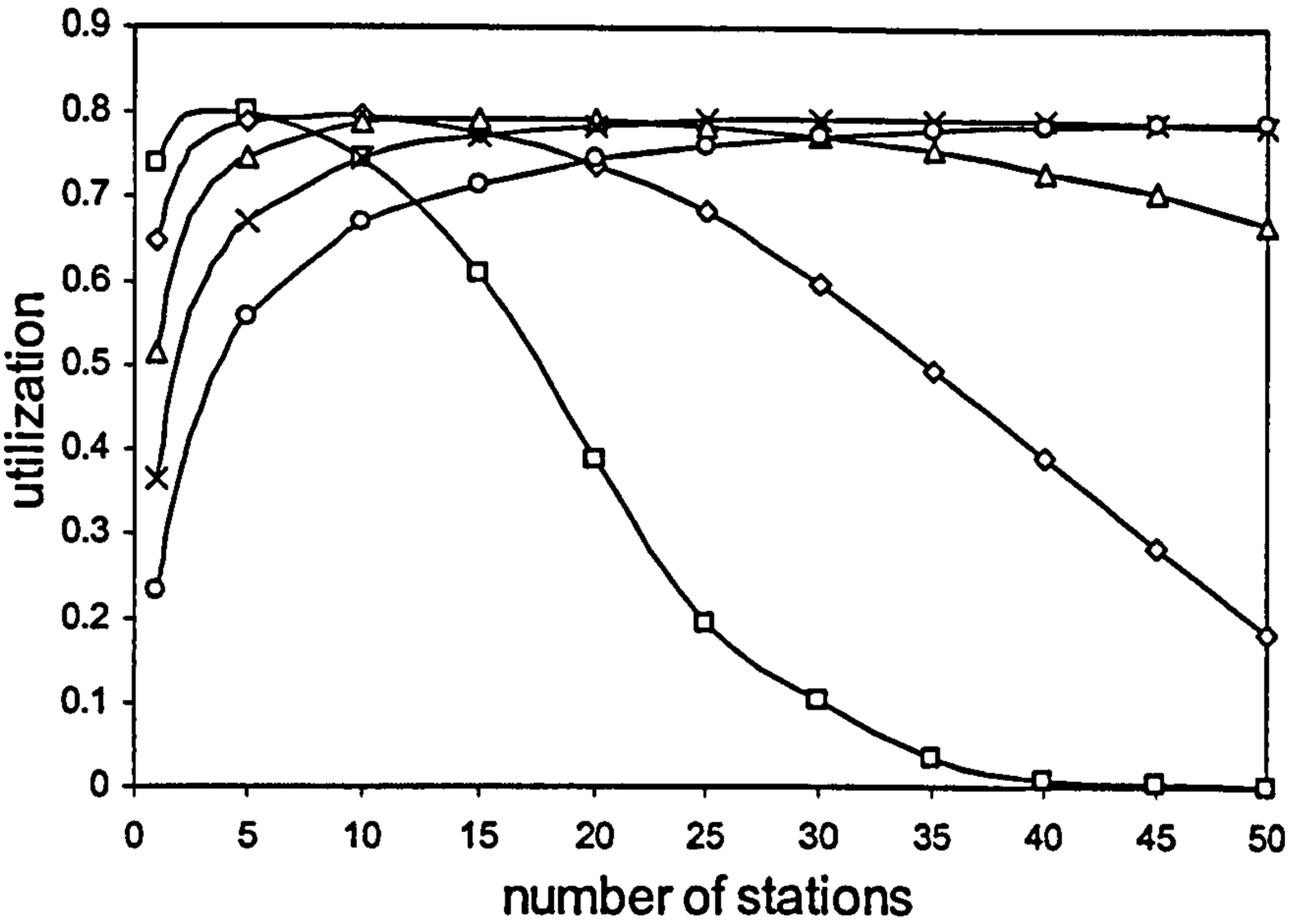

Figure 5.11 Utilization versus n for fixed CW, C=4 Mbit/s, l=16 Kbits, w=4

unsuccessful reservation attempts cause successive *CW* increments and a fairness problem. Employment of the Unreserved transfer mode should be avoided in LANs with many transmitting stations.

5.8 Simulation results for the Reserved transfer mode with sequenced data

Simulation results for LAN scenarios with all *n* stations employing the Reserved transfer mode with sequenced data are produced (Fig. 5.7(c)). Stations transmit *w* SDATA frames in every successful reservation attempt where *w* is the window size. SDATA frames always carry 16Kbits of payload data at RR=1 for the 4Mbps data rate. Simulations run for 15 sec.

Fig. 5.11 plots utilization versus network size for various fixed *CW* values. If a small *CW* is implemented, utilization seriously degrades when the number of stations increases due to the increased number of collisions. If a large *CW* is used, utilization degradation is observed for a few contending stations caused by the large number of empty CAS. Thus, optimum *CW* implementation becomes of key importance if maximum utilization is to be achieved. Fig. 5.11 reveals the interesting result that maximum utilization when the optimum *CW* value is employed for the specific network

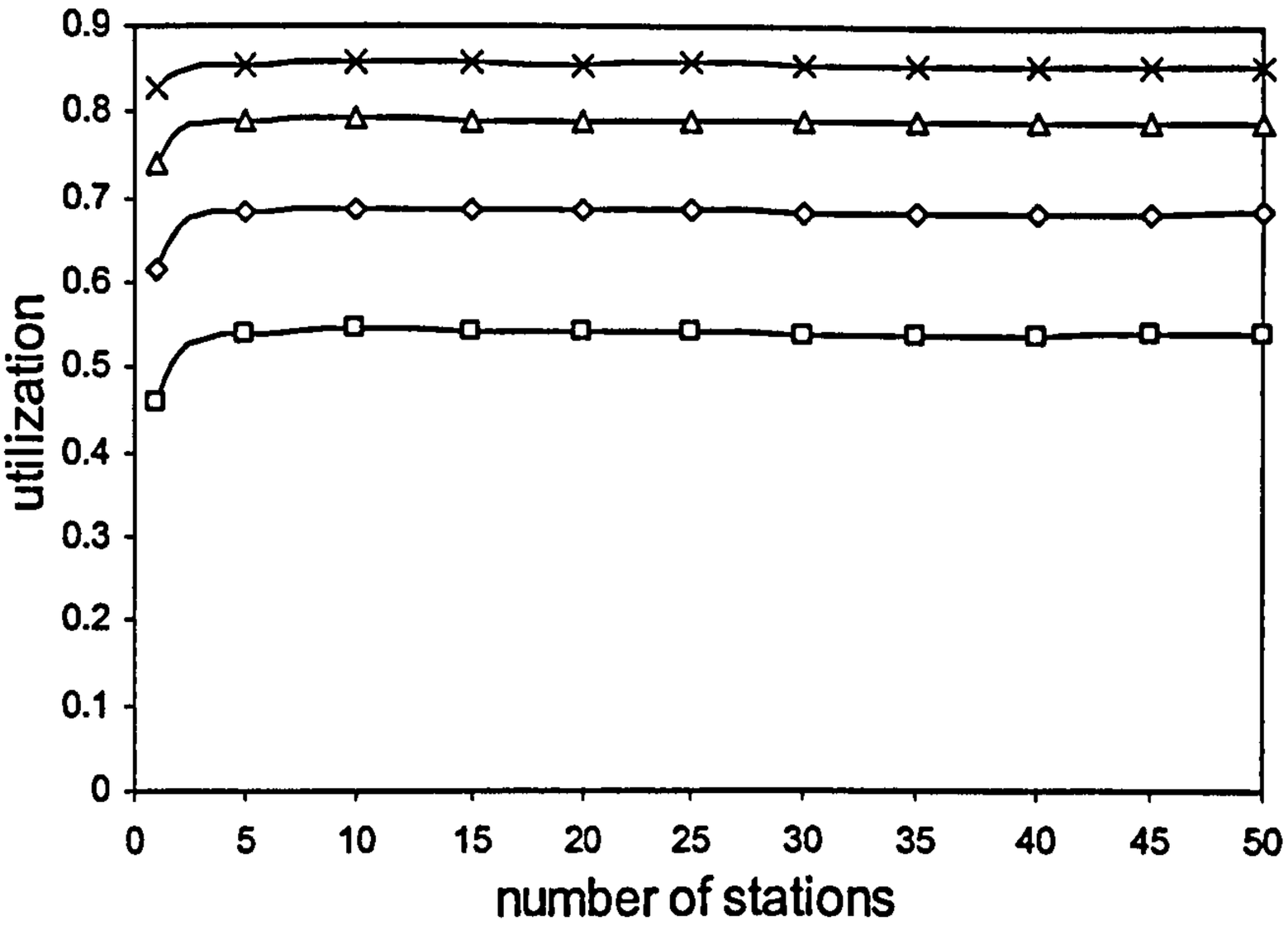

□ *w=1* ◇ *w=2*

△ *w=4* x *w=8*

Figure 5.12 Utilization versus n, C=4 Mbit/s, l=16 Kbits

size is practically independent of the network size.

Fig. 5.12 plots utilization versus network size for various *w* values when the proposed CW adjustment algorithm is implemented. It shows that utilization is relatively very low for low *w* values. This is an important conclusion because the considered SDATA frame transmissions incur the least overhead, the maximum frame size is used, no hidden stations are considered and, more important, an error free medium is assumed. As real life AIr networks may not be able meet these conditions, a lower utilization performance is expected. Fig. 5.12 also reveals that utilization is practically independent of network size when *n* is greater than 5 but lowers for LANs with less than five transmitting stations. Utilization reaches its lowest value when only one station is transmitting, a usual real life scenario. This is an unexpected result because no collisions occur in this case. These results call for further study of the collision avoidance procedures of the AIr protocol. Thus, an analytical model for these procedures is developed in the next chapter. This model is expected to reveal the effectiveness of PHY and MAC parameters on utilization. Please note that the same figures (Fig. 6.5 and 6.8) are produced by employing the proposed analytical model.

CHAPTER 6

Advanced Infrared Collision Avoidance Procedures

This chapter presents an analytical model for the Collision Avoidance (CA) procedures of the Reserved transfer modes of the AIr MAC protocol. It also employs this model to study the effectiveness of the CA procedures on channel utilization assuming an error free channel and no Repetition Rate implementation (RR=1). Chapter 7 employs the model developed in this chapter and derives new analytical models for the AIr retransmission schemes to study utilization performance when transmission errors occur and RR coding is implemented.

The CA procedures are summarized as follows. A station wishing to transmit first contends for medium access. The contention period is slotted and a contending station can only transmit at the beginning of a slot. The slot period is referred to as Collision Avoidance Slot (CAS). To minimize collision probability with other contenting stations, a station first selects a number of CAS to wait and assigns the selected value to the CAS timer. This number is randomly selected from the range (0,*CW*-1), where *CW* is the current Contention Window (CW) size. If during the deferral period a reservation from another station is observed, the station stops the CAS timer and decreases it again when the current transmission is over and the next contention period is started. The station transmits when the CAS timer reaches zero. As the hidden station problem [31][61] is likely to appear in infrared LANs, the AIr protocol defines a long CAS duration. The CAS duration σ is greater than the RTS transmission time plus TAT plus the time required to hear the beginning portion (PA and SYNC fields) of the responding CTS frame ($\sigma > T_{RTS}+\mathrm{TAT}+TT_{PA}+TT_{SYNC}$). Such a long CAS duration ensures that contending stations hidden from the RTS transmitter (and thus not being able to hear the RTS frame) but not from the receiver will receive the beginning of the CTS frame within a single CAS duration. As a result, contending stations with even a single CAS difference at the beginning of the contention period will not collide even if they are hidden from each other.

This approach provides an effective solution to utilization degradation caused by collisions from hidden stations. However the long CAS duration may still degrade utilization if the number of empty and colliding CAS during the contention periods is

high. This number depends on the number of the competing stations and on the *CW* values used by these stations. As stations can only adjust their *CW* values after successful reservations and collisions, the implemented *CW* adjustment algorithm becomes of great importance if maximum utilization is to be achieved.

This chapter is outlined as follows. Section 6.1 defines saturation utilization and the parameters used in the analysis. Section 6.2 presents a simple and accurate analytical model to calculate the performance of the CA procedures of the AIr protocol assuming a finite number of stations. The model is based on the CW adjustment procedures proposed in AIr LM specification [42]. The model is validated by comparing analytical with simulation results in section 6.3. Section 6.4 employs the analytical model to evaluate AIr utilization performance for SDATA frame employment under the assumption that no transmission errors occur. In particular, the effect of CW size to utilization is explored and the optimum CW size is derived by differentiating the utilization equation. The effectiveness to utilization of the proposed CW size adjustment scheme and of MAC and PHY layer parameters, such as the Turn Around Time (TAT), minimum and maximum CW size values, is finally explored.

6.1 Saturation utilization and parameter definitions

This work considers channel utilization which is defined in section 2.7 as the time portion during which the infrared medium successfully transfers payload data at the base rate (4 Mbit/s). Transmission of error frames does not contribute to channel utilization. According to the definition, if the transmitted information is repeated RR times, only the first transmission contributes to utilization. Thus, if the transmitter implements RR=2 to cope with transmission errors, utilization is halved.

It is known that several random access schemes show an unstable behavior when the offered load varies. A wide discussion of the instability problem can be found in [10]. The CA scheme of the 802.11 protocol is similar to that of the AIr protocol and exhibits some form of instability according to [21][38]. Simulation results for the 802.11 protocol when the offered load linearly increases with the simulation time are presented in [12]. When the offered load is low compared to channel capacity, 802.11 utilization closely follows the offered load. As load increases, utilization also increases until a maximum value is reached. Further increasing the offered load results in utilization degradation until a steady value is reached [12]. This steady value is referred

to as saturation utilization. Saturation utilization is lower than the maximum utilization the LAN can reach, when the offered load reaches a specific value. However, the maximum utilization figure is practically meaningless as the offered load is not a controllable parameter and the network can reach the maximum utilization figure only for short periods of time under varying load conditions. Saturation utilization is defined as the network utilization in steady state conditions. For simplicity, saturation utilization is referred to as 'utilization' in this work.

An infrared LAN consisting of n transmitting stations under saturation conditions is considered. In saturation status, it is assumed that a station always has a window of frames available for transmission. All stations employ the Reserved transfer mode with sequenced data, as described in section 5.3.2.3. When a station successfully captures the channel, it transmits a window of w frames with fixed payload size of l bits at C bit/s. Current analysis also assumes that reservation control frames (RTS, CTS, EOB and EOBC) are always received error free. This is a realistic assumption because, as described in section 5.2, control frames CTS, EOB and EOBC contain only an RH portion which is transmitted using the maximum repetition rate RR=16 to minimize transmission errors. The RTS control frame has also an MBR field consisting of only 48 bits, which is transmitted using variable RR. This MBR length is extremely small for the expected link quality and the assumption that the RTS frames are always received error free also holds true. As the considered indoor links operate at very short distances, current model also assumes that the one way propagation delay is very small and can be safely neglected.

The analytical model also assumes that there are no hidden stations. Thus, all stations will always receive the RTS and the CTS frames of a successful reservation. Therefore, there is no fairness problem as all stations have an equal chance to reserve the infrared medium. Based on AIr CA procedures, the current model considers a CW increase by 4 after a collision and a CW decrease by 4 after a successful reservation [42][96]. The specified CW lower limit of 8 and upper limit of 256 are also implemented. The time required for the transmission of reservation control frames and of frame elements is presented in Table 6.1 [94]. The implemented timers and time delay values are presented in Table 6.2. All suggested values by the standard are applied in the analysis and calculations with the exception of the Wait for CTS (WFCTS) time

frame / frame element		duration	time (μsec)
TT_{PA}	(frame element)	-	64
TT_{SYNC}	(frame element)	-	40
TT_{RH}	(frame element)	-	128
T_{RH}	(frame)	$TT_{PA}+TT_{SYNC}+TT_{RH}$	232
T_{RTS}	(frame)	$T_{RH}+48/(C * RR)$	244
T_{CTS}	(frame)	T_{RH}	232
T_{EOB}	(frame)	T_{RH}	232
T_{EOBC}	(frame)	T_{RH}	232

Table 6.1 AIr frame and frame element transmission times for C=4Mbit/s and RR=1.

timer/delay	restriction	suggested (μsec)	implemented (μsec)
Turn Around Time (*TAT*)	-	200	200
CAS duration (σ)	$>T_{RTS}+TAT+TT_{PA}+TT_{SYNC}$	800	800
WFCTS Timer	$>=TAT+T_{RH}$	632	556
EXIT1 Timer	$=TAT+T_{EOBC}+TAT$	632	632
EXIT2 Timer	$=TAT$	200	200

Table 6.2 AIr timers and time delays

out value. A contending station starts the WFCTS timer when it transmits an RTS frame and stops the timer when the corresponding CTS frame is received. If two or more stations are transmitting at the same CAS, the transmitted RTS frames collide, no CTS frames are generated and the WFCTS timer expiration that follows signals the collision to these stations. A WFCTS timer value that obeys the protocol restriction (T_{WFCTS}>=TAT+T_{RH}) and synchronizes the colliding with the remaining stations in contending for medium access at exactly the same time is implemented. The current model also adjusts CAS timers to the beginning of the next CAS when an RTS or a CTS frame is received.

6.2 Analytical model

The key assumption of our analytical model is that an RTS frame transmission collides with the same probability p regardless of the station's current CW value. It is assumed that, in saturation conditions, the collision probability is constant and independent of the experienced collisions and successful reservation attempts. The analytical model first examines the behavior of a single station in order to compute the collision probability p, as well as the probability τ that a station transmits in a randomly selected CAS for a network with n transmitting stations. Subsequently, by considering that only three events can occur in a CAS, a) a successful reservation, b) a collision and c) the CAS is empty, utilization and the average delay for a successful

reservation are expressed as a function of τ.

6.2.1 Transmission probability

As stations operate in saturation conditions, a station has immediately a window of frames ready for transmission after it successfully captures the channel and transmits a window of frames. Let *b(t)* be the stochastic process that represents the backoff time counter for a specific station. Process *b(t)* takes only integer values and represents the remaining CAS the station will defer before transmitting. Time scale *t* is also slotted and *t* takes only integer values; *t* represents the beginning of a CAS and *t*+1 represents the beginning of the next CAS. Stations increment *t* at the beginning of a CAS. We will use the term 'slot' to denote an increase in this discrete time scale. If the CAS is empty or contains a collision, an increase in the discrete time scale *t* (slot) corresponds to a CAS duration (σ) in the system time t_s. However, if the CAS contains a successful reservation, a slot corresponds to the total time required for a transmission of *w* frames during the successful reservation (see Fig. 6.1).

The stochastic backoff process *b(t)* decrements by one for every *t* increase. When *b(t)* reaches zero, the station transmits an RTS frame and the new *b(t)* value is randomly selected by a flat distribution in the range (0,*CW*-1). The current *CW* value depends on the number of successful reservations and collisions the station has experienced in the past. As a result, process *b(t)* is non-markovian. We use for convenience the notation $W=CW_{min}$. We define 'maximum backoff stage' *m* as $CW_{max}=W+4m$ and

$$W_i = W + 4i, \quad i \in (0, m) \tag{6.1}$$

where *i* is defined as the 'backoff stage'. According to the definition, $W=W_0=CW_{min}$ and $W_m=CW_{max}$. According to AIr LM specification [42], $CW_{min}=8$, $CW_{max}=256$ and $m=62$. We use $s(t)$ to denote the stochastic process representing the backoff stage $i \in (0,m)$ of the station at time *t*,

$$s(t) = i, \quad i \in (0, m) \tag{6.2}$$

Considering that W_i is the current *CW* value of a station and that process *b(t)* represents the remaining CAS a station will defer transmission, Figure 6.1 shows *s(t)* and *b(t)* values for the contention process presented in Figure 5.5. Figure also shows how discrete time scale *t* relates to system time t_S and presents the slot duration. Discrete time scale *t* increases only at the beginning of a CAS and takes only integer

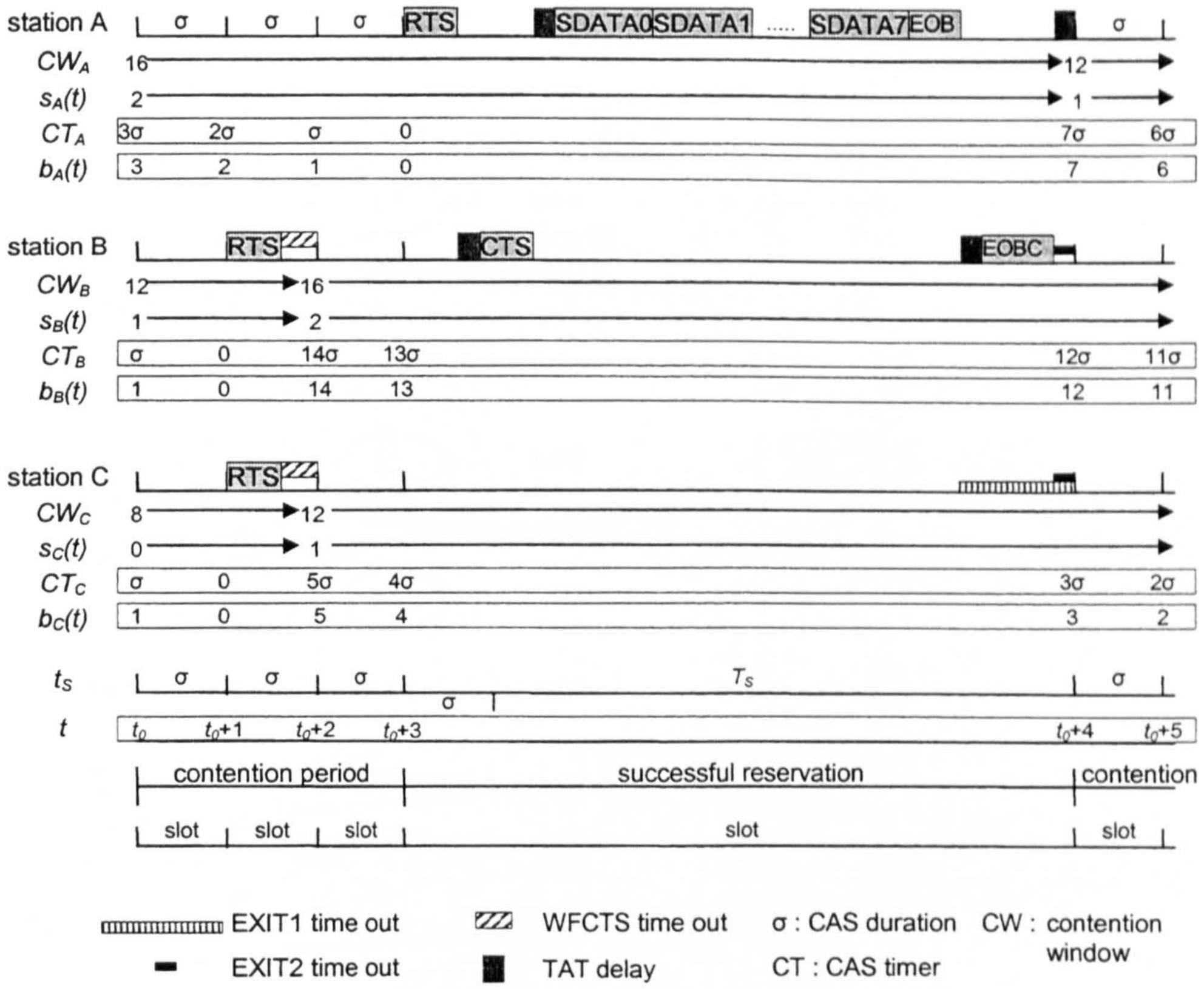

Figure 6.1. Stochastic processes $s(t)$ and $b(t)$

values. At the beginning of the contention ($t=t_0$), station A is at backoff stage 2 ($s_A(t_0)=2$) because its current CW value is 16 ($CW_A=16=8+4x2$). Station A also has $b_A(t_0)=3$ because it will defer for three CAS before transmitting an RTS. Similarly, station B has $s_B(t_0)=1$ and $b_B(t_0)=1$ and station C has $s_C(t_0)=0$ and $b_C(t_0)=1$. As the first CAS is empty, stations do not change backoff stage ($s_X(t_0+1)=s_X(t_0)$, $X=\{A,B,C\}$), decrement their $b(t)$ value ($b_X(t_0+1)=b_X(t_0)-1$, $X=\{A,B,C\}$) and the slot duration is σ. As the second CAS contains a collision of stations B and C, these stations increase their backoff stages ($s_B(t_0+2)=s_B(t_0+1)+1=2$ and $s_C(t_0+2)=s_C(t_0+1)+1=1$) and randomly select new $b(t)$ values ($b_B(t_0+2)=14$ and $b_C(t_0+2)=5$). Station A decreases its $b(t)$ value because it does not receive a valid frame and the slot duration is σ. The third CAS is empty and at (t_0+3) stations have $s_A(t_0+3)=2$, $b_A(t_0+3)=0$, $s_B(t_0+3)=2$, $b_B(t_0+3)=13$, $s_C(t_0+3)=1$ and $b_C(t_0+3)=4$. The fourth CAS contains a successful RTS transmission and, as discrete time scale t increases only at the beginning of a CAS, the slot duration is T_S and contains the successful RTS/CTS exchange, the transmission time of the SDATA

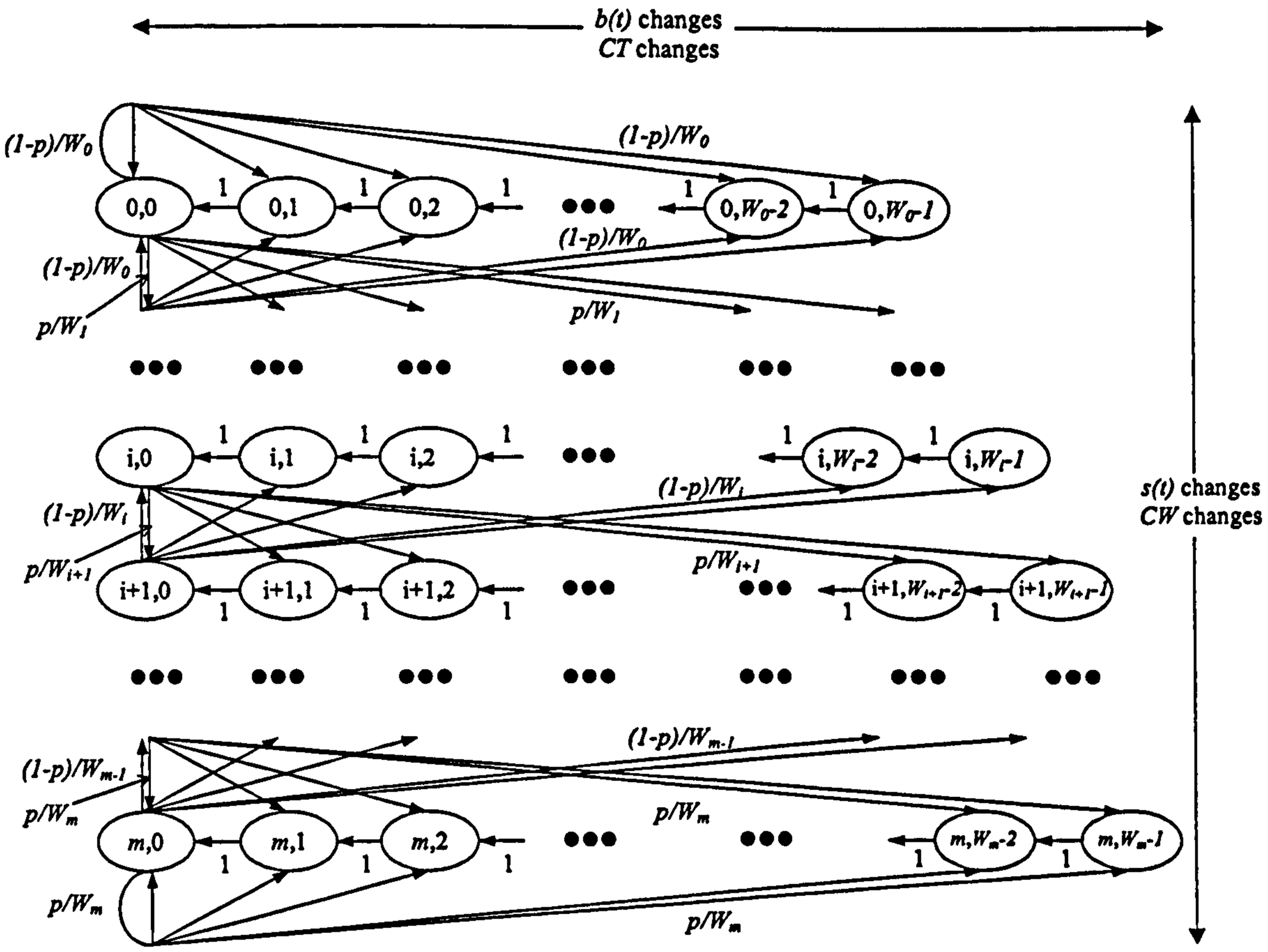

Figure 6.2 Markov Chain model for back off CW

frames and the EOB/EOBC frame exchange. Stations B and C decrease their $b(t)$ values ($b_B(t_0+4)=12$ and $b_C(t_0+4)=3$) and station A decreases its back off stage ($s_A(t_0+4)=1$) and randomly selects a new $b(t)$ value ($b_A(t_0+4)=7$) because it accomplished a successful reservation.

Assuming that the collision probability p is constant and independent of the CW used to select the current deferral period, the bidimentional process $\{s(t),b(t)\}$ can be represented by the discrete-time Markov chain drawn in Fig. 6.2. Lets assume that a station's bidimentional process $\{s(t),b(t)\}$ is currently at state (i,k), $i=0,1,...,m$, $k=0,1,...,W_i-1$. As $s(t)=i$, the station's current CW value is W_i; as $b(t)=k$, the station will defer k slots before transmitting an RTS. As $b(t)$ decrements at the discrete time scale, a decrement may correspond to an empty CAS or to an RTS collision by other stations or to a successful reservation of another station. After k steps, the station reaches state $(i,0)$ and transmits an RTS. As this transmission collides with probability p, the station will transition to state $(i+1,k)$ with probability p/W_{i+1}, where k is randomly selected in the range $(0,W_{i+1}-1)$; as this RTS transmission is successful with probability $(1-p)$, the

station will transition (at the end of the reservation, see Fig. 6.1) to state (*i-1*,*k*) with probability $(1-p)/W_{i-1}$, where k is randomly selected in the range $(0,W_{i-1}-1)$ in this case.

The only non-null one-step transition probabilities of the chain are (using the short notation $P\{i_1,k_1 \mid i_0,k_0\} = P\{s(t+1)=i_1, b(t+1)=k_1 \mid s(t)=i_0, b(t)=k_0\}$):

$$\begin{cases} P\{i,k \mid i,k+1\}=1 & k\in(0,W_i-2) \quad i\in(0,m) \\ P\{i,k \mid i+1,0\}=(1-p)/W_i & k\in(0,W_i-1) \quad i\in(0,m-1) \\ P\{i+1,k \mid i,0\}=p/W_{i+1} & k\in(0,W_{i+1}-1) \quad i\in(0,m-1) \\ P\{0,k \mid 0,0\}=(1-p)/W_0 & k\in(0,W_0-1) \\ P\{m,k \mid m,0\}=p/W_m & k\in(0,W_m-1) \end{cases} \tag{6.3}$$

The first equation in (6.3) accounts for the fact that the backoff time counter is decreased until it reaches zero. The second and third equations represent the *CW* decrease and the *CW* increase after a successful reservation and a collision respectively. The fourth equation considers that if the current backoff stage is 0, the *CW* value is not further decreased even after a successful reservation. Finally, the fifth equation considers that the *CW* is not increased after a collision if the maximum backoff stage m is reached.

We define that $b_{i,k} = \lim_{t\to\infty} P\{s(t)=i, b(t)=k\}$, $i\in(0,m)$, $k\in(0,W_i-1)$ represents the stationary distribution of the chain. Considering that $b_{00} = (1-p)b_{00} + (1-p)b_{10}$, b_{10} is given by:

$$b_{10} = \frac{p}{1-p} b_{00} \tag{6.4}$$

Since $b_{10} = pb_{00} + (1-p)b_{20}$, b_{20} is given by

$$b_{20} = \left(\frac{p}{1-p}\right)^2 b_{00} \tag{6.5}$$

Consequently, it can be easily shown that

$$b_{i0} = \left(\frac{p}{1-p}\right)^i b_{00},\ i\in(0,m) \tag{6.6}$$

Owing to chain regularities, for each $k\in(0,W_i-1)$,

$$b_{0k} = \frac{W_0-k}{W_0}\left(b_{10}(1-p)+b_{00}(1-p)\right)$$

$$b_{ik} = \frac{W_i - k}{W_i}\left(b_{i+1,0}(1-p) + b_{i-1,0}p\right),\ i \in (1, m-1) \qquad (6.7)$$

$$b_{mk} = \frac{W_m - k}{W_m}\left(b_{m-1,0}p + b_{m0}p\right)$$

After some algebra

$$b_{0k} = \frac{W_0 - k}{W_0} b_{00}$$

$$b_{ik} = \frac{W_i - k}{W_i} b_{i0},\ i \in (1, m-1) \qquad (6.8)$$

$$b_{mk} = \frac{W_m - k}{W_m} b_{m0}$$

Equations (6.8) can be rewritten as

$$b_{ik} = \frac{W_i - k}{W_i} b_{i0},\ i \in (0, m), k \in (0, W_i - 1) \qquad (6.9)$$

As a result, equations (6.6) and (6.9) express all $b_{i,k}$ values as a function of b_{00} and probability p. By applying the normalization factor

$$1 = \sum_{i=0}^{m}\sum_{k=0}^{W_i-1} b_{ik} = \sum_{i=0}^{m} b_{i0} \sum_{k=0}^{W_i-1} \frac{W_i - k}{W_i} = \sum_{i=0}^{m} b_{i0} \frac{W_i + 1}{2} = \frac{b_{00}}{2} \sum_{i=0}^{m} \left(\frac{p}{1-p}\right)^i (W_i + 1) \qquad (6.10)$$

and by substituting W_i form equation (6.1),

$$1 = \frac{b_{00}}{2}\left[(W+1)\sum_{i=0}^{m}\left(\frac{p}{1-p}\right)^i + 4\sum_{i=0}^{m} i\left(\frac{p}{1-p}\right)^i\right] \qquad (6.11)$$

After some algebra we derive

$$1 = \frac{b_{00}}{2}\left[(W+1)\frac{(1-p)^{m+1} - p^{m+1}}{(1-2p)(1-p)^m} + \frac{4p(1-p)}{(1-2p)^2}\left(1 - \frac{p^m(1+m) - p^{m+1}(2m+1)}{(1-p)^{m+1}}\right)\right] \qquad (6.12)$$

Equation (6.12) expresses b_{00} as a function of the collision probability p, the smallest contention window size W and the number of backoff stages m. This analysis allows us to evaluate the station's transmission probability τ. Considering that a station transmits when the backoff timer reaches zero,

$$\tau = \sum_{i=0}^{m} b_{i0} = b_{00} \sum_{i=0}^{m} \frac{p^i}{(1-p)^i} = b_{00} \frac{(1-p)^{m+1} - p^{m+1}}{(1-2p)(1-p)^m} \qquad (6.13)$$

Substituting the value of b_{00} from eq. (6.12) to eq. (6.13), τ is given by

$$\tau(p):\tau=\frac{2}{(W+1)+\frac{4p\left((1-p)^{m+1}+(2m+1)p^{m+1}-(m+1)p^{m}\right)}{\left((1-p)^{m+1}-p^{m+1}\right)(1-2p)}} \tag{6.14}$$

Equation (6.14) expresses probability τ as a function of the unknown probability p. Assuming that the number of transmitting stations n is constant and that all contending stations 'see' the discrete-time Markov chain drawn in Fig. 6.2 at the steady state and transmit with probability τ, the transmission collision probability p can be expressed as the probability that at least an extra one of the remaining (n-1) stations transmit at the chosen CAS

$$p=1-(1-\tau)^{n-1} \tag{6.15}$$

Equations (6.14) and (6.15) form a non-linear system with the unknowns τ and p which can be solved by employing numerical methods. Finally, τ and p are evaluated for a certain W, m and n combination. It is easy to demonstrate that there is only one solution to the non-linear system. Equation (6.15) can be rewritten as:

$$\tau^{*}(p):\tau=1-(1-p)^{1/(n-1)} \tag{6.16}$$

The function $\tau^{*}(p)$ is a continuous and monotonically increasing function in the range $p\in(0,1)$ and increases from $\tau^{*}(0)=0$ to $\tau^{*}(1)=1$. Function $\tau(p)$ is a continuous and monotonically decreasing function is the same range. It decreases from $\tau(0)=\frac{2}{W+1}$ to $\tau(1)=\frac{2}{W+1+4m}$. There is only one solution to the non-linear system because $\tau(0)>\tau^{*}(0)$ and $\tau(1)<\tau^{*}(1)$. Continuity of function $\tau(p)$ with respect to critical value p=1/2 is easily shown by taking into account that in this case equation (6.6) reduces to $b_{i0}=b_{00},\ i\in(0,m)$ and equation (6.10) becomes

$$1=\frac{b_{00}}{2}\sum_{i=0}^{m}(W_i+1)=\frac{b_{00}}{2}\sum_{i=0}^{m}(W+4i+1)=\frac{b_{00}}{2}\left((m+1)(W+1)+4\sum_{i=0}^{m}i\right) \tag{6.17}$$

and $b_{00}=\frac{2}{(m+1)(W+2m+1)}$. In this case $\tau(1/2)=(m+1)b_{00}=\frac{2}{W+2m+1}$.

6.2.2 Utilization analysis

Based on the calculated collision probability p and transmission probability τ, we can now analyse all possible events that can occur in a randomly chosen slot. Let P_{tr} be

the probability that at least one station transmits an RTS frame in the considered slot. For a LAN of n contending stations and a station transmission probability τ,

$$P_{tr} = 1-(1-\tau)^n \tag{6.18}$$

Let P_s be the conditional probability that an occurring RTS transmission is successful (P(success/trans)). P_s can be evaluated as the probability that, in the considered slot, one station transmits an RTS and the remaining (n-1) stations defer transmission provided that at least one station transmits an RTS,

$$P_s = \frac{P_{success}}{P_{tr}} = \frac{n\tau(1-\tau)^{n-1}}{1-(1-\tau)^n} \tag{6.19}$$

A successful reservation occurs with probability P_sP_{tr} in a randomly selected slot and the time utilized for transmitting payload information is wt, where w is the window size and t is defined as the time required for transmitting payload information data in an SDATA frame. The value of t is given by

$$t = \frac{RR\,l}{C} \tag{6.20}$$

where RR is the Repetition Rate, l is the payload data length and C is the base data rate. Considering that a randomly selected slot is empty with probability 1-P_{tr} and contains a collision with probability P_{tr}(1-P_s), utilization can be evaluated by dividing the time utilized for transmitting payload data by the average slot duration

$$U = \frac{1}{RR} \cdot \frac{P_{tr}P_s wt}{(1-P_{tr})\sigma + P_{tr}P_sT_s + P_{tr}(1-P_s)\sigma} \tag{6.21}$$

where T_s is the slot duration when a successful reservation is accomplished and σ is the CAS duration. Equation (6.21) considers that a collision lasts exactly one CAS duration. Utilization equation (6.21) can be easily reduced to

$$U = \frac{1}{RR} \cdot \frac{P_{tr}P_s wt}{P_{tr}P_sT_s + \sigma - P_{tr}P_s\sigma} \tag{6.22}$$

When the Reserved transfer mode with sequenced data is utilized

$$T_S = D + w(t + F_S + p_1) \tag{6.23}$$

where D is the reservation overhead that includes the transmission time of the RTS, CTS, EOB and EOBC frames and the TAT delays that follow these frames, F_S is the transmission time of the SDATA frame overhead (preamble, robust header, CRC etc.) and p_1 is the preparation time of an SDATA frame. Assuming that the RTS MBR field

is always transmitted using RR=1, D=1.74 msec. The value of F_S is given by

$$F_S = T_{RH} + \frac{RR\, l_S^{'}}{C} \tag{6.24}$$

where $l_S^{'}$ is the length of the MBR overhead of an SDATA frame and T_{RH} is as defined in section 5.2. T_{RH} is the transmission time of a frame with no MBR field. According to Fig. 5.3, $l_S^{'}$ =80 bits and section 5.2 evaluates that T_{RH}=232 μsec.

Our analytical model allows measurement of the time portion utilized on all tasks affecting AIr utilization. Such an evaluation reveals the impact of physical and link layer parameters to utilization. It is valuable for link designers in achieving high utilization at a reasonable cost and for link implementers in selecting suitable parameter values in order to maximize utilization. Considering that a randomly selected slot is empty with probability 1-P_{tr} and that the CAS duration is σ, the time portion utilized in empty CAS is given by

$$U_{empty} = \frac{(1-P_{tr})\sigma}{P_{tr}P_s T_s + \sigma - P_{tr}P_s\sigma} \tag{6.25}$$

A randomly selected slot contains a collision with probability P_{tr}(1-P_s) and the time portion utilized on collisions when two or more stations are simultaneously trying to reserve the infrared channel is

$$U_{coll} = \frac{P_{tr}(1-P_s)\sigma}{P_{tr}P_s T_s + \sigma - P_{tr}P_s\sigma} \tag{6.26}$$

The time portion utilized on transmitting data frame overheads, reservation control frames (RTS, CTS, EOB and EOBC) and the associated TAT delays is

$$U_{over} = \frac{P_{tr}P_s(T_s - wt)}{P_{tr}P_s T_s + \sigma - P_{tr}P_s\sigma} \tag{6.27}$$

The average contention period for a successful reservation, C_p, is given by

$$C_p = \frac{1-P_{tr}P_s}{P_{tr}P_s}\sigma \tag{6.28}$$

The calculated C_p value represents the overhead introduced by the CA procedures for a successful reservation and is particularly useful if the LC layer implements error control. In this case, a MAC successful reservation may contain only an LC acknowledgment frame that informs the transmitter of the correctly received frames in the previous window transmission. It will be used in chapter 7 which considers channel

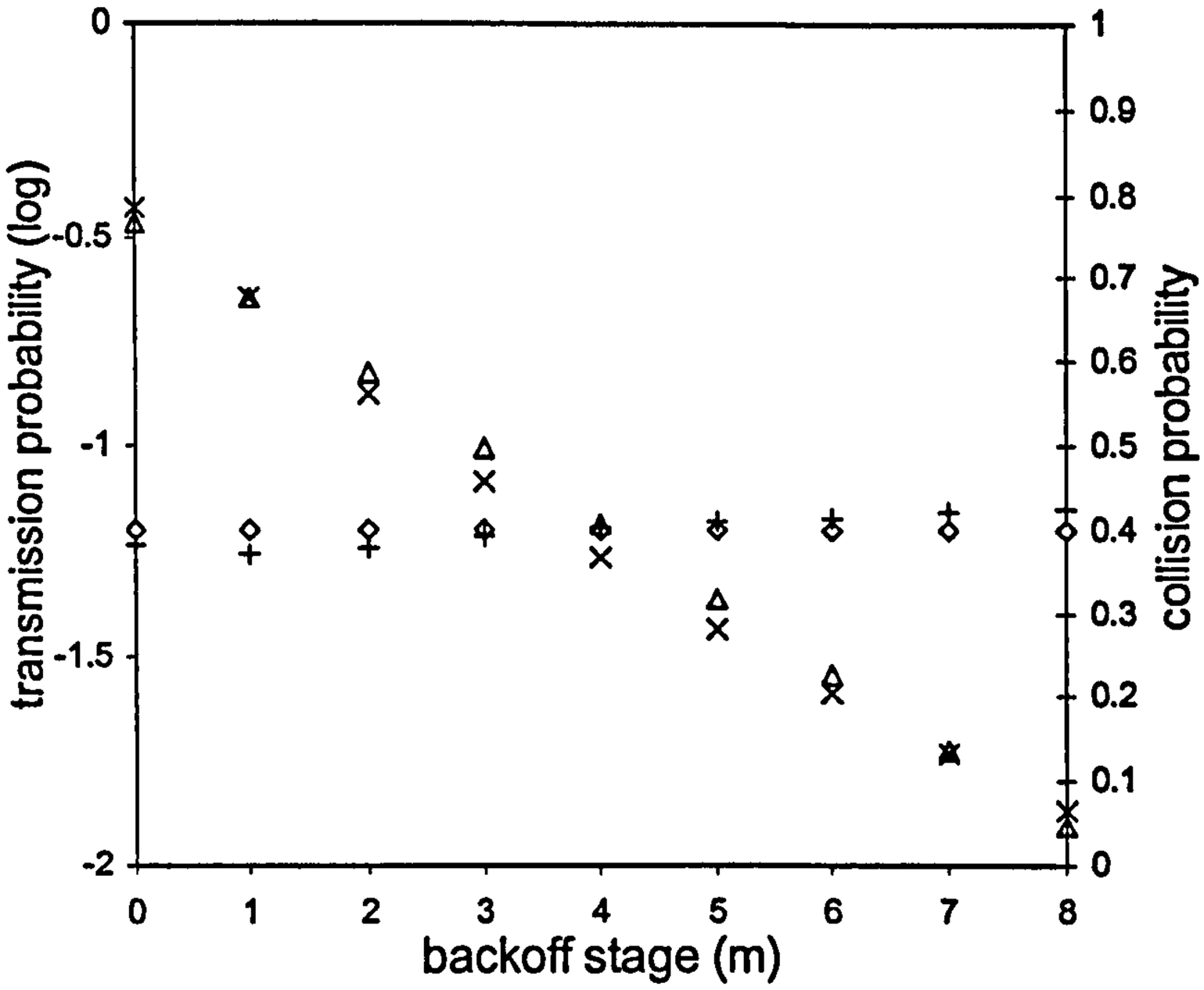

+ *collision probability p_i, simulation*
◇ *collision probability p, analysis*
× *transmission probability q_i, simulation*
△ *transmission probability q_i, analysis*

Figure 6.3 Transmission (q_i) and collision (p_i) probabilities versus back off stage, W=8, m=62, n=5

errors, LC acknowledgement overhead and retransmission delays.

6.3 Model validation

The model presented in the previous section is validated by comparing analysis with simulation results obtained from the OPNET simulator presented in section 5.6. We first focus on the behavior of a single station. The probability that a station's transmission is at stage i is denoted by q_i. The analytical model calculates probabilities q_i by

$$q_i = \frac{b_{i0}}{\tau}, \; i=0,1, \ldots ,m \tag{6.29}$$

Probability p_i is defined as the collision probability of a station's transmission at stage i. The average collision probability, p_{ave}, of a station's transmission is given by

$$p_{ave} = \sum_{i=0}^{m} q_i p_i \tag{6.30}$$

The key assumption of the analytical model can now be expressed as

$$p = p_{ave} = p_i, \; i=0,1, \ldots ,m \tag{6.31}$$

Fig. 6.3 compares simulation and analysis results for the q_i and p_i probabilities for a

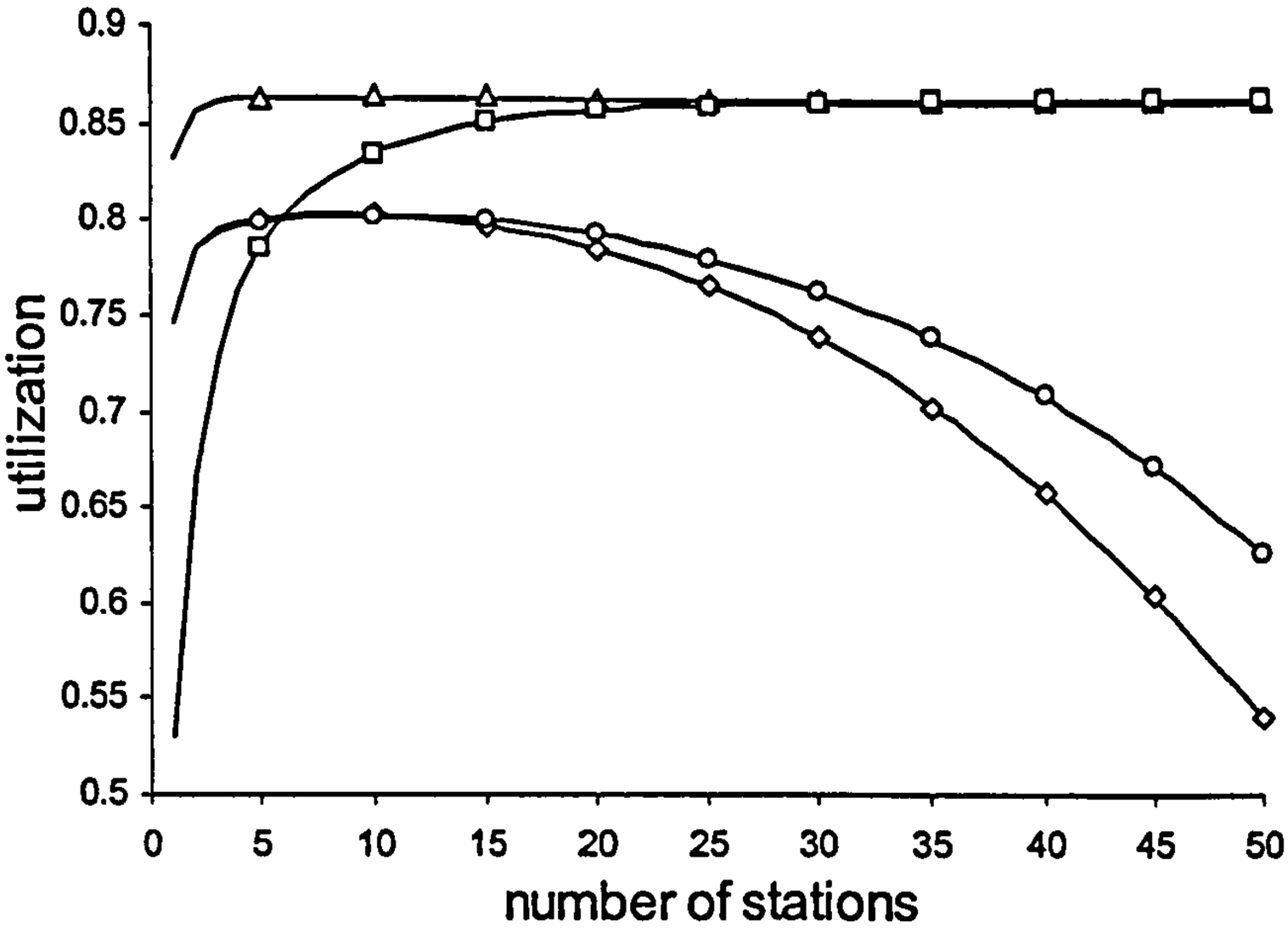

△ *W=8, m=62, l=16Kbits, w=8, C=4Mbit/s, RR=1*
□ *W=64, m=62, l=16Kbits,w=8, C=4Mbit/s, RR=1*
◇ *W=8, m=4, l=16Kbits, w=4, C=4Mbit/s, RR=1*
○ *W=8, m=5, l=16Kbits, w=4, C=4Mbit/s, RR=1*

Figure 6.4 Utilization: analysis versus simulation

network with five transmitting stations using the proposed values for W and m parameters. The figure includes only stages with transmission probability higher than 1% and shows that high back off stages are rarely used for n=5. Simulation results are acquired with a 95% confidence interval lower than 0.002. Slight differences are noticed between the p_i values and the p value that approximates them. The simulation calculated that the average collision probability p_{ave} is 0.385 and it is effectively approximated by the analytical model's constant collision probability p of 0.397. In addition, simulation results indicate that the collision probability p_i is not significantly different for higher stages, as it might have been expected. This result validates the key assumption of the proposed analytical model.

Considering the behavior of a network with n stations, analysis and simulation utilization versus network size is plotted in Fig. 6.4 for different W and m values. In all cases, the analytical model is proven extremely accurate as analytical results (lines) coincide with simulation results (symbols). Figure shows that the slight differences between p_i and p probabilities observed in Fig. 6.3 have negligible impact on utilization. Simulation results are again calculated with a 95% confidence interval lower than 0.002.

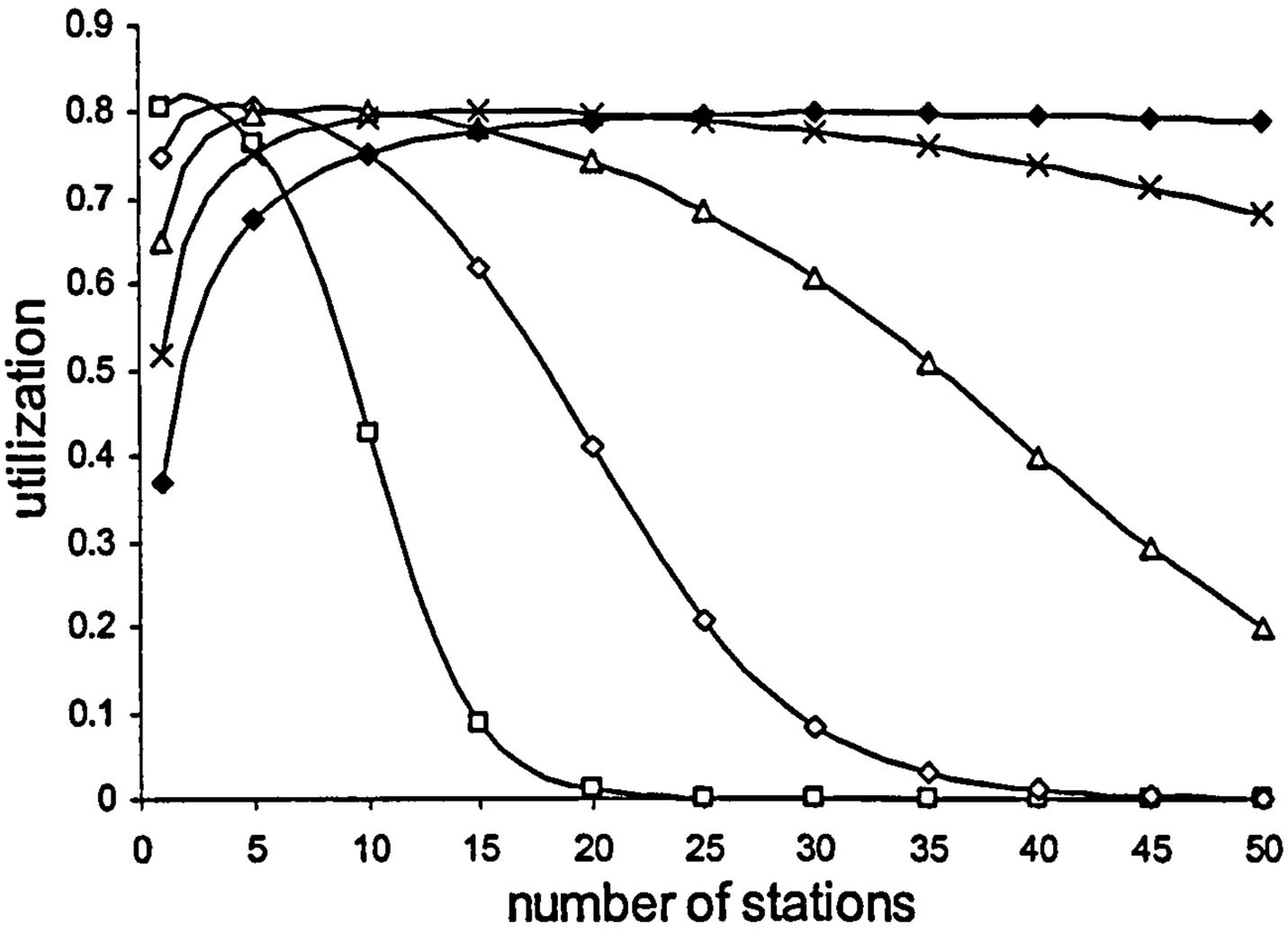

□ *CW (slots)=4*
◇ *CW (slots)=8*
△ *CW (slots)=16*
x *CW (slots)=32*
◆ *CW (slots)=64*

Figure 6.5 Utilization versus n for fixed CW size, l=16Kbits, w=4, C=4Mbit/s, RR=1

6.4 Performance evaluation

This section presents a performance evaluation of the AIr protocol by employing the analytical model developed in section 6.2. The considered SDATA frame employment is referred to as Sequential No Frame Level Acknowledgment (SEQ-NoFLACK) protocol in the next chapter. This evaluation assumes that p_l is 40 μsec, the infrared channel is error free and that no Repetition Rate coding (RR=1) is implemented.

6.4.1 The effect of Contention Window (CW) size

The impact of the CW size to utilization is considered first. Fig. 6.5 plots utilization versus number of stations for fixed *CW* values, i.e. no *CW* adjustment algorithm is enforced. Utilization results are calculated by employing the analytical model proposed in section 6.2 for no backoff stages (m=0). Results for n=1 are also included because n represents the number of the transmitting stations and not the number of the participating stations in the LAN. Fig. 6.5 shows that utilization is low for networks with a small number of transmitting stations when a large *CW* value is used. When the number of stations increases, maximum utilization performance is achieved. Further

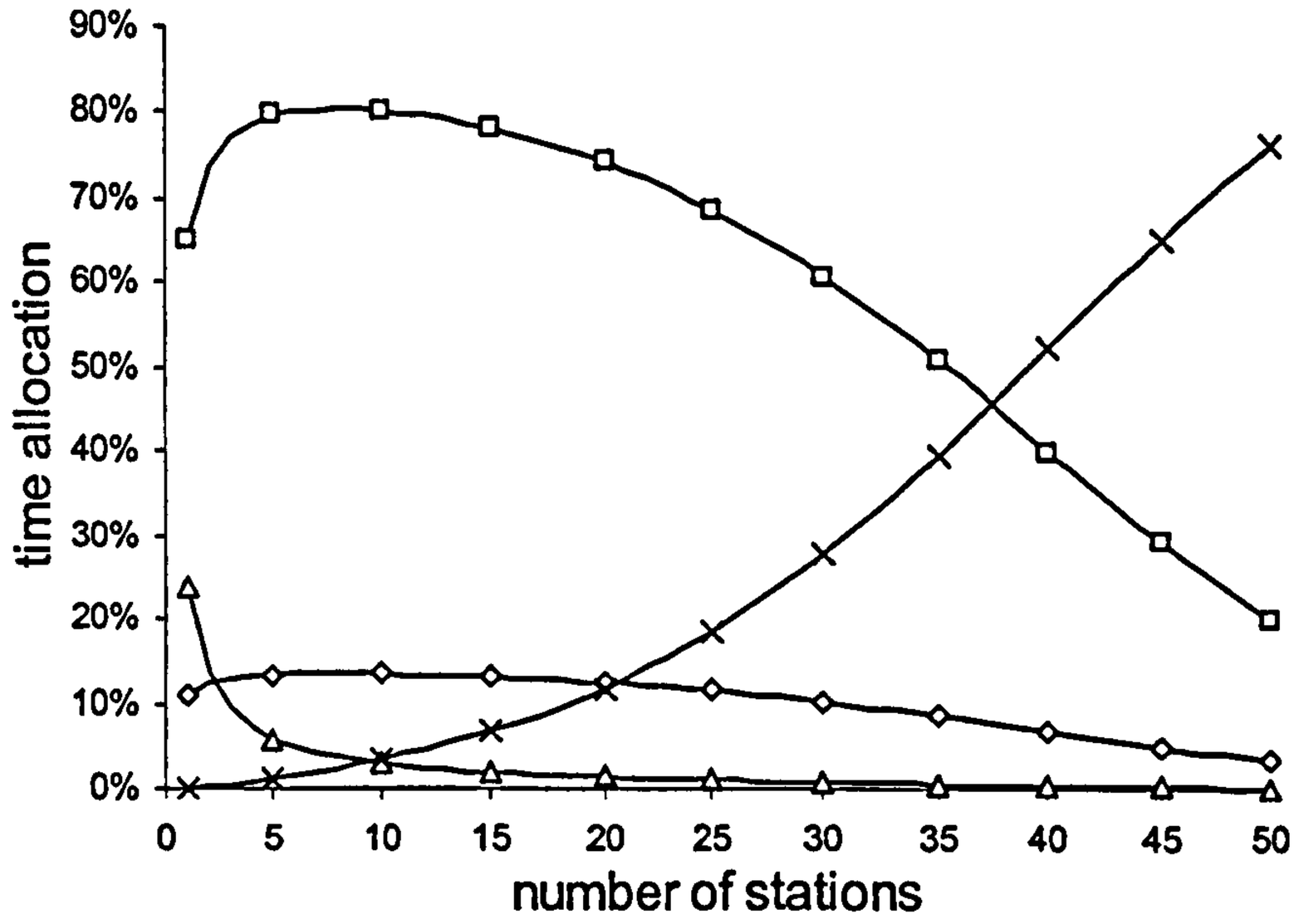

□ *payload data transmission (utilization)*
◇ *overheads*
△ *empty CAS*
x *collisions*

Figure 6.6 Time allocation of various AIr tasks versus n for fixed CW size=16 slots, l=16Kbits, w=4, C=4Mbit/s, RR=1

network size increase results in utilization degradation, especially for small *CW* values. Fig. 6.5 reveals that the *CW* value that results in maximum utilization increases if the number of transmitting stations increases. Utilization performance is significantly decreased if unsuitable *CW* values are implemented. Fig. 6.5 is identical to Fig. 5.11, which plots simulation results for the same network scenarios. This is an additional validation of the analytical model and of the results it produces. Fig. 6.6 plots all factors affecting utilization versus *n* for a fixed *CW* value of 16. Time portion utilized on empty CAS, collisions and overheads are plotted using eq. (6.25), (6.26) and (6.27) respectively. For small networks, utilization degrades mainly due to the increased number of empty CAS. For large networks, the increased number of collisions results in significant utilization degradation. Maximum utilization is observed when a suitable *CW* for the network size is used that results in a very small number of collisions and empty CAS simultaneously.

6.4.2 Optimum CW size

Optimum *CW* (W_{opt}) value for a LAN with *n* transmitting stations can be evaluated

by employing the proposed analytical model for m=0 and by setting the first derivative of the utilization equation versus τ equal to zero. When m=0, the model's key assumption that a transmission collides with the same probability regardless of the CW value used to select the deferral period is always true because CW is fixed in this case. By rearranging eq. (6.22)

$$U = \frac{wt/RR}{T_s - \sigma + \frac{\sigma}{P_{tr}P_s}} \tag{6.32}$$

Considering that w, t, T_s, RR and σ are constants, utilization is maximized when the expression

$$u = P_{tr}P_s \tag{6.33}$$

is maximized. By substituting P_{tr} and P_s values from equations (6.18) and (6.19), equation (6.33) becomes

$$u = n\tau(1-\tau)^{n-1} \tag{6.34}$$

By taking the first derivative of equation (6.34) versus τ and setting it equal to zero, after some algebra we obtain

$$\tau_{opt} = \frac{1}{n} \tag{6.35}$$

To reach optimum transmission probability τ_{opt} stations should employ the optimum CW size W_{opt}. When m=0, equation (6.14) reduces to

$$\tau = \frac{2}{W+1} \tag{6.36}$$

Combining equations (6.35) and (6.36)

$$W_{opt} = 2n - 1 \tag{6.37}$$

Maximum utilization can be evaluated from equation (6.32) if we substitute P_{tr} and P_s from equations (6.18) and (6.19) for τ_{opt} given from equation (6.35)

$$U_{max} = \frac{wt/RR}{T_s - \sigma + \sigma\left(\frac{n}{n-1}\right)^{n-1}} \tag{6.38}$$

As a result, maximum utilization depends on the number of transmitting stations in the LAN. However, for large n maximum utilization reaches a steady value. This

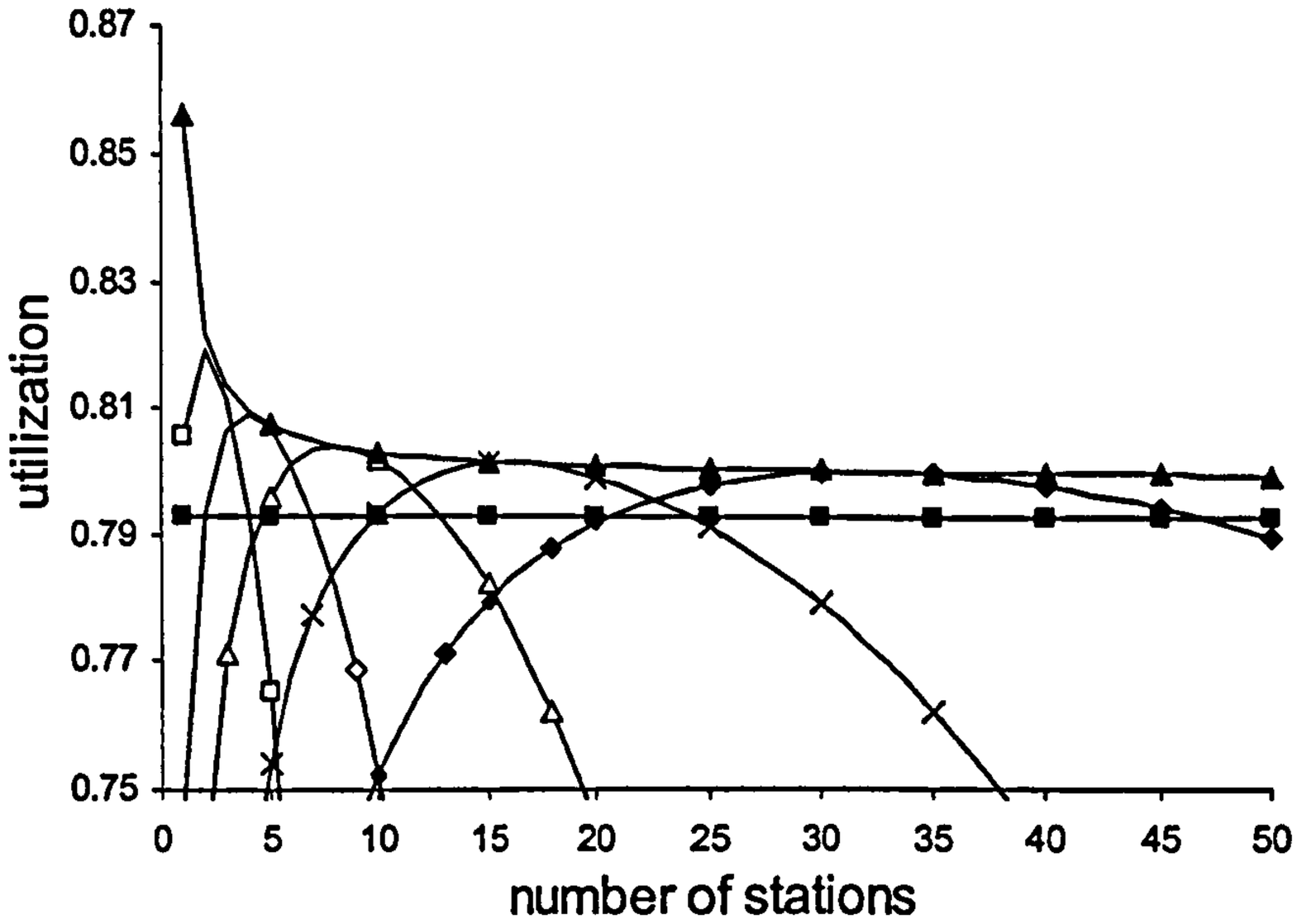

□ *CW (slots)=4*
◇ *CW (slots)=8*
△ *CW (slots)=16*
× *CW (slots)=32*
◆ *CW (slots)=64*
▲ *maximum* U_{max}
■ *maximum* U_{appr}

Figure 6.7 Utilization versus n for fixed CW size, l=16Kbits, w=4, C=4Mbit/s, RR=1

conclusion is slightly different with the expressed conclusion in [12][13] that maximum utilization is independent of n for the exponential backoff adjustment scheme of the IEEE 802.11 protocol although linear and exponential backoff schemes coincide when no adjustment (m=0) is allowed. Different conclusions arise from the approximations necessary for calculating maximum utilization in [12][13] because a collision lasts several CAS time periods in the 802.11 protocol. Fig. 6.7 plots utilization versus number of stations for fixed *CW* values and focuses on the maximum achievable utilization (note that the y-axis ranges from 0.75 to 0.87). It also plots U_{max} given from eq. (6.38) and the approximated maximum utilization U_{appr} calculated by performing the approximations presented in [12][13] for AIr's physical and link layer parameter values. The figure shows that when collisions last exactly one CAS duration, as in the AIr protocol, the approximations result in a lower calculated utilization, especially for very small LANs.

6.4.3 CW adjustment algorithm

The effectiveness of the proposed CW adjustment algorithm in estimating suitable

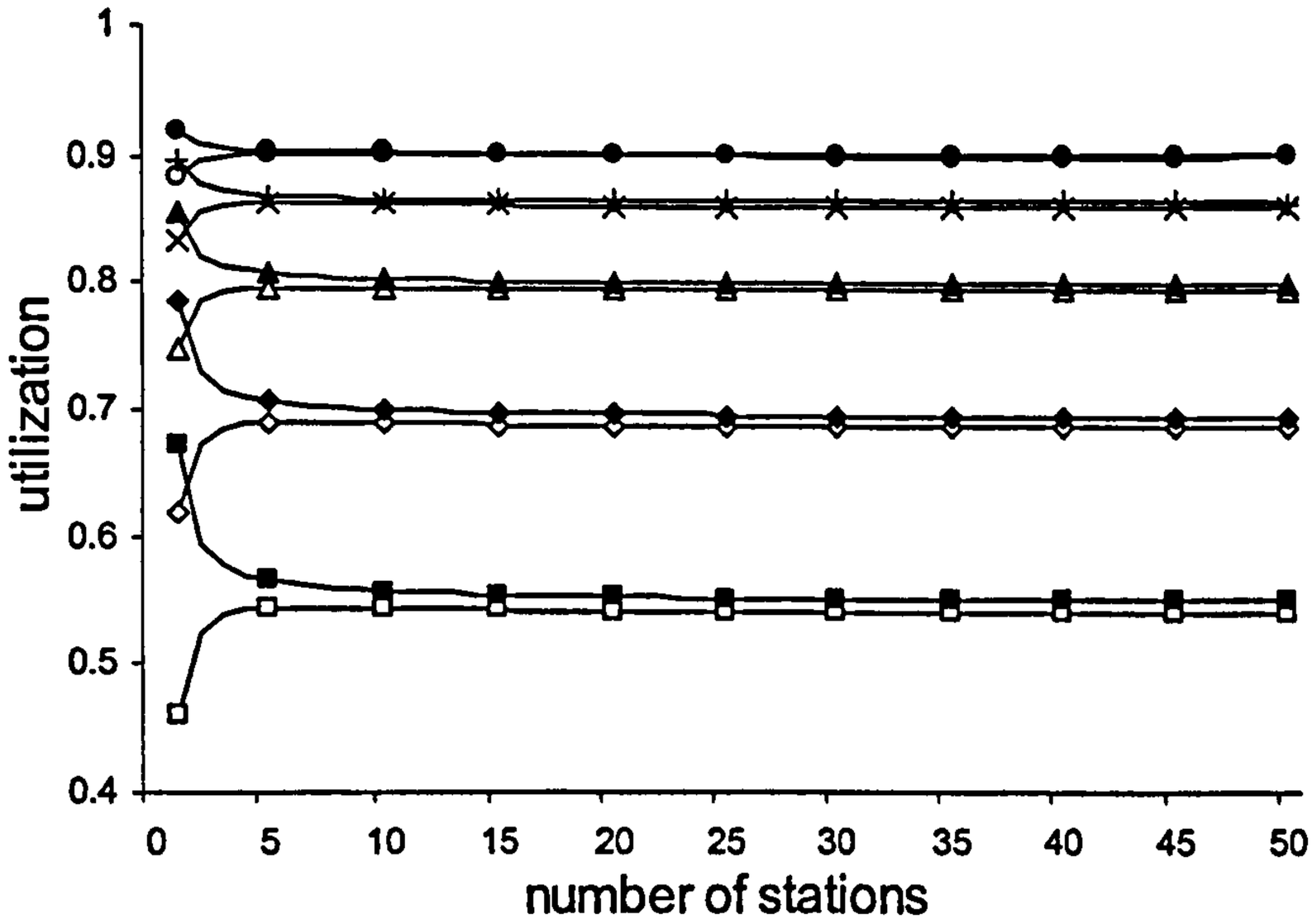

□ $w=1$
◇ $w=2$
△ $w=4$
x $w=8$
○ $w=16$

■ $w=1$, U_{max}
◆ $w=2$, U_{max}
▲ $w=4$, U_{max}
+ $w=8$, U_{max}
● $w=16$, U_{max}

Figure 6.8 Utilization versus n, l=16Kbits, W=8, m=62, C=4Mbit/s, RR=1

CW values is explored in Fig. 6.8, which compares maximum with achieved utilization for the protocol proposed CW_{min}=8 and m=62 values. The proposed algorithm performs effectively but for small networks the achieved utilization is significantly lower than the maximum possible. Fig. 6.8 also shows that utilization is very low when w is small and that applications should employ large window sizes in order to achieve high utilization. AIr is an inefficient choice for applications wishing to transmit small amounts of information data in every successful reservation.

Fig. 6.9 plots the time portion utilized by all time consuming tasks for the proposed parameter values. It also plots for comparison the same results when the optimum *CW* value (W_{opt}) is implemented. W_{opt} is calculated by eq. (6.37). For large networks, the proposed adjustment algorithm and parameter values result in more empty CAS and less colliding CAS than optimal. As utilization is slightly lower than optimal for large networks, the proposed adjustment algorithm is considered to perform satisfactorily. However, for small networks, the increased number of empty CAS results in a significantly lower utilization than optimal. Low AIr utilization for small networks was first noticed by evaluating simulation results presented in Fig. 5.12.

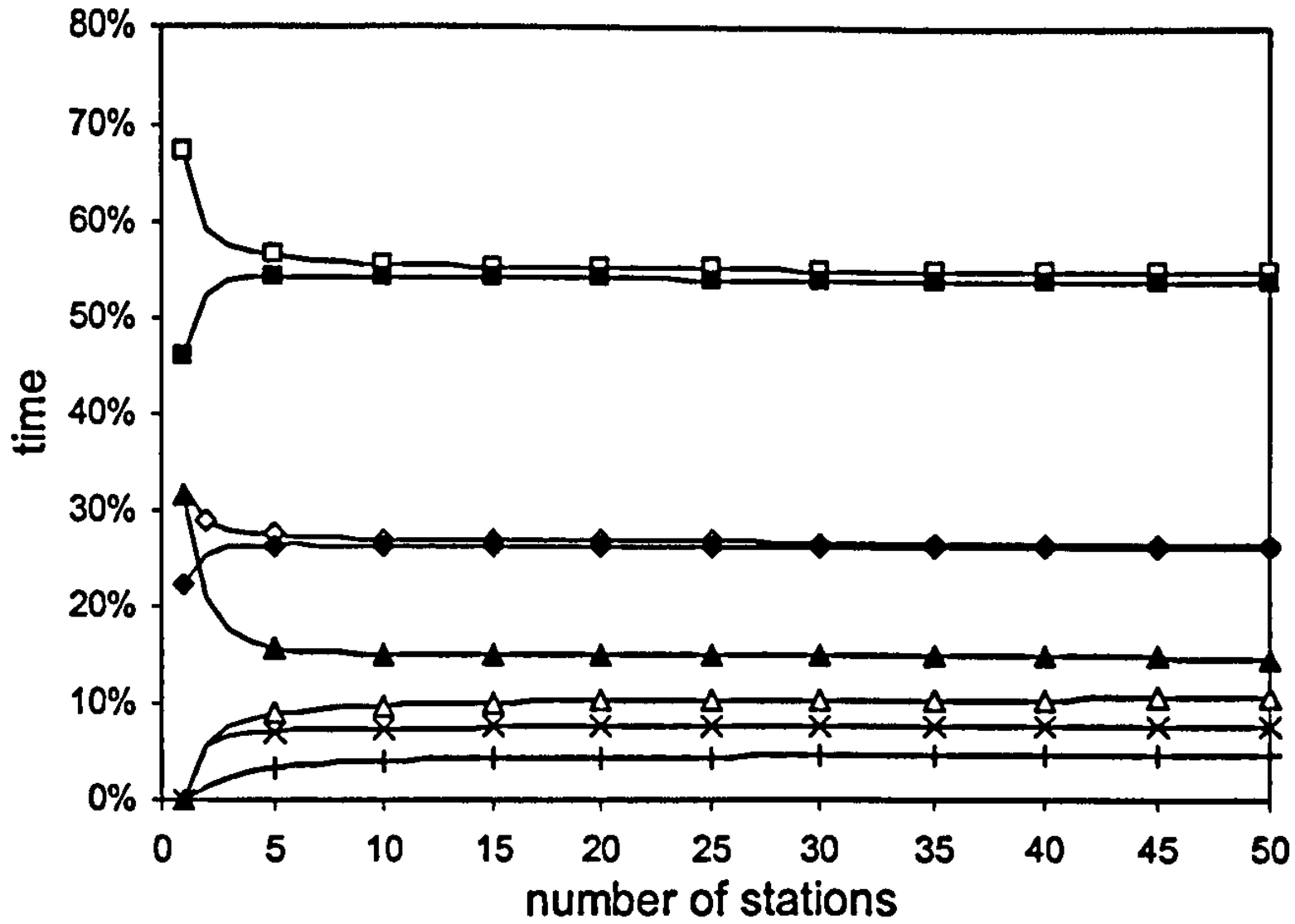

□ *payload data transmission (utilization) (optimal)*
■ *payload data transmission (utilization)*
◇ *overheads (optimal)*
◆ *overheads*
△ *empty CAS (optimal)*
▲ *empty CAS*
× *collisions (optimal)*
\+ *collisions*

Figure 6.9 Time allocation for various AIr tasks versus n, l=16Kbits, w=1, W=8, m=62, C=4Mbit/s, RR=1

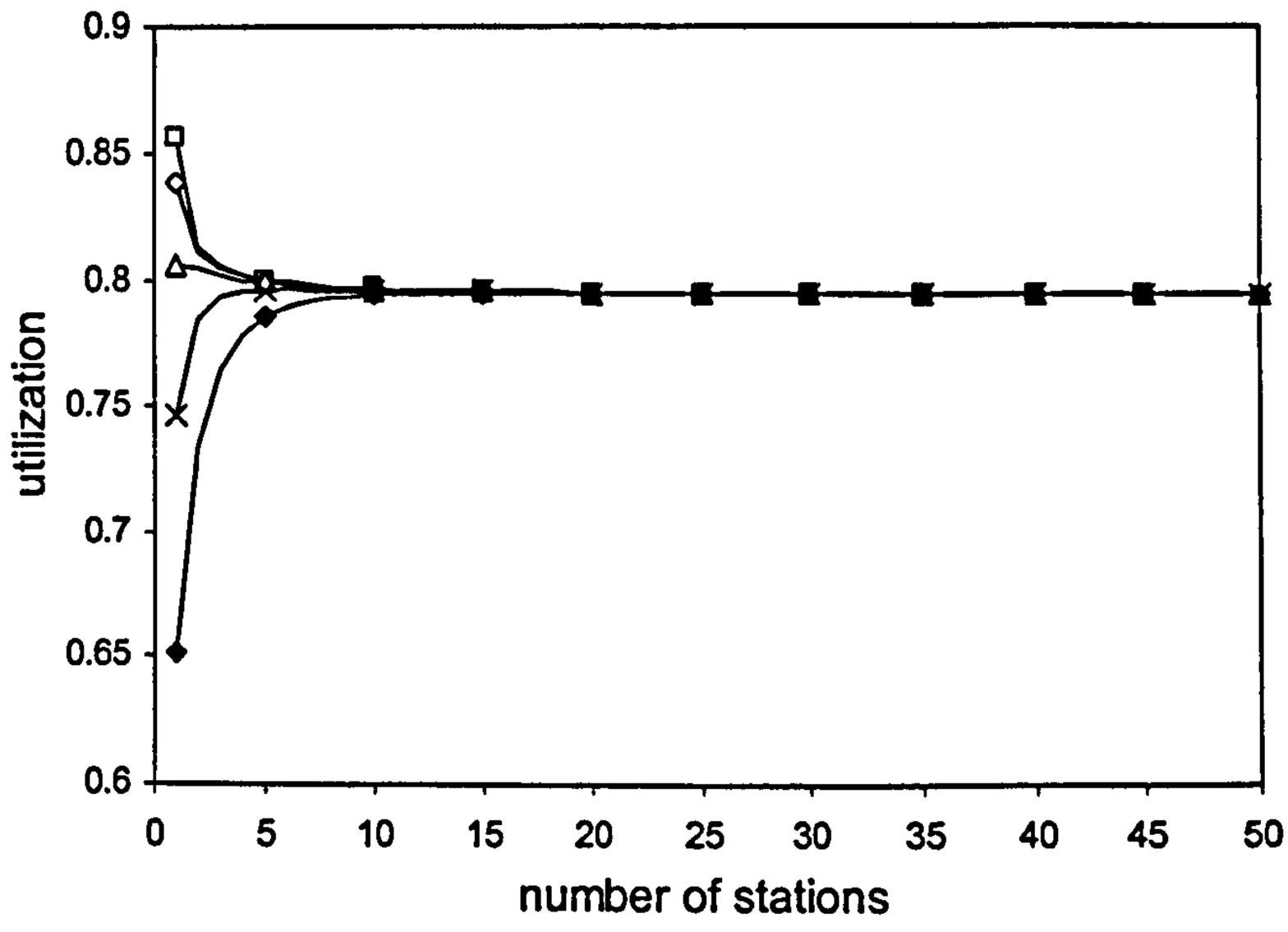

□ *W=1*
◇ *W=2*
△ *W=4*
× *W=8*
◆ *W=16*

Figure 6.10 Utilization versus n, m=62, l=16Kbits, w=4, C=4Mbit/s, RR=1

Fig. 6.10 considers the efficiency of the proposed parameter values for small networks by plotting utilization versus n for different CW_{min} (W) values. The figure

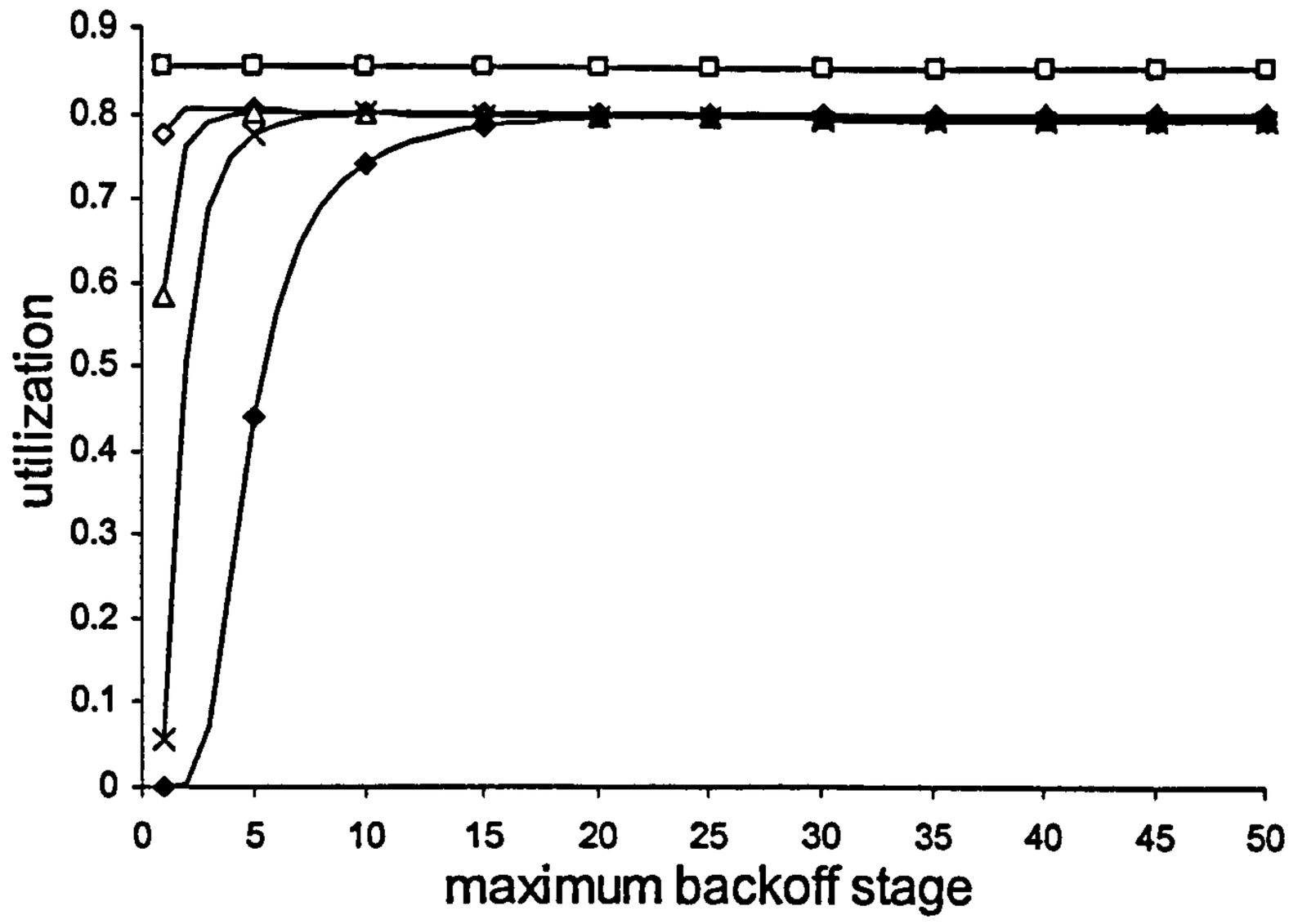

Figure 6.11 Utilization versus maximum backoff stage m, W=1, l=16Kbits, w=4, C=4Mbit/s, RR=1

shows that utilization is independent of W for large networks but highly increases for low W values for small networks. Significant utilization increase in observed by reducing W to one if only one or two stations contend for medium access, a usual case in real life wireless LANs. The situation is explained by considering that, for such small LANs, the proposed W value of 8 is significantly greater than the optimum W_{opt} value calculated by equation (6.37). Thus, utilization decreases due to the increased number of empty CAS. As a conclusion, for the considered network scenarios, W can be reduced to one in order to significantly increase utilization for small networks. Fig. 6.11 explores the suitability of the proposed CW_{max} value by plotting utilization versus maximum backoff stage m for different network sizes. Maximum backoff stage has minimal effect on utilization for small networks but a higher value is required for large networks. Utilization reaches its maximum value if m is greater than 20 even for LANs consisting of 50 transmitting stations. This value is significantly lower than the value of 62 proposed by the standard [42]. As a conclusion, new values for the W and m parameters are proposed; W=1 and m=20. Fig. 6.12 compares maximum with achievable utilization when the proposed W and m values are implemented. It shows that the achieved utilization is very close to the maximum. Direct comparison with Fig. 6.8 shows that

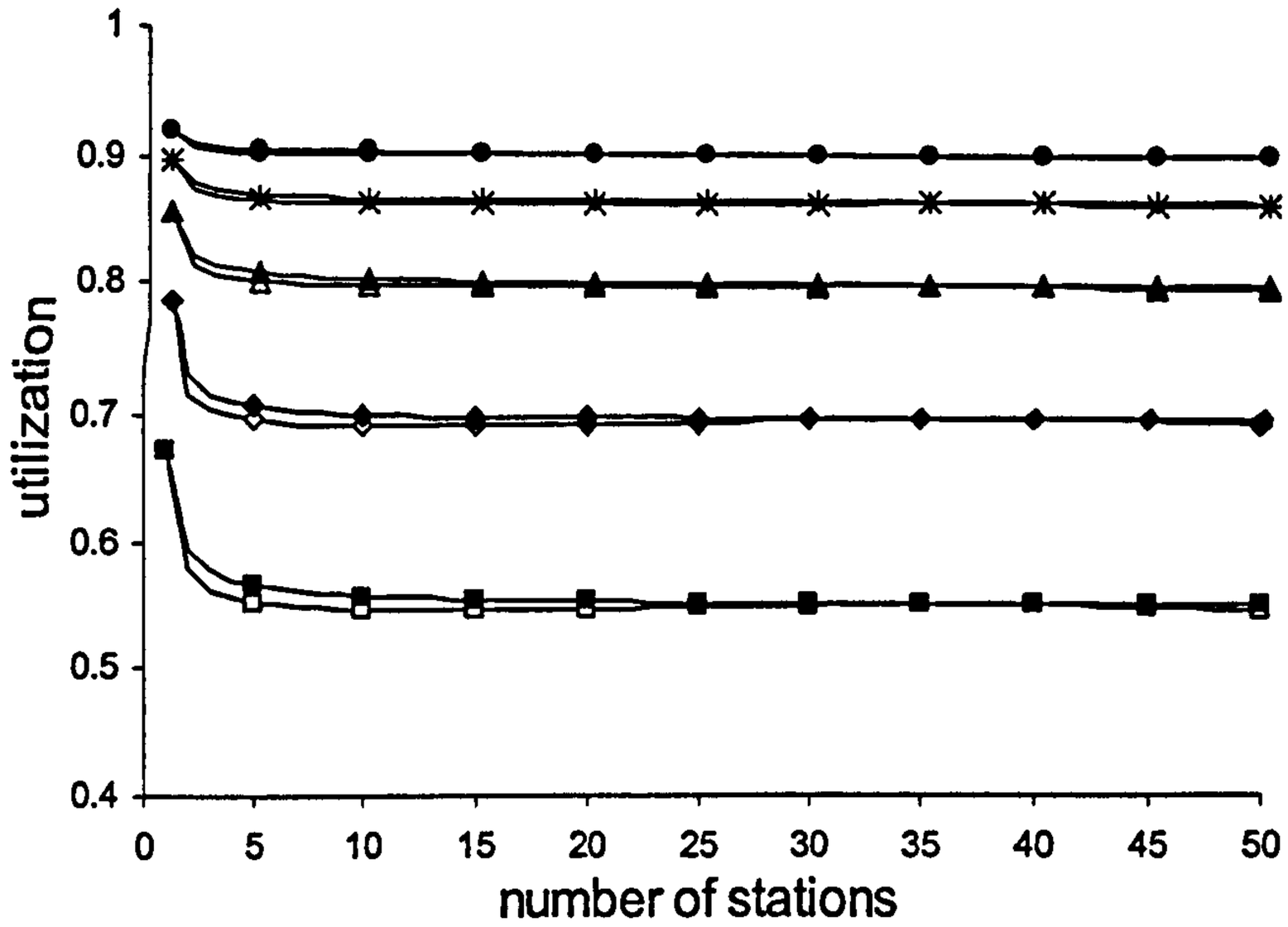

□ *w=1*
◇ *w=2*
△ *w=4*
x *w=8*
○ *w=16*

■ *w=1, U_{max}*
◆ *w=2, U_{max}*
▲ *w=4, U_{max}*
\+ *w=8, U_{max}*
● *w=16, U_{max}*

Figure 6.12 Utilization versus n, l=16Kbits, W=1, m=20, C=4Mbit/s, RR=1

utilization is greatly improved for small networks due to the implementation of the lower *W* value.

6.4.4 The effect of high RH RR value and TAT delay

Fig. 6.13 plots the time portion utilized by all time consuming tasks versus network size for two window size values (w=1 and w=4) to demonstrate the factors resulting in utilization impairment for small payload window sizes. It shows that a higher window size value (w=4) results in significant utilization improvement. Time portion utilized on empty CAS and collisions is always minimal but for the small w value of one, a significant time portion is utilized in overheads. This time portion includes a) SDATA frame header transmission, b) control (RTS/CTS/EOB/EOBC) frame transmission and c) the TAT delays that follow control frames. The situation is explained by considering that if w=1, four control frames are exchanged for every successful reservation that includes only one data frame transmission. The RH field of these control frames is always transmitted using RR=16 to ensure maximum coverage. As a result, to cope with potential hidden nodes, applications must transmit large amounts of information data

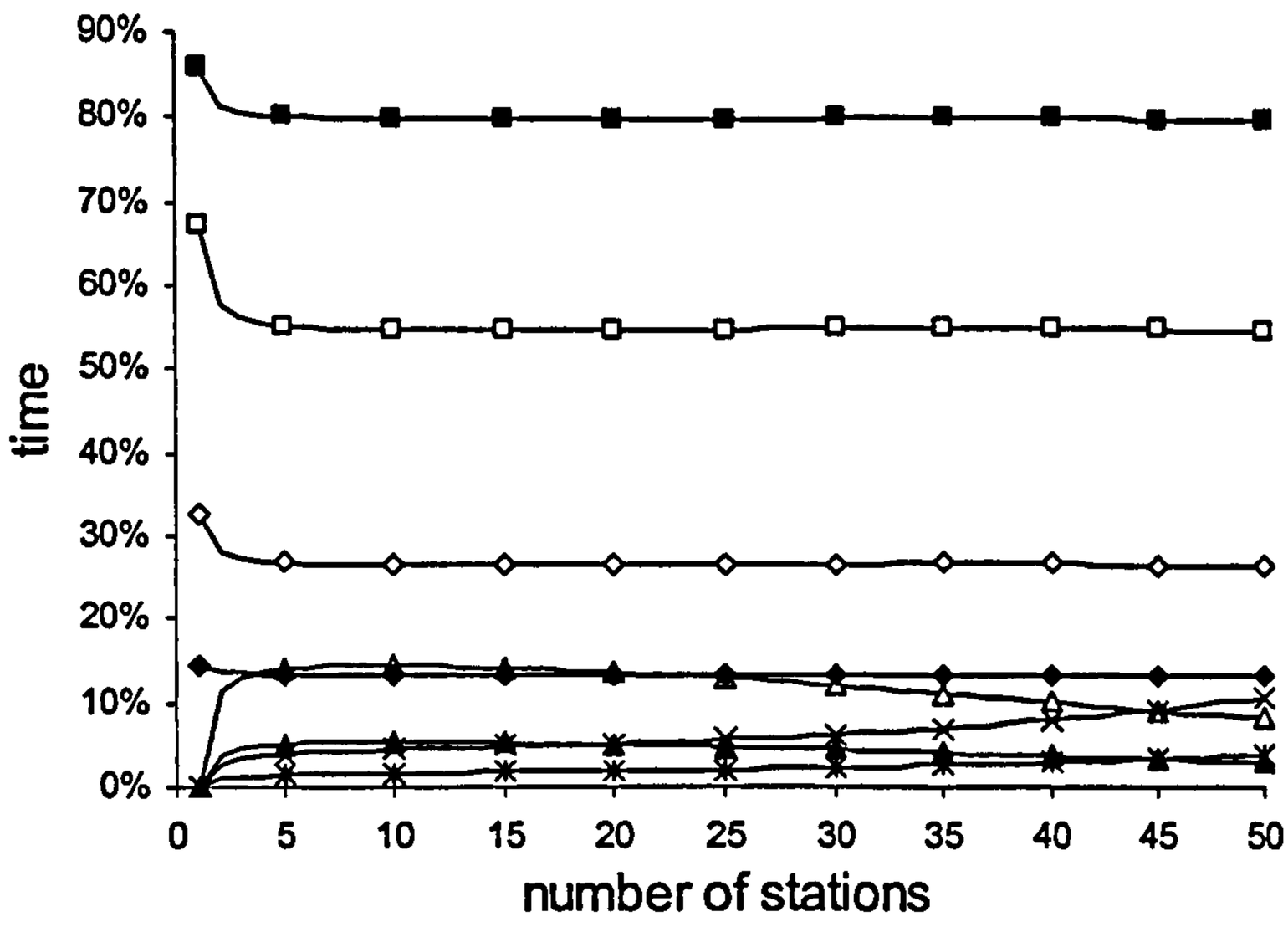

□ *payload data transmission (utilization), w=1*
◇ *overheads, w=1*
△ *empty CAS, w=1*
x *collisions, w=1*
■ *payload data transmission (utilization), w=4*
◆ *overheads, w=4*
▲ *empty CAS, w=4*
∗ *collisions, w=4*

Figure 6.13 Time allocation of various AIr tasks versus n, W=1, m=20, l=16Kbits, C=4Mbit/s, RR=1

during a successful reservation. As a conclusion, the long CAS duration and the proposed *CW* adjustment algorithm do not result in significant utilization degradation.

Fig. 6.14 presents the utilization improvement if the RH field is transmitted using *RR*=1 and/or if the TAT duration (a physical layer parameter) is reduced for applications transmitting only 16Kbits (*w*=1) of information data at *RR*=1 during a successful reservation. Small improvement is observed if only the TAT delay is reduced. However, transmitting the RH field using RR=1 results in significant utilization improvement. Further reducing the TAT delay is beneficial. For all cases, a smaller CAS duration is considered, always obeying the restriction that $\sigma >= T_{RTS}+TAT+TT_{PA}+TT_{SYNC}$ [45] to ensure that a station not capable of hearing the RTS frame will hear the beginning of the corresponding CTS frame in the CAS duration.

As a conclusion, the AIr protocol requires high window size implementation for achieving high utilization due to the high RR used in transmitting the RH field; the long CAS duration and the proposed CW adjustment algorithm do not result in significant utilization degradation. A high utilization can be achieved by transmitting the RH field

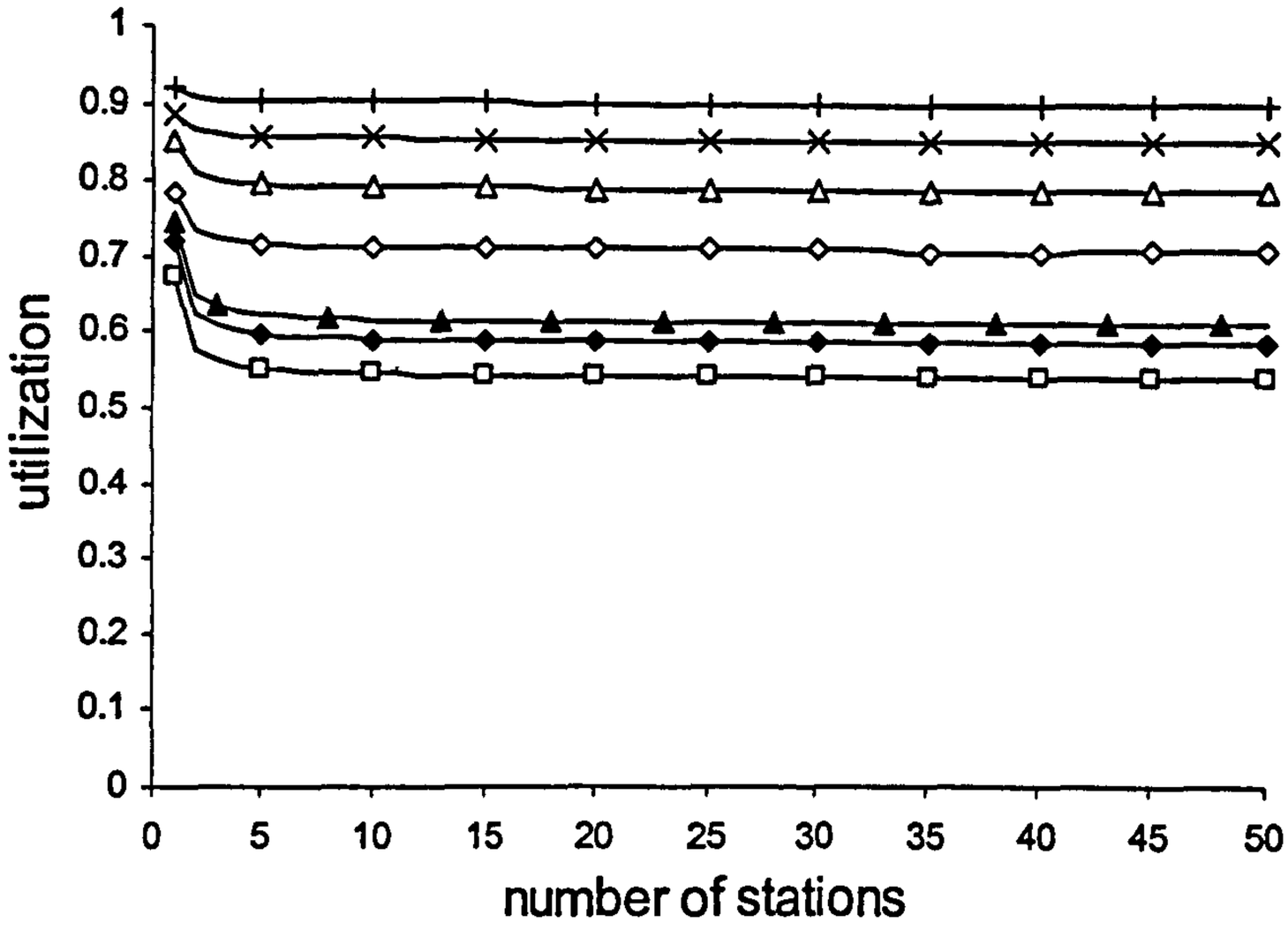

□ *RH field in RR=16, TAT=200μsec, σ=800μsec*
◆ *RH field in RR=16, TAT=100μsecs, σ=700 μsec*
▲ *RH field in RR=16, TAT=50μsec, σ=650μsec*
◇ *RH field in RR=1,TAT=200μsec, σ=300μsec*
△ *RH field in RR=1, TAT=100μsec, σ=200μsec*
× *RH field in RR=1, TAT=50μsec, σ=100μsec*
\+ *RH field in RR=1, TAT=10μsec, σ=50μsec*

Figure 6.14 Utilization versus n, W=1, m=62, l=16Kbits, w=1, C=4Mbit/s, RR=1

using RR=1, reducing the TAT delay and implementing the proposed CW adjustment algorithm.

CHAPTER 7

Advanced Infrared Link Control Layer

In the previous chapter, AIr performance was evaluated for error free transmissions; the frame error probability f_e was always zero. In addition, no Repetition Rate implementation was considered (RR=1). Only empty slots, collisions, reservation control frames and frame overheads could result in utilization degradation. In this chapter, the error free results will be re-examined in the light of realistic link error rate conditions due to noise.

Frame errors may result in significant delays and utilization degradation. In addition, retransmission schemes utilize acknowledgments that affect utilization. This chapter presents a complete AIr LC performance evaluation by considering delays arising from collision avoidance procedures, retransmission schemes and RR-coding. It focuses on the reliable information transfer procedures of the LC layer. The evaluation considers medium access delays by employing the analytical model presented in the previous chapter. It also considers acknowledgement and retransmission delays by developing analytical models for the AIr retransmission schemes. RR-coding delays are included using an analytical model that evaluates frame error rate for the receiver's signal to noise ratio and the frame RR value.

AIr protocol always employs an Automatic Repeat Request (ARQ) retransmission scheme to ensure correct reception of the transmitted information. AIr implements several ARQ schemes. The AIr MAC [45] sub-layer may:

a) not implement any retransmission scheme and not transmit any acknowledgments (DATA frames),
b) implement frame level acknowledgments (ADATA frames) or
c) sequence data frames and implement acknowledgments for a window of frames (SDATA frames).

The AIr LC sub-layer [43] implements a Go-Back-N (GBN) ARQ retransmission scheme to guarantee correct data reception. However, LC may rely on MAC retransmission procedures to guarantee that the transmitted data are successfully received by the remote device [43]. In this case, the remote device is not polled at the LC layer and no LC layer acknowledgments are transmitted. This chapter presents

analytical models for these ARQ schemes and employs the models to study AIr performance under different channel error conditions and for various parameters such as window size, frame length and turn around delays.

AIr may also employ Repetition Rate (RR) coding to cope with transmission errors. For stations far away from the transmitter with a low signal to noise ratio (SNR), a 4-PPM symbol is repeated RR times in order to increase the symbol capture probability at the receiver. RR is a way of adapting link rate to channel conditions. RR coding is not a reliable information transfer scheme but significantly reduces error rate. An analytical model that evaluates frame error rate as a function of RR and signal to noise ratio is presented. The analytical model is employed to study the effectiveness of the RR coding to channel utilization for the proposed ARQ schemes.

This chapter outline is as follows. Section 7.1 defines the proposed ARQ protocols that may be employed by AIr applications to successfully transmit data using the infrared medium. Section 7.2 develops analytical models that calculate the utilization of the proposed protocols and section 7.3 employs the analytical models to compare protocol performance for various link parameter values when RR coding is not implemented. Section 7.4 presents an analytical model that calculates frame error rate for a station's SNR when RR coding is implemented. Finally, section 7.5 studies the performance of the proposed ARQ protocols when RR coding is implemented and the suitable RR value for a station's SNR is used.

7.1 Protocol definition

7.1.1 FLACK and FLACK-M definition

AIr MAC layer may employ a Stop-and-Wait (SW) ARQ scheme or a GBN ARQ scheme or no ARQ scheme at all. SW ARQ scheme utilizes the Reserved transfer mode with acknowledgment; GBN ARQ scheme utilizes the Reserved transfer mode with sequenced data and if no ARQ scheme is employed, the Reserved transfer mode with DATA frame is utilized. The transfer modes are explained in section 5.3. When the Reserved transfer mode with DATA frame is utilized at the MAC layer, a MAC layer transmission indication to the upper layer means that the data are transmitted and not that the data are correctly received [45]. When an ARQ scheme is implemented at the MAC layer, a MAC layer transmission indication to the upper layer means that the data

are correctly received by the remote station.

Frame level acknowledgment (FLACK) protocol utilizes the GBN ARQ scheme at the LC layer and the SW ARQ scheme at the MAC layer (Fig. 7.1). FLACK is a two-level ARQ scheme as it separately acknowledges every frame at the MAC layer and every window of frames at the LC layer [72]. However, the AIr LC specification [43] defines that the LC layer may rely on the MAC reliable information delivery schemes to guarantee that the transmitted data frames are correctly received. In this case, the LC layer employs its GBN ARQ scheme only when no ARQ scheme is utilized at the MAC layer; no ARQ scheme is employed at the LC layer otherwise. Frame level acknowledgment MAC (FLACK-M) protocol employs the SW ARQ scheme at the MAC layer and no ARQ scheme at the LC layer (Fig. 7.2) [93]. FLACK and FLACK-M protocols can not take advantage of the sliding window mechanism but they can quickly adapt the implemented RR to channel conditions by means of the RR recommendations provided by the receiver's MAC ACK frames.

Figures 7.1 and 7.2 portray FLACK and FLACK-M operation respectively for a window size of 4. The transmitter captures the channel, sends an ADATA frame and waits for the responding MAC ACK frame. If the ADATA frame is received correctly, the receiver waits a turn around time (TAT) period to allow the transmitter's circuitry to recover and responds with an ACK frame. When the ACK frame is received, indicating successful reception of the ADATA frame, the transmitter proceeds with the transmission of the next frame. Assuming frame 3 is lost (Figures 7.1 and 7.2), the timer for the responding MAC ACK frame expires. The considered MAC ACK time out period equals the time required for receiving the MAC ACK frame. The transmitter terminates current reservation by means of an EOB frame and contends again for medium access in an effort to transmit the remaining frames during its next successful reservation. As FLACK and FLACK-M protocols can not use the sliding window mechanism, the next reservation contains only frames 3 and 4 and not a full window of frames in both cases. If FLACK-M protocol is implemented (Fig. 7.2), the transmitter does not set the Poll/Final (P/F) bit in the MGMT field of the last ADATA frame it transmits (frame 4) because FLACK-M does not employ a GBN ARQ scheme at the LC layer. If FLACK protocol is implemented (Fig. 7.1), the transmitter sets the P/F bit in the last ADATA frame it transmits and the receiver reserves the medium and responds

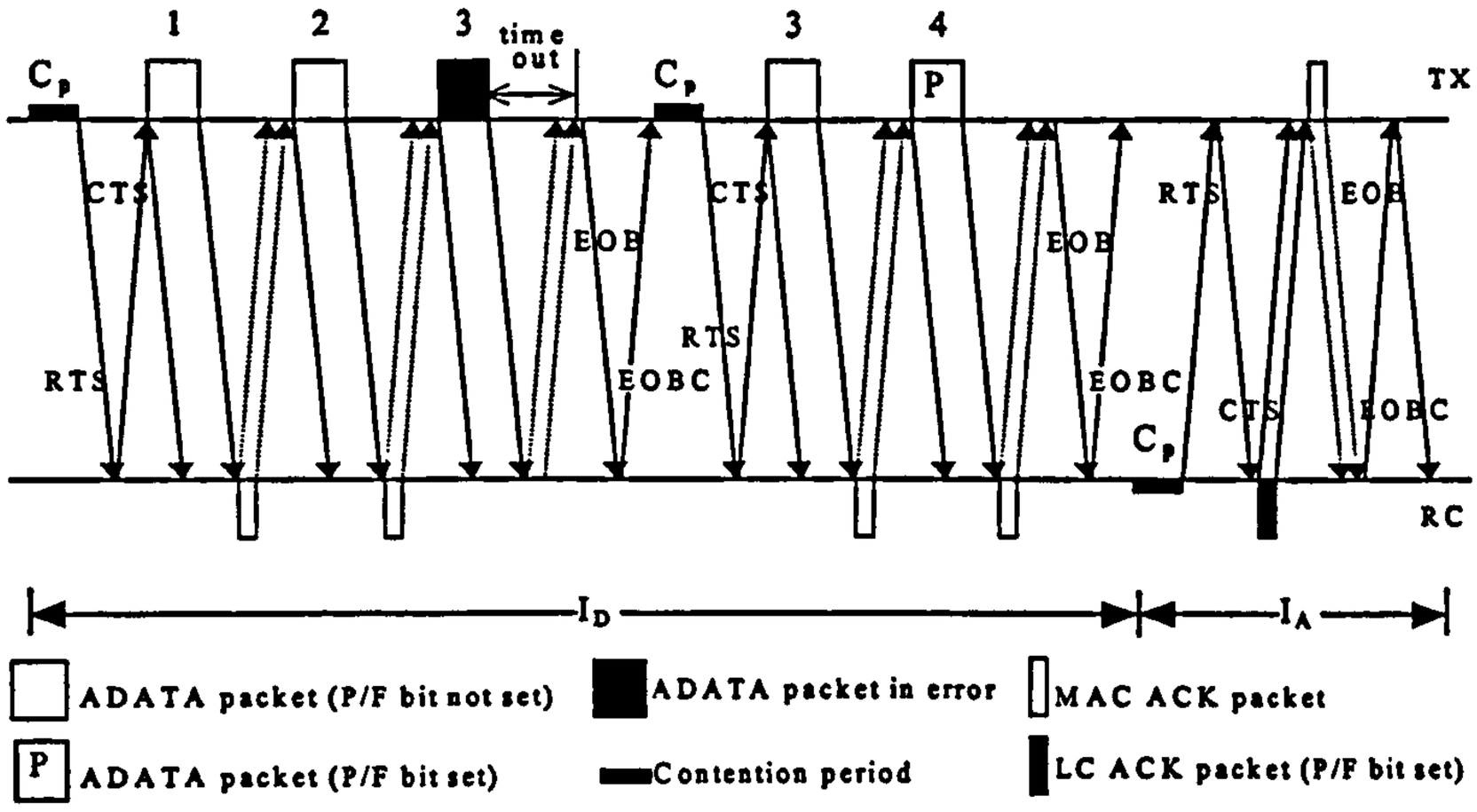

Figure 7.1 FLACK protocol (SW ARQ at the MAC layer and GBN at the LC layer)

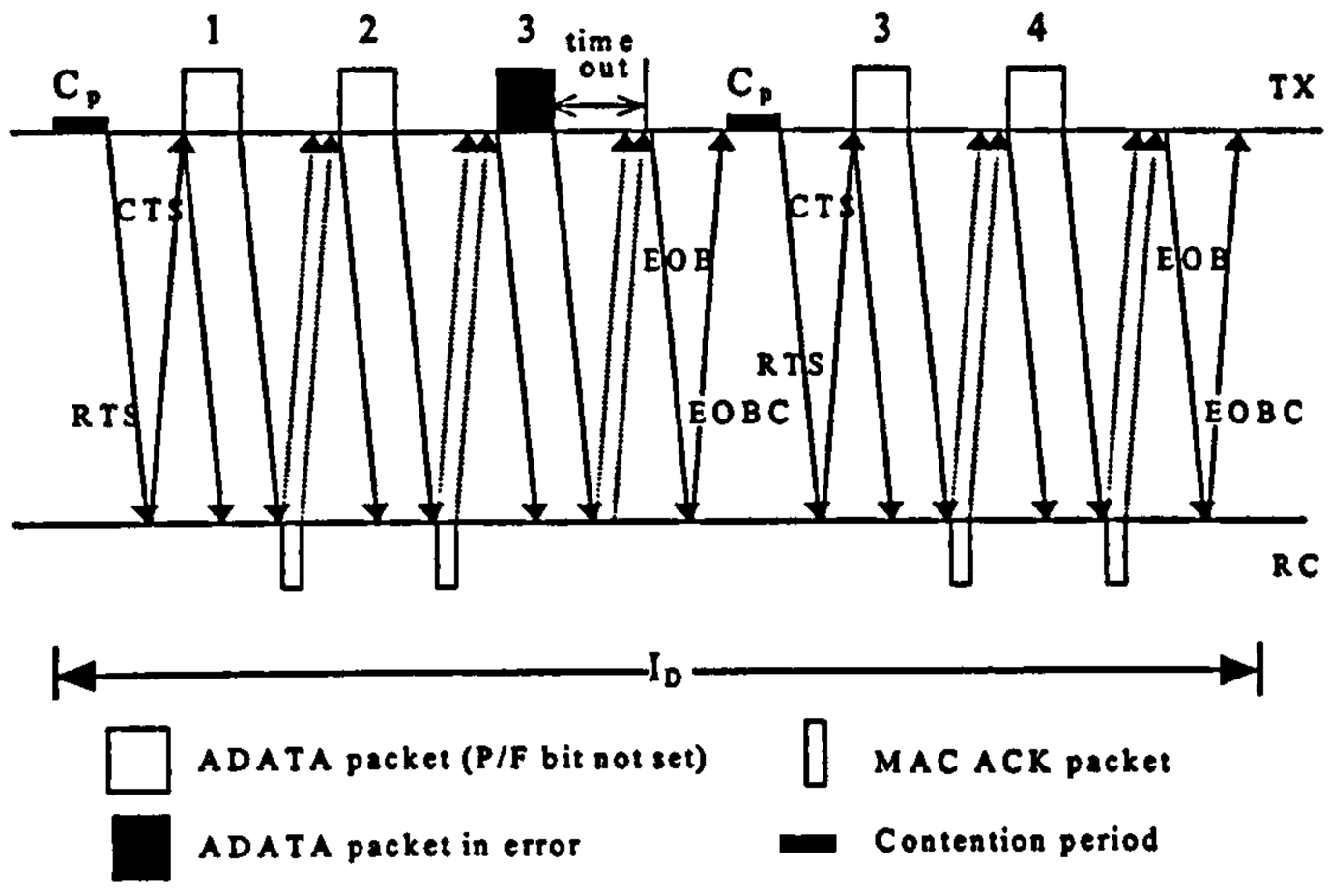

Figure 7.2 FLACK-M protocol (SW ARQ at the MAC layer and no ARQ scheme at the LC layer)

with an LC receive ready acknowledgment (LC ACK) frame. If the last ADATA frame carrying the P/F bit is lost, the transmitter immediately realizes the P/F loss by a time out expiration for the MAC ACK frame and contends again in order to retransmit the last ADATA frame.

7.1.2 NoFLACK and NoFLACK-ACK definition

An alternative is for the LC layer to employ its GBN ARQ scheme and to disable the MAC layer ARQ schemes [43]. LC GBN scheme sets the P/F bit in a transmitted frame to pass transmission control. AIr LC specification defines that the P/F bit may be set in a data or in an LC receive ready acknowledgment (LC ACK) frame. LC ACK frames are transmitted as MAC data frames with no information data. Thus, two

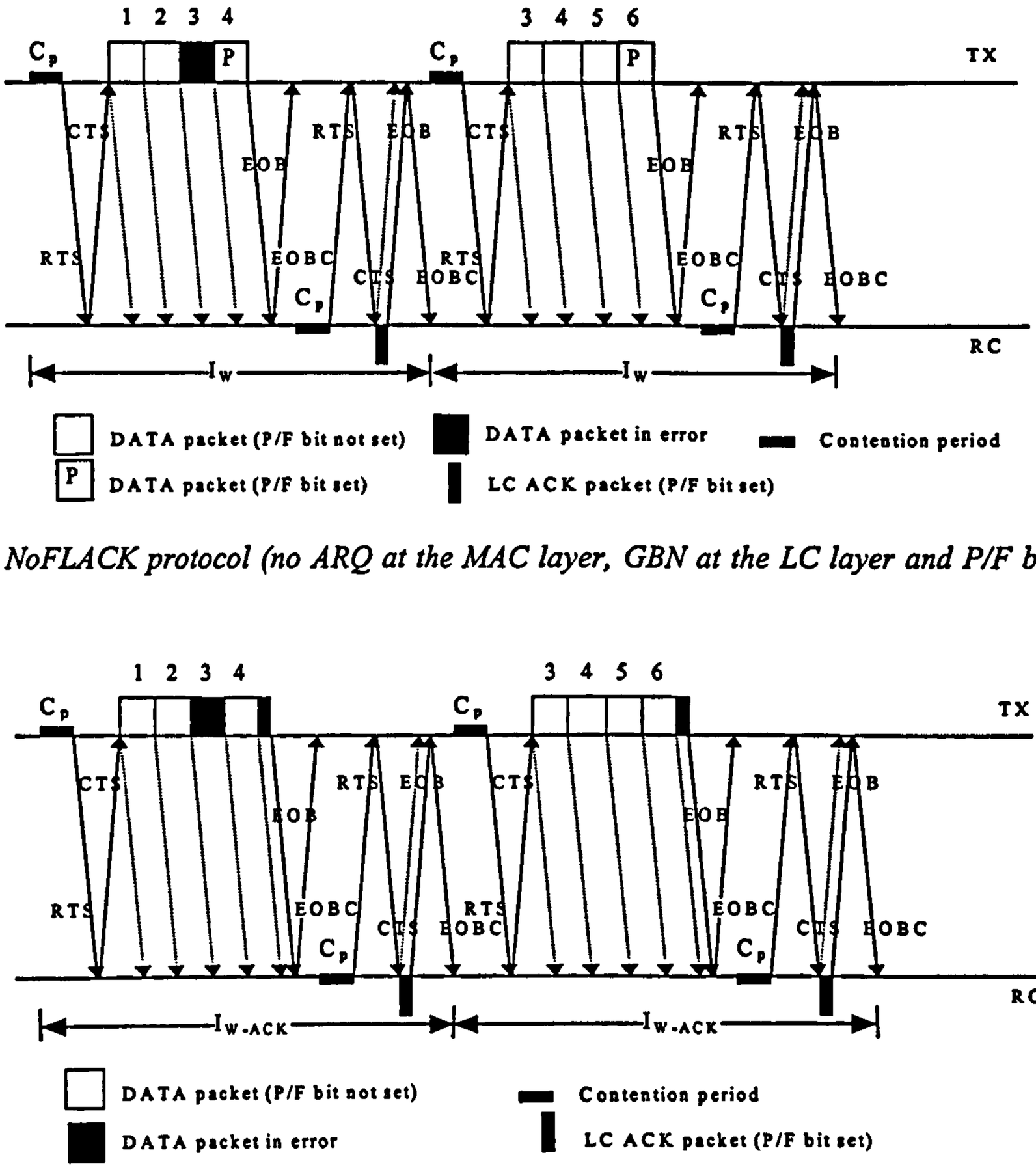

Figure 7.3 NoFLACK protocol (no ARQ at the MAC layer, GBN at the LC layer and P/F bit in DATA frame)

Figure 7.4 NoFLACK-ACK protocol (no ARQ at the MAC layer, GBN at the LC layer and P/F bit in ACK frame)

different operation modes are considered for the LC GBN ARQ scheme. The first always sets the P/F bit in the last DATA frame in a window transmission (Fig. 7.3); the second always sets the P/F bit in a special LC ACK frame that follows the last DATA frame in a window transmission (Fig. 7.4). No frame level acknowledgment (NoFLACK) protocol utilizes the GBN ARQ scheme at the LC layer, no ARQ scheme at the MAC layer and utilizes DATA frames to carry the P/F bit to the receiver (Fig. 7.3). No frame level acknowledgment protocol utilizing LC ACK frames (NoFLACK-ACK) protocol uses the GBN ARQ scheme at the LC layer, no ARQ scheme at the MAC layer and always utilizes LC ACK frames to carry the P/F bit to the receiver (Fig. 7.4) [93].

NoFLACK protocol sets the P/F bit in the last DATA frame in a window

transmission. The receiver acknowledges in-sequence correctly received frames and returns transmission control by setting the P/F bit in the responding LC ACK frame. When DATA frames contain a significant amount of information data and link error rate is high, the DATA frame carrying the P/F bit may be lost. In the case of a P/F bit loss, the receiver fails to acknowledge correctly received DATA frames because it assumes that the transmitter wishes to send more DATA frames before soliciting a response. The situation is resolved by a transmitter's LC layer time out expiration, following which the transmitter sends an LC ACK frame with the P/F bit set. The receiver responds with an LC ACK frame with the P/F bit set, acknowledging correctly received frames and returning transmission control. NoFLACK-ACK protocol reduces the P/F bit loss probability by not setting the P/F bit in the last DATA frame in a window transmission and by transmitting a new (and much smaller) LC ACK frame carrying the P/F bit which follows the last DATA frame in a window transmission. NoFLACK-ACK protocol reduces the P/F bit loss probability at the expense of transmitting a new LC ACK frame.

NoFLACK and NoFLACK-ACK protocols can use the sliding window mechanism but they can not quickly adapt their RR value to channel conditions because the receiver can only recommend new RR values by using the RR* field of the EOBC frame that terminates a reservation.

Figures 7.3 and 7.4 portray NoFLACK and NoFLACK-ACK protocol operation respectively. The transmitter transmits all frames upon gaining access to the infrared medium. As explained earlier, NoFLACK (Fig. 7.3) sets the P/F bit in the last DATA frame it transmits (frame 4 and 6); NoFLACK-ACK (Fig. 7.4) does not and sends a new LC ACK frame with the P/F bit set. Upon receiving a frame with the P/F bit set, the receiver, in both cases, responds with an LC ACK frame informing the transmitter of the in sequence correctly received frames. The LC ACK frame has the P/F bit set returning transmission control to the transmitter. If all frames are correctly received, the transmitter sends the next window of frames. Otherwise, it repeats the erred frame, retransmits all frames that followed the erred frame during the previous window transmission and, by taking advantage of the sliding window mechanism, the transmitter also sends new frames to form a complete window transmission. If again frame 3 is lost (Fig. 7.3 & 7.4), both protocols retransmit frames 3 and 4 and transmit new frames 5

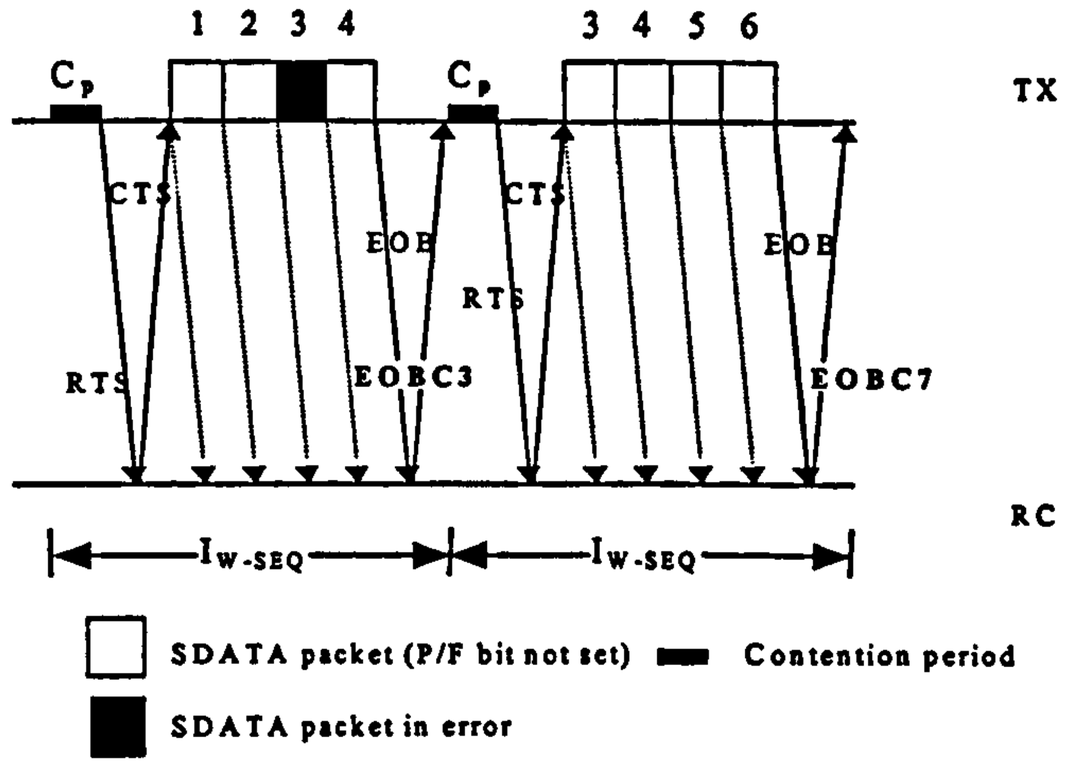

Figure 7.5 SEQ-NoFLACK protocol (GBN at the MAC layer and no ARQ scheme at the LC layer)

and 6 to form a complete window transmission. If the frame carrying the P/F bit is lost, the information transfer procedure is halted. The situation is resolved by a transmitter's LC time out expiration. The transmitter then sends an LC ACK frame with the P/F bit set forcing the receiver to acknowledge correctly received frames. Current analysis assumes that LC ACK frames are very small and are always correctly received.

7.1.3 SEQ-NoFLACK definition

Another alternative for the LC layer is to instruct the MAC layer to sequence data frames by employing the Reserved transfer mode with sequenced data. In this case, the EOBC control frame that terminates the reservation contains a sequence number that informs the transmitter of the next frame sequence number expected. This sequence number acknowledges in sequence correctly received frames, as described in section 5.3.2.3, and allows AIr MAC to implement a GBN ARQ retransmission scheme. Sequential no frame level acknowledgment (SEQ-NoFLACK) protocol implements the GBN ARQ scheme at the MAC layer and no ARQ scheme at the LC layer. SEQ-NoFLACK protocol incurs the least overhead because no special LC ACK or MAC ACK frames are transmitted and correctly received frames are acknowledged using the EOBC control frame that terminates a successful reservation. The SEQ-NoFLACK protocol can use the sliding window mechanism but it can not quickly adapt the implemented RR to channel conditions because the receiver can only recommend suitable RR values by using the RR* field of the EOBC frame.

Fig. 7.5 depicts SEQ-NoFLACK protocol operation. The transmitter sends a

window of SDATA frames after a successful RTS/CTS frame exchange. The SDATA frames contain frame sequence numbers. As no ARQ scheme is implemented at the LC layer, the P/F bit in the last SDATA frame is not set. However, the receiver informs the transmitter of the correctly received frames by using the Seq-R field of the EOBC control frame. If all frames are received successfully, the transmitter proceeds with the next window transmission. If again frame 3 is lost (Fig. 7.5), the transmitter contends again in order to retransmit frames 3 and 4. SEQ-NoFLACK protocol can use the sliding window mechanism and therefore new frames 5 and 6 are transmitted to form a complete window transmission during the next successful reservation.

7.2. Protocol analysis

Current analysis considers a LAN of n transmitting stations operating in saturation conditions, i.e. all n stations always have a window of frames ready for transmission. It is assumed that the LC ACK frames are small enough to be always received error free. The analysis considers the preparation time of a data frame and assumes that the processing time of a received data or ACK frame is smaller than the minimum turn around time (TAT) and can overlap with the TAT delay. Thus, no additional received frame processing time is calculated. The receiver processes the received frame and then waits until a total of TAT period is reached before transmitting the suitable response. It is also assumed that the processing time of a received frame can also overlap with the reception of the next frame and it is not additive.

7.2.1 FLACK utilization

The FLACK protocol utilization can be found by evaluating the number of reservations required to successfully transmit a window of w frames. For frame error rate f_e, the probability $P_{s/i}$ that i reservations are required to successfully transmit a window of frames is given by [76]

$$P_{s/i} = C_{i-1}^{w+i-2}(1-f_e)^w f_e^{i-1} \tag{7.1}$$

where

$$C_{i-1}^{w+i-2} = \frac{(w+i-2)!}{(i-1)!\,(w-1)!} \tag{7.2}$$

The transmission time of w frames if i reservations are required is given by

$$T_D(i) = i(C_p + D) + (w + i - 1)(t + F_A + p_1 + E) \tag{7.3}$$

where F_A is the transmission time of ADATA frame overhead (PA, RH, CRC etc.), E is the time required for a MAC acknowledgement and consists of the MAC ACK frame transmission time and of the TAT delays associated with this MAC ACK transmission and C_p, D, t and p_1 are as defined in the previous chapter. C_p is the average contention period (including empty and collision slots) for a successful reservation and is given by eq. (6.28), D is the reservation overhead that includes the transmission time of the RTS, CTS, EOB and EOBC frames and the TAT delays that follow these frames and equals 1.74 msec, t is the payload data transmission time and p_1 is the preparation time of a data frame. The value of t is given by

$$t = \frac{RR\, l}{C} \tag{7.4}$$

where RR, C and l are as defined in the previous chapter. RR is the Repetition Rate, C is the link base rate and l is the payload data length. The value of F_A is given by

$$F_A = T_{RH} + \frac{RR\, l_A^{'}}{C} \tag{7.5}$$

where $l_A^{'}$ is the length of the MBR overhead of an ADATA frame and T_{RH} is as defined in section 5.2. T_{RH} is the transmission time of a frame with no MBR field. According to Fig. 5.3, $l_A^{'}$ =72 bits and section 5.2 evaluates that T_{RH}=232 μsec.

The transmission time, I_D, for a complete w frame transmission can be calculated by

$$I_D = \sum_{i=1}^{\infty} P_{s/i} T_D(i) \tag{7.6}$$

As LC ACK frames are always transmitted error free, the transmission time of the LC ACK frame is given by

$$I_A = (C_p + D) + (t_A^{ack} + p_1 + E) \tag{7.7}$$

where t_A^{ack} is the LC ACK frame transmission time when ADATA frames are utilized and the other parameters are the same. E in eq. (7.7) stands for the time needed to acknowledge the LC ACK frame at the MAC layer. As the LC ACK frame does not contain payload data,

$$t_A^{ack} = F_A \tag{7.8}$$

The FLACK protocol utilization can now be derived as

$$U_{FLACK} = \frac{1}{RR}\,\frac{wt}{I_D + I_A} \tag{7.9}$$

7.2.2 FLACK-M utilization

The same analytical model can be applied to the FLACK-M protocol. Considering that the FLACK-M does not implement the GBN ARQ scheme at the LC layer and therefore no LC ACK frames are transmitted, the FLACK-M utilization can be evaluated by

$$U_{FLACK-M} = \frac{1}{RR}\,\frac{wt}{I_D} \tag{7.10}$$

where I_D is given by eq. (7.6).

7.2.3 NoFLACK-ACK utilization

As the NoFLACK-ACK protocol only implements the GBN ARQ scheme at the LC layer, its utilization can be found with the help of the analysis presented in section 3.4 for GBN protocols

$$U_{NoFLACK-ACK} = \frac{t}{RR}\,\frac{(1-f_e)}{f_e}\cdot\frac{\left(1-(1-f_e)^w\right)}{I_{W-ACK}} \tag{7.11}$$

where $I_{W\text{-}ACK}$, the window transmission time, is given by

$$I_{W-ACK} = 2(C_p + D) + w(t + F_D + p_1) + 2(p_1 + t_D^{ack}) \tag{7.12}$$

where F_D is the transmission time of DATA frame overhead, t_D^{ack} is the LC ACK frame transmission time when DATA frames are utilized and the other parameters are as defined for the FLACK protocol. The value of F_D is given by

$$F_D = T_{RH} + \frac{RR\, l_D^{'}}{C} \tag{7.13}$$

where $l_D^{'}$ is the length of the MBR overhead bits of a DATA frame and the other parameters are the same. According to Fig. 5.3, $l_D^{'}$ =72 bits. As the LC ACK frame does not contain payload data,

$$t_D^{ack} = F_D \tag{7.14}$$

The window transmission time, $I_{W\text{-}ACK}$, does not consider the P/F bit loss delay because NoFLACK-ACK sets the P/F bit in LC ACK frames only and current model assumes that LC ACK frames are small enough to be always received error free.

7.2.4 NoFLACK utilization

In the NoFLACK protocol, the information transfer procedure is halted when the P/F bit is lost and is restarted again when the LC timer expires. If one station is transmitting in the infrared LAN, this situation clearly results in link idle time and utilization degradation. However, if many stations are transmitting in the LAN, the utilization may not be significantly decreased if the probability that all transmitting stations suffer from P/F bit loss simultaneously is very low. If a few stations are transmitting in the LAN, utilization is decreased because the medium is idle when all stations lose the P/F bit simultaneously.

It is difficult and worthless to develop an analytical model that evaluates NoFLACK utilization as a function of the number of stations in the LAN. The reason is that when the P/F bit is lost, the transmitting station does not contend for medium access. As a result, the number of stations competing for medium access is not fixed and a new model that evaluates the average contention period (C_p) for a LAN with no fixed number stations is needed. However, the lower and upper limits of NoFLACK utilization can be evaluated for links with transmission errors. These limits are sufficient for the protocol comparison performed in this work.

The lower limit, $NoFLACK_1$, refers to the NoFLACK protocol scenario with only one transmitting station in the LAN. In this case, the infrared medium is idle for the entire LC time out period when a P/F bit is lost. The upper limit, $NoFLACK_N$, refers to NoFLACK protocol scenario with a significant (or infinite) number of transmitting stations. In this case, the infrared medium is equally utilized by the remaining stations in the case of one (or more) P/F bit loss. When one or more stations temporarily stop contending for medium access, the LAN utilization is not decreased but the utilization of every transmitting individual station is temporarily increased. Thus, all real life network scenarios implementing NoFLACK protocol will achieve a LAN utilization with an upper limit of the $NoFLACK_N$ utilization and a lower limit of the $NoFLACK_1$ utilization.

As NoFLACK implements only the GBN ARQ scheme at the LC layer, $NoFLACK_1$ utilization is given by

$$U_{NoFLACK_1} = \frac{t}{RR} \cdot \frac{(1-f_e)}{f_e} \cdot \frac{\left(1-(1-f_e)^w\right)}{I_{W-1}} \tag{7.15}$$

where $I_{w\text{-}1}$ is the average window transmission time and is given by

$$I_{W-1} = 2(C_p + D) + w(t + F_D + p_1) + (p_1 + t_D^{ack}) + f_e(T_t + C_p + D + p_1 + t_D^{ack}) \quad (7.16)$$

where T_t is the LC layer time out period and the other parameters are as defined for the NoFLACK-ACK protocol.

If the considered LAN has a significant number of transmitting stations and the infrared medium is always fully utilized during LC time out periods, the utilization is given by

$$U_{NoFLACK_N} = \frac{t}{RR} \cdot \frac{(1-f_e)}{f_e} \cdot \frac{\left(1-(1-f_e)^w\right)}{I_{W-N}} \quad (7.17)$$

and $I_{W\text{-}N}$ is given by

$$I_{W-N} = 2(C_p + D) + w(t + F_D + p_1) + (p_1 + t_D^{ack}) + f_e(C_p + D + p_1 + t_D^{ack}) \quad (7.18)$$

7.2.5 SEQ-NoFLACK utilization

The utilization of SEQ-NoFLACK protocol can be evaluated by the analysis of the GBN protocols

$$U_{SEQ-NoFLACK} = \frac{t}{RR} \cdot \frac{(1-f_e)}{f_e} \cdot \frac{\left(1-(1-f_e)^w\right)}{I_{W-SEQ}} \quad (7.19)$$

where $I_{W\text{-}SEQ}$, the window transmission time, is given by

$$I_{W-SEQ} = (C_p + D) + w(t + F_S + p_1) \quad (7.20)$$

and F_S is (as defined in the previous chapter) the transmission time of SDATA frame overhead and the other parameters are the same. The value of F_S is given by

$$F_S = T_{RH} + \frac{RR\, l_s^{'}}{C} \quad (7.21)$$

where $l_s^{'}$ is the length of the MBR overhead of a SDATA frame and the other parameters are the same. According to Fig. 5.3, $l_s^{'}$ =80 bits.

As the utilization analysis presented in the previous chapter for error free channels uses SDATA frames, it refers to SEQ-NoFLACK protocol analysis for f_e=0. If $f_e \to 0$, eq. (7.19) reduces to

$$U_{SEQ-NoFLACK} = \frac{wt}{RR\ I_{W-SEQ}} \quad (7.22)$$

From eq. (7.20) and eq. (6.23), we can deduce that

$$I_{W-SEQ} = C_p + T_s \tag{7.23}$$

By substituting C_p from eq. (6.28)

$$I_{W-SEQ} = \frac{1-P_{tr}P_s}{P_{tr}P_s}\sigma + T_s \tag{7.24}$$

and from eq. (7.24) and eq. (7.22)

$$U_{SEQ-NoFLACK} = \frac{1}{RR}\cdot\frac{wt}{\frac{1-P_{tr}P_s}{P_{tr}P_s}\sigma + T_s} = \frac{1}{RR}\cdot\frac{P_{tr}P_s wt}{P_{tr}P_s T_s + \sigma - P_{tr}P_s\sigma} \tag{7.25}$$

which is identical to eq. (6.22).

7.3. Performance comparison

Based on the analytical models presented in the previous section, protocol performance is compared under the assumption that no Repetition Rate (RR=1) coding is implemented. First, FLACK and FLACK-M protocols are compared and results indicate that FLACK-M offers a significantly higher utilization for the same link layer parameter values. Then, NoFLACK and NoFLACK-ACK protocols are compared and results indicate that NoFLACK-ACK is usually a better choice. Finally, NoFLACK-ACK, FLACK-M and SEQ-NoFLACK protocols are compared for different link layer parameter values.

7.3.1 FLACK versus FLACK-M

Fig. 7.6 compares FLACK and FLACK-M utilization versus frame error rate (FER) for various window size values. It shows that FLACK utilization is significantly lower than FLACK-M utilization for the same window size implementation. This result is explained by considering that FLACK is a two-way ARQ system. It implements an additional GBN ARQ scheme at the LC layer resulting in the transmission of additional LC ACK frames, additional RTS/CTS frame exchanges, contention periods, etc. Fig. 7.6 also shows that the FLACK protocol needs to double the implemented window size to reach a utilization figure close to FLACK-M protocol utilization. Utilization results produced for smaller l values indicate that this conclusion is always true and independent of the implemented frame size. Considering the conclusion derived in the previous chapter that the AIr protocol achieves high utilization only for high window size values and as the window size parameter is application dependent and thus not

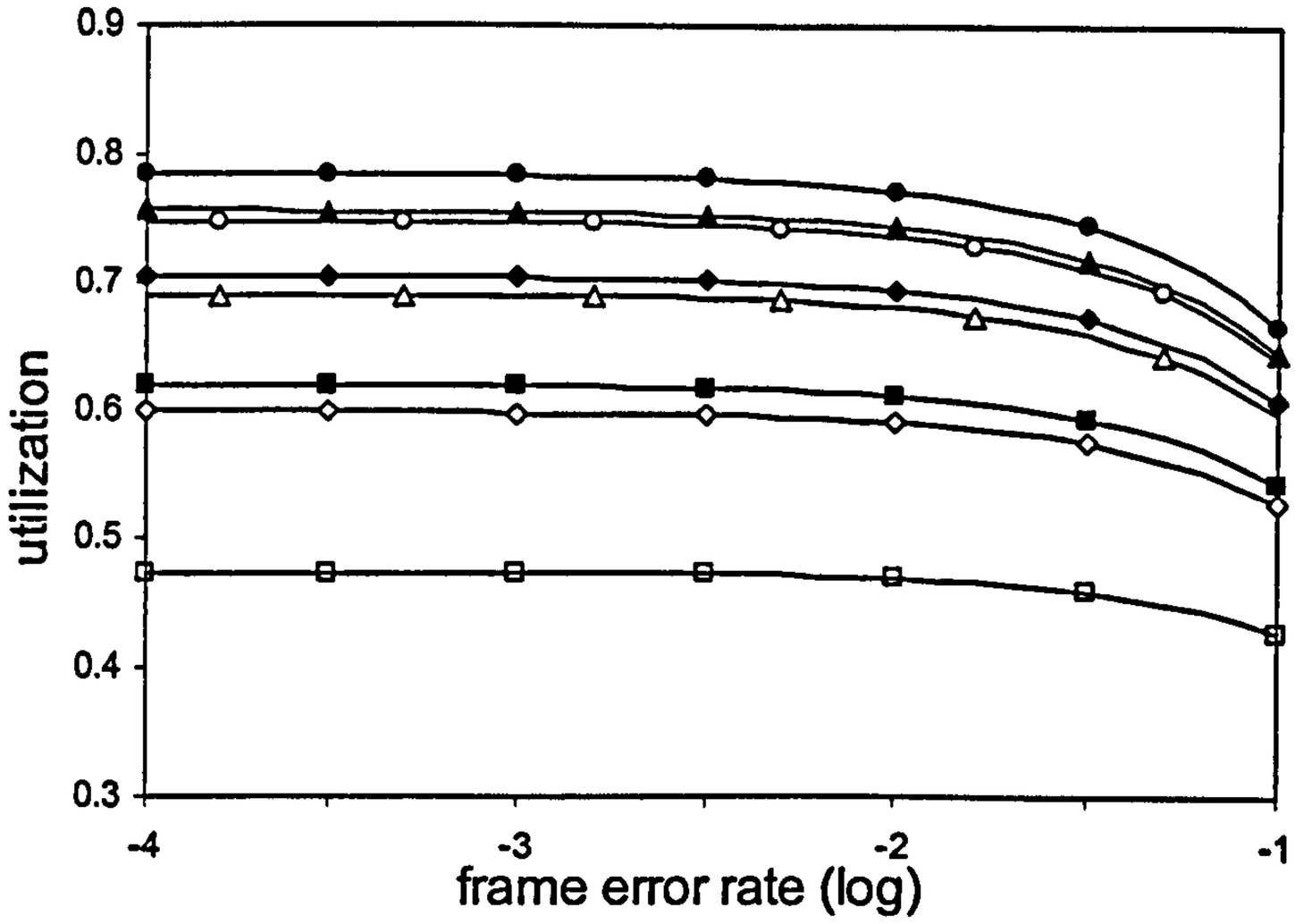

□ *FLACK, w=2 frames*
◇ *FLACK, w=4 frames*
△ *FLACK, w=8 frames*
○ *FLACK, w=16 frames*
■ *FLACK-M, w=2 frames*
◆ *FLACK-M, w=4 frames*
▲ *FLACK-M, w=8 frames*
● *FLACK-M, w=16 frames*

Figure 7.6 Utilization versus frame error rate for various w values, C=4Mbit/s, l=2Kbytes, T_t =5sec, W=8, m=62, n=5 stations

directly controllable at the MAC layer, the FLACK-M protocol is a much better choice. Therefore, the FLACK-M protocol is chosen for the rest of this evaluation. As a conclusion, when the LC layer utilizes the MAC SW ARQ scheme, it should not employ its GBN ARQ scheme and should rely on MAC layer reliable data delivery techniques to guarantee that the transmitted information is actually received by the remote station. Implementation of an additional GBN ARQ scheme at the LC layer, which is very close to the MAC layer, results in significant delays and no significant benefits.

7.3.2 NoFLACK versus NoFLACK-ACK

Fig. 7.7 plots NoFLACK utilization versus FER for LANs with one (n=1) and ten (n=10) transmitting stations. $NoFLACK_1$ utilization is taken for n=1; $NoFLACK_N$ utilization is taken for n=10 assuming that the infrared medium is equally utilized during T_t time out periods for ten transmitting stations. As $NoFLACK_1$ and $NoFLACK_N$ utilization also serve as NoFLACK utilization lower and upper limit respectively, it is expected that NoFLACK utilization for LANs with more than one and less than ten

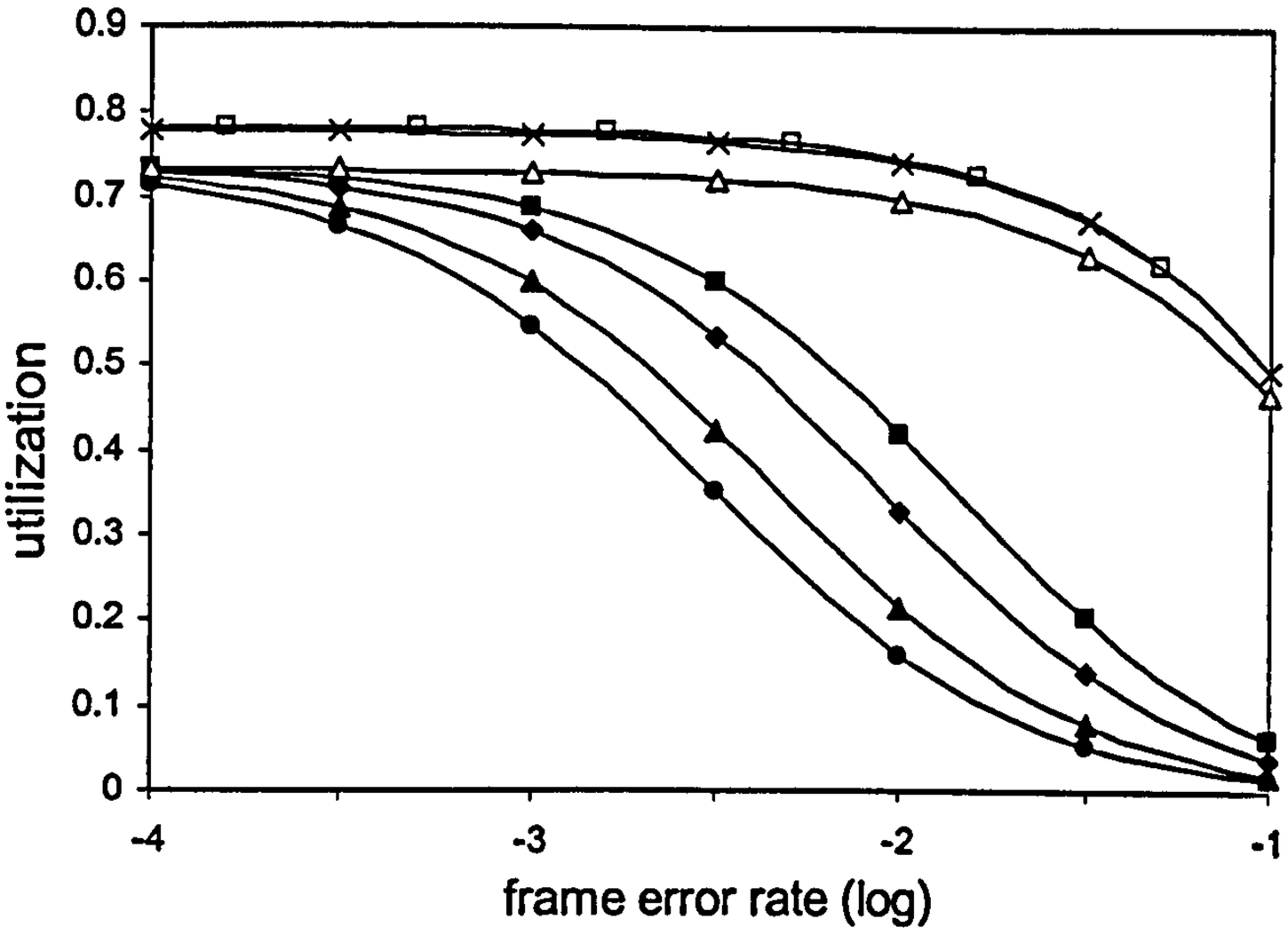

■ *NoFLACK$_1$, T_t =3 sec, n=1 station*
◆ *NoFLACK$_1$, T_t =5 sec, n=1 station*
▲ *NoFLACK$_1$, T_t =10 sec, n=1 station*
● *NoFLACK$_1$, T_t =15 sec, n=1 station*
□ *NoFLACK$_N$, T_t =3,5,10,15 sec, n=10 stations*
△ *NoFLACK-ACK, T_t =3,5,10,15 sec, n=1 station*
x *NoFLACK-ACK, T_t =3,5,10,15 sec, n=10 stations*

Figure 7.7 Utilization versus frame error rate for various T_t values, w=8 frames, C=4Mbit/s, l=2Kbytes, W=8, m=62

transmitting stations will fall between these limits. The reason is that the infrared medium will be partly utilized in the event of one or more P/F losses.

Fig. 7.7 shows that NoFLACK utilization degrades with FER increase and that it is more sensitive for n=1. In this case, utilization drop worsens with T_t value increase. The reason is that NoFLACK relies on the successful transmission of the last DATA frame to carry the P/F bit to the receiver. If the last DATA frame is lost, the station refrains from transmitting until the LC timer expires. As the NoFLACK$_1$ protocol scenario does not utilize these T_t periods, utilization degradation is increased for higher T_t values. NoFLACK$_N$ utilization is independent of T_t because the LC time out periods are fully utilized by the remaining stations.

Fig. 7.7 also plots NoFLACK-ACK utilization. NoFLACK-ACK utilization is always independent of T_t. The reason is that NoFLACK-ACK always sets the P/F bit in an LC ACK frame which is very small and has an extremely low (practically zero) error rate probability. Fig. 7.7 shows that for n=1, NoFLACK-ACK is a much better choice

than $NoFLACK_1$ because it is robust to FER increase. For n=10, the NoFLACK-ACK protocol achieves a slightly lower performance (practically identical) than the $NoFLACK_N$ protocol scenario. The reason is that the additional LC ACK frame utilized by the NoFLACK-ACK protocol causes a small additional delay compared with other protocol delays such as contention periods, RTS/CTS exchanges etc. Considering that a) if NoFLACK protocol is implemented, the LAN utilization ranges from $NoFLACK_1$ utilization to $NoFLACK_N$ utilization, b) NoFLACK-ACK for n=1 performs better that $NoFLACK_1$, c) NoFLACK-ACK for large n reaches a practically identical to $NoFLACK_N$ performance, and d) NoFLACK does not in practice outperform NoFLACK-ACK and suffers from LC time out delays under certain conditions, we can conclude that the NoFLACK-ACK protocol is a much better choice than the NoFLACK protocol. Therefore, the NoFLACK-ACK protocol is selected for the rest of this evaluation. As a conclusion, the P/F bit should be set only in LC ACK frames if the MAC's SW ARQ scheme is not employed.

7.3.3 Comparison of FLACK-M, NoFLACK-ACK and SEQ-NoFLACK protocols

Fig. 7.8 compares FLACK-M and NoFLACK-ACK utilization for different window size values. It reveals that for low FER, the FLACK-M protocol performs better than the NoFLACK-ACK protocol for small window size values but the situation is reversed for high window size values. A 'critical' value of six frames exists where both protocols achieve the same utilization. Fig. 7.9 plots SEQ-NoFLACK utilization for the same parameter values. It shows that SEQ-NoFLACK protocol outperforms FLACK-M and NoFLACK-ACK protocols for all window sizes if FER is low. Figures 7.8 and 7.9 show that NoFLACK-ACK and SEQ-NoFLACK utilization decrease with FER increase but FLACK-M is more robust to FER increase. We can conclude that for low FER, the SEQ-NoFLACK protocol is the best choice and that the FLACK-M protocol is preferable to the NoFLACK-ACK protocol for window transmissions consisting of less than 6 frames; NoFLACK-ACK is better otherwise.

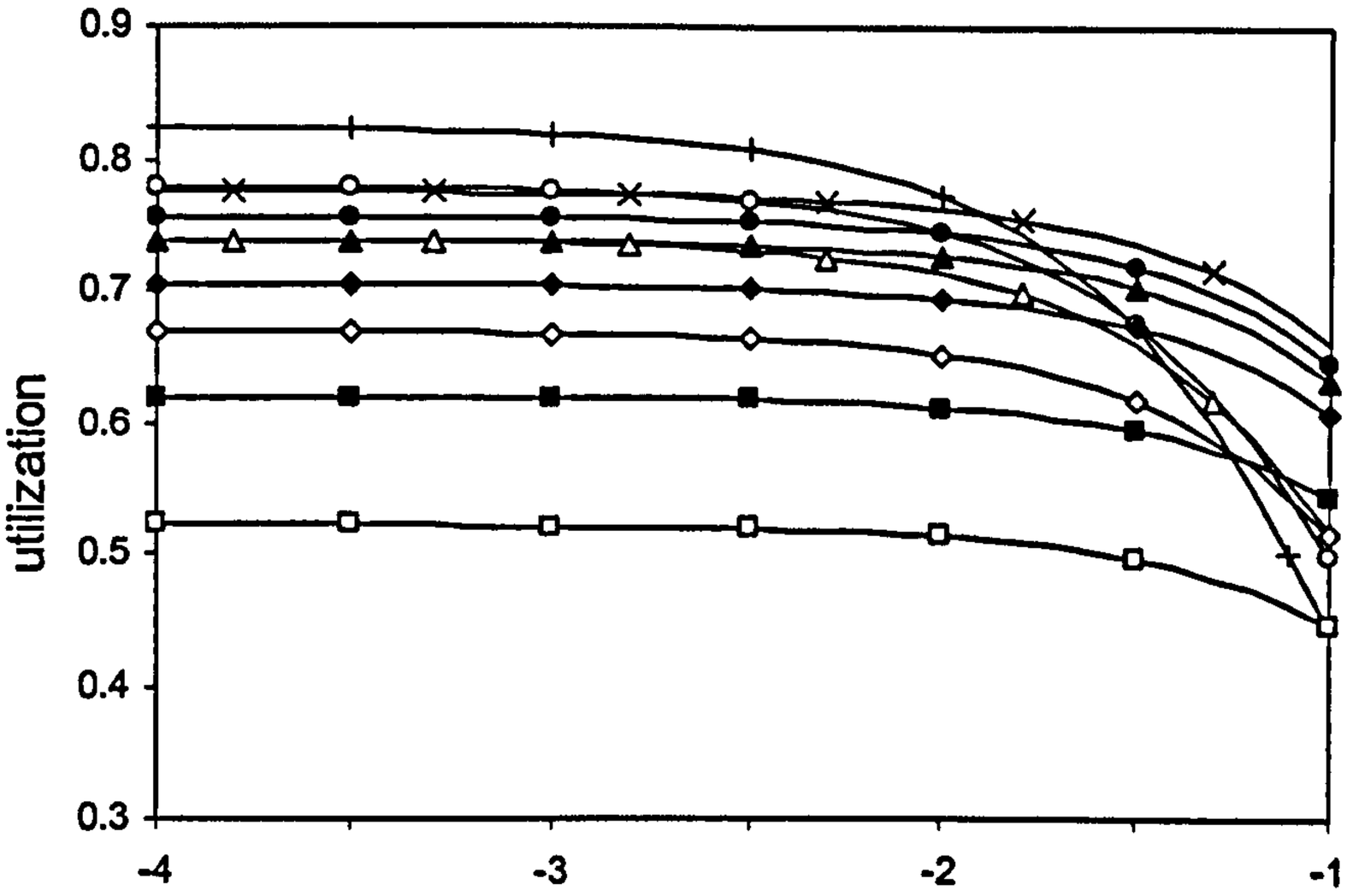

□ *NoFLACK-ACK, w=2 frames*
◇ *NoFLACK-ACK, w=4 frames*
△ *NoFLACK-ACK, w=6 frames*
○ *NoFLACK-ACK, w=8 frames*
\+ *NoFLACK-ACK, w=12 frames*
■ *FLACK-M, w=2 frames*
◆ *FLACK-M, w=4 frames*
▲ *FLACK-M, w=6 frames*
● *FLACK-M, w=8 frames*
x *FLACK-M, w=12 frames*

Figure 7.8 Utilization versus frame error rate for various w values, C=4Mbit/s, l=2Kbytes, T_t =5sec, W=8, m=62, n=5 stations

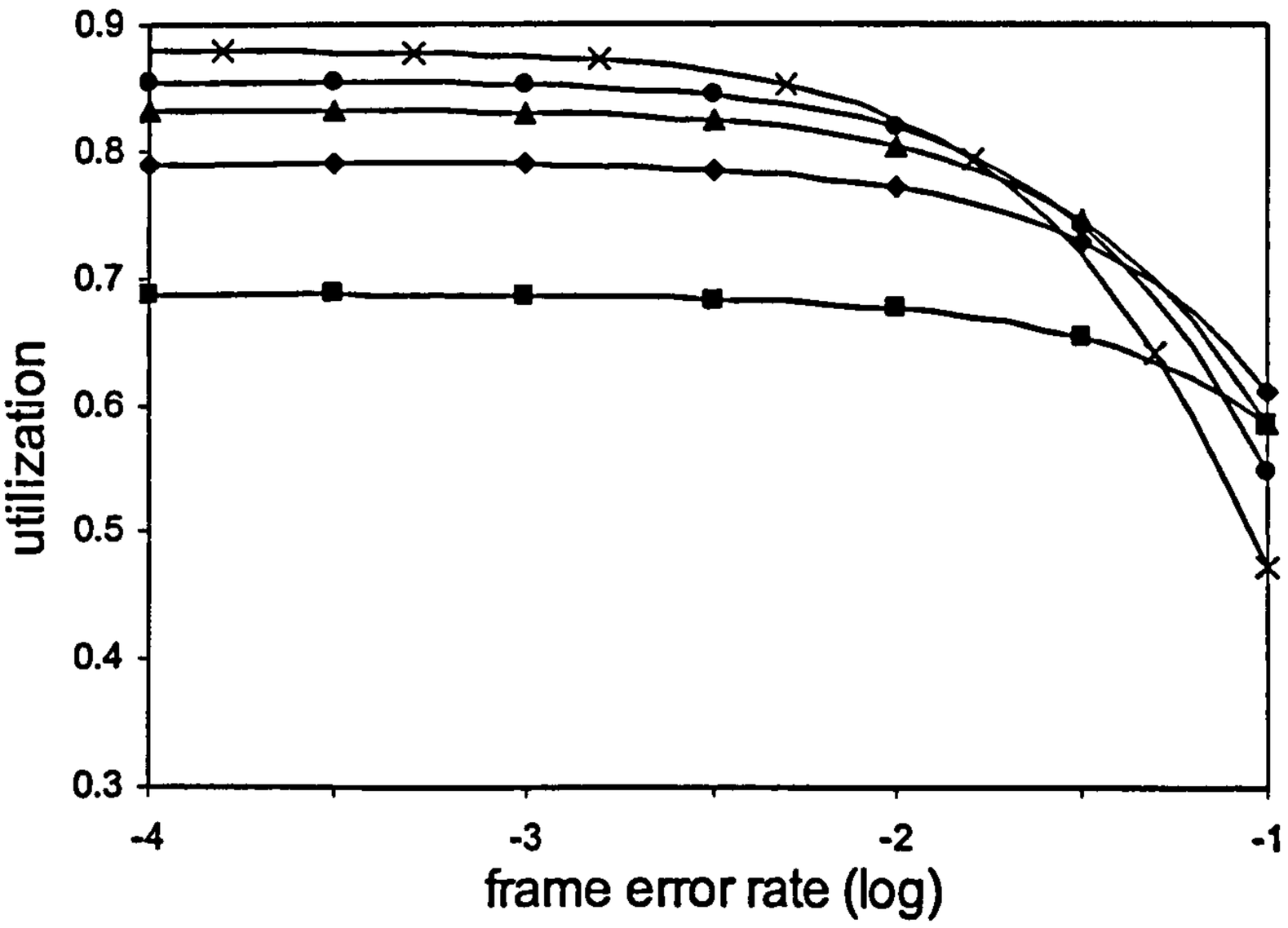

■ *SEQ-NoFLACK, w=2 frames*
◆ *SEQ-NoFLACK, w=4 frames*
▲ *SEQ-NoFLACK, w=6 frames*
● *SEQ-NoFLACK, w=8 frames*
x *SEQ-NoFLACK, w=12 frames*

Figure 7.9 Utilization versus frame error rate for various w values, C=4Mbit/s, l=2Kbytes, T_t =5sec, W=8, m=62, n=5 stations

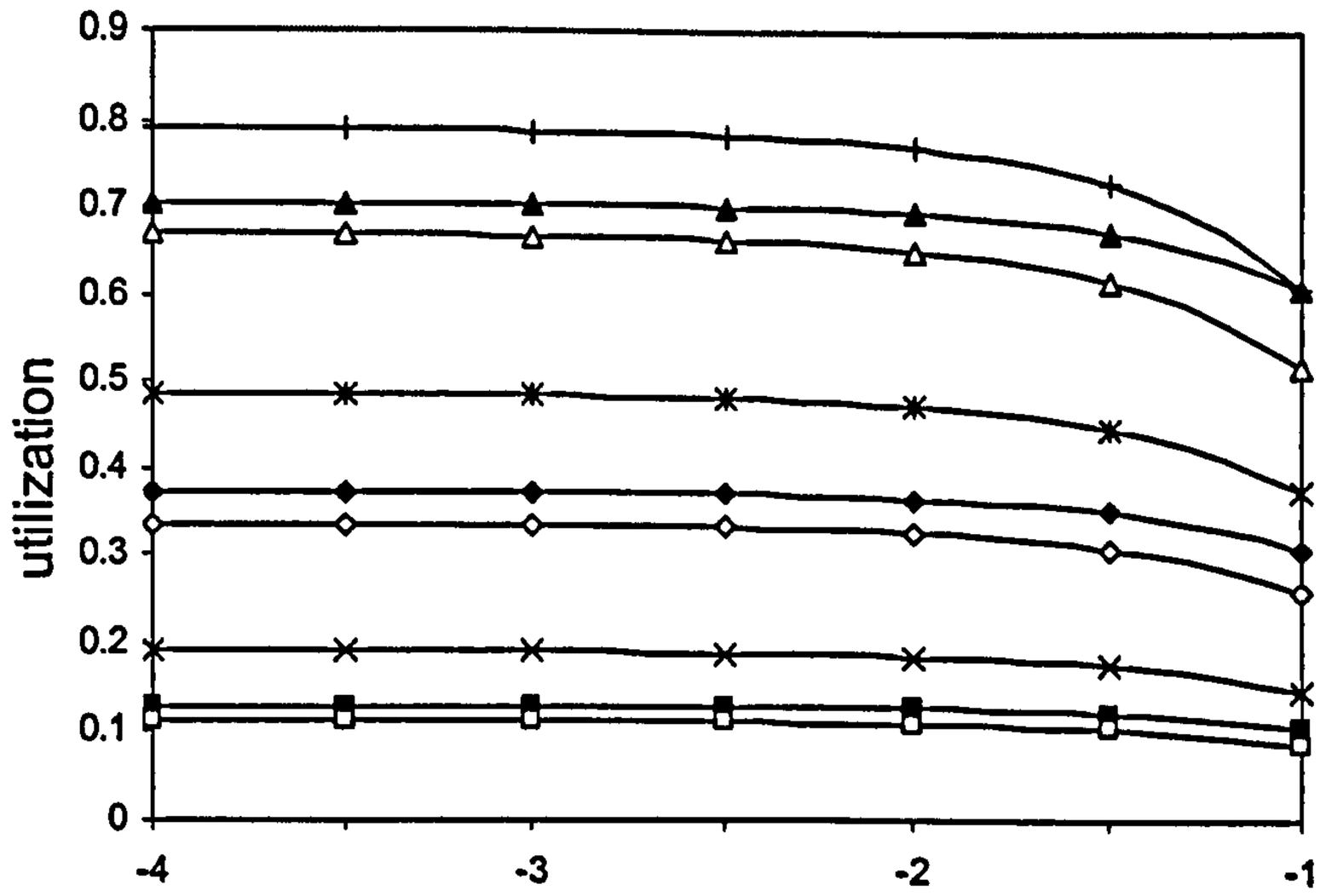

Figure 7.10 Utilization versus frame error rate for various l values, C=4Mbit/s, w=4 frames, T_t =5sec, W=8, m=62, n=5 stations

Fig. 7.10 shows the effect of frame size to utilization for a window size of four. Utilization is very low for small frame sizes and a high frame size implementation is needed in order to achieve high utilization. The SEQ-NoFLACK protocol always achieves a higher utilization than FLACK-M and NoFLACK-ACK. The FLACK-M protocol always outperforms the NoFLACK-ACK protocol because the implemented window size is less than the 'critical' value of six. FLACK-M is robust to FER increase but NoFLACK-ACK and SEQ-NoFLACK are also robust because a small window size is implemented. Fig. 7.11 plots the same results for a window size of sixteen. For low FER, SEQ-NoFLACK reaches the highest utilization figure and NoFLACK-ACK outperforms the FLACK-M protocol because the window size is greater than six. For high FER, FLACK-M is robust but NoFLACK-ACK and SEQ-NoFLACK protocol utilization strongly decrease because the window size is high. As a conclusion, the SEQ-NoFLACK protocol is always the best choice for small window sizes. For high window sizes, SEQ-NoFLACK is again the best choice for low FER but FLACK-M should be chosen if FER is high because it is more robust. Figures 7.10 and 7.11 show that a high frame size should be used in order to achieve high utilization. We can also conclude that AIr applications should employ a high window size and the maximum

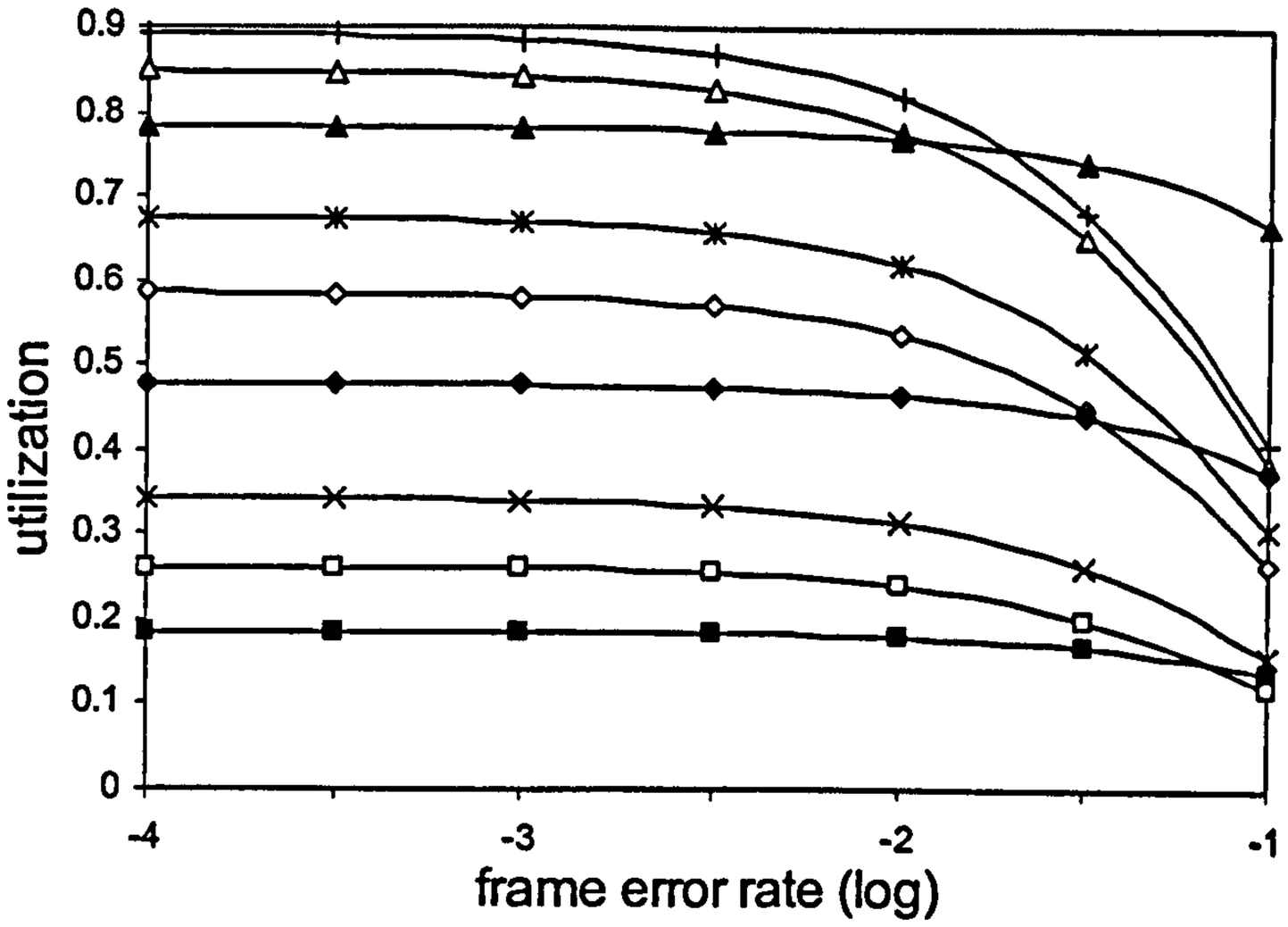

□ *NoFLACK-ACK, l=128bytes* ■ *FLACK-M, l=128bytes* x *SEQ-NoFLACK, l=128bytes*
◇ *NoFLACK-ACK, l=512bytes* ◆ *FLACK-M, l=512bytes* ✱ *SEQ-NoFLACK, l=512bytes*
△ *NoFLACK-ACK, l=2Kbytes* ▲ *FLACK-M, l=2Kbytes* + *SEQ-NoFLACK, l=2Kbytes*

Figure 7.11 Utilization versus frame error rate for various l values, C=4Mbit/s, w=16 frames, T_t =5sec, W=8, m=62, n=5 stations

frame size (16Kbits) at the MAC layer in order to achieve high utilization.

7.4. RR evaluation

The performance of *L*-PPM links has been studied in the literature [1][72][79] and the successful and unsuccessful symbol capture probabilities for stations experiencing a specific SNR for different RR are derived. This section presents an analytical model that evaluates the frame error rate (f_e) as a function of SNR and RR. Based on this model, FLACK-M, NoFLACK-ACK and SEQ-NoFLACK protocol performance is studied when RR coding is employed to reach stations with low SNR. The link quality for which RR adjustment is beneficial is finally examined.

Lets assume that a symbol transmission has L slots, T is the symbol duration and that only one pulse is transmitted in one of the L slots with power $P\sqrt{LT}$, where P is constant. All the remaining L-1 slots are empty or 'zero'. It is assumed that the transmitted pulse is a raised cosine signal given by

$$y(t) = \left| \frac{\sin(\pi t)}{\pi t} \cdot \frac{\cos(\pi \alpha t)}{1 - 4\alpha^2 t^2} \right| \tag{7.26}$$

where α is a raised cosine factor in the range [0,1]. Transmissions from other stations

may interfere with this transmission. The interfering signal is also assumed to be of raised cosine shape and given by

$$s(t)=\left|\frac{s_{\max}\sin(\pi t)}{\pi t}\cdot\frac{\cos(\pi\alpha t)}{1-4\alpha^2t^2}\right| \tag{7.27}$$

where $s_{\max}=ISR\cdot P\sqrt{LT}$ and ISR is the interference-to-signal ratio. The interfering signal is assumed to have a random phase with respect to the transmitted signal. Thus, the amplitude of the interfering signal may have any value within the symbol period at the time of sampling at the receiver. To determine the effects of the interfering signal to the original signal reception, the interfering signal amplitude is quantized into a fixed number of discrete amplitude levels. If M levels are considered, the quantized levels are given by

$$s_i=\frac{s_{\max}(2i-1)}{2M},i=1,...,M \tag{7.28}$$

The probability that an interfering signal of a specific level is received at the time of sampling at the receiver is given by

$$p_i=\sum_k\frac{|t_k-t_{k+1}|}{T} \tag{7.29}$$

where t_k is the instant time that the interfering signal amplitude crosses the quantization level from (i-1) to (i) and is calculated from $s(t)|_{t=t_k}=s_i-\frac{s_{\max}}{2M}$,

$$\left|\frac{\sin(\pi t_k)}{\pi t_k}\cdot\frac{\cos(\pi\alpha t_k)}{1-4\alpha^2t_k^2}\right|=\frac{i-1}{M} \tag{7.30}$$

and t_{k+1} is the instant time that the interfering signal amplitude crosses the quantization level from (i) to (i+1) and is calculated from $s(t)|_{t=t_{k+1}}=s_i+\frac{s_{\max}}{2M}$,

$$\left|\frac{\sin(\pi t_{k+1})}{\pi t_{k+1}}\cdot\frac{\cos(\pi\alpha t_{k+1})}{1-4\alpha^2t_{k+1}^2}\right|=\frac{i}{M} \tag{7.31}$$

With probability p_i, the received power at a slot that a pulse is originally placed is

$$y_{1i}=P\sqrt{LT}\left[1-ISR(1-s_i^n)\right]+\eta \quad i=1,...,M \tag{7.32}$$

where $s_i^n=\frac{s_i}{s_{\max}}$ is the normalized quantized level and η is white Gaussian noise with zero mean and variance σ_v^2. With probability p_i, the received power at a slot where no

pulse is transmitted is given by,

$$y_{0i} = P\sqrt{LT}ISR(1-s_i^n)+\eta \quad i=1,...,M \tag{7.33}$$

The conditional pulse error probabilities for a 'pulse' and 'zero' (no pulse) slot in an *L*-PPM symbol are given by

$$p_{e1} = \sum_{i=1}^{M} p_i \mathbf{Q}\left(\frac{t_n - P\sqrt{LT}(1-ISR(1-s_i^n))}{\sigma_v}\right) \tag{7.34}$$

$$p_{e0} = \sum_{i=1}^{M} p_i \left(1-\mathbf{Q}\left(\frac{t_n - P\sqrt{LT}(ISR(1-s_i^n))}{\sigma_v}\right)\right) \tag{7.35}$$

where t_n is the normalized threshold and $\mathbf{Q}(y)$ is the Marcum error function defined as

$$\mathbf{Q}(y) = \frac{1}{\sqrt{2\pi}} \int_{\infty}^{y} e^{\frac{(x)^2}{2}} dx \tag{7.36}$$

Note that $t_n = 0.3P\sqrt{LT}(1+ISR_M)$ is used and that the SNR can be defined as $SNR = 10\log\left(\left(P\sqrt{LT}\right)^2/\sigma_v^2\right)$.

If the transmitter repeats a symbol RR times, the receiver implements L counters to track the number of received pulses in every symbol slot. If there is only one slot counter with the maximum value, the receiver captures the symbol in the corresponding slot. It is assumed that if two or more counters share the maximum value, the symbol is not captured, although the receiver may randomly select the correct slot. The probability that the 'pulse' slot counter has RR-*i* pulses is given by

$$\Phi_i^1 = \binom{RR}{i}(1-p_{e1})^{RR-i} p_{e1}^i \tag{7.37}$$

where i is the number of transmitted pulses that are not received. The probability that RR-*j* pulses are received in a 'zero' slot is given by

$$\Phi_j^0 = \binom{RR}{j}(1-p_{e0})^{j} p_{e0}^{RR-j} \tag{7.38}$$

The probability that all 'zero' slot counters have values less than RR-*i* is given by

$$\Phi^{L-1} = \left(1-\sum_{j=0}^{i}\Phi_j^0\right)^{L-1} \tag{7.39}$$

The successful symbol capture probability P_{sc} can be calculated from

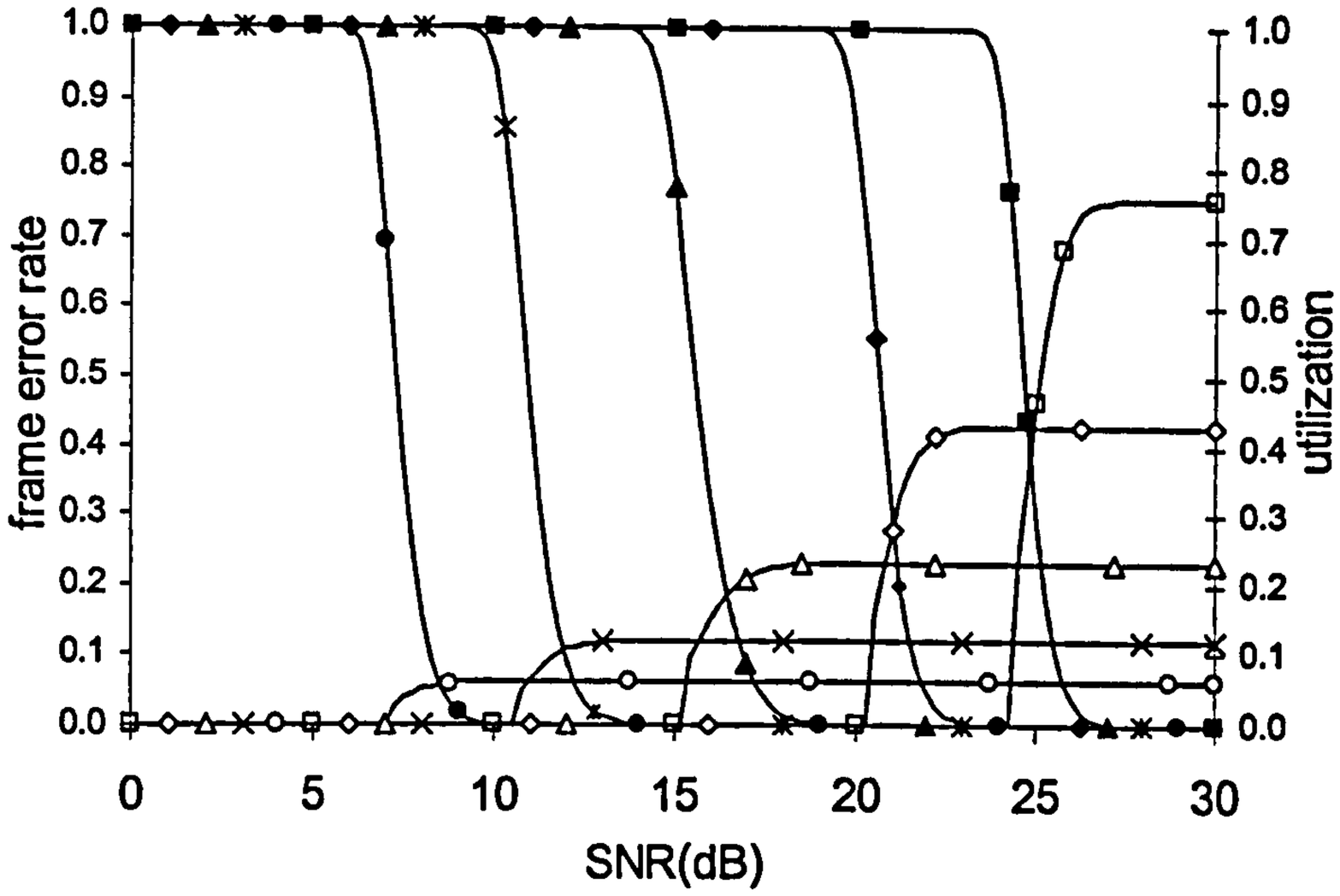

□ $U_{FLACK\text{-}M}$, $RR=1$ ■ f_e, $RR=1$
◇ $U_{FLACK\text{-}M}$, $RR=2$ ◆ f_e, $RR=2$
△ $U_{FLACK\text{-}M}$, $RR=4$ ▲ f_e, $RR=4$
× $U_{FLACK\text{-}M}$, $RR=8$ ✱ f_e, $RR=8$
○ $U_{FLACK\text{-}M}$, $RR=16$ ● f_e, $RR=16$

Figure 7.12 Utilization and frame error rate versus SNR for various RR values, C=4Mbit/s, w=8 frames, l=2Kbytes, T_t =5sec, W=8, m=62, n=5 stations, ISR=10%, t_n=0.3, α=0.75, M=16

$$P_{sc} = \sum_{i=0}^{RR-1}\left[\Phi_i^1\left(1-\sum_{j=0}^{i}\Phi_j^0\right)^{L-1}\right] \tag{7.40}$$

Finally, the frame error rate, f_e, is given by

$$f_e = 1-P_{sc}^{(l+l_A')/\log_2 L} \tag{7.41}$$

when ADATA frames are utilized. Similarly,

$$f_e = 1-P_{sc}^{(l+l_D')/\log_2 L} \tag{7.42}$$

when DATA frames are used and finally,

$$f_e = 1-P_{sc}^{(l+l_S')/\log_2 L} \tag{7.43}$$

when SDATA frames are utilized. Parameters l, l_A', l_D' and l_S' are as defined in section 7.2; l is the payload data length and l_A', l_D' and l_S' are the MBR overhead bit lengths of the ADATA, DATA and SDATA frames respectively.

Fig. 7.12 plots utilization and frame error rate (FER) versus SNR for all proposed RR values for the FLACK-M protocol for l=16Kbits, ISR=10%, t_n=0.3, α=0.75 and M=16. It shows that doubling RR provides approximately a 3-4dB SNR gain in FER.

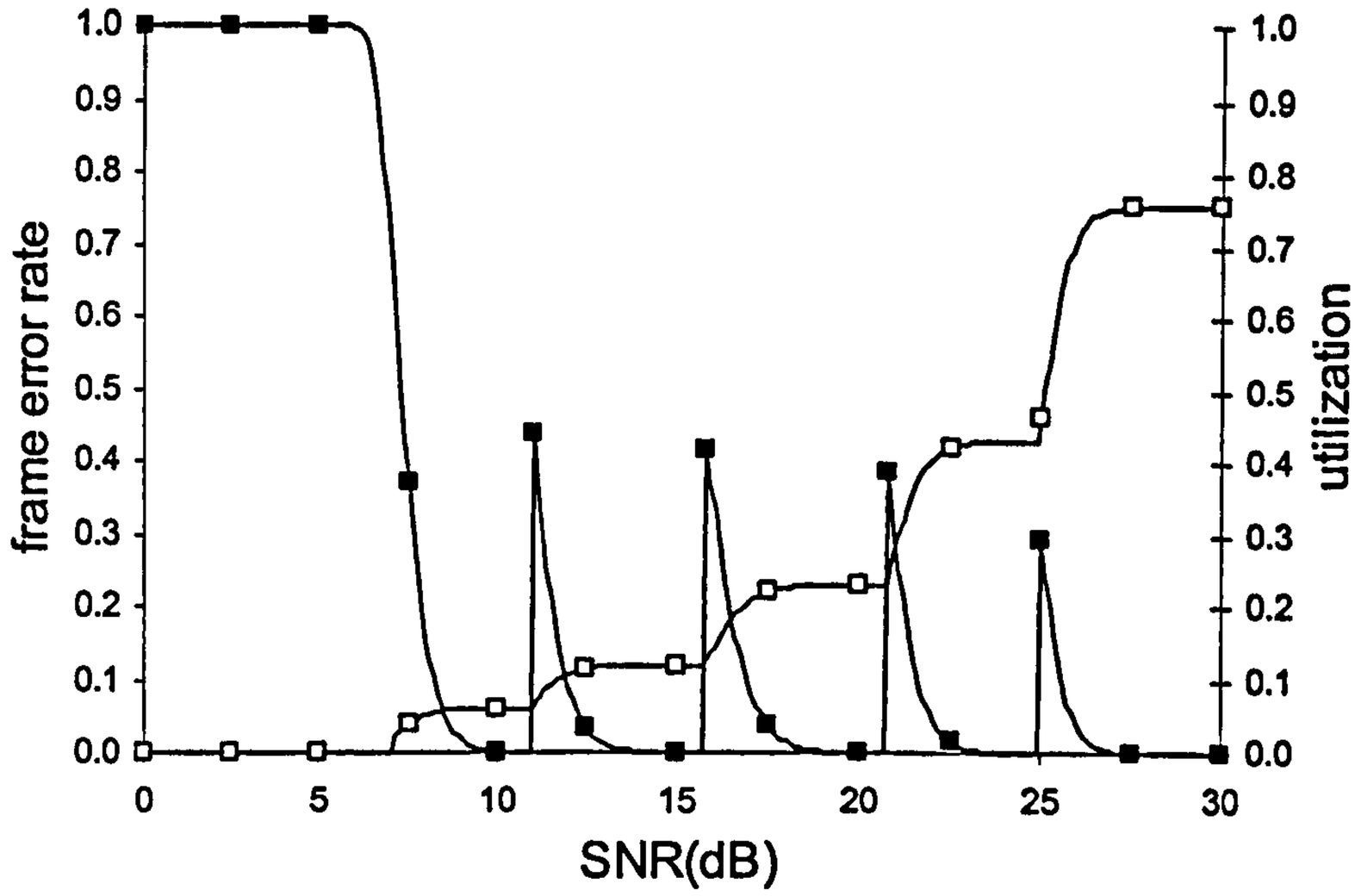

□ $U_{FLACK\text{-}M}$, *optimum RR*

■ f_e, *optimum RR*

Figure 7.13 Maximum utilization and frame error rate versus SNR for optimum RR values, C=4Mbit/s, w=8 frames, l=2Kbytes, T_t =5sec, W=8, m=62, n=5 stations, ISR=10%, t_n=0.3, α=0.75, M=16

The figure shows that for a specific SNR, the smallest RR value that results in low FER should be employed. If the SNR lowers resulting in a high FER value, doubling RR results in very low FER and a LAN utilization very close to half of the original utilization.

7.5 Effectiveness of RR coding on protocol performance

When should the transmitter double the RR it implements to increase utilization? The receiver should monitor link quality and if the FER it evaluates is greater than a threshold, it should advise the transmitter to double the RR it implements. This threshold value depends on the implemented ARQ protocol.

7.5.1 FLACK-M protocol

Fig. 7.13 plots FLACK-M utilization and the corresponding FER versus SNR when RR is adjusted to the optimum value that results in maximum utilization for the specific SNR. It shows that for the considered parameter values, RR should be adjusted if FER becomes greater than approximately 0.4. This high threshold value can be explained as follows. The FLACK-M protocol implements the SW ARQ scheme at the MAC layer and employs the Reserved transfer mode with acknowledgement. Thus, a frame loss is

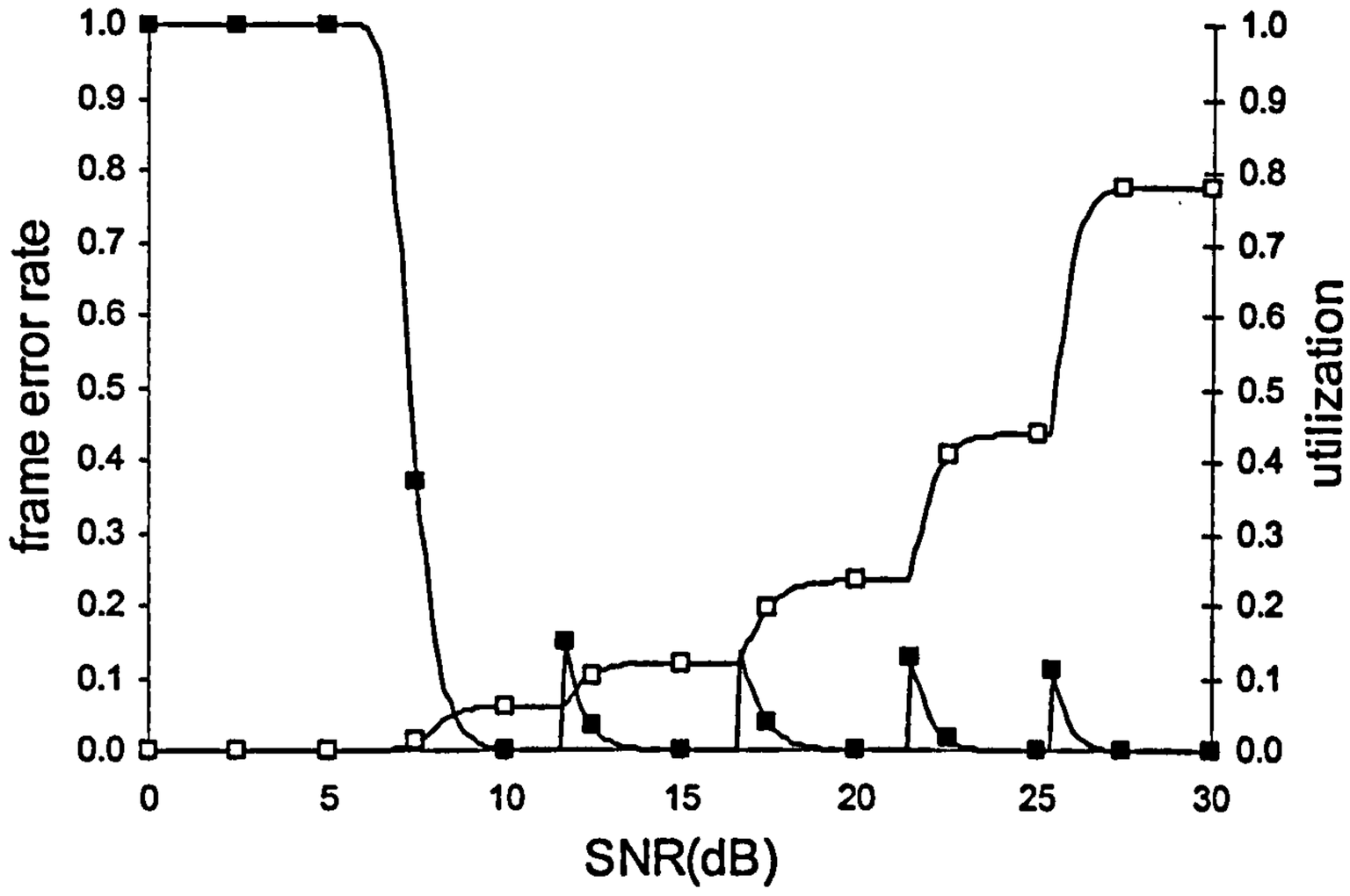

□ $U_{NoFLACK\text{-}ACK}$ *optimum RR*
■ f_e *optimum RR*

Figure 7.14 Maximum utilization and frame error rate versus SNR for optimum RR values, C=4Mbit/s, w=8 frames, l=2Kbytes, T_t =5sec, W=8, m=62, n=5 stations, ISR=10%, t_n=0.3, α=0.75, M=16

immediately realized by a missing MAC ACK frame. According to the utilization definition (sections 2.7 and 6.1), if RR is doubled to cope with transmission errors, utilization is halved. Thus, if significantly more than half of the transmitted frames are received correctly, RR should not be doubled. Results produced for different window and frame sizes indicate that the FER threshold is practically independent of the window size and that it lowers for lower frame sizes.

7.5.2 NoFLACK-ACK protocol

Fig. 7.14 plots NoFLACK-ACK utilization and the corresponding FER versus SNR when RR is adjusted to the optimum value for the specific SNR. The FER threshold lowers to approximately 0.15. The reason is that the NoFLACK-ACK protocol implements a GBN ARQ scheme and correctly received frames following an error frame in a window transmission are considered as out of sequence and are discarded by the receiver. As a result, a frame error causes the retransmission of the error frame and of the frames following it in the same window. Thus, NoFLACK ACK protocol is more sensitive to FER increase than FLACK-M protocol and a lower FER threshold is needed. Produced results also indicate that the FER threshold lowers with window size increase and increases for smaller window sizes. The FER threshold also depends on

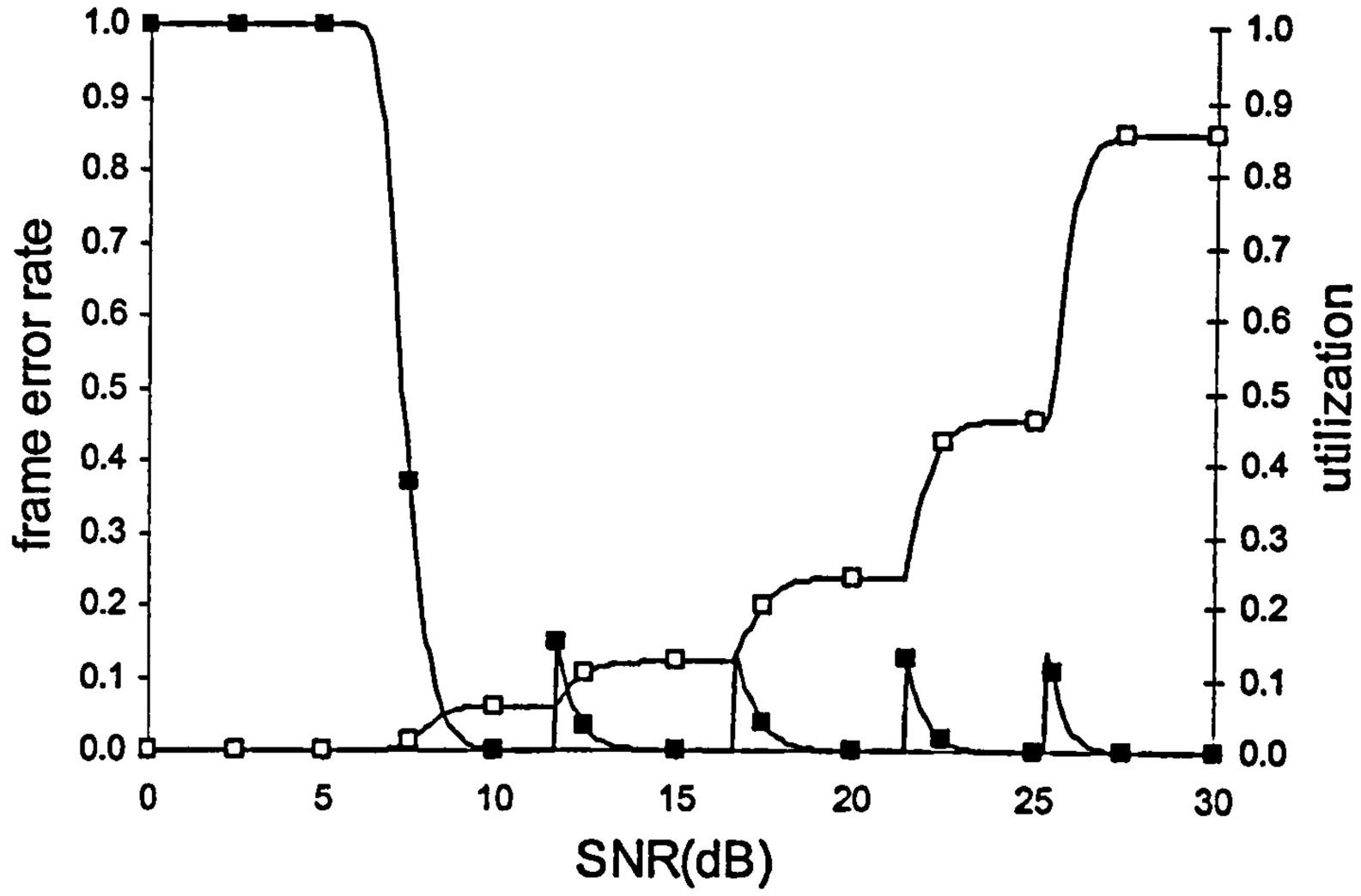

□ $U_{SEQ\text{-}NoFLACK}$, *optimum RR*
■ f_e *optimum RR*

Figure 7.15 Maximum utilization and frame error rate versus SNR for optimum RR values, C=4Mbit/s, w=8 frames, l=2Kbytes, T_t =5sec, W=8, m=62, n=5 stations, ISR=10%, t_n=0.3, α=0.75, M=16

frame size and lowers when a smaller than the maximum (=16Kbits) frame size is employed. However, as discussed in section 7.3, a low frame size implementation results in low utilization.

7.5.3 SEQ-NoFLACK protocol

Similarly, Fig. 7.15 plots SEQ-NoFLACK utilization and the corresponding FER versus SNR for optimum RR adjustment. Direct comparison with Fig. 7.14 shows that the FER threshold of the SEQ-NoFLACK is identical to that of the NoFLACK-ACK protocol. This result can be explained by considering that both protocols implement a GBN ARQ scheme and retransmit the same frames in the case of a frame loss. However, as SEQ-NoFLACK incurs smaller delays, a higher utilization is achieved.

7.5.4 Performance evaluation

Fig. 7.16 compares utilization versus SNR for optimum RR values for the FLACK-M, NoFLACK-ACK and SEQ-NoFLACK protocols. It shows that FLACK-M always achieves a higher utilization than NoFLACK-ACK protocol because, as discussed in section 7.3.3, the implemented window size of four frames is less than the 'critical' value of six frames. SEQ-NoFLACK always achieves the highest utilization among the

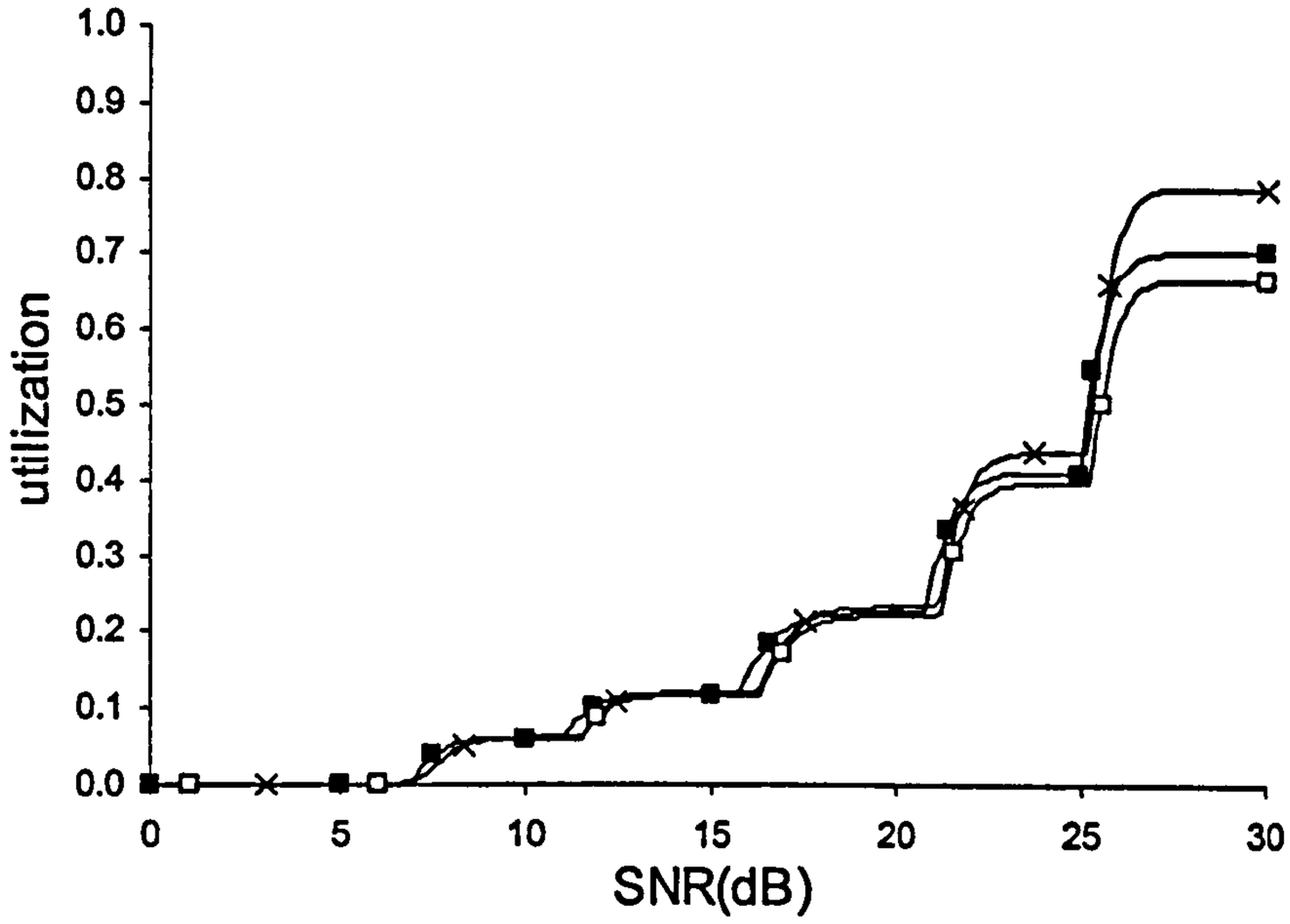

□ *NoFLACK-ACK, optimum RR*
■ *FLACK-M, optimum RR*
x *SEQ-NoFLACK, optimum RR*

Figure 7.16 Utilization versus SNR for optimum RR values, C=4Mbit/s, w=4 frames, l=2Kbytes, T_t =5sec, W=8, m=62, n=5 stations, ISR=10%, t_n=0.3, α=0.75, M=16

considered protocols. These results can be explained by considering that for small window sizes (four for example) all protocols are robust to FER increase, a conclusion drawn in the previous section. The protocol that incurs the least overhead always achieves the highest utilization. Fig. 7.17 plots the same utilization results for a window size of twelve. In this case, a different behavior is observed. SEQ-NoFLACK always outperforms NoFLACK-ACK; NoFLACK-ACK outperforms FLACK-M for most SNR values because the implemented window size of twelve is greater that the 'critical' value of six. However, as discussed in section 7.3.3 for large window size values, the SEQ-NoFLACK and NoFLACK-ACK protocols are not robust to FER increase; FLACK-M remains robust. As a result, for certain SNR values FLACK-M highly outperforms SEQ-NoFLACK and NoFLACK-ACK protocols. For example, if the SNR is 25.5 dB, FLACK-M reaches a 0.65 utilization figure and highly outperforms the SEQ-NoFLACK utilization of 0.47. The reason is that when the SNR results in low FER values, utilization slightly drops for the robust FLACK-M protocol; utilization highly drops for the non-robust SEQ-NoFLACK and NoFLACK-ACK protocols forcing a higher RR value employment and a utilization drop.

We can conclude that for low window sizes, SEQ-NoFLACK is always the best

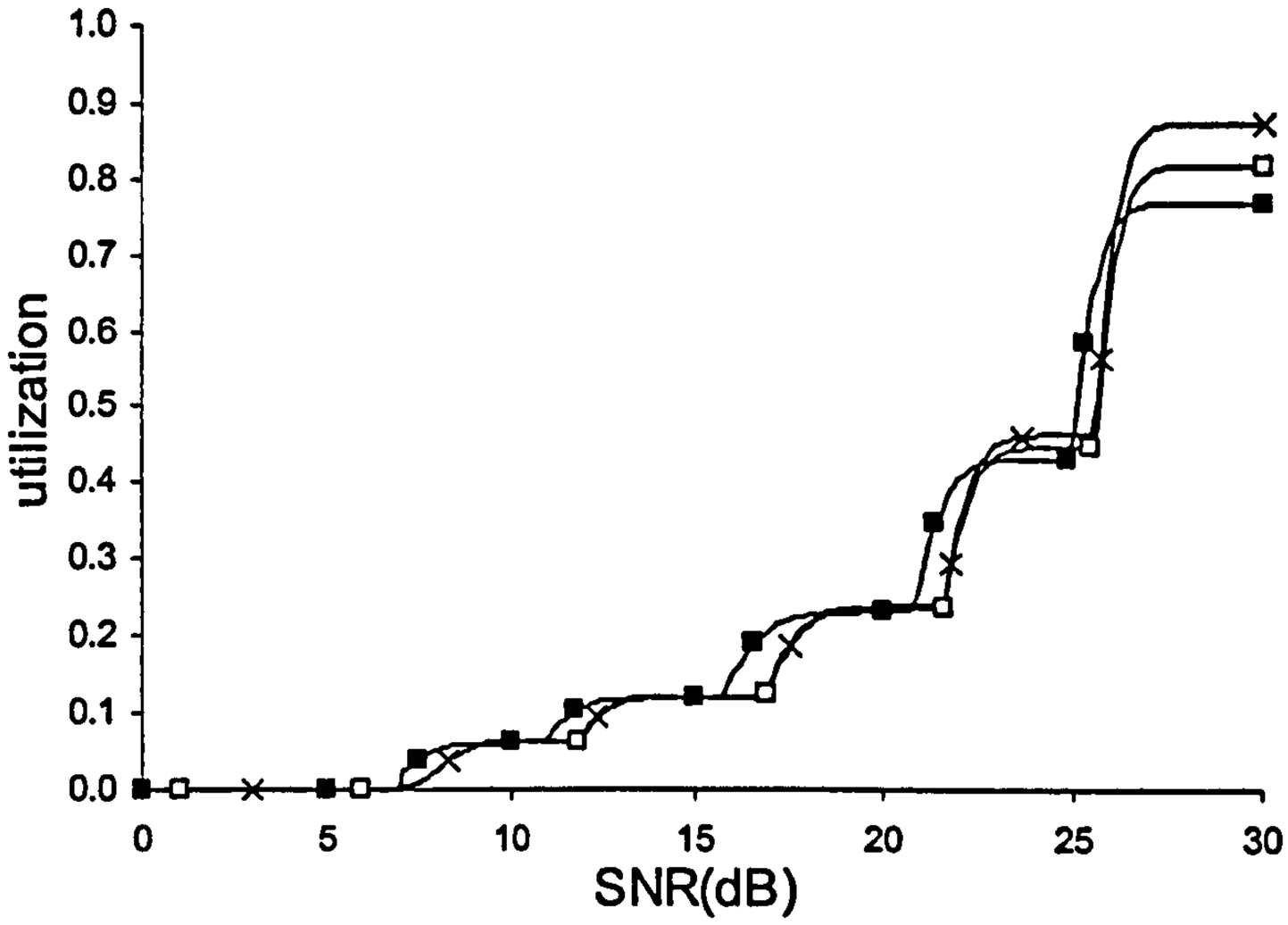

□ *NoFLACK-ACK, optimum RR*
■ *FLACK-M, optimum RR*
x *SEQ-NoFLACK, optimum RR*

Figure 7.17 Utilization versus SNR for optimum RR values, C=4Mbit/s, w=12 frames, l=2Kbytes, T_t =5sec, W=8, m=62, n=5 stations, ISR=10%, t_n=0.3, α=0.75, M=16

choice and FLACK-M outperforms the NoFLACK-ACK protocol. For high window sizes, SEQ-NoFLACK always outperforms the NoFLACK-ACK protocol. FLACK-M offers the best choice for a few SNR value intervals but, at the same time, the worst choice for the remaining SNR values. Thus, maximum utilization is achieved if the suitable ARQ protocol is selected for the enforced window size and for the receiver's SNR.

CHAPTER 8

Conclusions and Suggestions for Future Research

8.1 Conclusions

The aim of this thesis in analysing the performance of indoor infrared links and proposing implementation issues and protocol modifications that improve the operation of short range infrared links has been achieved. Two protocol stack proposals developed by the Infrared Data Association (IrDA) have been considered; the widely used IrDA 1.x proposal for indoor point to point links and the recently developed AIr proposal for indoor infrared LANs. The following protocol stack layers have been studied:

- IrDA 1.x IR Link Access Protocol (IrLAP)
- Advanced IR Medium Access Control layer (AIr MAC)
- Advanced IR Link Control layer (AIr LC)

The main contributions of this thesis are:

a) The derivation of simple equations that calculate optimum values for the window size and frame length link layer parameters of the IrDA 1.x protocol. These optimum values can be implemented easily in order to maximize the performance in high BER point to point IR links.

b) The proposal of link layer parameters and retransmission scheme that maximize the performance for a specific link quality in indoor AIr LANs. This work also considers the network scenarios that render AIr connectivity beneficial.

8.1.1 Conclusions for the IrDA 1.x IrLAP

a) The link turn around time due to hardware latency is of key importance in IR point to point links as it may significantly decrease performance. Two proposals are considered to address this problem in high speed IR links: a) the employment of IR ports with smaller hardware latency time periods and b) the implementation of higher window sizes (from 7 to 127 frames) at the link layer in order to reduce the link turn-around frequency. High window size employment increases performance at low BER, especially when link turn around time is high. The price we pay for

using high window sizes is that link performance becomes sensitive to BER increase because an error frame causes the retransmission of a significant number of out of sequence frames.

b) The maximum value for the minimum turn around time parameter of the future IrPHY specifications (40 Mbit/s or 100 Mbit/s) should not be less than 0.1ms when the IrDA links are expected to operate in good conditions of low BER. In this case, IrLAP should utilize the maximum allowed window size of 127 frames. If it is desired that the future high speed links should be more robust to BER increase, then a lower value of 0.01 ms should be defined for the minimum turn around time parameter. In this case, IrLAP should utilize the maximum window size of 127 frames at low BER and a reduced (or optimum) window size value when BER increases.

c) The implementation of optimal window and frame size values simultaneously results in maximum utilization and significant performance improvement, especially at high BER links. The minimum turn around time (hardware latency) and the F-timer time-out period are the main detrimental factors on performance in this case. Reducing the hardware latency of the IR ports significantly improves utilization.

d) The following modification in IrLAP operation is proposed to address delays arising from the F-timer expiration when optimum window and frame size values are implemented. The transmitter should not pass transmission control by setting the P-bit in the last I-frame it transmits, but set the P-bit in a new Receive Ready (RR) S-frame that follows the last I-frame transmission. This modification successfully minimizes delays arising from F-timer expiration at the expense of a small RR frame transmission and improves utilization. The implementation of simultaneously optimal window and frame size values, combined with the S-frame modification and IR ports with small hardware latency results in significant IrLAP performance figures on high BER links.

e) When optimal window and frame size values are simultaneously implemented, the optimum frame size values balance the time consumed on retransmitting error frames with the time consumed on transmitting overheads; the optimum window size values balance the time utilized in retransmitting out of sequence frames with the time utilized on acknowledgments.

f) Implementation of optimum window and/or frame size values is very simple and effective if the transmitter implements optimum values based on its estimation of link BER. Simulation results indicate that if the transmitter implements (a) only eleven different sets for both optimum window and frame size values, (b) simple rules for estimating link BER and (c) both optimum window and frame size values, a significant and very close to the maximum IrLAP performance can be achieved.

8.1.2 Conclusions for the AIr standard

a) AIr applications should utilize a high window size and the maximum frame size (16Kbits) at the MAC layer in order to achieve high channel utilization. The reason is that the essential PHY and MAC information transmitted in the Robust Header field of the reservation control frames is always transmitted using maximum Repetition Rate (RR=16) to ensure maximum coverage. As a result, the time required for medium reservation is increased and the transmission of significant amounts of information data during successful reservations is necessary for high utilization. The proposed Collision Avoidance procedures perform very effectively; these procedures include the Contention Window adjustment algorithm and the large Collision Avoidance Slot (CAS) duration that avoids collisions from hidden stations.

b) When there are no hidden stations, the proposed lower and upper limits for the Contention Window (CW) size result in utilization degradation. The lower limit of 8 slots should be lowered to 1 and the upper limit of 256 should also be lowered to 65. The proposed upper limit value of 65 corresponds to 21 backoff stages (65=1+21x4), when every stage utilizes the contention window size of the previous stage increased by 4. The new lower limit results in significant utilization improvement when one or a few stations are transmitting in the LAN.

c) The proposed Repetition Rate (RR) coding is proven very effective in reaching stations with low Signal to Noise Ratio (SNR). Doubling RR provides a 3-4 dB gain in SNR. The frame error rate (FER) threshold that renders doubling RR beneficial depends on the employed retransmission scheme. Assuming that RR coding is effectively implemented and the optimum RR value that results in maximum link utilization for a station's SNR is utilized:

i) if the application utilizes a small payload window size, the Reserved transfer

mode with sequenced data at the MAC layer should always be employed.

ii) if the application utilizes a high payload window size, the Reserved transfer mode with sequenced data at the MAC layer is usually the best choice. However, for certain SNR values, the Reserved transfer mode with acknowledgment achieves a higher utilization.

d) When the MAC SW ARQ scheme is utilized, the LC GBN ARQ scheme should be disabled and the LC layer should rely on the MAC SW scheme to guarantee that the transmitted information is correctly received by the remote station. Implementation of the GBN ARQ scheme at the LC layer, which is very close to the MAC layer, results in significant delays and no significant benefits.

e) When a reliable information transfer procedure is not utilized at the MAC layer and the LC layer implements its GBN ARQ scheme, the LC layer should poll the remote station by setting the P/F bit in a special Receive Ready acknowledgment (LC ACK) frame and not in a data frame. The reason is that the LC ACK frame is very small, it is seldom lost and significant delays caused by a possible P/F bit loss are avoided. The delay for the additional LC ACK frame transmission is very small compared to other protocol delays, such as the transmission time of control frames, TAT delays and contention periods.

f) If RR coding is not employed and a small window size is utilized, the transmitter should always employ the Reserved transfer mode with sequenced data at the MAC layer. If a high window size is utilized, the Reserved transfer mode with sequenced data at the MAC layer is again the best choice for error free links. For links with transmission errors, applications utilizing high window sizes should employ the Reserved transfer mode with acknowledgment at the MAC layer. In all cases, the LC layer retransmission scheme should be disabled.

g) Unreserved transfer mode should rarely be used at the MAC layer, especially in LANs with many transmitting stations. Unreserved transfer mode incurs the least overhead because it does not reserve the infrared medium using the RTS/CTS control frame exchange. However, if a data frame in the Unreserved mode collides, the remaining stations are unaware of the collision because the AIr physical layer does not indicate the medium busy condition. Contending stations transmit during the collision causing a fairness problem and utilization degradation.

8.2 Suggestions for future research

a) Collision avoidance procedures with hidden stations: In this thesis, an analytical model for the collision avoidance scheme of the AIr protocol is developed for WLAN scenarios with no hidden stations. As the presence of hidden stations is probable in infrared WLANs, the development of an analytical model that evaluates the performance of the collision avoidance procedures considering hidden stations is an open challenge. Such an analysis could examine the suitability of the proposed values for minimum and maximum CW size parameters for all network scenarios. The proposed analysis could also evaluate the implications of hidden stations for medium access delays and on ARQ scheme and RR value selection for AIr WLANs.

b) The presented analysis for the IrDA 1.x performance confirms that the implementation of optimum window and frame size values significantly improves the performance of point-to-point links at high BER. The AIr protocol introduces significant turn around delays arising from the collision avoidance procedures and from the RTS/CTS/EOB/EOBC frame exchange. In addition, it implements RR coding to cope with transmission errors. The derivation of optimum window size, frame length and RR value that maximize performance for the proposed ARQ schemes in the AIr protocol is an open issue. The AIr protocol stack implements receiver's recommendations of the RR value the transmitter should implement for maximum performance. The receiver may also recommend suitable window and frame size values that the transmitter should implement. Such an analysis will reveal the effectiveness of adapting window and frame size to cope with transmission errors in infrared multipoint wireless communications.

REFERENCES

[1] Audeh M.D., Kahn J.M. and Barry J. R. "Performance of pulse-position modulation on measured non-directed indoor infrared channels", IEEE Transactions on Communications, vol. 44, no. 6, pp. 654-659, June 1996.

[2] Bantz D.F. and Bauchot F.J., "Wireless LAN design alternatives", IEEE Network, vol. 8, no. 2, pp. 43-53, Mar/Apr. 1994.

[3] Barker P. and Boucouvalas A.C., "A simulation modeling of IRDA infrared communication protocol", 1st International Symposium on Communication Systems and Digital Signal Processing, Sheffield, UK, 6-8 April 1998, pp. 2-5.

[4] Barker P. and Boucouvalas A.C., "Performance analysis of the IrDA protocol in wireless communications", 1st International Symposium on Communication Systems and Digital Signal Processing, Sheffield, UK, 6-8 April 1998, pp. 6-9.

[5] Barker P. and Boucouvalas A.C., "Performance modeling of the IrDA protocol for infrared wireless communications", IEEE Communications magazine, vol. 36, no. 12, pp. 113-117, Dec. 1998.

[6] Barker P., Boucouvalas A.C. and Vitsas V., "Performance modelling of the IrDA infrared wireless communications protocol", International Journal of Communication Systems, vol. 13, pp. 589-604, 2000.

[7] Barker P., Vitsas V. and Boucouvalas A.C., "Simulation analysis of the Advanced Infrared (AIr) MAC wireless communications protocol", accepted for publication in IEE Proceedings Circuits and Systems.

[8] Barry J.R., Wireless Infrared Communications, Kluwer Academic Publishers, 1994.

[9] Benelli G., "A Go-Back-N protocol for mobile communications", IEEE Transactions on Vehicular Technology, vol. 40, no. 4, pp. 714-720, Nov. 1991.

[10] Bestekas D. and Gallager R., Data Networks, Prentice Hall, 1992.

[11] Bharghavan V., Demers A., Shenker S. and Zhang L., "MACAW: A media access protocol for wireless LANs", Proc. of the conference on Communications architectures, protocols and applications, SIGCOMM'94, Oct. 1994, pp. 212-225.

[12] Bianchi G., "Performance analysis of the IEEE 802.11 Distributed Coordination Function", IEEE Journal on Selected Areas in Communications, Wireless Series, vol. 18, no. 3, Mar. 2000.

[13] Bianchi G., "Throughput evaluation of the IEEE 802.11 Distributed Coordination Function", Proc. of the 5th Intl. Workshop on Mobile Multimedia Communications, MoMuc'98, Oct. 12-14, 1998, Berlin.

[14] Boucouvalas A.C. and Barker P., "Asymmetry in optical wireless links", IEE Optoelectronics, vol. 147, no.4, pp. 315 –321, Aug. 2000.

[15] Boucouvalas A.C. and Barker P., "IrLAP protocol performance analysis of IrDA wireless communications", IEE Electronics Letters, vol. 34, no. 25, pp. 2380-2381, 1998.

[16] Boucouvalas A.C. and Ghassemlooy Z., Editorial, Special Issue on Optical Wireless Communications, IEE Proceedings J, Optoelectronics, vol. 147, pp. 279, Aug. 2000.

[17] Boucouvalas A.C. and Vitsas V., "100 Mbit/s IrDA protocol performance evaluation", Proc. of the IASTED International Conference on Wireless and

Optical Communications (WOC 2001), Banff, Canada, June 27-29, 2001, pp. 49-57.

[18] Boucouvalas A.C. and Vitsas V., "Optimum window and frame size for IrDA links", IEE Electronics Letters, vol. 37, no. 3, pp. 194-196, Feb 2001.

[19] Bux W., Kummerle K. and Truong H.L., "Balanced HDLC procedures: A performance analysis", IEEE Transactions on Communications, vol. 28, no. 11, pp.1889-1898, Nov. 1980.

[20] Bux W. and Truong H.L., "High level data link control traffic considerations", 9th Int. Teletraffic Congress, Session 17, Torremolinos, Spain, Oct. 18-24, 1979.

[21] Chhaya H and Gupta S., "Performance modeling of the asynchronous data transfer methods of the IEEE 802.11 MAC protocol", Wireless Networks, vol. 3, pp. 217-234, 1997.

[22] Chiasserini C.F. and Rao R.R., "Performance of IEEE 802.11 WLANs in a Bluetooth environment", IEEE Wireless Communications and Networking Conference (WCNC), vol. 1, pp. 94-99, 2000.

[23] Chow F., "Effect of non-reciprocity on infrared wireless Local Area Networks", M.S. Report, University of California, Berkeley, December 1998.

[24] Chow F. and Kahn J.M., "Effect of non-reciprocity on infrared wireless Local Area Networks", Proc. of the IEEE Global Telecommunications Conference, Rio de Janeiro, Brazil, Dec. 5-9, 1999, vol. 1a, pp. 330-338.

[25] Comer D.E., "Computer Networks and Internets with internet applications", Prentice Hall, 2001.

[26] Crow B.P., Widjaja I., Kim J.G. and Sakai P.T., "IEEE 802.11 wireless Local Area Networks", IEEE Communications Magazine, vol. 35, no. 9, pp. 116-126, Sep. 1997.

[27] Dutta-Ray A., "Netwoks for homes", IEEE Spectrum, vol. 36, no. 12, pp. 26-33, Dec. 1999.

[28] Gfeller F. and Hirt W., "A robust wireless infrared system with channel reciprocity", IEEE Communications Magazine, vol. 36, no. 12, pp. 100-106, 1998.

[29] Gfeller F. and Hirt W., "Advanced Infrared (AIr): Physical layer for reliable transmission and medium access', Proc. of the 2000 International Zurich Seminar on Broadband Communications, pp. 77-84, 2000.

[30] Gfeller F., Hirt W., de Lange M. and Weiss B., "Wireless infrared transmission: How to reach all office space", IEEE 46th Vehicular Technology Conference, vol. 3, pp. 1535-1539.

[31] Gummalla A.C.V. and Limb J.O., "Wireless medium access control protocols", IEEE Communications Surveys, Second Quarter 2000, (available at: http://www.comsoc.org/pubs/surveys).

[32] Haartsen J.C., "The bluetooth radio system", IEEE Personal Communications, vol. 7, no. 1, pp. 28-36, Feb. 2000.

[33] Haarsten J., Naghshineh M., Inouye J., Joeressen O. and Warren A., "Bluetooth: vision, goals and architecture", ACM SIGMOBILE Mobile Computing and Communications Review, vol. 2, no. 4, pp. 38-45, Oct 1998.

[34] Harsall F., "Data Communications, Computer Networks and Open Systems", Addison-Wesley, 1996.

[35] Heatley D.J.T. and Neild I., "Optical wireless-the promise and the reality", IEE Colloquium on Optical Wireless Communications, pp. 1/1-1/6, Savoy Place,

London, 1999.
[36] Higginbottom G.N., "Performance Evaluation of Communication Networks", Artech House, 1998.
[37] Hirt W., Hassner M. and Heise N., "IrDA-VFIr (16 Mb/s): modulation code and system design", IEEE Personal Communications, vol. 8, no. 1, pp. 58-71, Feb. 2001.
[38] Ho T. and Chen K., "Performance analysis of the IEEE 802.11 CSMA/CA medium access control protocol", Proc. of PIMRC 1996, Taipei, Taiwan, Oct. 1996, pp. 407-411.
[39] IEEE 802.11, IEEE International Standard for Wireless LAN Medium Access Control (MAC) and Physical Layer (PHY) specifications, First Edition, 20/8/99.
[40] IrDA: "Advanced Infrared Draft Physical Layer Specification (AIr-PHY) – version 0.2", (IrDA, 1997).
[41] IrDA: "Advanced Infrared Draft Physical Layer Specification (AIr-PHY) – version 0.4", (IrDA, 1998).
[42] IrDA: "Advanced Infrared Link Manager (AIrLM) Draft Specification – version 0.3", (IrDA, 1999).
[43] IrDA: "Advanced Infrared Logical Link Control (AIrLC) Specification, version 0.1", (IrDA, 1999).
[44] IrDA: "Advanced Infrared Market Requirements - version 0.45", (IrDA, 1998).
[45] IrDA: "Advanced Infrared Medium Access Control (AIrMAC) Draft Protocol Specification - version 1.0", (IrDA, 1999).
[46] IrDA: "Advanced Infrared Physical Layer Specification (AIrPHY) – version 1.0", (IrDA, 1998).
[47] IrDA: "IrBurst High-speed Object Transmission Profile – version 0.1", (IrDA, 2002).
[48] IrDA: "Link Management Protocol (IrLMP) – Version 1.1", (IrDA, 1996).
[49] IrDA: "Serial Infrared Link Access Protocol (IrLAP) – version 1.1", (IrDA, 1996).
[50] IrDA: "Serial Infrared Physical Layer Specification (IrPHY) – version 1.0", (IrDA, 1994).
[51] IrDA: "Serial Infrared Physical Layer Specification (IrPHY) – version 1.1", (IrDA, 1995).
[52] IrDA: "Serial Infrared Physical Layer Specification (IrPHY) – version 1.4", (IrDA, 2001).
[53] IrDA: "Serial Infrared Physical Layer Specification for 16Mb/s Addition (VFIR)–Errata to version 1.3", (IrDA, 1999).
[54] IrDA: "Technical Overview of an Advanced IrDA Link Access Protocol and Physical Layer – Request for Comments – version 0.1", (IrDA, 1997).
[55] Johnsson M., "HIPERLAN/2 - The broadband radio transmission technology operating in the 5 GHz frequency band", HiperLAN/2 Global Forum ver 1.0, 1999 (available at www.hiperlan2.com).
[56] Jungnickel V., Forck A., Haustein T., Krüger U., Pohl V. and von Helmolt C., "Wireless infrared communication beyond 100 Mbit/s: System design, transmission experiments and potential", World Multiconference on Systemics, Cybernetics and Informatics, SCI 2001/ISAS 2001, Orlando, Florida, July 22-25, 2001, vol. IV, pp. 413-420.
[57] Kahn J.M. and Barry J.R., "Wireless infrared communications", Proc. of the

IEEE, vol. 85, pp. 265-298, Feb. 1997.
[58] Kahn J.M., Barry J.R., Audeh M.D., Carruthers J.B., Krause W.J. and Marsh G.W., "Non-directed infrared links for high-capacity wireless LANs", IEEE Personal Communications, vol. 1, no. 2, pp. 12-25, Second Quarter 1994.
[59] Karaoguz J., "High-rate wireless personal area networks", IEEE Communications Magazine, vol. 39, no. 12, pp. 96-102, Dec. 2001.
[60] Karn P., "MACA – A new channel access method for packet radio", ARRL/CRRL amateur radio 9th computer networking conference, Sep. 1990, pp. 134-140.
[61] Kleinrock L. and Tobagi F., "Packet switching in radio channels, part II – the hidden terminal problem in carrier sense multiple access and the busy tone solution", IEEE Transactions in Communications, vol. 23, no.12, pp. 1417-1433, Dec. 1975.
[62] Knutson C.D., Joos D., Woodings R., "Infrared data communications in wireless personal area networks", Proc. of the 5th World Multi-Conference on Systemics, Cybernetics, and Informatics, Orlando, USA, 2001, vol. IV, pp. 427-431.
[63] Kristensen F. and Sandgren M., "A system simulation of wireless local area networks operating in the 5 GHz band", Master's thesis, Lunds Institute of Technology, Sweden, 2001.
[64] Lansford J.; Stephens A. and Nevo R., "Wi-Fi (802.11b) and Bluetooth: enabling coexistence", IEEE Network, vol. 15, no. 5, pp. 20-27, Sep-Oct. 2001.
[65] LaMaire R.O., Krishna A. and Bhagwat P., "Wireless LANs and mobile networking: standards and future directions", IEEE Communications Magazine, vol. 34, no. 8, pp. 86-94, Aug. 1996.
[66] Lin S., Costello D.J.Jr. and Miller M.J., "Automatic-repeat-request error-control schemes", IEEE Communications Magazine, vol. 22, no. 12, Dec. 1984.
[67] Millar I., Beale M., Donoghue B.J., Lindstrom K.W. and Williams S., "The IrDA standard for high-speed infrared communications", The Hewlett-Packard Journal, vol. 49, no. 1, pp. 10-26, 1998.
[68] Modiano E., "An adaptive algorithm for optimizing the packet size used in wireless ARQ protocols", Wireless Networks, vol. 5, pp. 279-286, 1999.
[69] van Nee R., Awater G., Morikura M., Takanashi H., Webster M. and Halford K.W., "New high-rate wireless LAN standards", IEEE Communications Magazine, vol. 37, no. 12, pp. 82-88, Dec. 1999.
[70] Negus K.J., Stephens A.P. and Lansford J., "HomeRF: wireless networking for the connected home", IEEE Personal Communications Magazine, vol. 7, no. 1, pp. 20-27, Feb. 2000.
[71] OPNET™ modeller, MIL3 Inc., 3400 International Drive NW, Washington DC 20008, USA
[72] Ozugur T., "Advanced Infrared Local Area Networks", Ph.D. Thesis, Georgia Institute of Technology, June 2000.
[73] Ozugur T., Copeland J.A., Naghshineh M. and Kermani P., "Next-generation indoor infrared LANs: issues and approaches", IEEE Personal Communications, vol. 6, no. 6, pp. 6-19, Dec. 1999.
[74] Ozugur T., Naghshineh M. and Kermani P., "Comparison of go-back-N and selective reject ARQ modes of HDLC over half-duplex and full-duplex IR links and the effects of window size and processor speed in utilization", Proc of the 9th IEEE International Symposium on Personal, Indoor and Mobile Radio

Communications (PIMRC), 1998, vol. 2, pp. 708-712.
[75] Ozugur T., Naghshineh M.; Kermani P. and Copeland J.A., "Fair media access for wireless LANs", IEEE Global Telecommunications Conference (GLOBECOM '99), 1999, vol. 1b, pp. 570-579.
[76] Ozugur T., Naghshineh M., Kermani P. and Copeland J.A., "On the performance of ARQ protocols in infrared networks", International Journal of Communication Systems, vol. 13, pp. 617-638, 2000.
[77] Ozugur T., Naghshineh M., Kermani P., Olsen C.M., Rezvani B. and Copeland J.A., "ARQ protocol for infrared wireless LANs: packet-level ACK or no-packet-level ACK?", IEEE International Conference on Universal Personal Communications, (ICUPC '98), 1998, vol. 2, pp. 1235-1239.
[78] Ozugur T., Naghshineh M., Kermani P., Olsen C.M., Rezvani B. and Copeland J.A., "Balanced media access methods for wireless networks", Proc. of IEEE/ACM MobiCom'98, Oct. 1998, pp. 21-32.
[79] Ozugur T., Naghshineh M., Kermani P., Olsen C.M., Rezvani B. and Copeland J.A., "Performance evaluation of L-PPM links using repetition rate coding", Proc. of the IEEE PIMRC'98, Boston, USA, Sept. 1998, pp. 698-702.
[80] Pahlavan K., "Trends in Local Wireless Networks", IEEE Communications Magazine, vol. 33, no. 3, pp. 88-95, Mar. 1995.
[81] Paulson L.D., "Exploring the wireless LANscape", Computer, vol. 33, no. 10, pp. 12-16, Oct. 2000.
[82] Punnoose R.I., Tseng R.S. and Stancil D.D., "Experimental results for interference between Bluetooth and IEEE 802.11b DSSS systems", IEEE VTC 54th Vehicular Technology Conference, VTC 2001 Fall, vol. 1, pp.67-71.
[83] Ritter M.B., Gfeller F., Hirt W., Rogers D. and Gowda S., "Circuit and system challenges in IR wireless communication", 1996 IEEE International Solid-State Circuits Conference (42nd ISSCC), Digest of Technical Papers, 1996, pp. 398-399, 480.
[84] Robertson M.G., Hansen S.V., Sorenson F.E. and Knutson C.D., "Modeling IrDA performance: the effect of IrLAP negotiation parameters on throughput", Proc. of the 10th IEEE International Conference on Computer Communications and Networks, 2001, pp. 122-127. , 2001
[85] Sakidu M.N.O., Optical and Wireless Communications – Next Generation Networks", CRC press, 2002.
[86] Stallings W., "Wireless Communications and Networks", Prentice Hall, 2002.
[87] Tanenbaum A.S., "Computer Networks", Prentice Hall, 1996.
[88] Varshney U. and Vetter R., "Emerging mobile and wireless networks", Communications of the ACM, vol. 43, no. 6, pp. 73-81, June 2000.
[89] Vitsas V. and Boucouvalas A.C., "Automatic repeat request schemes for infrared wireless communications", IEE Electronics Letters, vol. 38, no. 5, pp. 254-246, 28 Feb 2002.
[90] Vitsas V. and Boucouvalas A.C., "Effectiveness of packet level acknowledgement in infrared wireless LANs", IEEE 55th Vehicular Technology Conference 2002, VTC Spring 2002, vol. 4, pp. 1814-1818, Birmingham, AL, May 6-9, 2002.
[91] Vitsas V. and Boucouvalas A. C., "IrDA IrLAP protocol throughput performance", Proceedings of the 2nd International Workshop on Networked Appliances (IWNA 2000), New Jersey, USA, Nov. 30-Dec. 1, 2000.

[92] Vitsas V. and Boucouvalas A.C., "Optimisation of IrDA IrLAP link access protocol", accepted for publication in IEEE Journal on Selected Areas in Communications.

[93] Vitsas V. and Boucouvalas A.C., "Packet level acknowledgement and Go-Back-N protocol performance in infrared wireless LANs", submitted for publication in the International Journal of Communication Systems.

[94] Vitsas V. and Boucouvalas A.C., "Performance analysis of the Advanced Infrared (AIr) CSMA/CA MAC protocol for wireless LANs", accepted for publication in Wireless Networks.

[95] Vitsas V. and Boucouvalas A. C., "Performance analysis of the AIr-MAC optical wireless protocol", Proc. of the International Conference on System Engineering, Communications and Information Technologies, (ICSECIT 2001), Magallanes, Punta Arenas, Chile, April 16-19, 2001.

[96] Vitsas V. and Boucouvalas A.C., "Performance analysis of the collision avoidance procedure of the Advanced Infrared (AIr) CSMA/CA protocol for wireless LANs", IEEE 55th Vehicular Technology Conference 2002, VTC Spring 2002, vol. 3, pp. 1502-1506, Birmingham, AL, May 6-9, 2002.

[97] Vitsas V. and. Boucouvalas A.C, "Performance evaluation of IrDA Advanced Infrared AIr - MAC Protocol", Proc. of the 5th Multi-Conference on Systemics, Cybernetics, and Informatics, Orlando, USA, 2001, vol. IV, pp. 347-352.

[98] Vitsas V. and Boucouvalas A.C., "Simultaneous optimisation of window and frame size for IrDA IrLAP links", IEE Electronic Letters, vol. 37, no. 16, pp. 1042-1043, 2001.

[99] Vitsas V. and Boucouvalas A.C., "Throughput analysis of the IrDA IrLAP optical wireless link access protocol", Proc. of the 3rd Conference on Telecommunications (ConfTele 2001) , Figueira da Foz, Portugal, April 23-24, 2001, pp. 225-229.

[100] Vitsas V. and Boucouvalas A.C., "Window and frame size adaptivity for maximum throughput in IrDA links", Proc. of the 3rd Electronic Circuits and Systems Conference, Bratislava, Slovakia, September 5-7, 2001, pp. 147-152.

[101] Williams S., "IrDA: past, present and future", IEEE Personal Communications, vol. 7, no. 1, pp. 11-19, Feb. 2000.

[102] Wisely D., "A 1 Gbit/s optical wireless tracked architecture for ATM delivery", IEE Colloquium on Optical Free Space Communication, London, Feb'96, pp. 14/1-14/7.

[103] Woodings R.W., Joos D.D., Clifton T. and Knutson C.D., "Rapid heterogeneous ad hoc connection establishment: accelerating Bluetooth inquiry using IrDA", IEEE Wireless Communications and Networking Conference (WCNC), Mar. 17-21, 2002, vol. 1, pp. 342-349.

[104] www.bluetooth.com

[105] www.homerf.org

[106] www.microsoft.com/hwdev/tech/network/infrared/default.asp